
**Macrophage population diversity as a
determinant of primary and secondary
responses to LPS**

SHOUMIT DEY

*A thesis submitted in partial fulfillment of the requirements
for the degree of Doctor of Philosophy*

UNIVERSITY OF YORK

BIOLOGY

September 2019

Abstract

Tissue-resident macrophages are the first responder cells of the immune system that phagocytose, present antigens and promote inflammation by secreting soluble factors (cytokines, chemokines, nitric oxide, etc) that act in an autocrine and paracrine manner. This response has been shown to be heterogeneous at mRNA level in single cells suggesting not all macrophages ‘fire’ an equal response. Such heterogeneity can have implications on how inflammation is established or modulated when there is a pathogenic invasion locally such as in wounds or systemically, as in the case of severe blood infections. Here, we ask how single and repeated challenge with LPS affects heterogeneity of macrophage communities. Through combining empirical measurements of inflammatory proteins such as TNF, IL-6, NOS2, and IL-1 β Pro at the single-cell level with mathematical simulations, we show distinct heterogeneous communities of macrophages emerge following primary and secondary LPS challenges. Furthermore, we show that restricting inter-cellular communication or impairing microRNA-mediated silencing, a key cellular process thought to determine population heterogeneity, affect the composition of macrophage communities and responses to LPS. Overall, our results demonstrate that macrophage communities of diverse micro-composition can demonstrate similar macroscopic cytokine responses indicating that population-level robustness and plasticity underpin innate immunity to LPS.

Contents

Abstract	iii
Acknowledgements	xxi
Declaration of Authorship	xxiii
1 Introduction	1
1.1 Pathogens and innate immunity	1
1.1.1 Macrophages and their role in immunity	2
1.1.2 Pathogen recognition by innate immune cells	4
1.1.2.1 LPS as a PAMP	5
1.1.2.2 TLR4 as a PRR	6
1.2 Regulation of inflammation by cytokines and inflammatory mediators . . .	9
1.2.1 TNF	10
1.2.2 IL-6	12
1.2.3 NOS2 and nitric oxide	14
1.2.4 IL-1 β	15
1.2.5 Cytokine response upon a second LPS exposure	17
1.3 Heterogeneity in macrophages	20
1.3.1 Tissue and organ level heterogeneity	20
1.3.2 Heterogeneity within tissue	21
1.3.2.1 Quorum sensing in immune cells	22
1.3.3 Activation-induced heterogeneity	24

1.3.4	Why study immune-cell heterogeneity	26
1.4	microRNAs as non-coding regulatory RNAs	27
1.4.1	Biogenesis and mode of action	29
1.4.2	miRNAs and macrophages responding to LPS	30
1.4.3	miRNAs in protein expression noise and population variability . . .	33
1.5	Mathematical description of biological complexity	35
1.5.1	Probabilistic modelling and Markov process	38
1.6	Choice of the biological model	39
1.6.1	Macrophage-like RAW264.7 cells	39
1.6.2	Thioglycollate-elicited peritoneal macrophages	41
1.7	Motivation and hypothesis	41
1.7.1	Aims	42
2	Methods	43
2.1	Methods and Materials	43
2.1.1	Mammalian cell culture	43
2.1.1.1	Animals and ethics statement	43
2.1.1.2	Extraction/culture of peritoneal macrophages	43
2.1.1.3	RAW264.7 cell culture	44
2.1.1.4	HEK293T cell culture	44
2.1.2	LPS-induced challenge or hyporesponsiveness protocol	45
2.1.3	Flow Cytometry	48
2.1.4	ELISA	52
2.1.5	Greiss Assay	53
2.1.6	RNA interference	53
2.1.7	TNF neutralisation	53
2.1.8	Western Blotting	54
2.1.9	RNA Extraction	55

2.1.10	cDNA synthesis	56
2.1.11	qRT-PCR	56
2.1.12	CRISPR-Cas9 gene editing	56
2.1.13	Transformation	57
2.1.14	Lentiviral production and infection	58
2.1.15	Limiting Dilutions	59
2.1.16	Data Analysis	59
2.1.17	Statistics	59
3	LPS challenge and inter-cellular communication drive heterogeneity	61
3.1	Introduction	61
3.2	Aims	62
3.3	LPS induces pro-inflammatory cytokine secretion	63
3.3.1	RAW264.7 cells secrete TNF, IL-6 and nitric oxide upon LPS stimulus	63
3.4	Cytokine response at single-cell level is heterogeneous	63
3.4.1	Single-cell staining reveals cytokines have temporal profiles	63
3.4.2	LPS response spurs a heterogeneous community in RAW264.7 cells .	67
3.4.2.1	TNF, IL-6 and NOS2 positive cells can be visualised at 16 hours	67
3.4.3	LPS dose alters community consistency within a clonal population .	73
3.4.4	LPS induced community is variable but shows a trend	76
3.4.5	TLR4 expression and cell size do not contribute to response heterogeneity	82
3.5	First challenge of LPS shapes community composition	84
3.5.1	Inter-cellular communication drives macrophage community	84
3.6	Community-level effects are retained upon adding another cytokine	88
3.6.0.1	Restriction of secretion alters responses to LPS	90

3.6.0.2	Isolated communities resemble communities whose secretion is restricted	93
3.6.1	Anti-TNF treatment does not disrupt macrophage response community	95
3.6.2	Thioglycollate-elicited peritoneal macrophage response to LPS is heterogeneous	98
3.7	Discussion	103
3.7.1	Conclusions	103
3.7.2	Visualisation method	104
3.7.3	RAW264.7 macrophages respond as a community	105
3.7.4	Community communication	108
4	Macrophage heterogeneity in secondary LPS challenge	111
4.1	Introduction	111
4.2	Aims	111
4.3	Second dose of LPS induces a hypo-response	112
4.3.1	Upon secondary exposure to LPS RAW264.7 cells make less of TNF, IL-6 and nitric oxide	112
4.4	Community composition determines secondary response to LPS	114
4.4.1	Heterogeneous community responses can be identified by protein accumulation	114
4.4.2	Single-challenged communities undergo a compositional change at 8 hours of LPS stimulus	118
4.5	Discussion	123
4.5.1	Conclusions	123
4.5.2	Hypo-responsive communities	123
4.5.3	Summary and future work	124

5	Mathematical descriptions of population heterogeneity	127
5.1	Introduction	127
5.1.1	Aims	128
5.1.2	Modelling - Methods employed	129
5.2	Modelling paradigm	129
5.2.1	Gillespie-Doob Algorithm	130
5.2.2	Comparison with ODE and analytical solutions	132
5.3	Modelling cell populations responding to LPS	134
5.3.1	Positive-state model definition	134
5.3.1.1	Positive-state model simulation with arbitrary rates	136
5.3.2	Non-responsive (nr) model definition	139
5.3.2.1	nr model - Assumptions	141
5.3.3	Parameter estimation - nr model	142
5.3.3.1	TNF	144
5.3.3.2	IL-6	151
5.3.3.3	pro-IL-1 β	152
5.3.3.4	NOS2	155
5.3.3.5	Non-responding states vary for each protein	157
5.4	Modelling signalling in macrophage communities	159
5.4.0.1	cube model - Assumptions	160
5.4.1	Parameter estimation	162
5.4.1.1	Estimated parameters - signalling	162
5.4.1.2	Estimated parameters - secretion restriction	164
5.4.2	Simplified cube model did not fit experimental data	170
5.5	Discussion	171
5.5.1	Hypo-responsive populations modelled as distinct populations are different for different proteins	172
5.5.2	Modelling community inter-dependence	173

5.5.3	Summary and future work	174
6	Dicer knock down affects composition, distribution and variability	177
6.1	Introduction	177
6.2	Aims	178
6.3	Dicer expression in RAW264.7 cells can be knocked down for up to 72 hours	179
6.4	Dicer-knock down populations can make TNF and IL-6 and are hypo-responsive on secondary stimulus	179
6.5	Dicer knockdown induces changes in community composition	181
6.5.1	Twice challenged communities at 24 hours appear similar	184
6.6	Single positive pro-IL-1 β cells increase upon Dicer KD	188
6.7	pro-IL-1 β levels increase per cell upon Dicer knock down	190
6.8	TNF levels are affected at low dose of LPS upon knocking down Dicer . . .	191
6.9	Dicer knock down populations have higher median IL-6 staining at high doses of LPS	195
6.10	Dicer knock down decreases NOS2 levels in the population	195
6.11	Dicer knock down affects the cell-to-cell variability of proteins	197
6.12	<i>In-silico</i> cell states are sensitive to Dicer knockdown	202
6.13	Discussion	205
6.13.1	Conclusions	205
6.13.2	Dicer knock-down alters sub-population frequencies	206
6.13.3	Protein expression	207
6.13.4	Cell-to-cell variability	208
6.13.5	Summary and Future work	209
7	Discussion	211
7.1	Summary	211
7.1.1	Integration of mathematical modelling to experimental approaches in studying heterogeneity	213

7.1.2	Innate immune responses are community-led	214
7.1.3	Twice-challenged communities do not change in composition in response to LPS	216
7.1.4	MiRNAs can fine-tune expression but also community composition	217
7.1.5	Conclusion	219
8	Appendix	221
	References	229

List of Tables

2.1	Antibodies used for flow cytometry	50
2.2	Antibodies used for western blotting	55
2.3	crRNAs used for Edit-R Dharmacon transient transfection of Cas9 nuclease plasmids.	57
8.1	TargetScan search for miRNAs targeting mouse IL-1 β mRNA	226
8.2	TargetScan search for miRNAs targeting mouse NOS2 mRNA	226

List of Figures

1.1	Bi-phasic NF-κB activation due to TLR4 endocytosis	8
1.2	Hyporesponsive cytokine expression upon a second LPS exposure	18
1.3	Secreted TNF, IL-1β and IFN-β provide additional stimulus to the LPS response	26
1.4	Sources of population heterogeneity in macrophages responding to antigen (LPS)	28
1.5	microRNA biogenesis and mode of action	31
1.6	miRNA regulated inflammatory response and contribution to population heterogeneity	36
2.1	LPS stimulus protocol	46
2.2	LPS induced hypo-responsiveness protocol	47
2.3	Brefeldin A incubation for intra-cellular staining	49
2.4	TNF, IL-6, NOS2 positivity fractions as determined by respective isotype controls	51
3.1	RAW264.7 cells produce TNF, IL-6 and nitric oxide upon stimulation with LPS	64
3.2	Single cell staining reveals distinct kinetics for TNF and NOS2	66
3.3	Heterogeneous population response titrates to LPS dose	69
3.4	Visualising heterogeneous response as a community of sub-populations	72
3.5	Visualising LPS stimulated RAW264.7 cells reveal heterogeneous communities	74

3.6	LPS induced communities show inter-experimental variability	77
3.7	LPS induced communities are variable but underlying patterns are consistent	79
3.8	Low and high LPS doses and inflammatory perpetrators cluster by unbiased approaches	81
3.9	TLR4 expression distribution and cell-size effects are negligible in stimulated RAW264.7 cells.	83
3.10	Restricting secretion of signalling proteins can give visual insights on community composition	87
3.11	Community composition complexity is increased on adding another cytokine	89
3.12	LPS stimulated RAW264.7 macrophages show weak to no correlation to those that have their secretion restricted for longer than 8 hours.	91
3.13	LPS stimulated RAW264.7 macrophages with secretion restricted for lesser than 8 hours are show separation with LPS dose	92
3.14	Cells stimulated in isolation and allowed to secrete make communities that are similar to secretion restricted (>8hr) communities	94
3.15	Anti-TNF neutralising antibody suppresses IL-6, NOS2 and IL12p40 mRNA up to 20%.	96
3.16	Neutralising TNF increases the number of late phase TNF producing cells	97
3.17	Surface expression of F4/80 shows distinct populations in thioglycollate-elicited peritoneal macrophages	99
3.18	F4/80 expression is more uniform upon <i>in vitro</i> culture of peritoneal macrophages	100
3.19	Thioglycollate-elicited peritoneal macrophages for heterogeneous communities and are affected secretion restriction	102
4.1	Re-stimulated RAW264.7 cells are hypo-responsive	113

4.2	Hypo-responsive communities appear more pro-inflammatory at 16 and 24 hours	116
4.3	Hypo-responsive communities are more consistent in their response in the first 8 hours	120
4.4	Prolonged restriction of secretion is associated with more modest changes in cells stimulated twice with LPS compared to cells stimulated once	122
5.1	Gillespie model average represents the ODE solution and both are true to the analytical solution	133
5.2	Positive-state model description and output when there is no LPS in the environment	137
5.3	LPS dose affects the rise and fall of positive cells differentially	138
5.4	Two temporally separated LPS doses induces similar response from <i>in silico</i> cells.	140
5.5	nr model description	142
5.6	nr model example output	143
5.7	Parameters estimation for TNF+ dataset reveal average α values greater than the other parameters	146
5.8	Peak TNF positive proportion decreases at second stimulus	148
5.9	Non-responding TNF population increases with first and second dose.	150
5.10	IL-6 positive cells do not peak as high upon second dose of LPS	153
5.11	pro-IL-1 β non-responsive cells increase steadily to 30% at 48 hours	154
5.12	NOS2 non-responding populations comprise just 8% after first LPS dose	156
5.13	Non-responding states vary for each protein	158
5.14	8 sub-population of the community as represented on the vertices of the cube model	161
5.15	Parameter estimation of cube model based on empirical dataset	165

5.16	Parameter estimates for cube model (8/12hr secretion) show little to no correlation between them.	166
5.17	Parameter estimation of cube model based on empirical dataset	168
5.18	Parameter estimates for cube model (restricted secretion) show little correlation between them	169
6.1	Dicer knock down in RAW264.7 cells	180
6.2	Dicer knock-down RAW264.7 cells are hypo-responsive	180
6.3	Dicer knock-down have an effect on triple positive and negative sub-populations	183
6.4	Hyporesponsive communities change little between NTC and siDicer groups	186
6.5	Community compositions NTC and untransfected communities differ by LPS dose while hypo-responsive communities differ little.	187
6.6	Dicer knock down increases pro-IL-1 β positive cells	189
6.7	pro-IL-1 β shows positive fold change when compared to non-transfected controls.	193
6.8	Dicer knock-down has subtle effects on TNF but profound effects on pro-IL-1 β expression	194
6.9	Dicer knock down decreases NOS2 levels in the population while IL-6 levels remain unaffected	196
6.10	NOS2 fluorescence intensity shows negative fold change when compared to non-transfected controls.	198
6.11	Dicer knock affects the cell-to-cell variability of pro-IL-1 β and NOS2 . . .	200
6.12	Dicer knock does not affects the cell-to-cell variability of TNF and IL-6 .	201
6.13	<i>In-silico</i> cell states are sensitive to Dicer knockdown	204
8.1	Triple positive cells and TNF- double positive cells correlate and may constitute similar populations	222

8.2	IL-1β is secreted upon two doses of LPS in RAW264.7 cells	223
8.3	TNF, pro-IL-1β and GM-CSF communities appear to change in composition on restricting secretion	224
8.4	Single positive pro-IL-1β have distinct expression profiles and are low producers	225

Acknowledgements

...None of the work done in this thesis would have been possible without the kindness, patience and remarkable tolerance shown towards me by my supervisors, *Dr Dimitris Lagos* and *Dr Jon Pitchford*. Their knowledge, helpfulness, criticism and carefulness towards Science will continue to inspire me.

I am sincerely grateful to:

Dr Dan Jeffares for his supervision, mentorship and criticism during my Masters which inspired me to pursue an interdisciplinary PhD degree.

Dr James Hewitson for always helping me understand Immunology and for his guidance in the wet lab.

Dr Jamie Wood and *Dr Marika Kullberg* for their thoughtful insights and criticisms that helped me shape this thesis. A further thanks to Jamie for pointing out that equation 5.11 can be solved exactly.

To all the incredible scientists at the Bioscience Technology Facility, University of York who were always available for help, guidance and support.

To my degree cohort and fellow students *Helen, Rosie, Steve* and *Karinna* for the intellectual discussions and lunch breaks.

Dan, Dhara, Akshay, Dani, Christina, Sami, Stalo, Arka, Gaurav, Ruchi, Nimit for their friendship and visits to York to distract me.

My aunt *Sanjukta* and uncle *Sujit* who have encouraged and motivated me throughout the last four years.

My parents *Shyamal* and *Sutapa* for their unwavering confidence and love that has kept me going.

And *Nidhi* for her support and for being the reason I could take the step to return to academia which has given me great joy and satisfaction.

Declaration of Authorship

I, Shoumit Dey, declare that this thesis and the work presented in it are my own. I confirm that this thesis has not been previously presented at University of York or elsewhere for a degree or award. Work presented in this thesis is a result of my own research and any work mentioned in this thesis, that is not my own, has been explicitly referenced.

Signed:

Date:

Chapter 1

Introduction

1.1 Pathogens and innate immunity

The environment that we live in contains a plethora of pathogenic microbes and toxic substances; in order to survive, all animals must defend against the attack of these disease causing agents by recognising them as foreign and mounting an immune response (Chaplin, 2010).

In a typical infection, the immune response is classified into an innate response that is fast and broad acting, and adaptive mechanism which is highly specific to a pathogen (Janeway et al., 2001). The two responses are distinct in terms of specificity but are closely interconnected and are carefully orchestrated by specialised immune cells. In a simplified narrative, a pathogen (which can be bacteria, fungus or virus) must first traverse through the epithelial layer (first line of defence) which typically involves tissue damage that leads to damage signalling, activation of tissue-resident macrophages, and recruitment of neutrophils and monocytes which respond to the presence of the pathogen by phagocytosis and secretion of specialised proteins such as cytokines to signal other cells involved in the immune system (Turner et al., 2014) in an autocrine (self acting), paracrine (acting nearby) and endocrine (far acting) manner to initiate and propagate an immune response (Chaplin, 2010).

Professional antigen presenting cells (APCs) such as dendritic cells present peptides derived from the pathogen (antigens) to T cells. This event either triggers T-cell mediated killing by cluster of differentiation (CD) molecule 8+ (CD8+) T-cytotoxic cells that recognise the antigen and/or leads to the generation of memory B cells (mediated by CD4+ T-helper cells) that can facilitate the recognition of this antigen in a future infection. In this way, the adaptive immune system can mount a much stronger and specific response to that particular pathogen in a future encounter (Chaplin, 2010).

As a broad acting, non-specific arm of the immune system, innate immunity encounters the pathogen first, promotes inflammation, contains the infection and shapes the adaptive response. However, innate immune cells such as macrophages are also key in resolution of inflammation and tissue repair, not just initiation (Zhang and Mosser, 2008) as discussed in the sections ahead.

1.1.1 Macrophages and their role in immunity

The word macrophage in Greek means 'big eater' and true to their name these large cells phagocytose pathogens and dead cells upon encounter. Macrophages belong to a group of cells called leukocytes that include cells like neutrophils, eosinophils, basophils, megakaryocytes and monocytes derived from a common parent cell, the common myeloid progenitor. Macrophages are ubiquitous and found in almost all organs and tissues most of which are derived from embryonic progenitor populations such as the yolk-sac or foetal liver while some originate from the adult bone marrow. Macrophages derived from the bone marrow are, usually, monocytes that circulate in the blood as a patrolling population that are recruited to tissues upon infection or wound healing. This activates the monocytes to differentiate into monocyte-derived macrophages and dendritic cells which, in addition, to fighting the infection can replenish the resident-tissue macrophage population.

Most of the tissue-resident macrophages are of yolk-sac or foetal liver origin and are long-term residents that specialise considerably depending on the tissues they live in. While tissue-resident macrophages are self-persisting populations that can stay lifelong in some tissues, monocytes on the other hand have a short life-span and are replenished constantly by the haematopoietic stem cells in the bone marrow (Wynn, Chawla, and Pollard, 2013; Zhao et al., 2018).

Upon tissue injury or infection, resident macrophages recognise pathogen associated molecular patterns (PAMP) that are specific to pathogens or damage associated molecular patterns (DAMP) by specialised receptors such as pattern recognition receptors (or PRRs) and become activated. Activation leads to an enhanced ability of macrophages to phagocytose and, also, shape the ensuing inflammatory response by secreting small signalling proteins called cytokines and chemokines (CHEMOtactic cytoKINES) that can direct nearby macrophages to respond and even recruit neutrophils and monocytes (Bianchi, 2007; Mogensen, 2009).

The role of macrophages, however, is not limited to promoting inflammation. After an early inflammatory phase, macrophages assume a wound-resolving phenotype by producing growth factors (Shimokado et al., 1985; Willenborg et al., 2012; Rappolee et al., 1988; Chujo et al., 2009; Berse et al., 1992) like TGF- β that promote cell proliferation, wound healing and synthesis of extracellular-matrix components (Murray and Wynn, 2011). Next, assuming a more anti-inflammatory phenotype, these macrophages secrete interleukin-10 (IL-10), inhibitory factors like TGF- β and express cell surface receptors programmed cell death ligands 1 and 2 (PD-L1 and PD-L2) to dampen the immune response, which if left unchecked can cause cellular death and delay in tissue repair (Khalil et al., 1989; Said et al., 2010; Shouval et al., 2014; Zigmond et al., 2014). Recent research indicates that distinct macrophage and monocyte populations are involved in different stages of inflammation, repair and resolution (Gundra et al., 2014; Vannella

et al., 2014). It is, however, unknown whether an individual macrophage can adopt all these characteristics of being inflammatory, wound healing or anti-inflammatory at different times taking cues from the local tissue micro-environment or whether distinct functional macrophage and monocyte subsets are responsible to regulate these different activities (Wynn and Vannella, 2016).

Traditionally, macrophage response, as described above, has been either classical macrophage (M1) response which leads to the production of inflammatory cytokines such as tumour necrosis factor (TNF) and interleukins such as IL-6, IL-1 β etc or as M2 (alternatively activated) described as a more wound healing and repair oriented phenotype secreting the anti-inflammatory cytokine IL-10, growth factor TGF- β and Arg1. In recent years, this dichotomy has been challenged and macrophage response is considered highly dependent on the activating stimulus and that M1 and M2 responses are two extremes of an extensive spectrum of responses (Martinez and Gordon, 2014). A transcriptomic study in human macrophages experimentally showed the existence of a spectrum of phenotypes, and thus, expanding the M1 and M2 phenotypes to a range of activation profiles (Xue et al., 2014). Judith Allen and colleagues have since suggested a naming convention for macrophage phenotypes based on how they are activated. As an example, macrophages that are activated by lipopolysaccharide (LPS) treatment can be named as M(LPS) as per this nomenclature method (Murray et al., 2014). This understanding expands the phenotypic repertoire of macrophages and describes the heterogeneity of macrophage response in greater detail.

1.1.2 Pathogen recognition by innate immune cells

Macrophages recognise PAMPs from bacteria, fungus and viruses. PAMPs are recognised by PRRs that are either cellular membrane-bound PRRs (such as Toll-like Receptors and C-type Lectin Receptors) or cytoplasmic PRRs (RIG-1-like Receptors and NOD-like Receptors). Toll-like Receptors (or TLRs) are key immunological mediators of

response to a pathogenic encounter. There are 10 TLRs in humans (TLR1-10) and 12 in mice (TLR1-9; 11-13) each specialised to recognise non-self ligands from a variety of PAMP sources such as bacteria, fungus, protozoa, and viruses (Mogensen, 2009; Takeda and Akira, 2004).

Some TLRs recognize more than one type of pathogen. For example, TLR4, that recognises LPS from most gram-negative bacteria as well as glycoinositol phospholipids from protozoa and envelope glycoproteins from viruses. Similarly, TLR2, another toll-like receptor, can recognise zymosan from fungi, peptidoglycan from bacteria, GPI-mucin from protozoa and envelope glycoproteins from viruses (Yoshimura et al., 1999; Schwandner et al., 1999; Mogensen and Paludan, 2005). TLRs are not always surface-bound but can be cytoplasmic in location such as TLR3 that recognises double-stranded RNA from viruses (Liu et al., 2008).

Upon binding a TLR agonist, macrophages go through a signalling cascade via the TLR/agonist pathway that induces the translocation of inflammation-associated transcription factors such as NF- κ B, activating protein 1 (AP1) and interferon regulatory factors (IRFs) leading to transcription of pro-inflammatory cytokines like TNF, IL-6, IL-1 β and IL-12, type 1 interferon and chemokines (Zhang and Ghosh, 2001; Medzhitov, 2001; Takeda and Akira, 2004).

1.1.2.1 LPS as a PAMP

LPS, also referred to as endotoxin, is a large molecule found on the outer membrane of the cell wall of gram-negative bacteria and is an important PAMP recognised uniquely by TLR4 (Hoshino et al., 1999; Poltorak et al., 1998). Structurally, LPS comprises of a hydrophobic Lipid A and a hydrophilic polysaccharide chain which consists of an inner core, outer core and an O-antigen. The O-antigen is a highly variable unit in terms of number of repeating oligosaccharides. Gram-negative bacterial species are often

sub-classified into serovars to describe within species variation based on the O-antigen structure and has been shown to describe the virulence of a particular serovar. However, the main PAMP component of LPS for TLR based inflammatory signalling is the lipid A core. This component can contain different number of acylation chains which can show inter-species variability. Six acylated chains and diphosphorylation of Lipid A core in *Escherichia coli* have shown to elucidate a standard TLR4 response. Bacteria such as *Yersinia* spp. with fewer than six acyl chains in the Lipid A core of their LPS tend to have a dampened LPS/TLR4 inflammatory response (Montminy et al., 2006). *Francisella tularensis*, a human pathogen, shows an inability to elicit a TLR response and, thus, is able to escape the innate response. The Lipid A core of *Francisella* LPS is hypo-acylated and monophosphorylated (Tan et al., 2015). Thus, Lipid A core serves as the primary source of PAMP and pathogens modifying this core component have been shown to escape/alter the immune response (reviewed by Rosadini and Kagan, 2017).

1.1.2.2 TLR4 as a PRR

TLR4 receptors are expressed by a range of cells including monocytes, macrophages, myeloid-derived dendritic cells and microglia. LPS binds to TLR4 to elicit an inflammatory response in cells expressing TLR4. LPS binding to TLR4 is a complex process and requires several accessory proteins like LPS binding protein (LBP), cluster of differentiation molecule 14 (CD14) and MD2 (Lymphocyte antigen 96) (Wright et al., 1989; Wright et al., 1990; Shimazu et al., 1999). LBP which binds monomeric LPS molecules, can then bind to CD14 which then delivers LPS to a complex of TLR4/MD2 (Park and Lee, 2013). It has been shown, using surface plasmon resonance (SPR), that LPS binds to recombinant TLR4, CD14 and MD2 separately in that order of increasing affinity. This not only suggests that CD14 can transfer LPS to MD2 but also that LPS can bind directly to TLR4 or MD2 (Shin et al., 2007).

TLR4/MD2 complex upon binding to LPS, homodimerises leading to structural changes that bring the two intracellular Toll/IL-1 receptor (TIR) domains in close proximity. This then recruits TIR-domain containing adaptor proteins TIRAP (TIR domain containing adaptor protein) and TRAM (TRIF-related adaptor molecule) which then engages MyD88 (Myeloid Differentiation primary response gene 88) and TRIF (TIR domain containing adaptor inducing IFN- β) respectively (Horng, Barton, and Medzhitov, 2001; Fitzgerald et al., 2003).

The TLR4/MD2 signal transduction can proceed by the MyD88-dependent pathway and lead to the formation of a complex consisting of MyD88 and IL-1 receptor associated kinase 1,2,4 (IRAK1, IRAK2 and IRAK4) known as myddosome (Lin, Lo, and Wu, 2010). The myddosome activates TNF receptor-associated factor 6 (TRAF6) which further activates transforming growth factor- β -activated kinase 1 (TAK1) that activates the nuclear factor kappa-light-chain-enhancer of activated B cells (NF- κ B) and the mitogen activated protein kinase (MAPK) switching on inflammatory gene expression (Chen et al., 2001).

Alternatively, signal transduction from LPS binding can proceed via the MyD88-independent pathway or TRIF-dependent response as the LPS-bound TLR4 is endocytosed (??) by the macrophage (Kagan et al., 2008). TRIF-dependent pathway then activates the NF- κ B pathway and inducing interferon genes by activating the transcription factor Interferon Regulatory Factor 3 (IRF3). While activating IRF3-dependent interferon- β genes (Doyle et al., 2002), the MyD88 independent response also provides a second wave of translocation of NF- κ B to the nucleus, further activating pro-inflammatory genes (Yamamoto, Sato, and Hemmi, 2003).

Inflammatory responses that are TLR4 induced can be severe and cause a septic shock mediated by an overwhelming immune response that can lead to organ damage,

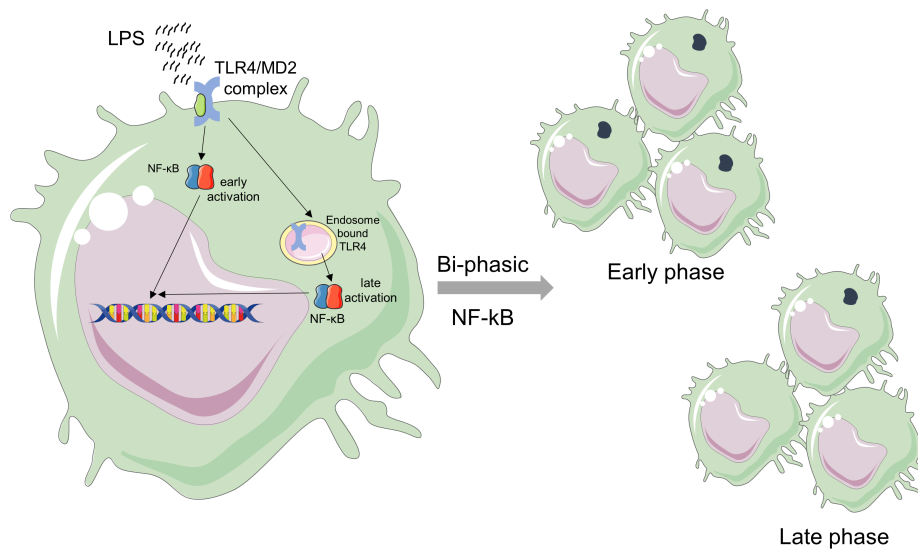


FIGURE 1.1: **Bi-phasic NF- κ B activation due to TLR4 endocytosis**

Transcription factor NF- κ B induction/translocation occurs by the downstream signalling of the TLR4/MD2 binding of bacterial LPS leading to the transcription of an early phase of protein expression. As the TLR4 receptor is endocytosed by the cell this leads to a second wave of late-phase NF- κ B activation.

thus, requiring the TLR4 pathway-induced gene expression to be tightly regulated. Indeed, TLR4 pathway is regulated at multiple levels starting at the top with radio protective 105 (RP105), a homolog of TLR4. RP105 complexes with MD1, a homolog of MD2, and then interacts with the TLR4/MD2 complex inhibiting the association of LPS (Divanovic et al., 2005). Downstream of the TLR4/LPS signalling there are many other proteins such as MyD88s (Janssens et al., 2003), IRAK-M (Kobayashi et al., 2002), A20 (Boone et al., 2004), TRAF1 (Su et al., 2006) that can inhibit MyD88, IRAKs, TRAF6, TRIF respectively, thus, regulating proteins of both the MyD88 dependent and independent pathway of TLR4/LPS response.

1.2 Regulation of inflammation by cytokines and inflammatory mediators

An efficient immune response is orchestrated by small secretory proteins and molecules that can act on cells producing them, nearby cells or by recruiting cells from blood vessels while facilitating movement by increasing vascular permeability. Innate immune cells can efficiently communicate with a variety of professional immune cells and other cells expressing cytokine receptors by secreting cytokines and by chemokines to encourage chemotaxis. In addition, growth factors and inorganic molecules such as nitric oxide (reviewed by Sharma, Al-Omran, and Parvathy, 2007) and reactive oxygen species (reviewed by Mittal et al., 2014) have important microbicidal and inflammatory roles.

Cytokines including chemokines and other mediators are able to influence a variety of immune cells and can also be redundant in their activity with different cytokines performing a similar function. The crude overall functions of this type of regulation is to effect either a pro-inflammatory or anti-inflammatory response (reviewed by Jun-Ming and An, 2007). TNF, IL-1 β , IL-6, IL-8, IL-18, nitric oxide are central to inflammatory action of innate immune response, and are expressed by numerous cell types and are

involved in a wide variety of biological activities, immune responses like cytokine production, chemotaxis, proliferation, survival and have pathological role in various diseases. A balance between such an inflammatory cocktail flowing around the site of infection (or systemically) and anti-inflammatory signals such as TGF- β , IL-10, IL-4, IL-13, eventually, leads to the resolution of inflammation (Turner et al., 2014; Dinarello, 2018; Hunter and Jones, 2015; Kalliolias and Ivashkiv, 2016; Sharma, Al-Omran, and Parvathy, 2007; Couper, Blount, and Riley, 2008). This balance is critical and, as an example, the ratio of IL-10 to TNF has been shown to be higher in non-survivors of systemic infections like sepsis compared to survivors (Gogos et al., 2002).

1.2.1 TNF

TNF is one of the most important secreted small protein that can shape the immune response by inducing inflammation, apoptosis or necroptosis. Many inflammation-led chronic conditions like rheumatoid arthritis (RA), inflammatory bowel disease (IBD), psoriasis etc are approved to be treated using commercially available TNF targeting neutralisation antibodies to reduce inflammation (Bradley, 2008; Kalliolias and Ivashkiv, 2016).

Tnf gene is a single-copy gene encoded in the 6th and 17th chromosome in humans and mouse genome respectively. TNF expression is regulated by the transcription factors NF- κ B and nuclear factor activated T-cells (NFAT). TNF is expressed as a transmembrane (27 kDa) protein (Kriegler et al., 1988) that can be proteolytically cleaved by the metalloprotease ADAM Metallopeptidase Domain 17 (ADAM17) also known as TNF Converting Enzyme (TACE) as shown by Bell et al., 2007.

TNF signals via TNF receptor 1 (TNFR1) and TNF receptor 2 (TNFR2) that are expressed on self or other (Hsu, Xiong, and Goeddel, 1995; Rothe et al., 1995). While TNFR1 is found to be expressed in almost all cells, TNFR2 is expressed more exclusively

on neurons, immune cells and endothelial cells (Yang et al., 2018).

The soluble form of the protein (17kDa) and the transmembrane TNF can bind to TNFR1 while only the transmembrane form can bind to TNFR2 (Grell et al., 1995). TNFR signalling based on the two receptors have been proposed to either promote inflammation (Waetzig et al., 2004) and tissue degeneration via TNFR1 route or tissue survival and regeneration via TNFR2 signalling (Fischer et al., 2011; Fischer et al., 2014).

Homotrimeric TNFR1 accepts homotrimers of TNF as ligand resulting in the recruitment of the TNFR1 associated death domain (TRADD) protein that then progresses through four possible pathways mediated either by a complex I or complex IIa, IIb and IIc. Complex I formation leads to the activation of NF- κ B and MAPKs while complex IIa and IIb progresses with the cysteine-aspartic protease Caspase-8 dependent cellular apoptosis (Micheau and Tschopp, 2003). Complex IIc, also known as the necrosome, directs the cell towards necroptotic pathway by activating mixed lineage kinase domain-like protein or MLKL (Degterev et al., 2005). TNFR1 signalling, thus, leads to a cellular decision of whether to initiate an inflammatory response or induce cellular death. Although not clearly understood, current understanding suggests that the abundance of anti-apoptosis protein such as cellular FLICE-inhibitory protein (c-FLIP_L) that binds to Caspase-8 to block the apoptotic signal may be crucial in determining which pathway is switched on (Micheau et al., 2001). Similarly, it has been shown, in mice, the deubiquitinating protein A20 can restrict the ubiquitination of Receptor-interacting serine/threonine-protein kinase 3 (RIPK3) that promotes the necrosome (complex IIc of TNFR1 pathway) formation and, in that way, stop the cell from undergoing necroptosis (Onizawa et al., 2015). The above mechanisms indicate ways in which the decision to switch on complex I-mediated TNFR1 pathway is selected and, thereby, leading to cell survival.

Cells of the myeloid lineage such as macrophages are the major producers of TNF and it is one of the early response cytokine secreted upon TLR4/LPS signal transduction.

1.2.2 IL-6

IL-6 is an important pro-inflammatory cytokine that can affect cells locally and systemically. IL-6 has been known by a variety of names such as B cell stimulatory factor 2 (BSF-2), interferon β 2, hepatocyte stimulating factor (HSF) until the discovery that all those proteins were, in fact, the same protein. As the old names suggest, IL-6 can differentiate B-cells into antibody producing cells, induce antiviral effects and upon reaching liver activate the production of acute-phase proteins exemplifying the diversity of its actions. One of the important inflammatory effects of IL-6 is to promote infiltration of neutrophils and, subsequently, of monocytes and T-lymphocytes. Monoclonal antibodies targeting the IL-6 receptor (IL-6R) have been used clinically to treat inflammatory arthritis suggesting its importance in inflammation-led diseases (Tanaka, Narazaki, and Kishimoto, 2014)

IL-6 is a 21-28 kDa glycosylated protein that is encoded in the 5th and 7th chromosome in mouse and human genome respectively. It is produced in response to PAMPS, TNF and IL-1 β by almost all immune and stromal cells. IL-6 signalling requires two receptors, IL-6 receptor (IL-6R) and glycoprotein 130 (gp130). IL-6 receptors are either membrane-bound (mIL-6R) or soluble (sIL-6R) and, similarly, membrane-bound gp130 and a soluble gp130 (sgp130) is also known (Yamasaki et al., 1988; Hibi et al., 1990; Novick et al., 1989). IL-6 induced signal transduction occurs through IL-6R and glycoprotein 130 (gp130) via classical and trans-signalling.

In classical signalling, IL-6 binds to mIL-6R and gp130 forming a hexamer (2 molecules of each, Skiniotis et al., 2005) or a tetramer (with 2 gp130 molecules, Murakami et al., 1993) and this requires the need for both IL-6R and gp130 to be

expressed as transmembrane proteins which only occurs in leukocytes, megakaryocytes and hepatocytes. Thus, classical signalling is limited only to a few type of cells. In contrast, trans-signalling occurs when sIL-6R binds to IL-6 and, then, binds to the membrane bound gp130 which is ubiquitously expressed in all cells. Trans-signalling has been shown to be associated with inflammation progression (Campbell et al., 2014; Jones et al., 2011).

As a regulatory mechanism, sgp130 can bind to sIL-6R and IL-6 to form a complex that blocks IL-6 trans-signalling (Narazaki et al., 1993). In order to show the effect of sgp130 induced trans-signalling blocking, transgenic mice that expressed the generated protein sgp130Fc (10-times more potent in inhibiting IL-6/IL-6R complex than sgp130) were used as a model of acute inflammation using the air pouch model. In comparison to wild-type mice the transgenics showed reduced recruitment of neutrophils and macrophages, thus, confirming the crucial role of IL-6 trans-signalling in inflammation progression (Chalaris et al., 2019).

The source of sIL-6R has been attributed to two independent mechanisms one of which involves the proteolytic cleavage of the membrane bound IL-6R through ADAM proteases. Human IL-6R are shed by ADAM10 and ADAM17 whereas in mice ADAM10 helps shed the receptor (Garbers et al., 2011). The second mechanism proposed as a source for sIL-6R utilises alternative splicing of the receptor without the transmembrane domain (Csilla Holub et al., 1999).

In both types of IL-6 signalling, gp130 bound to IL-6/IL-6R complex activates janus kinases 1 and 2 (JAK1, JAK2), tyrosine kinase (Tyk2), signal transducer and activator of transcription 1 and 3 (STAT1, STAT3) and the mitogen-activated protein kinase (MAPK) cascade (Murakami et al., 1993; Heinrich et al., 2003). STAT1, STAT3 mediated inflammation is tightly regulated by suppressors of cytokine signalling 3 or SOCS3

(Crocker et al., 2003), and absence of SOCS3 has been associated with IL-6 mediated induction of anti-inflammatory response by suppression of the pro-inflammatory TNF and IL-12 (Yasukawa et al., 2003).

1.2.3 NOS2 and nitric oxide

Nitric oxide synthases (NOS) are a group of enzymes that catalyse the formation of citrulline and nitric oxide (NO) from L-arginine at the expense of NADPH and oxygen. There are three known isoforms, NOS1 (neuronalNOS) and NOS3 (endothelialNOS) are constitutively expressed genes whereas NOS2 (inducibleNOS) is only induced upon LPS or cytokine stimulation. Nitric oxide levels (measured as nitrates) are highly enhanced in diseases like RA, osteoarthritis (OA) and ankylosing spondylitis establishing its critical role in inflammatory conditions (Sharma, Al-Omran, and Parvathy, 2007; Bogdan, 2015).

Nos2 gene is encoded by the 7th and 11th chromosome in humans and mouse respectively and remains completely silent until induced by a immune signal/stimulus in a calcium independent manner. In mice, NOS2, a 130 kDA protein, is expressed by macrophages stimulated by LPS, IFN- γ , IL-1 β , IL-6 and TNF (Kleinert et al., 2004). The transcription factors associated with these stimuli such as IRF-1, a complex of STAT1, STAT2 and IRF-9 known as the interferon-stimulated gamma factor (ISGF3) and NF- κ B have all been shown to interact with the *Nos2* promoter. *Nos2* transcription has been shown to require a sequential association of transcription factors. NF- κ B binding to the *Nos2* promoter leads to the general transcription factor II human (TFIIH; also found in mice) being recruited. TFIIH remains bound to the site even after NF- κ B is no longer associated where it awaits the arrival of a RNA Polymerase II that is recruited by ISGF3. Upon arrival, TFIIH phosphorylates the polymerase to begin transcription, thereby, creating a factor-recruitment model that fires only after NF- κ B and the IFN induced signal are both detected (Farlik et al., 2010).

Regulation of nitric oxide production by NOS2 is also affected by other metabolic and environmental states such as hypoxia. Limited availability of oxygen in hypoxia is required for NOS2-mediated NO catalysis. Further, under hypoxic conditions NOS2 is unable to attach to the actin cytoskeleton (mediated by α -actinin 4) which is a precondition for NOS2 activity. Other factors include the osmolarity of the inflammatory environment, it was shown that nitric oxide production is enhanced when concentration of Na⁺ is higher (Jantsch et al., 2015).

Nitric oxide is a highly potent pro-inflammatory molecule that can act as an autocrine/paracrine mediator due to its lipid solubility and, therefore, easy permeability across the cell membrane. However, the biological lifetime of nitric oxide is short (six seconds) which restricts its actions spatially and temporally. The mode of action of nitric oxide ranges from direct bactericidal/static effects by hindering growth in *E. coli* and *L. monocytogenes* (Liew et al., 1990) and in conjunction with other molecules to form S-nitrosothiols, superoxide anions, tyrosine nitrates etc.

1.2.4 IL-1 β

IL-1 β is an acute phase cytokine that has a role similar to TNF and can induce the production of TNF and IL-6 in macrophages. It can cause systemic changes by inducing fever upon reaching the hypothalamus and initiating acute phase proteins in the liver. Excessive IL-1 β production has been associated with many autoinflammatory diseases like the heritable Mediterranean Fever that causes fever and inflammation of the peritoneum, Muckle-Wells syndrome whose symptoms include periodic fever and urticaria, neonatal-onset multi system inflammatory disorder (NOMID) that causes persistent inflammation, particularly affecting the nervous system. All these diseases can be successfully treated with targeted therapy towards IL-1 β (Guo, Callaway, and Ting, 2015).

Mature IL-1 β is a 17.5 kDa protein that is encoded in chromosome 2 of the human and mouse genome. LPS induced activation of *Il1b* gene is under the control of the transcription factor NF- κ B (Hiscott et al., 1993) like TNF but can also be induced during glycolysis inhibition by hypoxia inducible factor or HIF-1 α (Tannahill et al., 2013). Upon transcription, IL-1 β is first translated into a pro-form of the protein which is 31 kDa and is inactive. The bioactive form of Pro-IL-1 β is dependent on the activation of the interleukin converting enzyme (ICE1) also known as caspase-1 that can proteolytically cleave pro-IL-1 β . Caspase-1 is under the control of a protein complex termed as the inflammasome. Inflammasomes are complexes of multiple proteins that assemble in the cytoplasmic matrix upon sensing PAMPs or DAMPs that regulate the activation of caspase-1. The inflammasome is named after the scaffolding protein involved in the complex formation. A Nod-like receptor (NLR), NLRP3 forms an inflammasome that is activated in response to many stimulus and must be primed by the binding of LPS to TLR4 (Guo, Callaway, and Ting, 2015). Following this step, a second priming like ATP can induce the inflammasome to make mature caspase-1 that can then lead to the formation of active IL-1 β from its pro-form. Thus, mature IL-1 β is not produced just by the stimulus provided by LPS and requires a second stimulus for the activation of caspase-1 in order for IL-1 β to be released (Netea et al., 2009; Xie et al., 2014).

After the immune response has been initiated, inflammasome is deactivated by T cell derived IFN- γ and other type I IFN, CD40L, miR-223 (reviewed by Latz, Xiao, and Stutz, 2013) and feedback loop on the duration of caspase-1 activity (Boucher et al., 2018). IL-1 β signalling is mediated by interleukin 1 receptors, IL-1R1 and IL-1R2 of which the former binds to IL-1 β resulting in the formation of an IL-1R1/IL-1R3 (IL-1 receptor 3) complex. IL-1R1/IL-1R3 complex both have an intracellular TIR domain that dimerise to attract MyD88 proteins (Muzio et al., 1997; Medzhitov et al., 1998; Burns et al., 1998). The death domain of MyD88 further recruits IRAK4 and then IRAK1. Hyperphosphorylated IRAK1 then recruits TRAF6, TAK1 leading to the degradation of IKK leading to NF- κ B

translocation to the nucleus (reviewed by Bent et al., 2018).

IL-1R2, on the other hand, is a decoy receptor and IL-1 β binding to the receptor does not take part in any signalling further and, therefore, blocks IL-1 β signalling cascade (Colotta et al., 1993). IL-1 β can also be blocked by the secreted soluble IL-1 receptor agonist (IL-1Ra) that can compete against IL-1R1 (Arend et al., 1998) while it does not bind to the decoy receptor IL-1R2.

1.2.5 Cytokine response upon a second LPS exposure

The adaptive immune cells exhibit immunological memory owing to the capability of T and B cells to act in an antigen specific manner. In contrast, the innate immune cells are better known for an immediate response to a broader spectrum of pathogens. In recent years, it has been proposed that innate cells can respond based on a previous stimulation with an antigen (Netea et al., 2016).

Macrophages stimulated with TLR agonists have been shown to be hypo-responsive upon re-stimulation and elicit a reduced pro-inflammatory response (Carey FJ and Zalesky, 1957; Flohé et al., 1999). Macrophage hypo-responsiveness termed as tolerisation (Figure 1.2) has not only been associated with the down regulation of TLRs (Medvedev, Kopydlowski, and Vogel, 2000; Medvedev et al., 2002), but, it also involves extensive gene reprogramming with the activation of alternative anti-inflammatory pathways and many anti-microbial genes (Foster, Hargreaves, and Medzhitov, 2007; Biswas and Lopez-Collazo, 2009; Mages, Dietrich, and Lang, 2008).

It has been shown that LPS tolerance regulates two type of genes, the non-tolerisable that do not get suppressed upon LPS re-stimulus or those that are not hypo-responsive (Foster, Hargreaves, and Medzhitov, 2007). It was also shown in the same study that histone trimethylation (H3K4) induced at promoters when responding to LPS is no

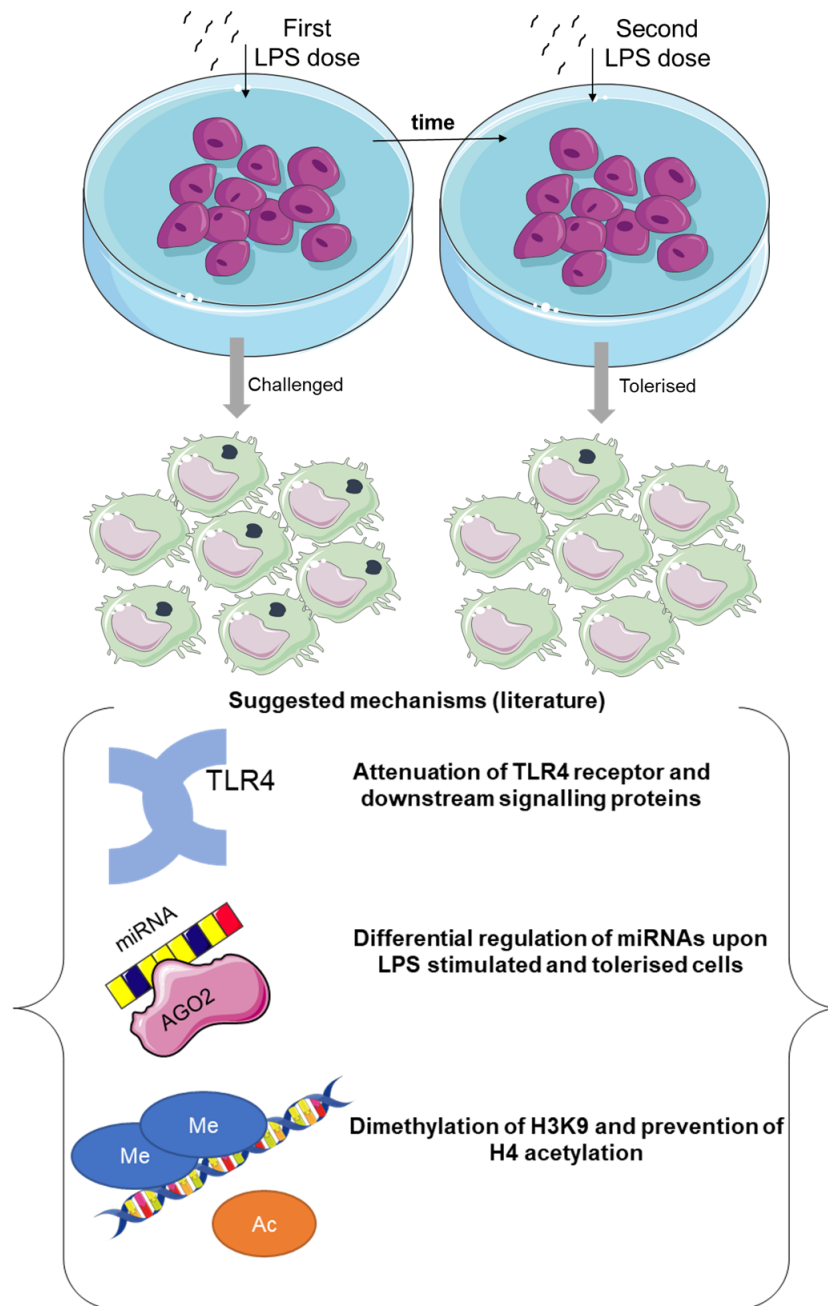


FIGURE 1.2: Hyporesponsive cytokine expression upon a second LPS exposure

Macrophages upon sensing LPS switch on a pro-inflammatory phase by producing cytokines that promote inflammation locally and systemically. However, a repeated dose (second LPS dose) renders them in a hypo-responsive state. Some of the molecular mechanisms that drive this are attributed to down-regulation of TLR4, miRNA-mediated regulation of inflammatory mediators and signalling proteins and by epigenetic regulation of tolerised genes such as methylation and deacetylation.

longer associated on secondary stimulus on genes like *Il6* (Foster, Hargreaves, and Medzhitov, 2007). *Tnf* and *Il1b* promoters are associated with H3K9 dimethylated histones to repress transcription in human monocyte-like THP1 cells. While these are remodelled at the first dose of LPS, they are also present in the secondary LPS stimulus, thus, conferring a tolerance or hypo-responsiveness (Chan et al., 2005; El Gazzar et al., 2007; Chen et al., 2009). A second layer of regulatory control is seen in the dependence of LPS-induced genes on the remodelling of the nucleosome by the SWI/SNF (SWItch/Sucrose NonFermentable) complex that seems to differentially affect LPS-induced genes. While *Tnf* is shown to be not dependent on the SWI/SNF remodelling induced expression, *Il6* and *Nos2* are dependent on this re-modelling (Ramirez-Carrozzi et al., 2006; Ramirez-Carrozzi et al., 2009). This suggests that LPS dose re-programs macrophages at the gene promoter level and, this describes an important molecular mechanism of LPS-induced tolerance or hyporesponsiveness (Seeley and Ghosh, 2017).

Antigen priming can have disparate consequences. Studies of vaccines in epidemiological studies showed that non-specific effects of certain vaccines like BCG protected the host from other diseases (Netea and Meer, 2017). This suggested an apparent protective effect of antigen-priming on innate cells. Upon secondary challenges, innate cells not only show a pronounced reduction in the pro-inflammatory response but also express anti-inflammatory cytokines like IL-10 and TGF β (Biswas and Lopez-Collazo, 2009). An overbearing immune response to wounds and infections often results in a serious life threatening condition known as sepsis. An abundance of pro-inflammatory cytokines released in sepsis leads to systemic inflammation. As the condition progresses the hyporesponsiveness, thus induced, creates an anti-inflammatory environment which has been related to higher incidences of secondary infections and death in clinical patients (Hotchkiss et al., 2009; Vught et al., 2016). As such, the innate immune system goes into a cycling of environments which can

rarely be ameliorated, highlighting the need to understand this hyporesponsive phenotype.

The above ascertains that tolerisation is a complex phenotypic change, and any heterogeneity associated with LPS tolerance or hypo-responsiveness may be an important area of focus to better understand a community of macrophages responding to repeated exposure to PAMPs.

1.3 Heterogeneity in macrophages

Macrophages are generally regarded as a heterogeneous cell population and this heterogeneity can be attributed to many factors such as their developmental-origin and maturation stages, tissue micro-environment and how they are activated. Here we discuss the heterogeneity associated with macrophages at an organ/tissue level, within tissue, and finally at level of antigen response.

1.3.1 Tissue and organ level heterogeneity

Macrophages can be thought of as a distributed organ-system that maintain homeostasis across the human body (reviewed here Gordon and Plüddemann, 2017). Although, their primary purpose may be to respond to infection, they don a variety of roles in the course of their long term development in the respective tissues. An early source of heterogeneity of macrophages is introduced based on their lineage that may be traced back to their developmental origin like yolk-sac progenitors, foetal liver progenitors or haemopoetic stem cells in the adult bone marrow.

Fate mapping analysis has shown that most tissue-resident macrophages are formed in the early embryo (Yona et al., 2013). These early macrophage progenitors also called erythromyeloid progenitors, are placed in tissues during organogenesis where they

persist into adult life eventually being termed tissue-resident macrophages. These are a self-persisting population, sometimes, for life. The heterogeneity of tissue-resident macrophages can be exemplified by the diverse functions that they are involved in. For example, microglia are a resident macrophage population of the central nervous system and apart from scavenging infectious organisms, are also able to interact with live and apoptotic neurons. Alveolar macrophages that serve on the frontline of alveolar-blood interface as a first line cellular defence against pathogens and particles also play an important role in surfactant metabolism. The surfactant reduces the breathing effort by lowering the surface tension at the alveolar epithelium which can lead to respiratory distress. Similarly, splenic red pulp macrophages have been shown to be distinct from monocyte-derived macrophages and can phagocytose IgG-opsonised red blood cells by activating Fc γ R receptors (Nagelkerke et al., 2018). The presence of such diverse tissue-resident macrophages were then shown to have unique gene expression by Gautier et al., 2012 between microglia, spleen, lung (alveolar) and peritoneal macrophages in mice and that such diversity due to the micro-environment may shape the chromatin landscape of these tissue-resident macrophages (Lavin et al., 2014).

1.3.2 Heterogeneity within tissue

While tissue-resident macrophages from different organs may be heterogeneous among themselves, resident population within a specific tissue is also known to be heterogeneous. Although self persisting, upon infection resident cells make cytokines and chemokines that attract neutrophils and monocytes patrolling the blood vessels encouraging them to extravasate into the infected tissue. This infiltration of monocytes and their subsequent differentiation into macrophages may increase/replace resident macrophages once the infection is resolved. Since these monocyte-derived macrophages are from a different lineage (derived from haemopoietic stem cell in the bone marrow) they introduce heterogeneity in the resident population. Kupffer cells that are known to be the largest resident macrophage population are often re-inforced by

monocyte-derived macrophages because the latter encounter PAMPs and DAMPs more often than other resident population due to their location in the liver. Previous research has shown that these monocyte-derived macrophages are easily distinguishable by the expression of the macrophage marker F4/80 levels. A general idea surrounding this is that embryonic origin macrophages self renew themselves whereas monocyte-derived macrophages cannot differentiate into a qualified resident population. Cardiac (Molawi et al., 2014) and intestinal macrophages (Bain et al., 2014) in mice, that are both of embryonic origin, self-renew slowly with age and stop after weaning respectively. Instead, monocyte-derived macrophages are recruited to replenish the resident population without renewal. Other studies have shown the opposite, where recruited monocyte-derived macrophages can gradually differentiate and adopt the transcription profile of a fully functional resident cell population as in the case of Kupffer cells in the liver (Scott et al., 2016).

Despite the presence of two models of replenishment of tissue-resident macrophages, considerable heterogeneity is introduced in the tissue micro-environment upon the recruitment of cells that become long-term residents either by being constantly replenished or by adopting the transcription profile of the host cells (Molawi et al., 2014; Bain et al., 2014; Scott et al., 2016).

1.3.2.1 Quorum sensing in immune cells

Quorum sensing is a process of communication between bacterial cells leading to the production chemical molecules (also called autoinducers). Sensing the diffusion gradient (Redfield, 2002) of these chemicals, bacteria can alter gene expression and regulate many critical processes like making biofilms, conjugation, virulence etc (Miller and Bassler, 2001). Similar to this, mammalian immune system exhibits such quorum sensing which has been shown recently. This type of sensing in immune-cell populations is unlike paracrine effect which affects a few cells around the cell producing the paracrine signal.

Immune quorum sensing spans longer space and induces an all or none population-level response when inducing proteins are present above a threshold concentration (reviewed by Antonioli et al., 2019).

Quorum sensing in immune populations has been suggested as a model of homeostasis in CD4+ T cells that is IL-2 mediated sensing of activated cells (Almeida et al., 2012) which Reynolds et al., 2014 further characterise using a stochastic Markov-based mathematical model, analysing the elimination of IL-2 and regulatory T cell populations post infection. Montaudouin et al., 2013 showed that B cells can detect immunoglobulin IgG by Fc γ RIIB receptor and, thereby, monitor the number of activated B cells. Further, they suggest that the number of activated immunoglobulin IgM-secreting B cells can be kept under check by this quorum sensing mechanism.

Quorum sensing has been proposed in macrophages as well (reviewed by Antonioli et al., 2019) which refers to, among others, two very interesting studies. Postat et al., 2018 found in *Leishmania major* infections (an intracellular parasite) mice show an increased recruitment of mononuclear phagocytes in the site of infection along with elevated levels of chemokines such as CXCL1, CXCL10, CCL2 and CCL3 upon treating the mice with a specific NOS2 inhibitor. Further, they showed that NOS2 suppressed cells produced more TNF, IL-1 β and CCL3 at the single-cell level. Then by comparing cellular metabolism in wild type and *Nos2*^{-/-} macrophages, they inferred that nitric oxide mediated suppression of respiration reduced the ATP:ADP ratio and, thereby, decreased macrophage activity. In order to check whether this effect was largely restricted to a single cell type, the authors mixed NOS2 competent cells with deficient cells to see if competent cells can affect the other cells. Although, they did not see such an effect at low densities but in a 1:1 ratio, respiration of *Nos2*^{-/-} cells was reduced. Such a density-based effect on respiration restriction was then shown *in vivo* to conclude that nitric oxide mediates the downregulation of inflammatory response and it is dependent on NOS2

producing cells being present in a minimum density of 5000 per cubic millimetre (Postat et al., 2018).

Chen et al., 2015 while studying hair plucking, and the consequent regeneration, in mice found that regeneration only occurs if the plucking density is greater than 10 squared millimetre. Intriguingly, this stimulated the plucked and the unplucked follicles to regenerate leading to more hair being regenerated than lost. Next, to understand mechanisms, microarray analysis was done to generate a sequence of events 12, 24, 48 and 96 hour post hair follicle injury. The authors find CCL2 as a key component of carrying the quorum signal to recruit TNF producing macrophages to the site, speculating that TNF may be stimulating hair regeneration through Wnt signalling in keratinocytes (Chen et al., 2015).

These studies together suggest that populations can show an all or none response to stimulus that is governed by a cell density-dependent diffusion sensing quorum effect.

1.3.3 Activation-induced heterogeneity

Interestingly, heterogeneity within a pure myeloid population activated by LPS has also been reported using single cell RNASeq study that found large-scale cell-to-cell variation in bone-marrow derived dendritic cells in their expression of cytokines suggesting population heterogeneity within a seemingly pure population (Shalek et al., 2013). In this study, 18 single cells along with three replicates of a population of 10,000 cells each were sequenced to look at the transcript signature at 4 hours post LPS stimulus. While gene expression between the replicates of population seem to correlate tightly (Pearson $r > 0.98$), individual cells showed large variation ($0.29 < r < 0.62$). Further, they found that a subset of the highly expressed genes (> 250 transcripts per million) in the single cell dataset had a higher co-efficient of variation (CV) along with bimodal expression patterns. mRNA levels in highly producing cells were one or more orders of magnitude

greater than the low producers. *Il6*, *Cxcl1*, *Cxcl10* mRNA were confirmed using RNA-fluorescence in situ hybridisation (FISH) as a visual confirmation of this bimodality (Shalek et al., 2013).

The above suggests that the bimodal response in cytokine production in the population along with the increased cell-to-cell variability in highly expressed genes can be attributed to heterogeneity in the responding population. Mechanisms that introduce antigen-induced heterogeneity may include bi-phasic NF- κ B signalling due to TLR4 endocytosis (as previously in **figure 1.1** and detailed later in **figure 1.6**) and, the additional TNFR1 and IFN- β signalling upon activation (**Figure 1.3**). Investigations in clonal populations have shown that TNF and LPS induced NF- κ B expression are distinct, with LPS inducing a less dampened NF- κ B expression in comparison. Further, Covert et al., 2005 suggest that this effect is seen because TLR4/LPS pathway involves MyD88 dependent and the TRIF-mediated pathways, that are on their own oscillatory and dampened, but together produced a more sustained NF- κ B expression. It can be speculated from this study that autocrine/paracrine TNF signalling may induce heterogeneous populations. Indeed, in a study from the same group (Lee et al., 2009) two distinct temporal LPS-induced NF- κ B nuclear localisation trajectories are presented that do not appear when either MyD88 or TRIF is knocked out. Individual knockouts could not, especially, explain why NF- κ B nuclear localisation persisted for hours in the wild-type model. It was then attributed to be an effect of paracrine signalling by TNF to drive a positive NF- κ B expression via the TNFR1 pathway. This was confirmed by neutralising TNF with soluble TNFR1 (Lee et al., 2009). Xue et al., 2015 using isolated single cells showed reduced secretion of LPS-induced cytokines such as IL-6 and IL-10 in a human monocytic cell line U937. Using modelling and experiments, they further showed that paracrine signalling by TNF by a small subset of cells (that highly expressed TNF) was necessary but not sufficient for producing IL-6 and IL-10 in large amounts.

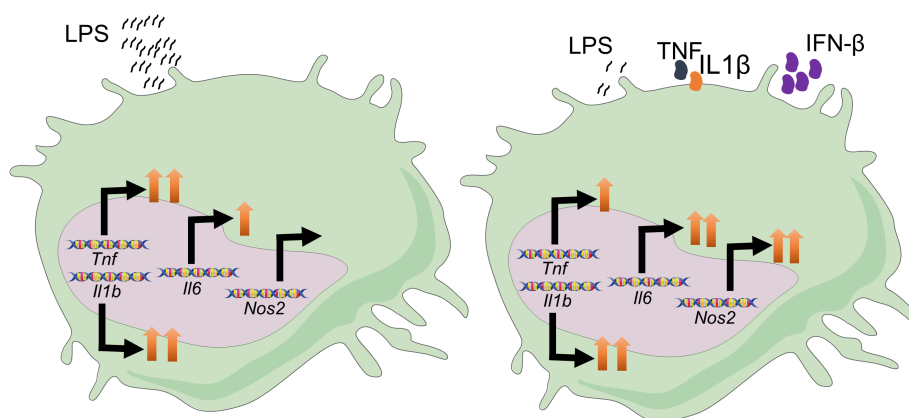


FIGURE 1.3: **Secreted TNF, IL-1 β and IFN- β provide additional stimulus to the LPS response**

LPS stimulation leads to the expression of TNF, IL-1 β , IL-6, IFN- β . The release of these into the extra-cellular space and binding to their respective surface receptors increase the initial LPS-mediated response to increase IL-6 expression. NOS2 expression depends on the IFN- β induced transcription factor activation.

Other sources of heterogeneity may be due to the effects of transcription-independent communication between heterologous and cytokine receptors (Bezbradica and Medzhitov, 2009). More recently, Allen and Medzhitov have suggested that the fraction of population responding by producing an inflammatory cytokine in response to LPS may be regulated by the circadian clock (Allen et al., 2019).

In summary, it has been shown by multiple studies that clonal macrophage populations can elicit heterogeneous responses to antigens like LPS and that this heterogeneity can be, in part, contributed by autocrine and paracrine effects.

1.3.4 Why study immune-cell heterogeneity

A heterogeneous response to antigens such as LPS as described can be biologically advantageous. Satija and Shalek reviewed phenotypic advantages that can be conferred on immune cells due to variability in protein production within a seemingly clonal population (Satija and Shalek, 2014). Variability in expression of receptor proteins such

as CD25 expression in CD8+ T cells has been shown to determine future outcome of T cells. Those CD8+ T cells that express high levels of CD25 become inclined to differentiate into memory cells that are long-lived (Kalia et al., 2010). Rand et al showed that individual cells producing IFN- β are stochastically limited and a reliable anti-viral response is co-ordinated by paracrine response amplification (Rand et al., 2012) allowing restraint and co-ordination. NF- κ B dynamics in response to TNF has been shown to be digital in lower doses whereas analogue responses are recorded at higher doses when all cells respond (Tay et al., 2010) suggesting immune cells may leverage ensemble coding as described in Satija and Shalek, 2014.

In this thesis we are interested in visually representing heterogeneity of cytokine expression in model macrophages and to quantitate the effect of disrupting established models (as illustrated in **Figure 1.4**) that can induce heterogeneity in cytokine response. Post transcriptional repression of protein expression has been associated with cell-to-cell variability (Garg and Sharp, 2016) and in the next few sections, miRNAs are introduced as a potential regulatory in mammalian cells to make a case why they should be considered in immune-cell responses and our hypothesis.

1.4 microRNAs as non-coding regulatory RNAs

Several studies show convincingly the role of miRNAs in regulation of macrophage activation, polarization and response to LPS (reviewed by Curtale, Rubino, and Locati, 2019) The discovery of microRNAs (miRNAs) in 1993 in *Caenorhabditis elegans* introduced a new class of evolutionarily conserved regulatory single stranded RNA. In *C. elegans*, downregulation of a protein, LIN-14, was essential for the larval stage to progress. This LIN-14 was found to be dependent on the transcription of lin-4. However, lin-4 was translated only into small RNA molecules but not translated. Later, it was found that the transcribed RNA showed antisense pairing to the 3' untranslated region (UTR) of the

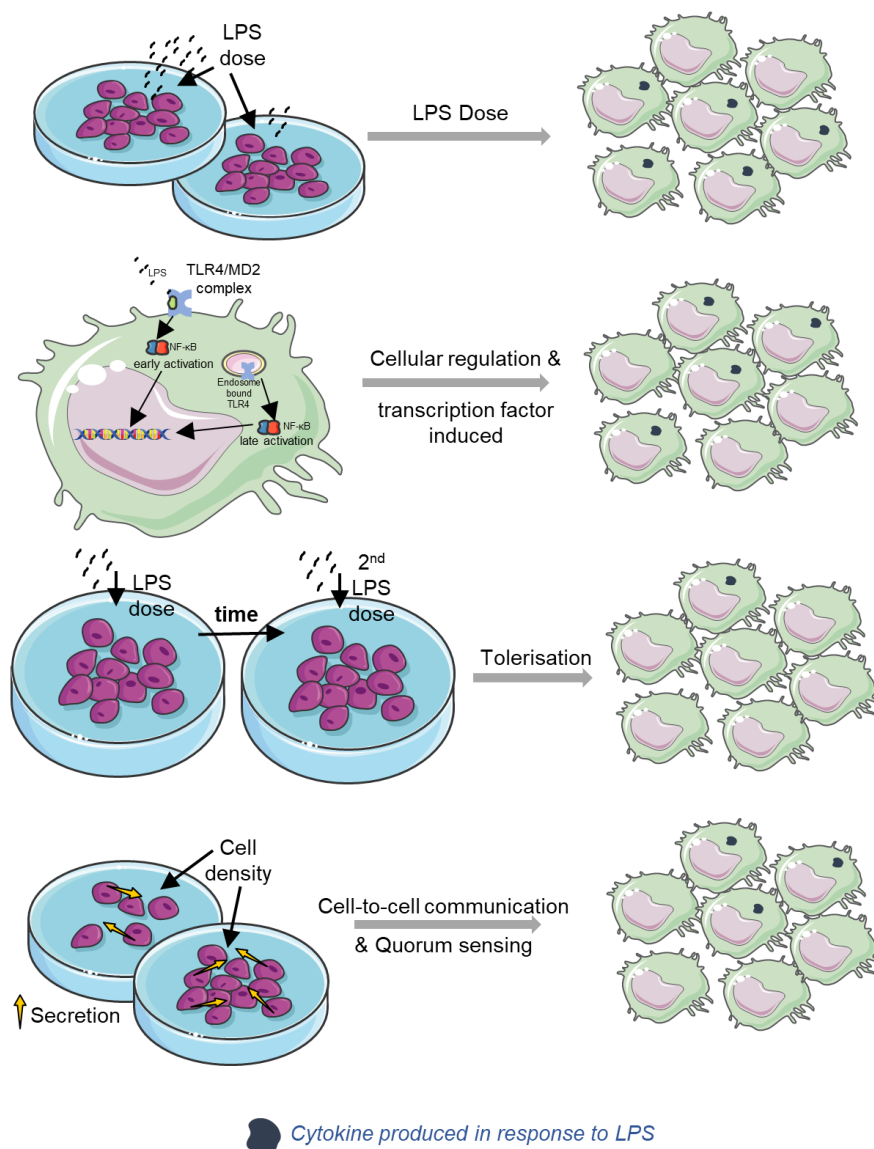


FIGURE 1.4: Sources of population heterogeneity in macrophages responding to antigen (LPS)

Cells (right panel) represent macrophage population response to LPS upon different perturbations (left panel) that can induce population level heterogeneity in terms of cytokine production such as LPS dose, transcription factor and regulation imposed, temporally distinct LPS treatments, secretory effects and quorum sensing.

lin-14 mRNA. Since then, many laboratories reported miRNAs in plants, animals and humans that are 22-24 nucleotide long, non-coding and bind target messengerRNA (mRNA) to repress its translation.

miRNAs are essential to development and homeostasis, as studies in mice have shown that loss of miRNA can lead to developmental defects in most organs along with physiological and behavioural defects. miRNAs show antisense pairing to their target mRNA, however, the seed sequence that pairs with the mRNA is short and between 6-8 nucleotides long at the 5' end of the miRNA. Short seed sequences can recognise 3' UTRs of many mRNA and, also, many miRNAs can target the same 3' UTR, often, resulting in a many to many relationship between miRNAs and mRNAs. There are 1234 mouse and 1917 human sequenced miRNAs that have been described and catalogued on miRBase (v22.1), an online repository that catalogues miRNAs. The human genome consists of around 21,000 protein coding genes, 60% of which are considered to have conserved miRNA targets (Friedman et al., 2009).

1.4.1 Biogenesis and mode of action

miRNAs are transcribed and transported to the ribosomes by a canonical pathway (Bartel, 2004) cleaved to an active form by Dicer (Harfe et al., 2005) and suppress mRNA expression by either disrupting translation or mRNA degradation.

Canonical miRNAs are transcribed by RNA polymerase II (Pol II) as a 1kb primary miRNA (pri-miRNA). These pri-miRNAs have a region that folds on itself to form a hairpin-like structure with single-stranded tails on the 5' and the 3' end. The microprocessor complex consisting of the ribonuclease III endonuclease Drosha and two molecules of the double-stranded RNA binding protein DiGeorge syndrome critical region 8 (DGCR8) that binds to the hairpin (**Figure 1.5**). The two RNase III domains of Drosha then clips the tails on the 5' and 3' end to form an approximate 60 base pair long

stem-loop that is termed as the precursor miRNA (pre-miRNA). In the next step, pre-miRNA is exported out of the nucleus by the protein exportin 5 (XPO5) and RAs-related Nuclear protein (RAN) GTP. Upon export into the cytoplasm, pre-miRNA is cleaved at the loop by the endonuclease DICER giving rise to a miRNA duplex that consists of the miRNA along with the passenger strand miRNA. DICER is assisted by its partner protein transactivating response RNA-binding protein (TRBP) and the protein activator of the interferon-induced protein kinase (PACT). The duplex, thus, formed has two nucleotide long overhangs on both the 3' end resulting from the cuts made first by Drosha and then by DICER. The duplex is then loaded onto an Argonaute2 (AGO2) protein (**Figure 1.5**) in an ATP dependent manner (Yoda et al., 2009). The duplex once loaded returns AGO2 to a lower energy state which encourages the passenger strand to be unloaded and degraded (Kawamata and Tomari, 2010).

The guide strand loaded on to the AGO2 protein is called the minimal RNA-induced silencing complex (miRISC). The miRISC then interacts with regions of the target mRNA that are called miRNA response elements (MREs). If the complementarity (**Figure 1.5**) is near-perfect the mRNA is degraded by AGO2-induced slicing of the mRNA via its endonuclease activity. However, animals seldom show perfect complementarity of miRNAs and MREs and, in case of imperfect complementarity, the silencing miRISC complex weakly binds to the mRNA while AGO2 and other factors repress translation and destabilisation of mRNA, finally leading to its degradation (Bartel, 2018) (**Figure 1.5**).

1.4.2 miRNAs and macrophages responding to LPS

Toll-like receptors on myeloid cells are central in the role of innate immunity as they detect PAMPs and initiate an inflammatory response by secreting cytokines, chemokines and other inflammatory mediators. The TLR-mediated gene expression is controlled

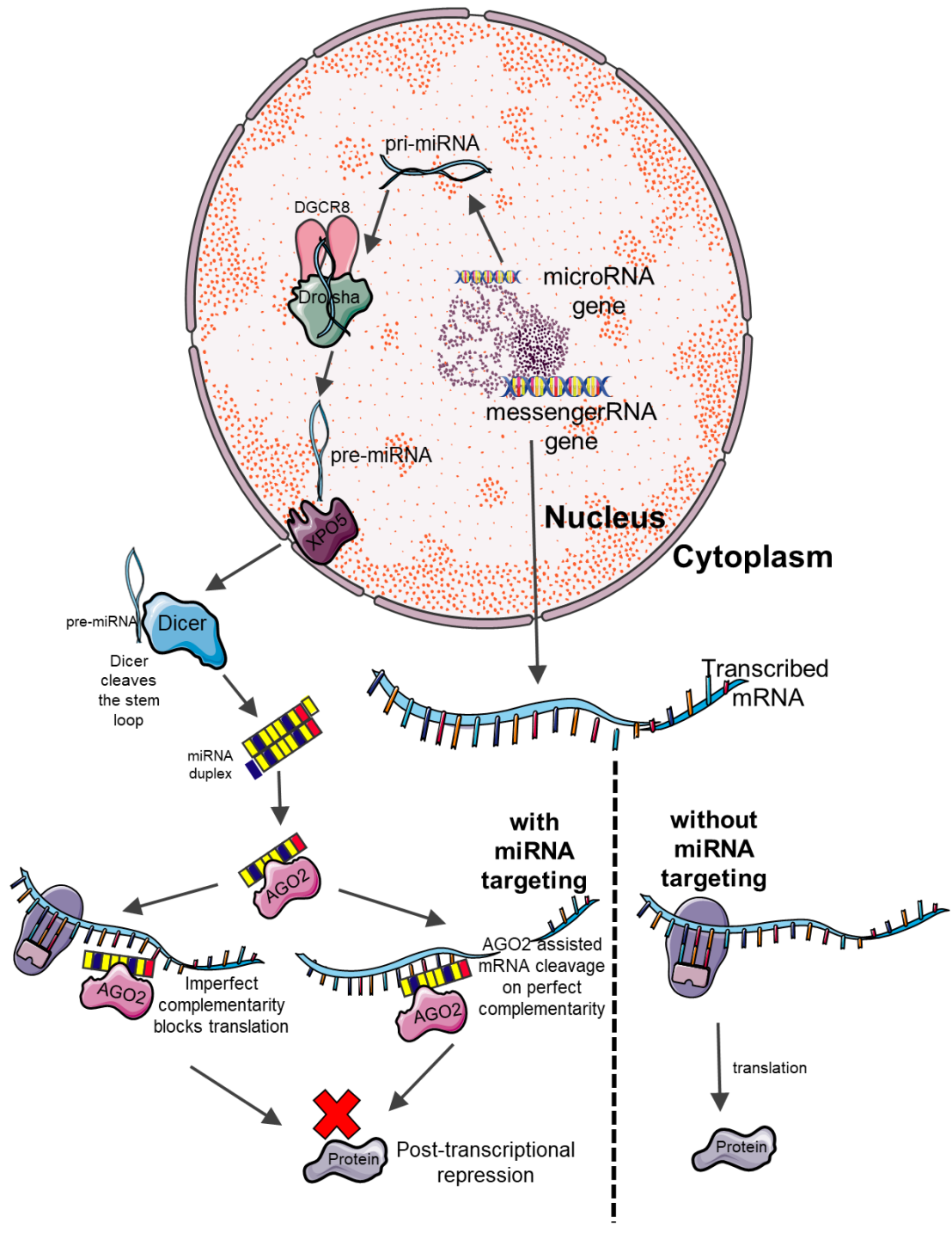


FIGURE 1.5: microRNA biogenesis and mode of action

Canonical miRNA biogenesis pathway showing pre-processing by DGCR8 and Drosha of primary miRNA transcript to pre-miRNA inside the nucleus. Once exported out to the cytoplasm pre-miRNA are cleaved to a mature form by Dicer. Mature miRNA is then loaded onto a RNA-induced silencing complex (AGO2 and associated proteins). mRNAs which are targeted by miRNAs are repressed by partial or perfect complementarity.

tightly by transcription factors and various signalling intermediates that signal via MyD88 or TRIF signalling routes that lead to translocation of NF- κ B, IRF3 and AP-1 to the nucleus. miRNAs are known to target many proteins involved in this pathway, thus, forming another layer of protein regulation (**Figure 1.6a**).

TLR4 is targeted by miRNA let-7b (Teng et al., 2013), let-7i (Chen et al., 2007) from the lethal-7 family and miR-181b (Jiang et al., 2018) and, as such, repressed upon LPS activation.

Downstream of the toll-like receptor, Inhibitor of nuclear factor kappa-B kinase subunit epsilon (IKK ϵ) has been shown to be targeted by miR-155 during *Helicobacter pylori* infection. IKK ϵ is a signalling protein in the TRIF mediated TLR4 pathway and activates the transcription factor IRF3. The overexpression of miR-155 in this context leads to the downregulation of the cytokines IL-8 and CXCL1 (Xiao et al., 2009). Up stream in the TRIF dependent TLR4/LPS pathway Zou et al., 2017 have shown miR-3178 can decrease the activation of NF- κ B by post-transcriptionally targeting TNF receptor-associated factor 3 (TRAF3). miR-124 is upregulated in RAW264.7 murine macrophage cell-line upon Bacillus Calmette-Guerin (BCG) infection in a MyD88 dependent manner while targeting multiple signalling components including TLR6, TRAF6, MyD88 and TNF (Ma et al., 2014). IRAK1 mRNA in RAW264.7 cells are targeted and negatively regulate TNF, NF- κ B and IL-6 (Xu et al., 2013). miR-132 reduces expression of IL-6 and IL-1 β by decreasing levels of its target protein p300 (Lagos et al., 2010). miR-146a (Taganov et al., 2006) have been shown to negatively regulate IRAK1 and TRAF6.

Negative regulators of the TLR4/LPS signalling pathway such as A20 which inhibits signal transduction to the sequestered NF- κ B complex has also been shown to be targeted by let-7f in the context of *Mycobacterium tuberculosis* infection in RAW264.7 cells

and bone-marrow derived macrophages (Kumar et al., 2015).

The above suggests that miRNAs can act as positive and negative modulators of the LPS induced inflammatory response. It is difficult to ascertain whether miRNAs in a concerted manner promote or suppress inflammation.

1.4.3 miRNAs in protein expression noise and population variability

miRNA can have profound effects in disease, cancer and development, that is why as a system of regulatory RNAs their global role in protein expression has also intrigued scientists. Bartel and Chen, 2004 proposed the idea that miRNAs render precision to protein expression by comparing miRNA induced silencing to a adjustable resistor or rheostat in an electric circuit, suggesting miRNA expression in a cell type can be adjusted to have different effects on a target mRNA. Since, multiple miRNAs can target the same mRNA, they suggested by varying the expression level of the miRNA and depending on its complementarity to the target a range of outcomes can be achieved. Thus, allowing the possibility of tuning mRNA targets meaning that the protein expression is not repressed but only fine-tuned to an active yet dampened level (Bartel and Chen, 2004).

Protein expression is noisy (Thattai and Oudenaarden, 2010) in a population of cells and within a single cell over time. This variability in expression of a protein has been described mathematically and experimentally (in *E. coli*) as the sum of two orthogonal components, intrinsic and extrinsic noise (Swain, Elowitz, and Siggia, 2002; Elowitz, Levine, and Siggia, 2002). This was confirmed to be true in mammalian cells (Raj et al., 2006) and shown to propagate in gene networks (Pedraza and Oudenaarden, 2005), thus, suggesting their role in introducing heterogeneity in clonal populations. Intrinsic noise was defined as inherent stochasticity in reactions related to transcription and translation whereas extrinsic noise a consequence of by the stochastic variation in concentrations of molecules such as polymerases and regulatory proteins required in the expression of the

target protein (Swain, Elowitz, and Siggia, 2002; Elowitz, Levine, and Siggia, 2002). Schmiedel et al., 2015 experimentally and mathematically probed the idea that miRNAs can render precision to protein expression by affecting intrinsic and extrinsic noise in protein expression.

Using a two reporter system (fluorescent) with a bidirectional reporter, Schmiedel et al., 2015 quantified protein levels and any corresponding noise in mouse embryonic stem cells. By appropriately binning from bi-plots of the two fluorescent signals obtained from flow cytometry experiments they quantified the noise (defined as standard deviation/mean) or the co-efficient of variation when the reporter transcript had 3' UTR that was miRNA targeted or not. Their experiments showed that variance was indeed decreased when protein expression was low but, intriguingly, noise in expression increased when the protein was expressed at higher levels. In order to understand this effect they described the problem mathematically which predicted that while intrinsic noise did indeed reduce with miRNA induction, with the increased expression of the protein, the extrinsic noise increased as well as leading to an overall increase in the noise (Schmiedel et al., 2015). This increase in the extrinsic noise associated with gene expression is due to the variation in the expression of miRNAs. The two opposing results due to miRNA-induced post-transcriptional repression is depicted in figure **1.6b**.

Studies on heterogeneity have found that housekeeping genes tend to be normally (or log normally) distributed in single cell populations (Shalek et al., 2013; Kumar et al., 2014; Klein et al., 2015) while there is a subset of cells that display increased cell-to-cell variability whose distribution is bi-modal or heterogeneous. Further Kumar et al., 2014 also showed that knocking out microRNA biogenesis proteins (*Dicer*^{-/-} and *DGRC8*^{-/-}) in mouse pluripotent stem cells, result in a population with little variation in the pluripotency genes (or 'ground state') that are highly variable in wild-type. Garg and Sharp, 2016 speculate if extrinsic noise contributed by miRNA pool that increases

variance in highly expressed genes (Schmiedel et al., 2015) can contribute in the variability in wildtype pluripotency factors as shown by Kumar et al., 2014; Klein et al., 2015.

In another study, Blevins et al., 2015 in developing mouse thymocytes showed that miRNA-deficient cells have increased population CV (co-efficient of variation) in the expression of T-cell activation marker suggesting the role of miRNAs in regulating cell-to-cell variability in immune cells. Overall, this shows that miRNAs as global regulators of protein expression can not only suppress translation but can contribute to population heterogeneity and, even, be a determinant of phenotypic changes.

1.5 Mathematical description of biological complexity

Biological systems such as biochemical pathways, cells, tissues, organs, and uni- and multi-cellular organisms can be all described as complex systems. To understand these systems, careful biological experiments and statistical methods need to be employed to dissect mechanisms, and these approaches may consider scales ranging from biochemistry and molecular biology to large-scale tissue function and interactions within an organism or between organisms. Because of this complexity, ascertaining how a biological system interacts with numerous biological entities is not easy to understand (Martins, Ferreira, and Vilela, 2010; Walpole, Papin, and Peirce, 2013; Ji et al., 2017). For example, how a whole organ may respond to cancer is difficult to delineate using only molecular biology approaches and statistical comparisons, because each cell must be viewed in the context of its immediate neighbourhood and its broader ecological context within the tissue and organism (Ferreira, Martins, and Vilela, 2003; Owen, Byrne, and Lewis, 2004). Such systems-level understanding requires the usage of mathematical, and often computational, methods to help define the biological system in question, as well as

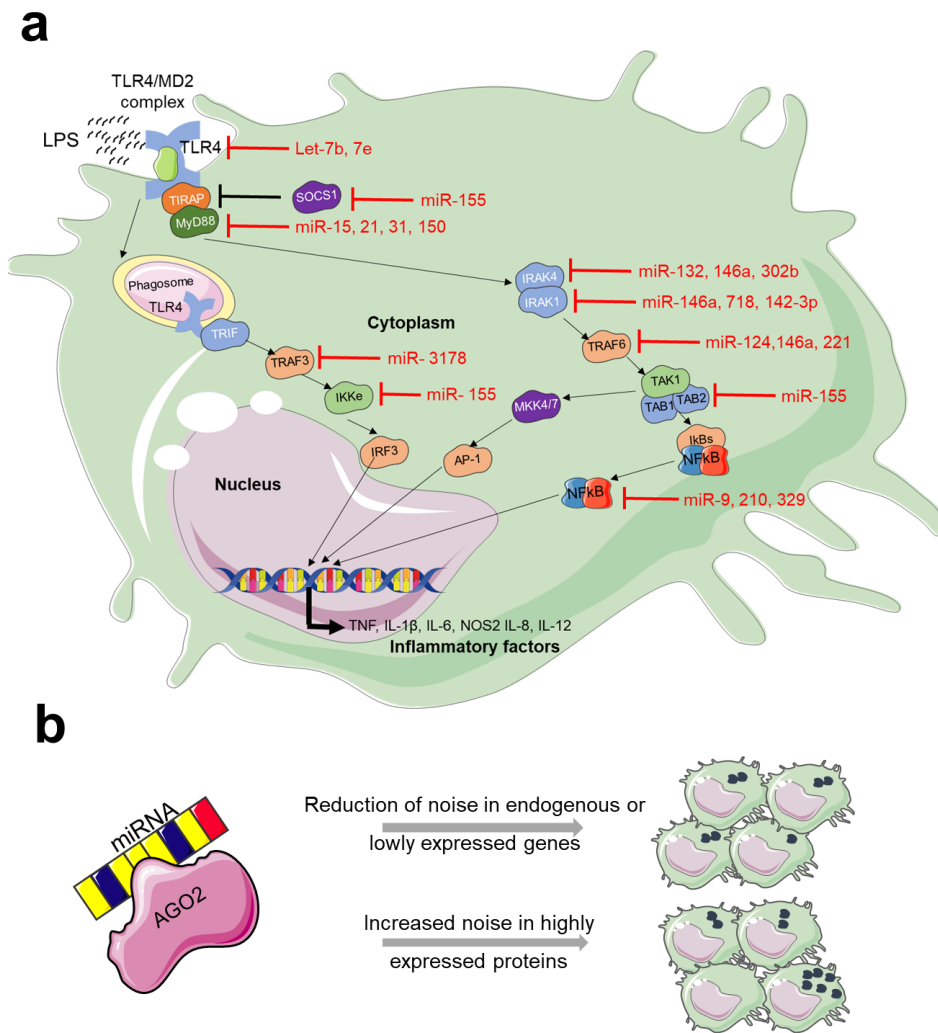


FIGURE 1.6: miRNA regulated inflammatory response and contribution to population heterogeneity

a LPS-induced TLR4 signaling pathway leads to the downstream induction of three major transcription factors, NF-κB, IRF3 and AP-1 that contribute to the inflammatory gene signature of a macrophage. Proteins regulating this pathway (positively or negatively) are in turn post-transcriptionally regulated by miRNAs as depicted in the cartoon. b miRNAs have also been shown to introduce cell-to-cell variability in a population of seemingly identical cells i) by reducing intrinsic noise in endogenous genes and, consequently variability or ii) by increasing the extrinsic noise in a highly-expressed gene.

a theoretical model (Kitano, 2002; Tomlin and Axelrod, 2007).

In the last two decades with the human genome being sequenced and sequencing costs becoming economically feasible, and not limited to specialist laboratories, the amount of data available to a biologist about their model organism has increased many folds. Sequencing can not only inform about the genetic code but also what is being expressed (transcriptomics) with temporal resolution. This, then demands the need for computational analysis of these gene networks to understand cellular or population behaviour (Smolen, Baxter, and Byrne, 2000; Ay and Arnosti, 2011; Grimes, Potter, and Datta, 2019).

Besides de-constructing large network models, mathematical modelling can help to describe a complex process with simplified parameters that can be estimated by calibrating the model outputs to empirical outputs. This approach not only helps in model validation in describing large-scale phenomenological results (Wood and Coe, 2007; Wood et al., 2008) but also to deduce parameters to describe interesting features such as kinetics over time or threshold values of a complex process or events (Renshaw, 1993; Lema-Perez et al., 2019)

Biological systems modelling has mostly relied on continuous deterministic solutions using ordinary differential equations (ODE) to describe the biological problems being studied. This is a particularly useful paradigm when, for example, the abundance of the reacting species in the system can be quantified in terms of concentration (Murray, 2002). The ODE approach assumes that these concentrations change via fixed deterministic trajectories. These models can elucidate average behaviour of systems but sometimes fail to capture the inherent stochastic nature of many biological processes (McAdams and Arkin, 1997; Gillespie, 2007; Wilkinson, 2009) such as gene expression where noise (or stochasticity) can be associated with low copy numbers of reacting molecules such as

DNA and transcription factors (Guptasarma, 1995; Paulsson, Berg, and Ehrenberg, 2000; Paulsson, 2005). Deterministic systems fail to capture the effects of low copy numbers that can result in a noisy trajectory where no two cells have the same trajectory associated with protein expression. Comparisons of deterministic and stochastic models of the prokaryotic *lac* operon has illustrated the role of stochasticity in modulating system behaviour (Stamatakis and Mantzaris, 2009). In order to capture such heterogeneity, probability theory based methods can be an effective way of accounting for the unpredictability of a complex biological system (McAdams and Arkin, 1997; Gillespie, 2007; Wilkinson, 2009).

1.5.1 Probabilistic modelling and Markov process

Probability-theory based modelling of biological events is different from the ODE based approach in the fundamental sense that the reactions (or other biological interactions) do not have associated deterministic rates governing a continuous state-space, but instead consider discrete events with an associated probability per unit time of occurring. This modelling paradigm, as such, associates a chance associated with an event and removes the certainty of an event to happen with a said rate. Given a low number of reactants, models based on probability can add a stochastic flavour to the outputs of the master equation, which can be thought of as an equation which captures the probabilistic changes within a system (Gillespie, 1977). Explicitly solving a probability master equation analytically although possible (Jahnke and Huisinga, 2007; Shahrezaei and Swain, 2008) is often an intractable task, and thus there is a need to approximate the master equation (Kampen, 2007) or simulate the time-evolution using algorithms which accurately represent the behaviour of the underlying master equation (Gillespie, 2007).

A mathematical system that allows probability-theory based deductions of a complex system is a Markov chain. The key defining property of a Markov chain is that, conditional on knowledge of the present state of the system, the future behaviour of the

system is independent of the system's state at any earlier time i.e. the system is memoryless. Markov chains have been extensively used to model biological systems, which can be thought of mathematically as being defined by the states of an n -dimensional system along with the probabilities of switching from one state to another (Gillespie, 1992). For example, a cell that is expressing a gene or not, represents two states that have probabilities associated with switching on or off from that state. The important characteristic of the Markov chain, that it has no memory such that the transition from one state to another only depends on the current state, makes this mathematical framework appropriate for a wide range of biological models (Wilkinson, 2009).

The Doob-Gillespie algorithm is an exact algorithm which can provide fast and accurate solutions for models based on Markov chains; it simulates a sample trajectory from the probability mass function of a master equation using the Markov property. It was first described by Joseph Doob in 1945 (Doob, 1945) and then presented by Dan Gillespie (Gillespie, 1976) in a very well-described paper with simulations comparing ODE solutions with the Doob-Gillespie algorithm. The algorithm traces the time-evolution of species of a system by choosing the time to next reaction and the reaction that describes the system in time.

1.6 Choice of the biological model

1.6.1 Macrophage-like RAW264.7 cells

As a model system, we chose RAW264.7 cells that are adherent murine macrophage-like cell line that were derived from the ascites of a tumour induced in a male BAB/14 mouse injected with a preparation of Abelson murine leukemia virus. This immortalised cell-line shows the properties of macrophages and can partake in neutral red dye endocytosis, secretion and synthesis of lysozyme, and zymosan and latex bead

phagocytosis. This macrophage cell line can also mediate lysis and phagocytosis of sheep erythrocytes which is antibody-mediated. The cells are LPS sensitive and cell growth is inhibited (50% of the population) by 0.5 ng/ml of LPS and a 100ng/ml dose stalls growth of all cells for upto four days (Raschke et al., 1978). Since the cell line was created using a viral transformation it is possible that viral particles remain in the cell line, however, no viral activity was detected by fibroblast focus-forming assay or by the plaque assay to detect the presence of retroviruses (Raschke et al., 1978).

RAW264.7 cells express cluster of differentiation molecule 11B (CD11b) and EGF-like module-containing mucin-like hormone receptor-like 1 (also known as F4/80) both macrophage markers associated with cell adherence stably over multiple passages (20) in culture. Many other genes have tested to be stably expressed in this cell-line over passages such CD14, iNOS (or NOS2), hypoxia-inducible factor 2 α (HIF-2 α), cluster of differentiation molecule 11c also known as CD11c (Taciak et al., 2018).

In this thesis, we measure four pro-inflammatory proteins produced by macrophages in response to LPS. TNF, IL-1 β , IL-6 and NOS2 are all expressed by RAW264.7 cells and the bi-phasic NF- κ B expression induces an early TNF response with an increased IL-6 and NOS2 expression is seen at later time points (Xue et al., 2005; Wang et al., 2008). It was also indicated that RAW264.7 cells closely mimic primary bone-marrow derived macrophages in the expression of surface receptors and the response to microbial ligands (Berghaus and Moore, 2010).

However, it must be noted that RAW264.7 cells are immortalised and, thus, represent cells that otherwise would not have proliferated *in vivo*. This makes them an artificial model system for macrophages that can change with continuous culture.

1.6.2 Thioglycollate-elicited peritoneal macrophages

In order to confirm our findings in primary cells we extracted peritoneal macrophages from C57BL/6 female mice. Peritoneal macrophages are a well-researched macrophage type that is tissue-resident and elicit an inflammatory response (Cassado, D'Império Lima, and Bortoluci, 2015). It is however, duly noted that the peritoneal macrophages in our study were thioglycollate-elicited and, therefore, were a mix of resident and monocyte-derived macrophages (Ghosn et al., 2010).

1.7 Motivation and hypothesis

We have discussed inherent macrophage heterogeneity in the previous sections and how this heterogeneity in a seemingly clonal population can manifest, discussing contributing factors like antigen dose and pre-exposure, gene activation, inter-cellular communication, quorum sensing and, at a more fundamental level, by noisy expression in highly expressed genes targeted combinatorially by miRNAs (**Figure 1.4**).

Putting the above in the context of immune cells and immune response, we hypothesise that single-cell protein measurements in clonal macrophage population can be used to show and represent heterogeneity in response to single, repeated doses of LPS or to miRNA depletion.

We question if we can capture and visually represent the pro-inflammatory response to an antigen in a clonal population of RAW264.7 cells in the context of variability. Are there sub-populations in the cell community (those responding to antigen) that, in principle, play a similar inflammatory role and, if so, do these communities respond to LPS dose(s), intercellular communication, cellular density and global miRNA regulation. We quantitate pro-inflammatory TNE, IL-6, NOS2 (and IL- β in later experiments) to identify and track sub-populations in the community to see if this response is robust or is

their plasticity in these communities. Further, in order to see how such communities evolve over time and whether or not they have an effect in shaping the response, we use simple mathematical models to predict temporal trajectories of empirical outcomes to fit underlying parameters that may contribute to the qualitative and quantitative changes to the community structure.

1.7.1 Aims

1. Capture and visually represent heterogeneous macrophage response to primary and secondary challenges of LPS and develop methods to compare heterogeneous communities composed of cells expressing TNF, IL-6, NOS2 and IL-1 β (**Chapter 4**)
2. Use mathematical models to simulate time evolution of these communities to obtain rate vectors that describe transitions between sub-populations. (**Chapter 5**)
3. Show how sub-populations are affected by depleting the miRNA bio-machinery proteins such as Dicer (**Chapter 6**)

Chapter 2

Methods

2.1 Methods and Materials

2.1.1 Mammalian cell culture

2.1.1.1 Animals and ethics statement

Wild type C57BL/6 mice were bred in the animal facility at University of York and cages were ventilated individually. Animal welfare and care were considered foremost and UK home office guidelines, complying with the ASPA act, 1986, were followed for all animal protocols .

2.1.1.2 Extraction/culture of peritoneal macrophages

4-6 week old C57BL/6 wild type mice were injected with 200 μ l of 4% thioglycolate in the peritoneal cavity to induce macrophage recruitment (Zhang, Goncalves, and Mosser, 2008). After four days the mice were euthanised by overdose of anaesthesia. The cells were then extracted by lavage in ice cold Gibco Roswell Park Memorial Institute (RPMI) 1640 medium supplemented with 1% streptomycin-penicillin mixture, 1% L-glutamine and 10% fetal calf serum (Hyclone). After centrifuging at 4°C at 1500RPM for 5 minutes, cells were resuspended in red blood lysing buffer (Hybri-Max, Sigma) and left to stand at room temperature for 5 minutes. Finally, harvested cells were plated and let to stand for adhering to tissue culture plate at 37°C and 5% CO₂. The cells were then washed

with phosphate-buffered saline (PBS, Gibco) to remove non-adherent cells. Media was replaced and cells were used for further experiments.

2.1.1.3 RAW264.7 cell culture

Murine macrophage-like cell line, RAW264.7 were obtained from frozen stocks at the Lagos laboratory. Cells were cultured in Dulbecco's Modified Eagle Medium (DMEM) supplemented with 1% streptomycin-penicillin mixture, 1% L-glutamine and 10% fetal calf serum (Hyclone) in Corning T25 flasks and then passaged onto T75 flasks (Corning). Cells were detached for passaging using 1x Trypsin-EDTA (Invitrogen) by incubating at 37°C for 10 minutes. Cells were detached completely by gently scraping with cell scraper with a cross-ribbed handle (VWR). Upon reaching 70-80% confluency, cells were either cryopreserved in a mixture of 90% FCS and 10% dimethyl sulfoxide (DMSO) in Corning cryogenic vials or plated in 24 well plates for further experiments at passage 4 or 5. RAW264.7 cells were centrifuged at 1500RPM at 25°C for 5 minutes for the purposes of washing or re-suspending.

2.1.1.4 HEK293T cell culture

Human embryonic kidney 293 cells with a mutant version SV40 T antigen (HEK293T) were obtained from frozen stocks at the Lagos laboratory. Cells were cultured in Dulbecco's Modified Eagle Medium (DMEM) supplemented with 1% streptomycin-penicillin mixture, 1% L-glutamine and 10% fetal calf serum (Hyclone) in 10cm dishes and passaged upon 60-70% confluency. Cells were detached for passaging using 1x Trypsin-EDTA (Invitrogen) by incubating at 37°C for 5 minutes and gentle tapping. Cells were cryopreserved as above or used for experiments at passage 4. HEK293T cells were centrifuged at 1200RPM at 25°C for 5 minutes.

2.1.2 LPS-induced challenge or hyporesponsiveness protocol

Thioglycollate-elicited peritoneal macrophages (TPEMs) were plated at 1,000,000 cells per well for a minimum of 4 hours prior to experiments. 200-250,000 RAW264.7 cells were plated overnight before experiments. All cells were plated in a Corning 24 well plate in 500 μ l of DMEM.

For LPS titration experiments, cells were either stimulated with purified *Escherechia coli* lipopolysaccharide (LPS; Sigma-Aldrich) or were left in media (untreated) on day 1 (**Figure 2.1**). Cells were challenged with 1, 10, 100 or 1000 ng/ml of LPS. Supernatant was collected at 24 hours for ELISA and stored at -20°C. Cells were harvested for flow cytometry at 16 or 24 hour from LPS stimulus.

For inducing hyporesponsiveness, cells were either stimulated with 10 or 1000 ng/ml of LPS or left untreated in media on day 0 (**Figure 2.2**). After 24 hours (day 1), cells were washed twice with PBS and replaced with media (Media/Media) or with media containing 1000 ng/ml of LPS (10/1000; 1000/1000 or Media/1000) as represented in **Figure 2.2**. Challenged (Media/1000) and twice-challenged (10/1000; 1000/1000) were compared to ascertain hyporesponsiveness by measuring TNF and IL-6 by ELISA in the supernatant.

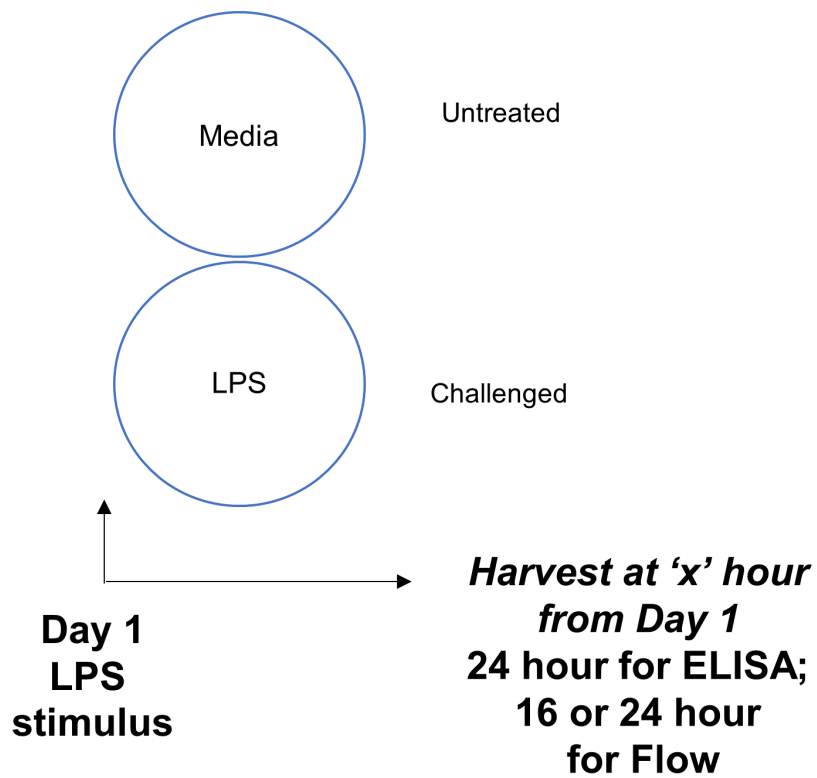


FIGURE 2.1: LPS stimulus protocol

Cells were either left untreated in media or challenged with LPS (1, 10, 100, 1000 ng/ml) on day 1 (lower panel) and harvested for flow cytometry at 16 or 24 hours post stimulus. Supernatant was collected at 24 hour for ELISA.

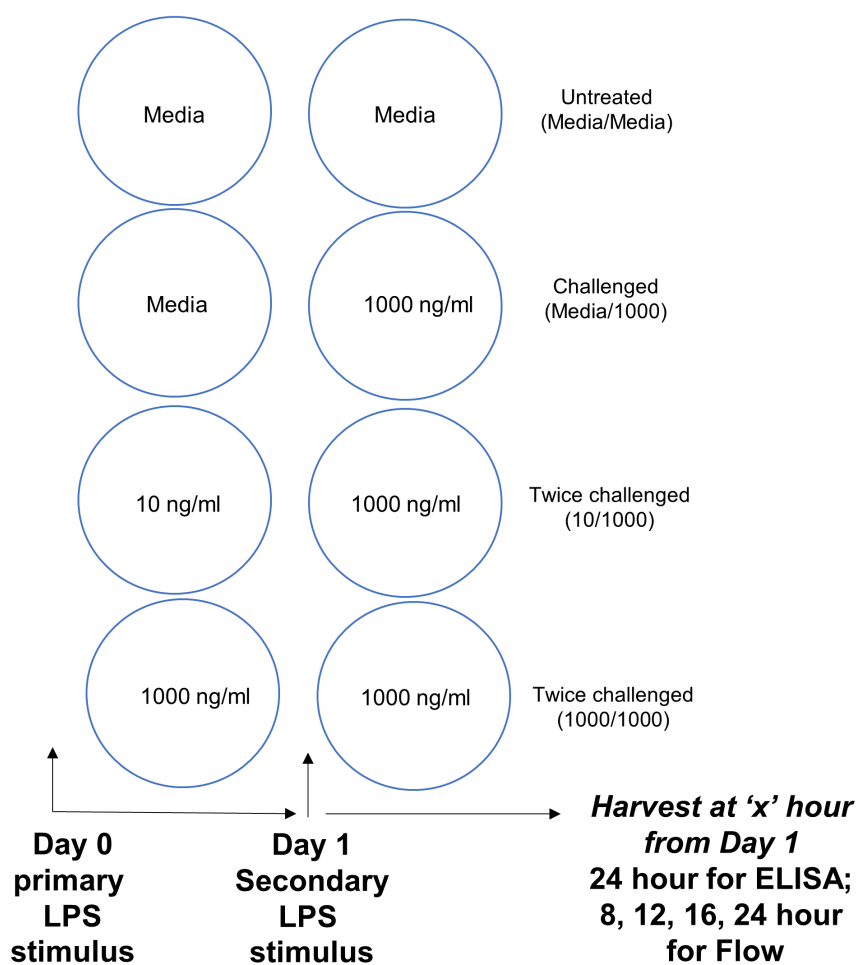


FIGURE 2.2: LPS induced hypo-responsiveness protocol

Cells were either left untreated in media or stimulated with LPS (10 or 1000 ng/ml) on day 0 (lower panel). On day 1 cells were either left untreated (Media/Media) or challenged with 1000 ng/ml LPS (Media/1000; 10/1000; 1000/1000). 10/1000 and 1000/1000 received two doses of LPS while Media/1000 represented cells that were only challenged once. Cells were then harvested for flow cytometry at 8, 12, 16 or 24 hours post secondary challenge (day 1). Supernatant was collected at 24 hour post day 1 for ELISA.

2.1.3 Flow Cytometry

RAW264.7 or thioglycollate-elicited peritoneal macrophages were collected after washing in ice-cold PBS and then detaching the cells with Accutase (Biolegend). Prior to collection, cells were incubated in 10ug/ml of Brefeldin A (BFA) to block protein transport (Misumi et al., 1986). BFA incubations were used at varying durations as described in **Figure 2.3** as an example and is, also, explicitly mentioned in each experiment.

Cells and all reagents were maintained at 4°C throughout the intra-cellular staining protocol. Harvested cells were washed twice in PBS and re-suspended in approximately 50µl of PBS. Cells were stained with 100µl of 1:1000 Zombie Aqua live/dead stain (Biolegend) in PBS on ice for 8-10 minutes in the dark. Cells were then washed with Flow cytometry staining (FACS) buffer (PBS, 0.5% BSA, 0.05% sodium azide), aspirated and re-suspended in 50µl FACS buffer. F_C receptors were blocked with 5µl of 2mg/ml rat IgG for five minutes. Cells were then stained with surface receptor antibodies for 20 minutes on ice in the dark. Cells were washed with FACS buffer and then fixed with BD Cytfix for 20 minutes on ice in the dark. Cells were washed twice with permeability buffer (BD Cytoperm). Intracellular staining was performed with the cocktail of antibodies made in permeability buffer. The list of the antibodies for surface and intra-cellular staining are listed in table **2.1**. Intracellular stains were washed off with FACS buffer after staining for 20 minutes on ice in the dark. Cells were washed again with FACS buffer, re-suspended in about 400µl FACS buffer and run on BD LSR Fortessa.

Single stain controls and isotype controls were used in all experiments. An example of gating strategy used for intracellular staining along with its isotype control is shown in **Figure 2.4**. FCS 3.0 files from Fortessa runs were recorded on FACS Diva software. Unless mentioned explicitly, cells were pre-gated on live cells, singlets, forward scatter and side scatter (for gating intact cells), F4/80+ and/or CD11b+ using FlowJo.

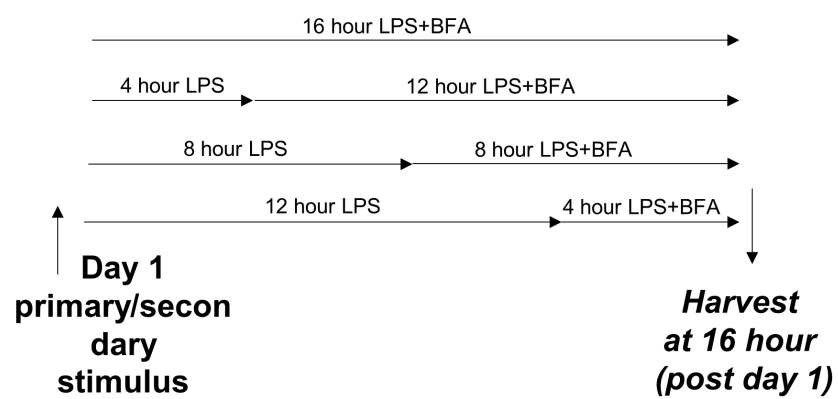


FIGURE 2.3: **Brefeldin A incubation for intra-cellular staining**

Cells on day 1 were stimulated with LPS and BFA to obtain shorter or longer periods of intra-cellular staining as described in the cartoon and harvested for flow cytometry staining at the end of the incubations.

Manufacturer	Antibody against	Clone	Fluorophore	Isotype	Dilution
Biolegend	TNF	MP6-XT22	BV421	IgG1	1:300
Biolegend	IL-6	MP5-20F3	APC	IgG1	1:200
Biolegend	GM-CSF	MP1-22E9	PE-Cy7	IgG2a	1:400
Biolegend	CD11b	M1/70	PE-Cy7	IgG2b	1:400
Biolegend	F4/80	BM8	FITC	IgG2a	1:200
Biolegend	CD64	X54-5/71	PerCP/Cy5.5	IgG1	1:200
Biolegend	TLR2	CB225	PE	IgG2a	1:200
Biolegend	TLR4	APC	SA15-21	IgG2a	1:200
Biolegend	CD86	PE	GL-1	IgG2a	1:200
ThermoFisher Scientific	NOS2	CXNFT	e-Fluor 610	IgG2a	1:300
ThermoFisher Scientific	IL-1 β Pro	NJTEN3	PE	IgG1	1:200

TABLE 2.1: Antibodies used for flow cytometry

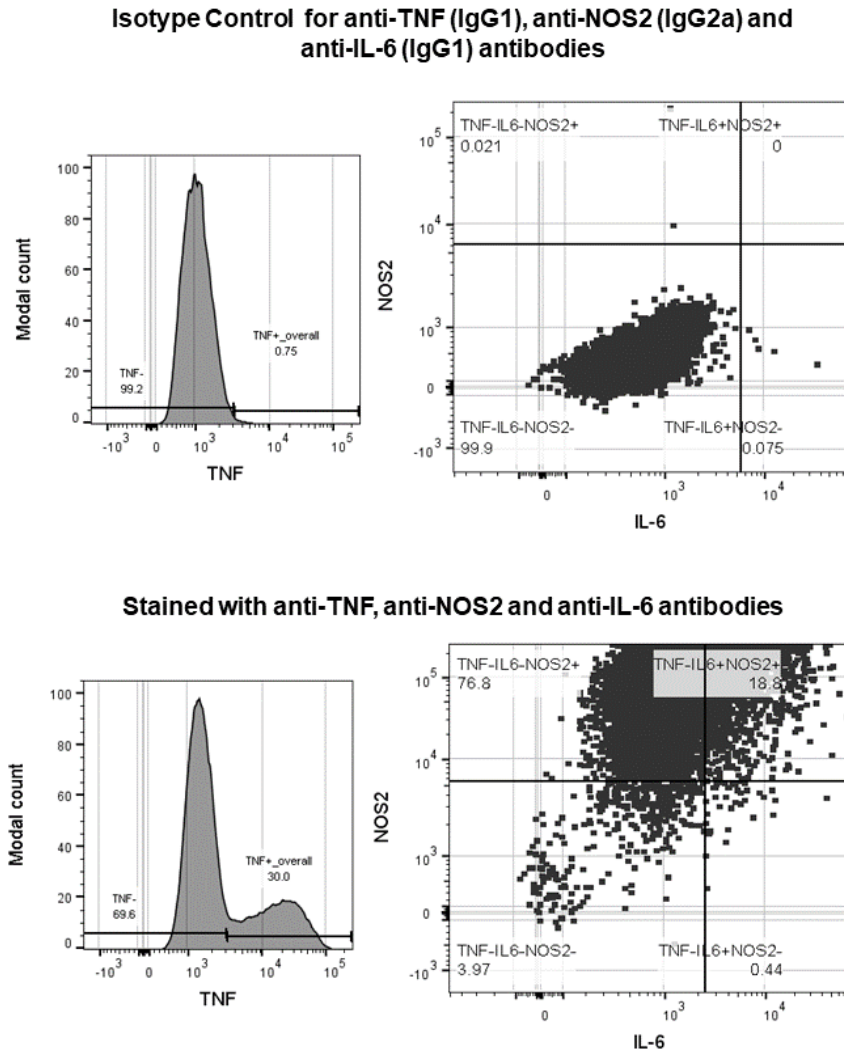


FIGURE 2.4: TNF, IL-6, NOS2 positivity fractions as determined by respective isotype controls

Cells were pre-gated for live, single, intact cells, CD11b and F4/80. CD11b⁺ F480⁺ populations were then used to gate TNF⁺ and TNF⁻ populations. TNF⁺ and TNF⁻ sub-populations were individually gated to IL-6⁺ and NOS2⁺ sub-populations using bi-plots. The resulting 8 sub-populations were then used to calculate their individual percentage in all CD11b⁺ F480⁺ population. Top row shows the isotype control TNF, IL6 and NOS2 based on which the positive/negative gates were established and applied to sample (bottom row)

2.1.4 ELISA

IL-6, TNF and IL-1 β concentrations in the cell culture supernatant were measured by enzyme-linked immunosorbent assay (ELISA). Nunc Maxisorp flat-bottom 96-well plates from ThermoFisher Scientific were used for all ELISA experiments. Biolegend ELISA MAX Standard kits for TNF, IL-6 and IL-1 β were used to measure the respective cytokine levels. Capture antibodies were added to wells at 1 in 200 dilution in coating carbonate buffer (Biolegend). After an overnight incubation at 4°C for coating of the plates with capture antibodies, the wells were blocked with 10% FCS in tris-buffered saline (TBS) or TBST (20mM Tris hydrochloride pH 7.4, 150mM NaCl with 0.05%TWEEN) for 2 hours at 37°C. Standards (Biolegend) and samples were diluted appropriately and added in duplicates to wells. Plates were incubated for 2 hours at 37°C at room temperature. Wells were washed in TBST 4–5 times and then biotinylated antibodies (1:500 in 10% FCS in TBST) were added to the wells. After incubation at 37°C for 1 hour, plates were washed in TBST and Biolegend Avidin horseradish peroxidase (HRP, 1:10000) was added to the wells for 30 minutes. TMB buffer or 3,3',5,5'-tetramethylbenzidine (Biolegend) was used as a substrate for HRP. The reaction was stopped using 2N sulfuric acid. Absorbance was read at 450nm with a wavelength correction at 570nm using a VersaMax Microplate Reader (Molecular Devices). Standard curves were generated using 4-parameter non-linear fitting to known standard concentrations using SoftMax Pro software. Optical density of the unknowns that fit within the linear range of the standard curve was used to calculate the concentration of the sample.

2.1.5 Greiss Assay

Greiss assay was used to measure nitrite concentrations in the supernatants. Diazotization reaction in Greiss assay was carried out as per manufacturer's instructions (Promega) by adding sulfanilamide to the supernatant and then NED (0.1% N-1-naphthylethylenediamine dihydrochloride) in a 96-well plate. Plates were incubated at room temperature for 5-10 minutes to allow for colour to develop. Standards were run in duplicates or triplicates to determine nitrite concentration. Plates were read on VersaMax microplate reader capturing absorbance between 520 and 550nm.

2.1.6 RNA interference

RAW264.7 cells were plated at 50,000 cells per well in a 6 well plate overnight. The next day, the cells were transfected with 50nM siRNA ON-TARGET^{plus} mouse Dicer siRNA SMARTPOOL at 50nM or a non-targeting control procured from Dharmacon. The transfection was facilitated using TransIT-siQUEST (Mirrus Bio) in reduced serum Opti-MEM (Gibco) as the transfection mixture. Opti-MEM was replaced with full DMEM 5-6 hours post transfection. Cells were checked for siRNA efficiency by western blot 24-48 hours post transfection. Cells treated with Dicer siRNA were referred to as the siDicer group.

All LPS titration and hyporesponsiveness experiments for siDicer treated cells were carried as per protocol described in sub-section 2.1.2 but in 6-well plates in 2ml of media

2.1.7 TNF neutralisation

MP6-XT22 monoclonal anti-TNF- α antibody was used to neutralise soluble TNF- α in cell culture supernatants. Antibody was a gift from Dr. Louis Boon (Bioceros). Antibody neutralisation efficiency was measured by mRNA levels of IL-6, NOS2, IL-12p40 and IL-1 β and by measuring protein concentration of TNF and IL-6 in cell culture supernatants.

2.1.8 Western Blotting

Cells were washed with ice cold PBS. Protein extracts were prepared by treating cells with RIPA or radio-immunoprecipitation assay (RIPA) buffer (150mM NaCl, 10mM Tris HCL pH 7.2, 5mM EDTA, 0.1% Triton X-100, 0.1% SDS and 1% sodium deoxycholate) and then scraped directly from the plate. To inhibit protease activity, a cocktail of protease inhibitors P0044, P8340, P57266 (Sigma) were added in a 1 in 100 volume to RIPA buffer. The cell lysate was then collected and centrifuged at 10000g for 15 minutes after letting it stand on ice for 10 minutes. Lysates were stored in -20°C.

Total protein concentration was determined by a BCA (Bicinchoninic acid) assay from ThermoFisher Scientific. Samples were diluted 1 in 6 before quantification. 5 μ l of diluted sample and standards were added to the wells of a 96 well plate along with the working solution for BCA assay (made as per manufacturer's instructions). Plate was incubated at 37°C for 30 minutes for colour to develop and read on Molecular Devices VersaMax plate reader at 562nm. Standard curves were generated using bovine serum albumin (BSA) and from which the sample concentration was determined. Appropriate amounts of sample volume were determined to load 10 μ g of protein per lane in an SDS-page gel containing acrylamide. Samples were denatured by mixing them with sample loading buffer(4x, 250 mM Tris HCl pH 6.8, 8% SDS, 40% glycerol, 5% β -mercaptoethanol and 0.05% bromophenol blue) incubating them in heating block at 95°C for 10 minutes.

Samples were loaded onto an 8% SDS-page gel and run on a Bio-Rad PowerPac at 120V for 60–90 minutes for resolving proteins. After the run, gel was cut and sandwiched between blotting papers and with a polyvinylidene difluoride or PVDF membrane underneath to encourage transfer on a semi-dry western transfer unit (Bio-Rad) at 0.2A and limited to a maximum voltage of 25V. The PVDFs were activated by washing them in methanol for 1 minute before setting up the transfer cell. Upon successful transfer, membrane was blocked in 5% non-fat dry milk (Sigma-Aldrich) in

TBST with 0.1% TWEEN for 1 hour at room temperature. Membranes were left overnight in primary antibodies at 4°C with constant rolling in a falcon tube. HRP-conjugated secondary antibodies were added to the membranes thereafter at room temperature for 1 hour. The membranes were washed in TBST in-between and after antibody incubations 5 minutes each time for three times. After secondary incubation, the membrane was incubated in room temperature using ECL (GE Healthcare), a chemiluminescent substrate for HRP. The luminescence was developed on film and band quantification was done using ImageJ (National Institutes of Health, NIH). Quantification of target proteins were normalised to the loading controls, β -actin and GAPDH. Antibodies used are listed in table 2.2.

2.1.9 RNA Extraction

Cultured cells in wells were washed with PBS and then lysed in 700 μ l QIAzol (Qiagen) for processing the same day or stored in -80°C if RNA extraction was conducted on a later date. RNA extraction of lysed cells in QIAzol was done using Direct-zol mini prep (Zymoresearch) or using miRNAeasy kit (Qiagen) according to the manufacturer's instructions. RNA was eluted in nuclease free water and stored in RNase-free tubes (Appleton Woods). RNA quality was gauged on ThermoFisher's NanoDrop ND 2000 spectrophotometer based on A260/280 and A260/230 ratios.

Manufacturer	Antibody against	Clone	Dilution
Cell Signalling	Cas9	7A9-3A3	1:1000
Biolegend	Dicer1	N167/7	1:100
Abcam	β -Actin	AC-15	1:5000
Abcam	GAPDH	6C5	1:5000

TABLE 2.2: Antibodies used for western blotting

2.1.10 cDNA synthesis

Purified RNA was reverse transcribed to make cDNA using random hexamers (Promega). 50-200ng of RNA was loaded per cDNA sample in PCR tubes with 1 μ l of random hexamers, 1 μ l of 10 μ M dNTPs along with upto 13 μ l nuclease-free water. The sample strips were centrifuged briefly and then placed in a thermocycler (BIO-RAD) at 65°C for 5 minutes and then cooled to 4°C. 4 μ l of First strand buffer, 0.5 μ l of RNaseOUT, 2 μ l of 0.1M DTT, and 0.5 μ l of 200U/ μ l Superscript III (all from Invitrogen) were then added to each PCR tube. The samples were kept in the thermocycler for 10 minutes at 25°C, 50 minutes at 50°C and then finally, 5 minutes at 85°C to stop the reaction. Samples were stored at -20°C.

2.1.11 qRT-PCR

SYBR Green master mix (Applied Biosystems) was used to quantify mRNA expression. 10 μ l of SYBR Green per reaction was added along with 0.6 μ l of 10 μ M forward and reverse primers and 7.8 μ l of nuclease free water to MicroAmp Fast Optical 96-well plates (Applied Biosystems). 1 μ l of cDNA was then added directly into the master mix in the wells. Plates were sealed with adhesive films (Applied Biosystems), centrifuged at 1200g for 90 seconds and run on StepOnePlus Real-Time PCR Systems (Applied Biosystems) for 40 amplification cycles (95°C-60°C). *Hprt* and/or *Gapdh* were used as loading controls and analysis was done using the $\Delta\Delta$ CT (comparative cycle threshold) method.

2.1.12 CRISPR-Cas9 gene editing

RAW264.7 cells were plated at a density of 100,000 cells per well in a 24 well plate the night before transfection. Edit-R Cas9 Expression plasmids with puromycin resistance gene and synthetic RNAs (GE Dharmacon) were used to transfect RAW264.7 cells. Three pre-designed Edit-R crRNAs (CRISP RNA) for Dicer as per table 2.3 were selected for

knocking out Dicer. Cas9 nuclease expression plasmid (Dharmacon) was mixed with tracrRNA (trans-activating crRNA; Dharmacon) and crRNA (Dharmacon) in eppendorfs to obtain a final concentration of 25nM of the guide RNA (tracrRNA+crRNA) and 1 μ g/well of Cas9 plasmid in serum free media. The mix was allowed to stand in room temperature for 5 minutes. 50 μ l of 60 μ g/ml DharmaFECT Duo transfection reagent (Dharmacon) was added to the plasmid and guide mixture and incubated at room temperature for 20 minutes. The final volume of the mix was brought up to 500 μ l with antibiotic-free DMEM. The transfection mix was added and the cells were incubated in 37°C with 5% CO₂ for 48 hours. Cells were then split into DMEM containing 5 μ g/ml puromycin (Fisher Scientific) for selecting clones.

2.1.13 Transformation

Agilent XL-1 Blue supercompetent cells were used to amplify plasmids required for lentiviral assembly. Pre-made ampicillin (Sigma) supplemented agar plates were kept at room temperature to warm up. 30-50 μ l of XL-1 bacteria were added in a tube. The tube was swirled gently and then the 50-500ng of the required plasmid (with a ampicillin resistance gene) was added to the bacteria. The tube was incubated on ice for 30 minutes. The bacteria-plasmid mixture was given a heat pulse in a 42°C water bath for 45 seconds. After a brief incubation on ice for 2 minutes, 900 μ l of pre-warmed SOCS media (2% tryptone, 0.5% yeast extract, 10 mM NaCl, 2.5 mM KCl, 10 mM MgCl₂, 10 mM MgSO₄, and 20 mM glucose) was added. Finally, about 80 μ l of transformed bacteria were plated on agar plates with ampicillin. Appropriate negative and positive controls were used to confirm ampicillin based selection. Single colonies were picked from Agar

Target	crRNA sequence	Manufacturer	Part number
Dicer	GCTCGAAGAGGTGAGTTAAT	Dharmacon	CM-040892-01-0002
Dicer	GTGTTGAGTGGTACAATAAC	Dharmacon	CM-040892-02-0002
Dicer	CAAATTCTGAATGGGATATG	Dharmacon	CM-040892-04-0002

TABLE 2.3: crRNAs used for Edit-R Dharmacon transient transfection of Cas9 nuclease plasmids.

plates with ampicillin to culture transformed bacteria further. Plasmids were purified by Qiagen HiSpeed Midi kit using resin based binding of DNA. Resin-bound DNA was then eluted by QIAprecipitators using isopropanol as per manufacturer's instructions.

2.1.14 Lentiviral production and infection

Lentiviruses were packaged in HEK293T cells obtained from frozen stocks in the Lagos laboratory. Transfection was carried out in 10cm tissue culture dishes (Corning) with $3-4 \times 10^6$ cells plated a day before the transfection in full DMEM. On the day of the transfection, media was replaced with 8ml of warm reduced serum media Opti-MEM (Gibco) per plate. The plasmids lentiCrisprV2 (Addgene-52961), VSV-G (Addgene-14888) and $\Delta 8.14$ (Addgene-79047) were gifts from Dr. Tyson V Sharp (Barts Cancer Institute, London). 15 μ l Transfection reagent FuGENE (Promega) was added to 35 μ l Opti-MEM directly avoiding the tube walls per plate in an eppendorf. The mixture was allowed to stand for 5 minutes at room temperature. Approximately 1.5-2 μ g of DNA each for the transfer, packaging and envelope plasmid was then added to 50 μ l of Opti-MEM in a separate eppendorf. Finally, the DNA and FuGENE mix were added to each other to make up the total volume upto 100 μ l and allowed to stand at room temperature for 20-30 minutes. Effectively, the final transfection mix contained about 3 μ l of FuGENE per μ g of plasmid DNA. The transfection mixture was added onto plates dropwise. Control green fluorescence protein (GFP) expressing plasmids (pCSGW; Bainbridge et al., 2001, available in Lagos laboratory) were used to check if transfection was successful. 60 hours post transfection, viruses were harvested by passing the culture supernatant through a 0.45 μ m filter. Viruses harvested from different plates were pooled and aliquoted into 1ml eppendorfs and frozen at -80°C for later use

100,000 RAW264.7 cells were seeded in a six well plate a day before lentiviral infection. 1ml aliquots lentiviruses were thawed and warmed to 37°C for 2-3 minutes. Media from the wells were replaced with 1ml of lentiviruses. Lentiviral infection was confirmed

using GFP viruses 24 hours after infection. Cells infected with lentiCrisprV2 were split into puromycin for selection.

2.1.15 Limiting Dilutions

Monoclonal cell populations were selected by limiting dilutions in 96 well tissue culture plates (Corning) in full DMEM with 5 μ g/ml puromycin. Cells from transfection or lentiviral infections were grown in puromycin and then collected, counted and diluted to approximately 50-100 cells per 10ml of media. The cell suspension was well mixed by vortexing and 100 μ l of the suspension was added to each well to achieve a rough cell density of 0.5-1 cell per well. Plates were then left undisturbed for 10-15 days and then observed under a light microscope to look for wells with monoclonal colonies. These clones were further expanded for analysis.

2.1.16 Data Analysis

FlowJo (FlowJo LLC) was used to analyse all flow cytometry data. StepOne Software (Applied Biosystems) was used to analyse and export raw qPCR data which was further processed on Microsoft Excel.

2.1.17 Statistics

Statistical analysis was done using Graphpad Prism 6, Matlab and R. Statistics used were mentioned in figure legends. In general, goodness of fit was measured by the R^2 statistic. Treatment groups were compared using paired t-tests. Pie charts compositions were compared using Pearson's correlation matrix, Bray Curtis metric or t-SNE. Linear models were fitted by specifying the response and predictor variables in our empirical dataset in MATLAB 2017a.

Chapter 3

LPS challenge and inter-cellular communication drive macrophage population heterogeneity

3.1 Introduction

Clonal populations like pluripotent stem cells have been shown to have a variable gene expression landscape. Genes related to endogenous housekeeping roles are normally distributed and stably expressed in the population while genes involved in development and metabolism have been shown to be differentially expressed with bimodal distribution patterns (Kumar et al., 2014; Klein et al., 2015). A parallel of this response has been seen in differentiated but homogeneous myeloid cells that show instability or heterogeneity in the expression of key inflammatory proteins when stimulated with LPS (Shalek et al., 2013). Such bi-modality in the response in key inflammatory cytokines can play a critical role in response outcomes (Satija and Shalek, 2014) of immune cells. The challenge is to understand contributing factors that leads to this variability and how this can then be used to modulate outcome. In **Chapter 1**, possible contributory factors were discussed, especially in the context of a clonal population of cells responding to LPS. In response to LPS pro-inflammatory cytokines and mediators such as TNF, IL-6, NOS2 and

IL-1 β are expressed and/or secreted by macrophages. At the population level, LPS can have an effect on the amount of pro-inflammatory cytokines expressed both when LPS concentration in the environment is altered (Amura et al., 1998; Yang et al., 2017; Matsuura et al., 2010).

In this chapter, using flow cytometry, we look at expression of pro-inflammatory proteins at single-cell level to describe temporal snapshots of heterogeneous communities within a clonal population responding to LPS and show that these communities vary when the size of the LPS dose is perturbed. Further, we show that the community compositions can be significantly altered even with a crude disruption to inter-cellular communication and change in cellular density.

3.2 Aims

The prominent aim of this chapter was to determine if RAW264.7 cells respond heterogeneously to LPS and, if this heterogeneity can differentiate between primary LPS challenge as described below:

1. To describe a method to capture and visually represent population heterogeneity of LPS-induced pro-inflammatory response of RAW264.7 cells as a function of proteins measured at a single-cell level.
2. Compare population heterogeneity between LPS dose, inter-cellular communication and cell density to show if perturbing each of these factors can affect heterogeneity.

3.3 LPS induces pro-inflammatory cytokine secretion

3.3.1 RAW264.7 cells secrete TNF, IL-6 and nitric oxide upon LPS stimulus

As key inflammatory mediators, TNF (Kallioli and Ivashkiv, 2016), IL-6 (Hunter and Jones, 2015) and NOS2 (Bogdan, 2015) were chosen as our experimental outputs of an inflammatory response. We stimulated our macrophage model, RAW264.7 cell line with LPS to check cytokine secretion at 24 hours. Both TNF and IL-6 were found to be present in the culture supernatant. In addition, nitric oxide was found in the supernatant while none of the three inflammatory mediators were found at detection levels in untreated cells (**Figure 3.1**). Numerous studies have shown cytokine secretion in RAW264.7 cells upon LPS stimulus (Xiang et al., 2009; Kong et al., 2007; Dai et al., 2019; Zhuang and Wogan, 1997) and confirm our finding that RAW264.7 cell line, can secrete TNF, IL-6, nitric oxide upon stimulus with LPS.

3.4 Cytokine response at single-cell level is heterogeneous

3.4.1 Single-cell staining reveals cytokines have temporal profiles

To see how population level results translate to single-cell, we measured TNF, IL-6 and NOS2 upon LPS stimulus by flow cytometry. NOS2, the enzyme that catalyses the production nitric oxide, was measured to get an indirect representation of nitric oxide levels (Griffith and Stuehr, 1995). We stained our selected markers after 4 hours (**Figure 3.2a**) with LPS and Brefeldin A (BFA) to block secretion such that TNF and IL-6 could be stained intracellularly. We also stained cells after 24 hours (**Figure 3.2b**) of activation which included a 4 hour BFA incubation at the end (20 hour LPS + 4 hour LPS+BFA).

Labelling cells with an antibody against TNF, revealed that TNF expresses earlier than IL-6 or NOS2, staining positive in more than half the population (**Figure 3.2a**) at higher doses of LPS (10 and 100 ng/ml). Also, small differences between 100 and 1000

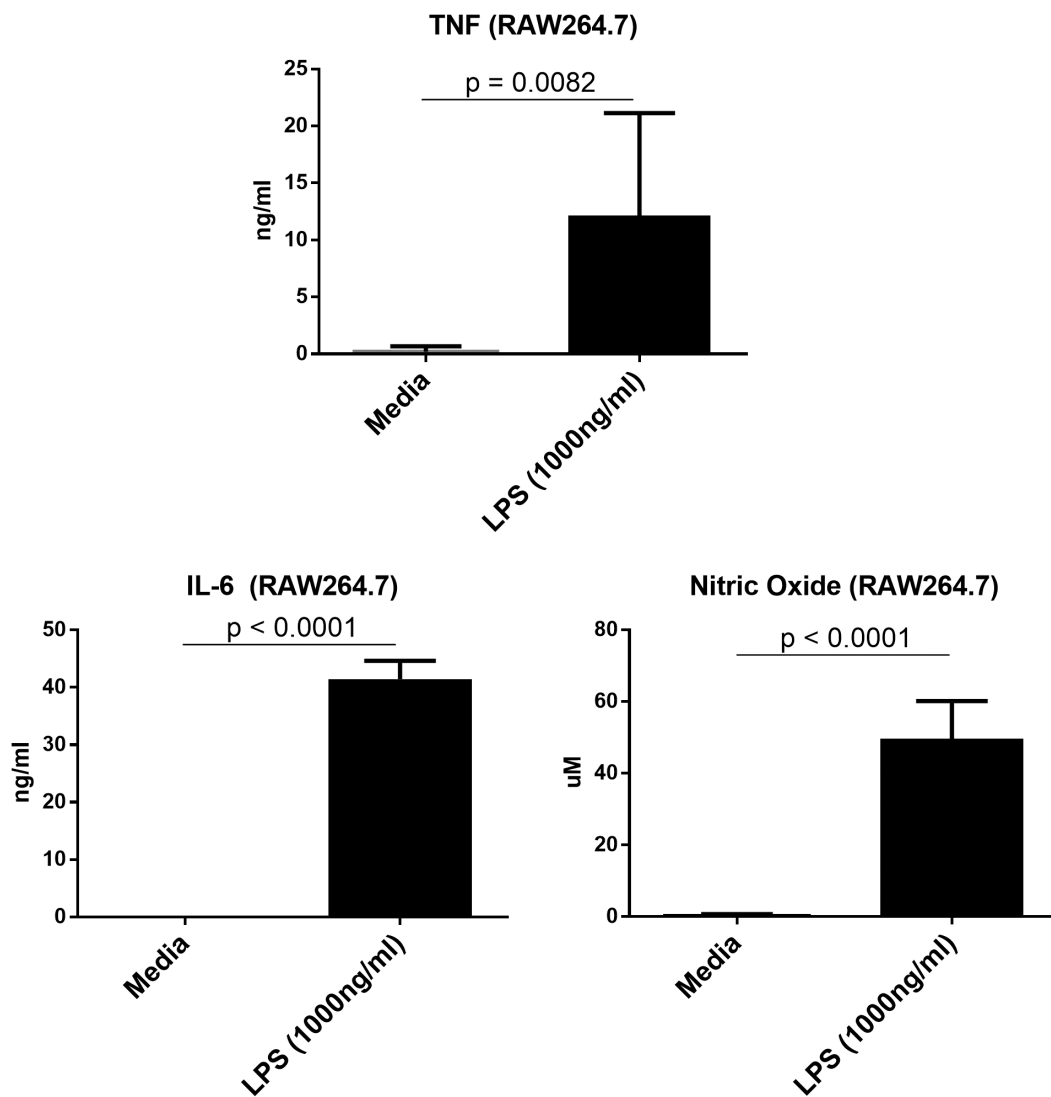


FIGURE 3.1: RAW264.7 cells produce TNF, IL-6 and nitric oxide upon stimulation with LPS

Bar plots showing TNF, IL-6 and nitric oxide (NO) levels in control and LPS-treated (1000 ng/ml, 24 hour) RAW264.7 cells. p-values were calculated using paired t-tests (n=6-10).

ng/ml of LPS in terms of frequency and median fluorescence was observed in TNF expression (**Figure 3.2**). At a low dose of 1 ng/ml, TNF positive cells are fewer than 50%, suggesting LPS dose to have an effect, at a single cell level, on how many cells respond to the stimulus. 24 hours of LPS stimulus with a 4hr BFA incubation showed only a small fraction of TNF+ cells **Figure 3.2b**. The median fluorescence intensity of these small fraction in all three LPS doses (when compared to untreated cells/media) showed an increase after 24 hours (**Figure 3.2c** for TNF). These positive fractions that appeared to express TNF in an analog way did not titrate to LPS dose (**Figure 3.2b** and **c** for TNF)

No IL-6 staining was detected at 4 hours of LPS stimulus suggesting IL-6 is made by RAW264.7 cells late into the LPS stimulus, whereas an increase in the mean fluorescence intensity was observed at 24hr (**Figure 3.2c** for IL-6). Since IL-6 was detected at the population level in the culture supernatant after a 24 hour LPS stimulus (**Figure 3.1**), this suggested that the empirical time points may be insufficient to capture the appearance and disappearance of IL-6 positive cells (**Figure 3.2a&b** for IL-6). No LPS dose induced difference was noticed in the staining for IL-6 at 24 hours.

NOS2+ cells appeared late into LPS stimulus with more than 50% cells staining positive for NOS2 at the highest dose of 1000 ng/ml and more than 20% cells responding at lower doses of LPS (**Figure 3.2b** for NOS2). In addition to LPS dose-dependency of NOS2 positivity, there was also an increase in the amount of NOS2 being produced at higher doses as indicated by an increased fraction of cells in the highest log-bin of **Figure 3.2b** fluorescence intensity and is represented by the consequent jump in the median fluorescence of NOS2 (**Figure 3.2c**). No NOS2 staining was detected within four hours of LPS stimulus across the LPS doses (**Figure 3.2a**).

Overall, these single-cell temporal snapshots showed these proteins have distinct temporal profiles and that LPS dose induces heterogeneity in the response to LPS with

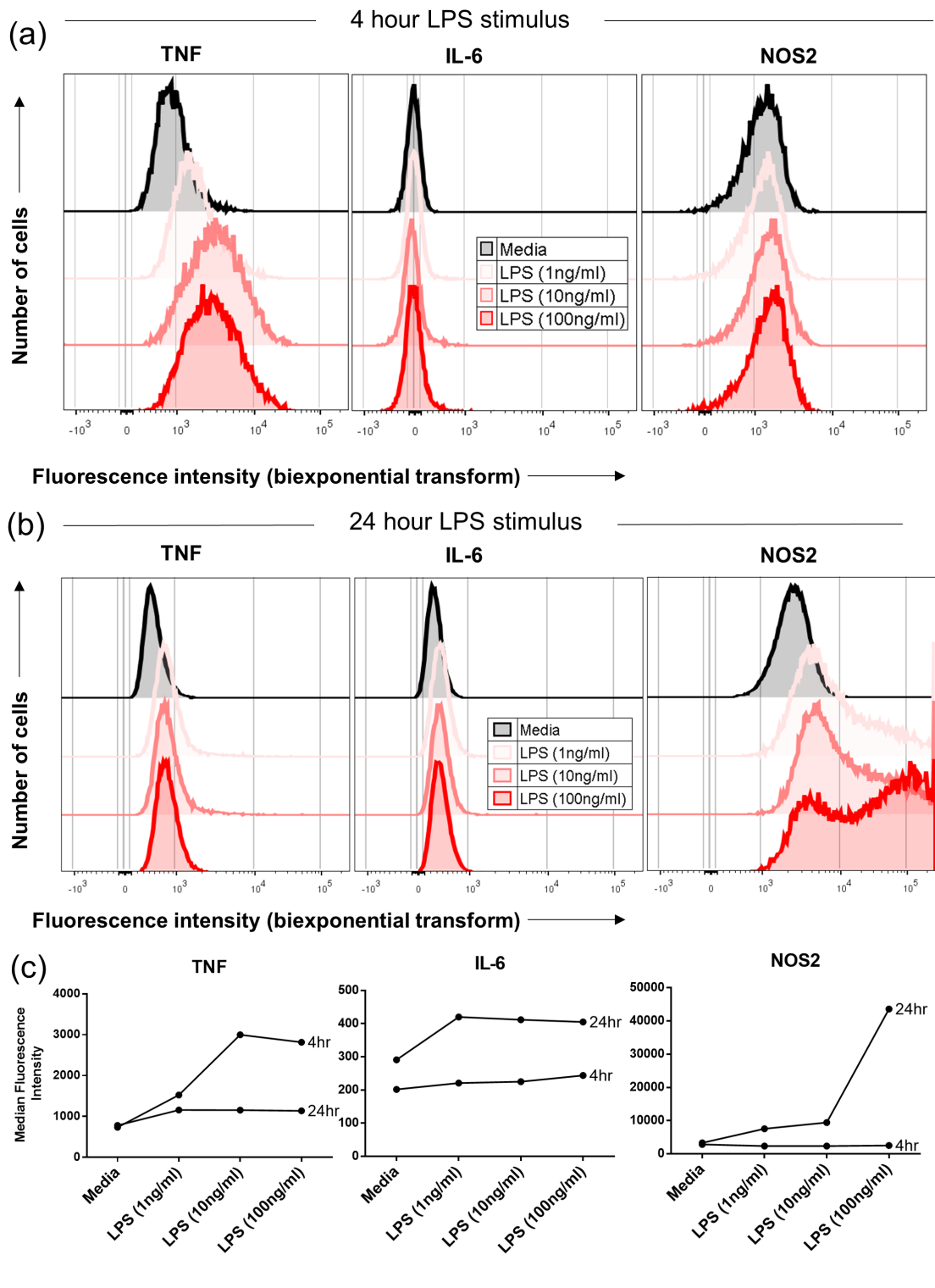


FIGURE 3.2: Single cell staining reveals distinct kinetics for TNF and NOS2

Histograms showing distribution of fluorescence intensity for TNF, IL-6 and NOS2 in RAW264.7 cells cultured in media only or at 1, 10 and 100 ng/ml concentration of LPS for **a** 4 hour (LPS+BFA) and **b** 24 hour (20 hour LPS + 4 hour LPS+BFA). **c** Before-after plots showing median fluorescence intensity of TNF, IL-6 and NOS2 for Media, and LPS doses of 1, 10, 100 ng/ml at 4 and 24 hour. Count of cells=50-100,000

fractions of populations responding to stimulus (TNF and NOS2 at 4hr and 24hr, **Figure 3.2a** and **b**) and, further, that a fraction of cells may even remain positive even after the rest of the population switches off, as seen in the case of TNF and IL-6 (**Figure 3.2a** and **b**) negating any all or none response in any of the measured proteins.

3.4.2 LPS response spurs a heterogeneous community in RAW264.7 cells

3.4.2.1 TNF, IL-6 and NOS2 positive cells can be visualised at 16 hours

We then stimulated RAW264.7 cells for 16 hours in LPS (12 hours in LPS plus 4 hours with the addition of BFA) to see if all three proteins can be visually represented and quantitated. Indeed, at 16 hours we could obtain a temporal snapshot of protein expression of TNF, IL-6 and NOS2. This temporal snapshot represents protein accumulation in a period of 4 hours (i.e. the duration of BFA incubation) between 12hr and 16hr of LPS stimulus and captures phenotype in terms of protein expression. Any fluctuations that may be present in a period less than 4 hours is ignored. To this effect, it has been reported that pre-made cytokines, such as TNF, can take about 30 minutes to be released (Salamanca et al., 2008) or can take up to 2 hours for *de novo* synthesis such as IL-6 that takes about an hour for gene expression and another hour for protein expression (Hoadley and Hopkins, 2003). As such we assume that a minimum 4 hour BFA incubation can capture the 'phenotypic' state of a single RAW264.7 cell based on whether it stains positive or negative for TNF, IL-6 and/or NOS2.

TNF expression (accumulation between 12-16 hours of LPS stimulus) titrated between LPS doses (**Figure 3.3a&b** for TNF) whereas median fluorescence was much higher for 1000ng/ml dose in comparison to the lower doses. In fact, the lower doses did not show a big difference between their median fluorescence suggesting, although more cells became positive as the dose of LPS increased between 1 ng/ml to 100 ng/ml on average they made similar amounts. In contrast, 1000 ng/ml of LPS not only increased

the frequency of cells expressing TNF but also increased the intensity of expression (**Figure 3.3c**). TNF expression snapshot between 12-16 hours was bi-modal in comparison to **Figure 3.2a** suggesting, especially at higher doses, most cells start expressing TNF early and, while some switch off expression, some continue to make TNF (**Figure 3.3a**).

IL-6 expression titrated almost equally well in terms of the frequency of positive cells and median fluorescence intensity of the population to the LPS dose suggesting that IL-6 expression of RAW264.7 cells, at least, at this time point is affected by LPS dose (**Figure 3.3**). Approximately, 50-75% of cells at higher doses of LPS (100 and 1000ng/ml respectively) and 13-21% of cells were positive at lower doses (**Figure 3.3b**), thus, showing IL-6 to be heterogeneously expressed based on the amount of LPS in the environment.

NOS2 expression upon LPS stimulus for 16 hours indicated that by this time point almost all cells start switching on NOS2 at high doses while there are about 27% cells at the lowest dose of LPS that do not switch on NOS2 production (**Figure 3.3b**). Interestingly, the range of NOS2 positive cells in the higher doses (10, 100 and 1000ng/ml) is narrow at 87-96% of the population suggesting that the size of the LPS dose may not have effect on whether NOS2 is switched on or not. However, on analysing the median fluorescence intensity, it is revealed that although most cells do switch on NOS2 production at low doses, the amount they make is much lesser than at higher doses of LPS (**Figure 3.3**). When NOS2 amount and frequency are both considered NOS2 response is heterogeneous and titrates to LPS dose.

Labelling cells with respective antibodies at this timepoint revealed that all three of the measured inflammatory mediators are LPS dependent and that each have a distinct behaviour. IL-6 expressing cells varied most (13%-75%) while TNF positive cells

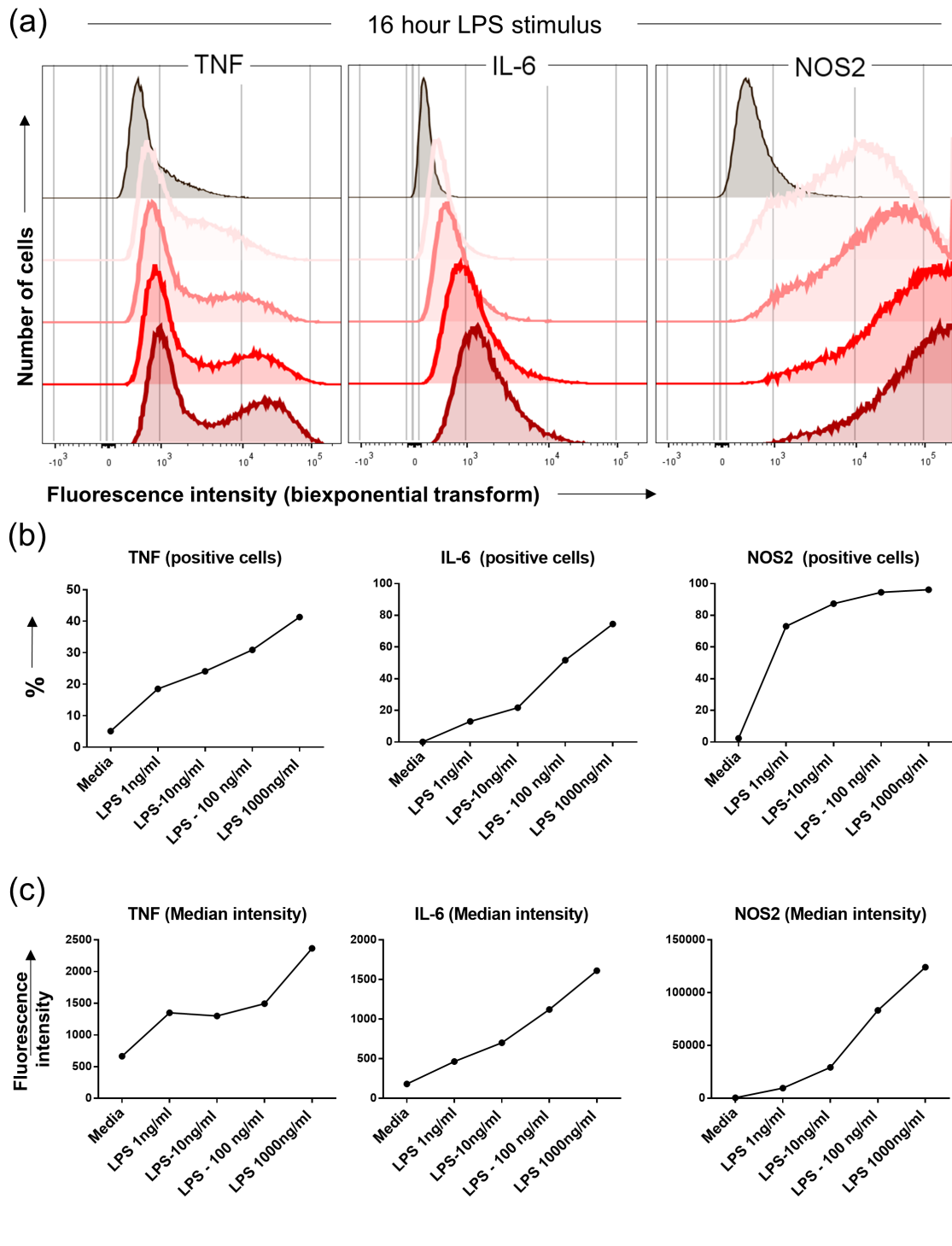


FIGURE 3.3: Heterogeneous population response titrates to LPS dose

a Histograms showing distribution of fluorescence intensity for TNF, IL-6 and NOS2 in RAW264.7 cells cultured in media only or at 1, 10, 100 and 1000 ng/ml concentration of LPS for 16 hours (12 hours LPS + 4 hours LPS+BFA). Before-after plots showing **b** percentage positive of total cells and **c** median fluorescence intensity of TNF, IL-6 and NOS2. Count of cells=100,000

(18%-41%) and NOS2 positive cells (73%-96%) showed lower variation to LPS dose respectively. The results also suggested that there are some cells within the responding population that when responding to a high dose of LPS are possibly high producers of TNF (**Figure 3.3a&c**). Similarly, IL-6 staining, although uni-modal showed a right tail which appeared more prominent at higher LPS doses suggesting the presence of a heterogeneous population of cells that maybe high producers of IL-6 (**Figure 3.3a**). The distribution of NOS2 expression, on the other hand, in all doses of LPS showed a small population of cells that were either negative or made less NOS2 in comparison to the majority of the population (**Figure 3.3a**).

Next, in order to capture the temporal snapshot at 16 hours of LPS stimulation for all the three proteins, we then looked at fluorescence intensity (of TNF, IL-6 and NOS2 antibodies) per cell to obtain information on whether, on an individual basis, cells were TNF, IL-6 and NOS2 positive. As such, leading to 8 possible sub-populations within the parent population such as cells that were positive for all three proteins (TNF+IL6+NOS2+) and triple negative cells (TNF-IL6-NOS2-). The other possible combinations consist of single and double positive cells and are represented as a pie chart and enumerated in the legend in **Figure 3.4**. These sub-populations are represented as slices of the pie to visualise macrophage heterogeneity as community composition of the RAW264.7 population.

To draw these pie charts (technique inspired from SPICE, Roederer, Nozzi, and Nason, 2011), we obtained the information for the pie by first gating on live cells. Next, we gated on the live population for single cells by selectively gating out populations that have higher forward scatter width in comparison to their forward scatter area to reject cells that may have clumped together. Further cells were subjected to a forward scatter versus side scatter gate for cell size and granularity to select intact cells. Next, cells that stained positive for both CD11b and F4/80, as canonical macrophage surface markers

(Taylor et al., 2005), were included in our analysis. Suitable isotype controls (**Figure 2.4** in **Chapter 2**) were then employed to identify background fluorescence of TNF, IL-6 and NOS2 in stimulated RAW264.7 cells.

Next we gated on TNF positive cells using a histogram to identify cells that expressed TNF against the isotype background. The TNF positive and negative populations were then gated separately to make bi-plots for IL6 and NOS2 to fragment the populations into the subtypes as described in **Figure 3.4**. Pies obtained with the above method represent population heterogeneity as community composition and can be used to compare treatments visually to draw insights of population heterogeneity in LPS-induced response.

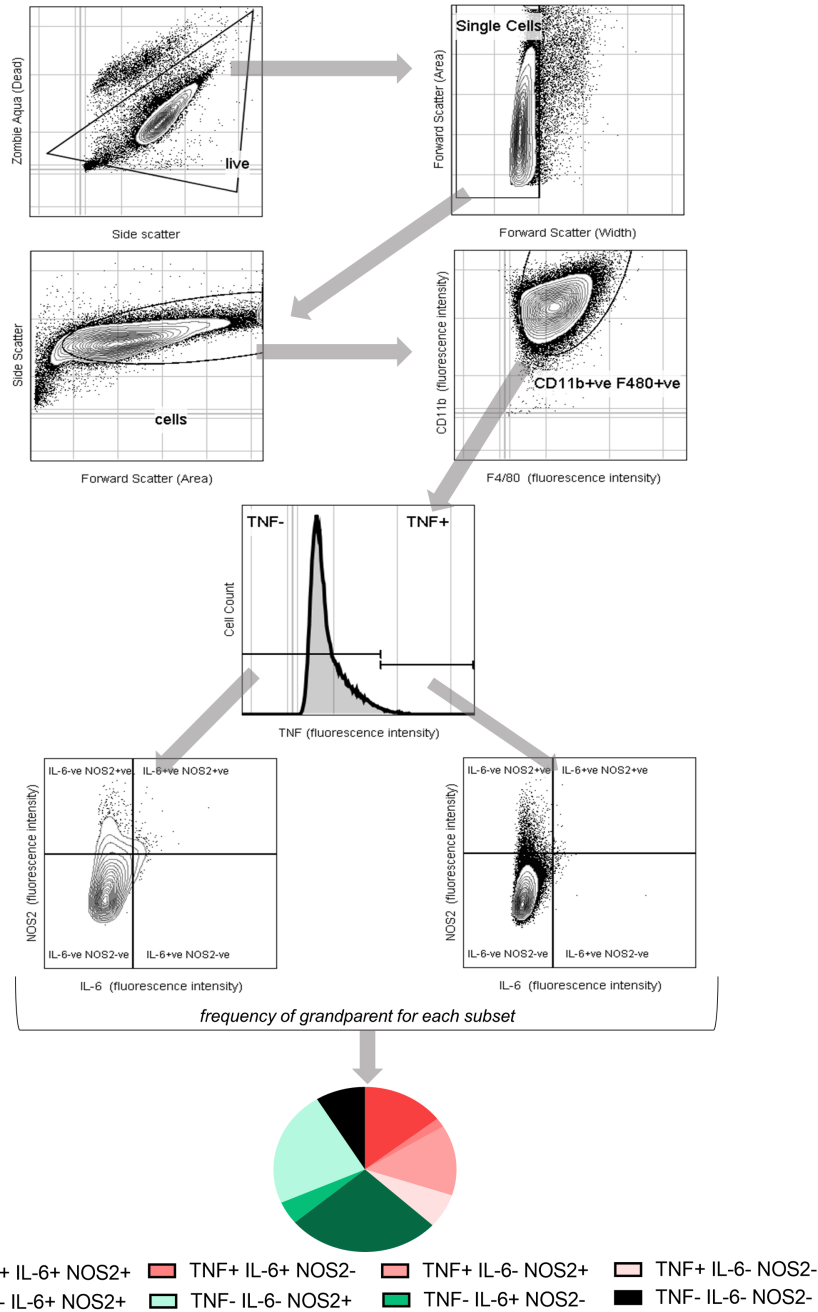


FIGURE 3.4: Visualising heterogeneous response as a community of sub-populations

Cells were pre-gated for live, single, intact cells, CD11b and F4/80. CD11b⁺ F480⁺ population was then used to create TNF⁺ and TNF⁻ sub-populations. TNF⁺ and TNF⁻ sub-populations were individually gated to IL-6⁺ and NOS2⁺ sub-populations using bi-plots. The resulting 8 sub-populations were then used to calculate their individual percentage in all CD11b⁺ F480⁺ population. The frequency data was then plotted as a pie chart with each pie slice representing a subset as enumerated in the legend.

3.4.3 LPS dose alters community consistency within a clonal population

We next compared temporal snapshots of community compositions across LPS doses to visually depict differences between the effects of LPS dose (**Figure 3.5a**). The media only or untreated cells depicted a homogeneous community which composed primarily of triple negative cells (TNF-IL-6-NOS2-) and some TNF+ cells (approximately 4%). Pie charts depicting community composition of cells stimulated with low doses (1 and 10 ng/ml LPS) and higher doses (100 and 1000ng/ml) were visually different and distil the underlying information of the histograms (**Figure 3.2a**) of all three proteins for an individual cell. The communities indicate a fundamental difference between dose response where higher doses tend to increase the frequencies of cells that have the strongest inflammatory response by making all three of the measured proteins while lower doses have a sizeable proportion of cells that are negative for any one, two or three of these proteins.

Double positive cells TNF+IL-6+NOS2- cells form a negligible proportion of cells (less than 1%) across LPS doses and, it may be inferred, that cells making both TNF and IL-6 but not NOS2 are rare, although, this may be a temporal effect. Cells making both TNF and NOS2 but not IL-6 (TNF+IL-6-NOS2+) form about 10-15% of the population and are consistent across LPS doses while TNF-IL-6+NOS2+, another double positive subset consistently increased with increasing LPS dose (**Figure 3.5a**).

Among single positive populations (those that were positive for only one of the three proteins) single positive TNF cells seem to be higher (5-9% versus 1-2%) in lower doses of LPS. Single positive IL-6 cells constituted a small sub-population (0.5-2%) increasing with LPS dosage. Single positive NOS2 cells formed a sizeable proportion of the population in 1, 10 and 100ng/ml LPS doses whereas it halved at the highest LPS dose (1000 ng/ml) (**Figure 3.5a**).

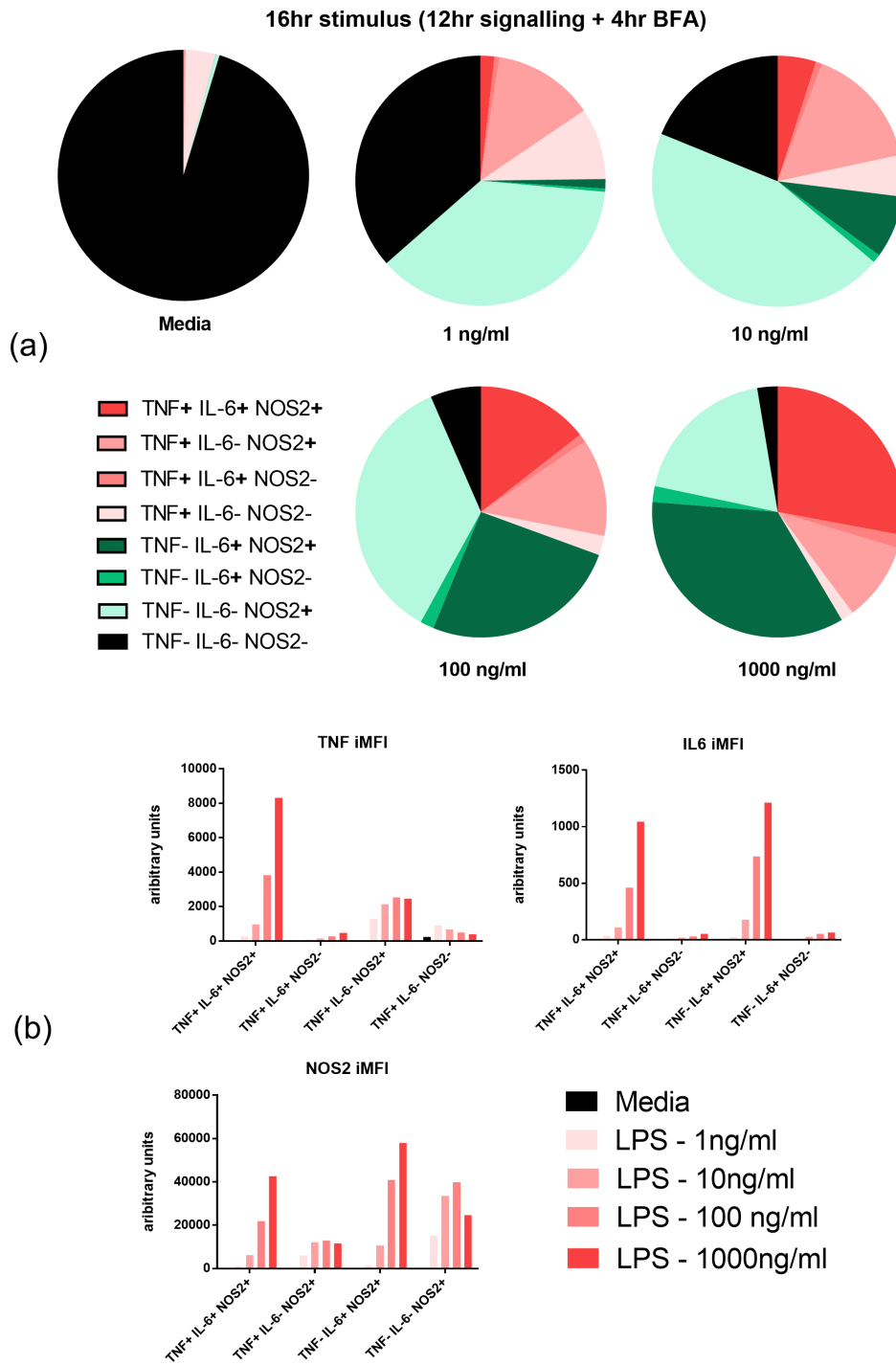


FIGURE 3.5: Visualising LPS stimulated RAW264.7 cells reveal heterogeneous communities

a Pie charts representing sub-population frequencies of RAW264.7 cells stained for TNF, IL-6 and NOS2 cultured in Media, or 1, 10, 100 and 1000 ng/ml of LPS. **b** integratedMFI (iMFI) bar plots to show TNF, IL-6 and NOS2 amounts as calculated from subset frequency and mean fluorescence intensity.

We then analysed if these sub-populations showed differential expression intensity of an individual protein i.e. whether triple positive TNF cells had a higher fluorescence intensity than single positive TNF cells. For this, we calculated the magnitude of the response also known as the integratedMFI (iMFI, Shooshtari et al., 2010) by multiplying sub-population frequency with mean fluorescence intensity. Triple positive cells produced most TNF at high doses (100 and 100ng/ml) whereas in low doses double positive cells for TNF and NOS2 but not IL-6 (TNF+IL-6-NOS2+) expressed more TNF (**Figure 3.5b**). Double positive cells for TNF and IL-6 but not NOS2 (TNF+IL-6+NOS2-) that were shown earlier to be a negligible sub-population, as expected, did not contribute much in TNF amount while, in contrast, single positive TNF+IL-6-NOS2- sub-populations made small contributions to the overall TNF amount despite being present (at about 10-15%) across all LPS doses (**Figure 3.5a&b**). This may indicate that some sub-populations, although positive for TNF, are low producers and, as such, further contribute to the heterogeneity in TNF secretion.

IL-6 amount was unaffected by TNF+IL-6+NOS2- (as in the case of TNF) and the single positive IL-6 sub-population, constituting a small proportion of cells, were part of this group. In addition, the mean fluorescence intensity of these sub-populations for IL-6 was not higher than the other sub-populations to have any affect in overall IL-6 expression. Double positive cells for IL-6 and NOS2 but not TNF (TNF-IL-6+NOS2+) and the triple positive sub-populations were the highest producers of IL-6. Interestingly, double positive population (TNF-IL-6+NOS2+) that increased with higher LPS dose produced more IL-6 than the triple positive population (**Figure 3.5a&b**).

NOS2 staining intensity when multiplied by various NOS2 positive sub-populations suggested a similar pattern with respect to double (TNF-IL-6+NOS2+) and triple positive populations contributing to most of the protein expression. Double positive cells IL-6 and NOS2 but not TNF made up to twice more NOS2 at higher doses of 100 and

1000ng/ml LPS. At low doses, however, NOS2 production could be attributed to single positive NOS2 cells (TNF-IL-6-NOS2+) or the double positive cells for TNF and NOS2 but not IL-6 (TNF+IL6-NOS2+).

Thus far, we have described a method to qualitatively visualise the heterogeneity in protein production of a population responding to LPS in terms of response-community composition. Further, utilising the mean fluorescence intensity (iMFI) of a sub-population we have then shown how much a sub-population contributes to the protein expression within the community. In this particular case, we demonstrate that heterogeneous response induced by LPS in RAW264.7 cells can be visually represented, quantified and that there are distinct sub-populations that manifest upon LPS activation of a macrophage community. It is shown that certain sub-populations of the LPS induced pro-inflammatory community, produce less or more protein compared to others as a function of how many cells there are in the sub-population and how much, on average, they make.

3.4.4 LPS induced community is variable but shows a trend

We then repeated experiments as described in **Figure 3.5** to obtain RAW264.7 community compositions responding to LPS at 16 hours to show that considerable plasticity underpins LPS response as visually apparent in **Figure 3.6** the pie slices of which are quantified in **Figure 3.7b**. Untreated cells did not show variability in their composition across the experiments, however, each of the LPS dose showed considerable variability between experiments. This variability appeared to be more pronounced as the LPS dose increased, as such, 1000 ng/ml LPS dose showed greater fluctuations to community composition than the lowest dose. This suggests that cells responding to high doses of LPS may be more susceptible to the unevenness in the response.

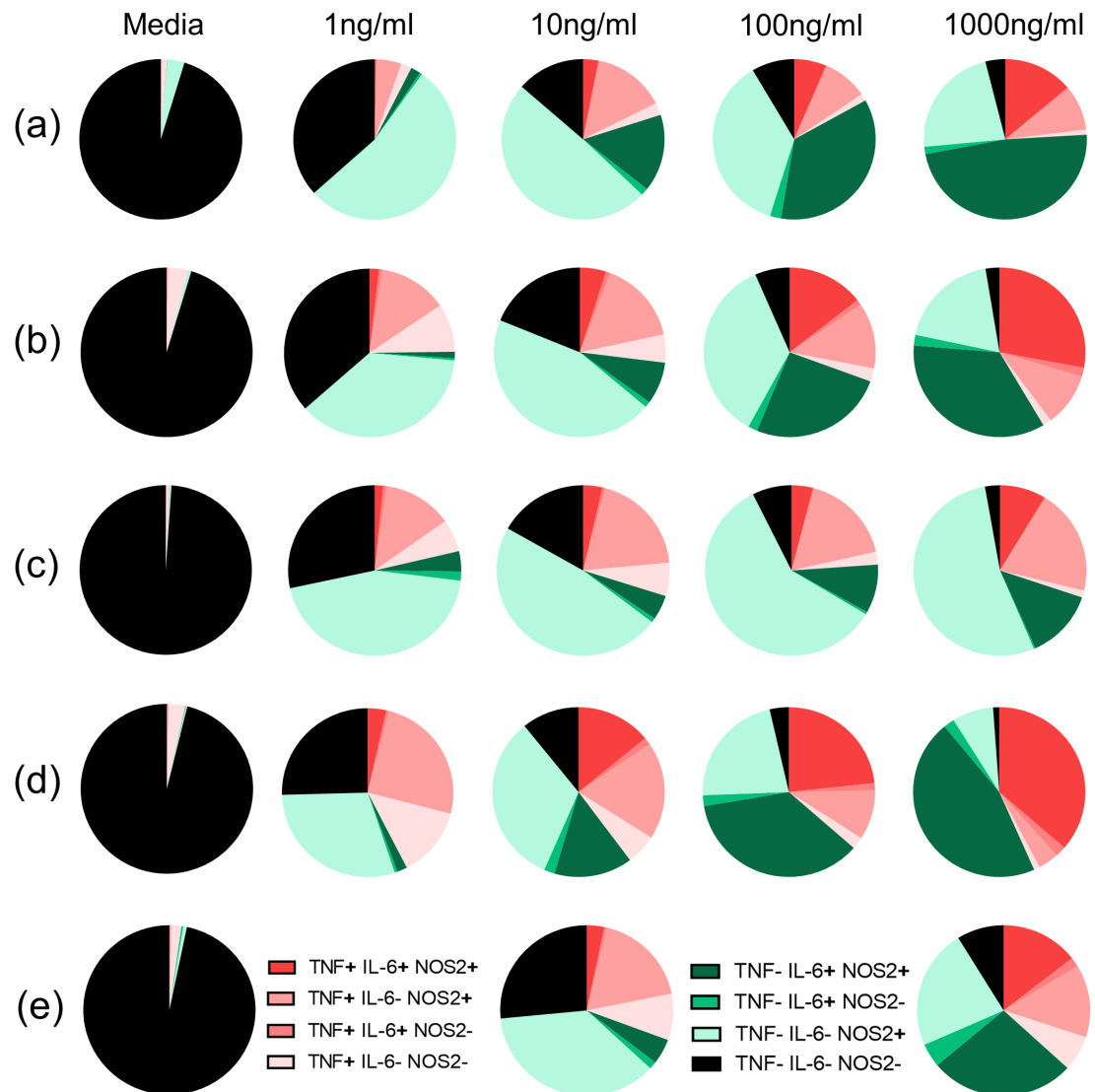


FIGURE 3.6: LPS induced communities show inter-experimental variability

Pie charts representing sub-population frequencies of RAW264.7 cells stained for TNF, IL-6 and NOS2. Count of cells=50,000-100,000. a, b, c, d and e represent individual experiments.

We then quantified the frequency of cells overall positive for TNF, IL-6 and NOS2 to check if dose-induced effects of LPS can be uniquely identified on these three species as independent measures (**Figure 3.7a**). Mean TNF+ cells after 16 hours of LPS stimulus remained between 23-35% between the lowest and highest LPS dose. NOS2+ cells titrated to LPS doses with mean NOS2+ cells between 59%-90% between lowest and highest dose of LPS and with a greater range between high and low of dose LPS in comparison to TNF. However, mean NOS2+ cells showed low variability (75%-90%) between 10, 100 and 1000 ng/ml of LPS and, thereby, offering low predictability between higher doses (**Figure 3.7a**). IL-6+ cells predict LPS dose most effectively with mean IL-6+ cells rising incrementally at 5, 17, 41 and 57% for 1, 10, 100 and 1000ng/ml LPS treatment. In addition to variability between LPS doses, IL-6+ cells were highly variable among experiments across all species for all doses with an average co-efficient of variation or CV (standard deviation/mean, expressed as a percentage) of 41% as compared to 30% and 6% for TNF+ and NOS2+ cells respectively. Intriguingly, TNF+ cells are the most variable with a CV of 52% at 1 ng/ml when a single dose of LPS is considered (calculation not shown, **Figure 3.7a**). From these results, it can be speculated that a population of RAW264.7 are variable in the production of TNF when LPS doses are low while IL-6 production is generally variable and with higher doses of LPS more prone to higher variability in IL-6+ cells.

In **Figure 3.7b**, we checked if the variability, in community composition shown between experiments show any overall consistency to discriminate between LPS doses. We speculate that the presence of TNF+IL-6+NOS2+ and TNF-IL-6+NOS2+ sub-populations are a determinant of high doses of LPS whereas higher proportions of TNF-IL-6-NOS2- cells are a key component of the community responding to low doses of LPS. Using t-SNE based unbiased clustering reveals triple positive cells and TNF-IL-6+NOS2+ to separate out as a distinct cluster (**Figure 3.8a**) while clustering on the basis of sub-populations separate low to high doses of LPS (**Figure 3.8b**).

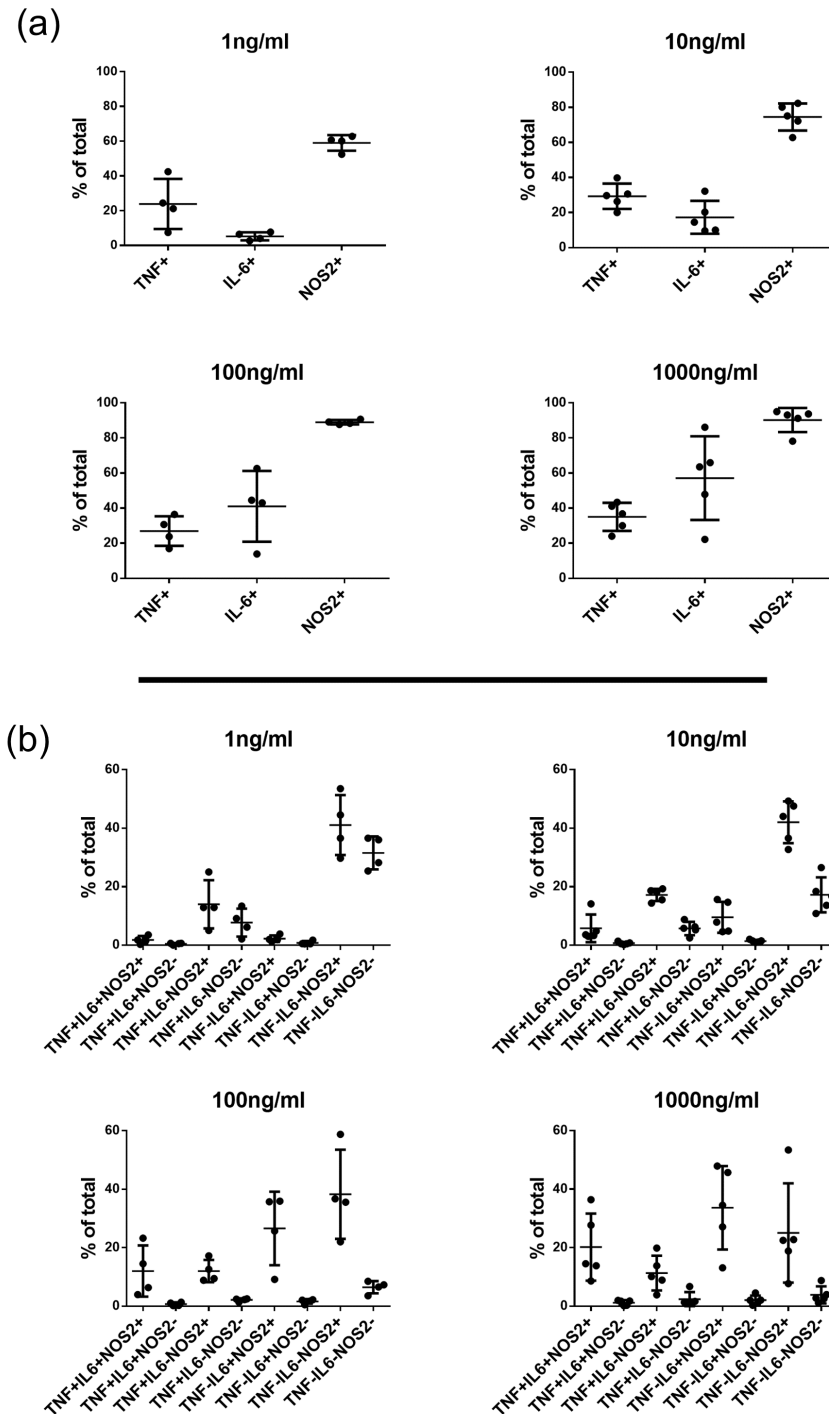


FIGURE 3.7: LPS induced communities are variable but underlying patterns are consistent

Scattered dot plots showing mean and standard deviation of **a** TNF+, IL6+ and NOS2+ **b** TNF, IL6, NOS2 sub-populations of RAW264.7 cells cultured in 1, 10, 100 and 1000 ng/ml LPS.

Individual dots in both **a** and **b** represent independent experiments. n=4-5

Interestingly, these two sub-populations also correlated well with $R^2 = 0.64$ (**Appendix Figure 8.1**).

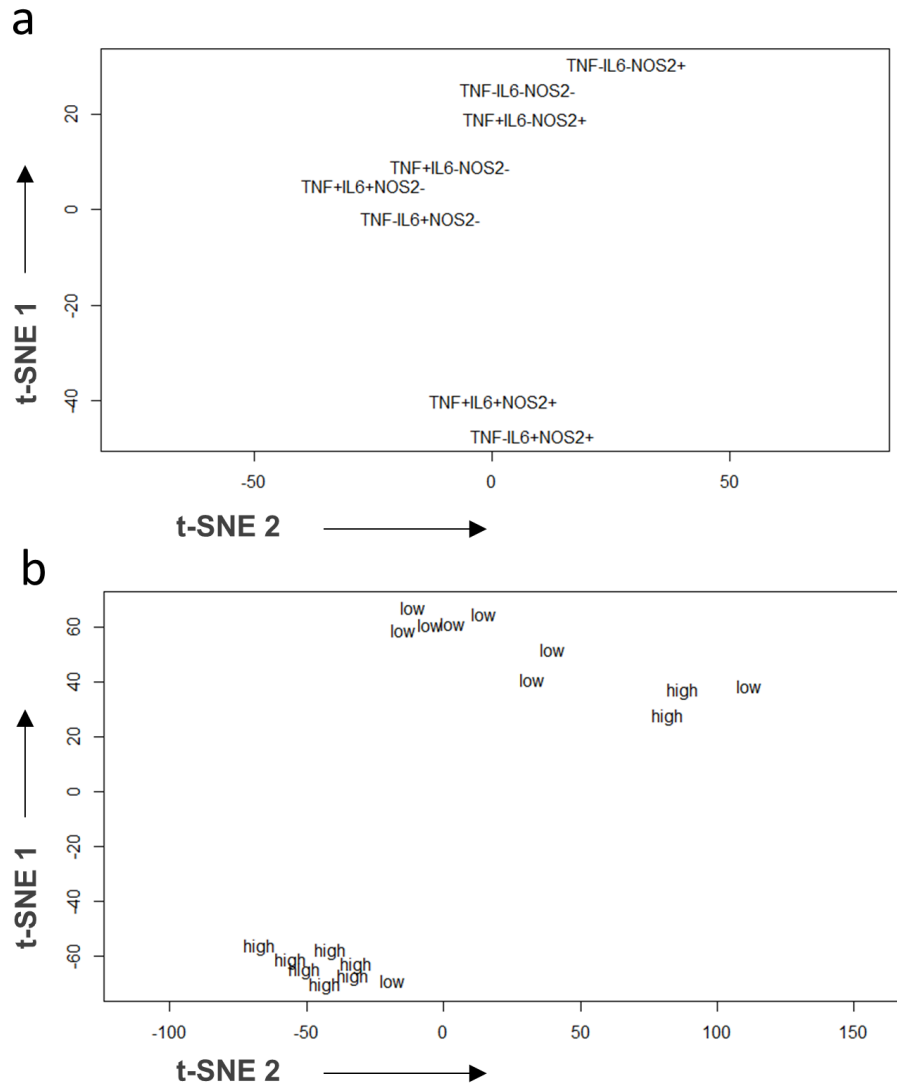


FIGURE 3.8: **Low and high LPS doses and inflammatory perpetrators cluster by unbiased approaches**

Clustering analysis using t-SNE with a perplexity value of 5 for: **a** RAW264.7 community sub-populations as from **Figure 3.7 b** With LPS doses shown as either low (1 and 10ng/ml) or high (100 and 1000ng/ml)

3.4.5 TLR4 expression and cell size do not contribute to response heterogeneity

We next wanted to see if this LPS induced heterogeneous response had a simple explanation based on heterogeneous expression of the surface receptor TLR4 that initiates the LPS-induced response. We found that it is expressed uni-modally in untreated cells (**Figure 3.9a**). This suggested TLR4 is tightly expressed and, as such, absence of any underlying sub-populations with differential TLR4 expression. 12 hours of LPS stimulus resulted in the down regulation of TLR4 approximately half as much as higher doses (10, 100 and 1000ng/ml; **Figure 3.9b**). While low dose of LPS effect may lead to a weaker downstream response, the distribution of TLR4 expression itself may not contribute to the heterogeneous response (**Figure 3.9a**).

We also looked at the expression of co-stimulatory cluster of differentiation molecule 86 (CD86), as an activation marker of macrophages (Delgado et al., 1999; June et al., 1994) which appeared to be bi-modally expressed in a clonal population. Upon LPS stimulus, however, CD86 was upregulated with the population median increasing towards a more uniformly activated distribution (**Figure 3.9a&b**). Again, like TLR4, CD86 activation was half as much at the lowest dose than the higher doses. CD86 may be further examined as a determinant of the heterogeneous outcomes to LPS (**Figure 3.9a**) but was not the focus of this study. We then looked at cell size and found that there was no difference in the expression levels of TNF, IL-6 or NOS2 across sizes of cells as measured by forward scatter and seemed to uniformly fill the log-decades of fluorescence intensity for all three proteins as compared to untreated cells (**Figure 3.9c**). Based on this we infer that size of RAW264.7 cells may not be the cause for a heterogeneous response to LPS.

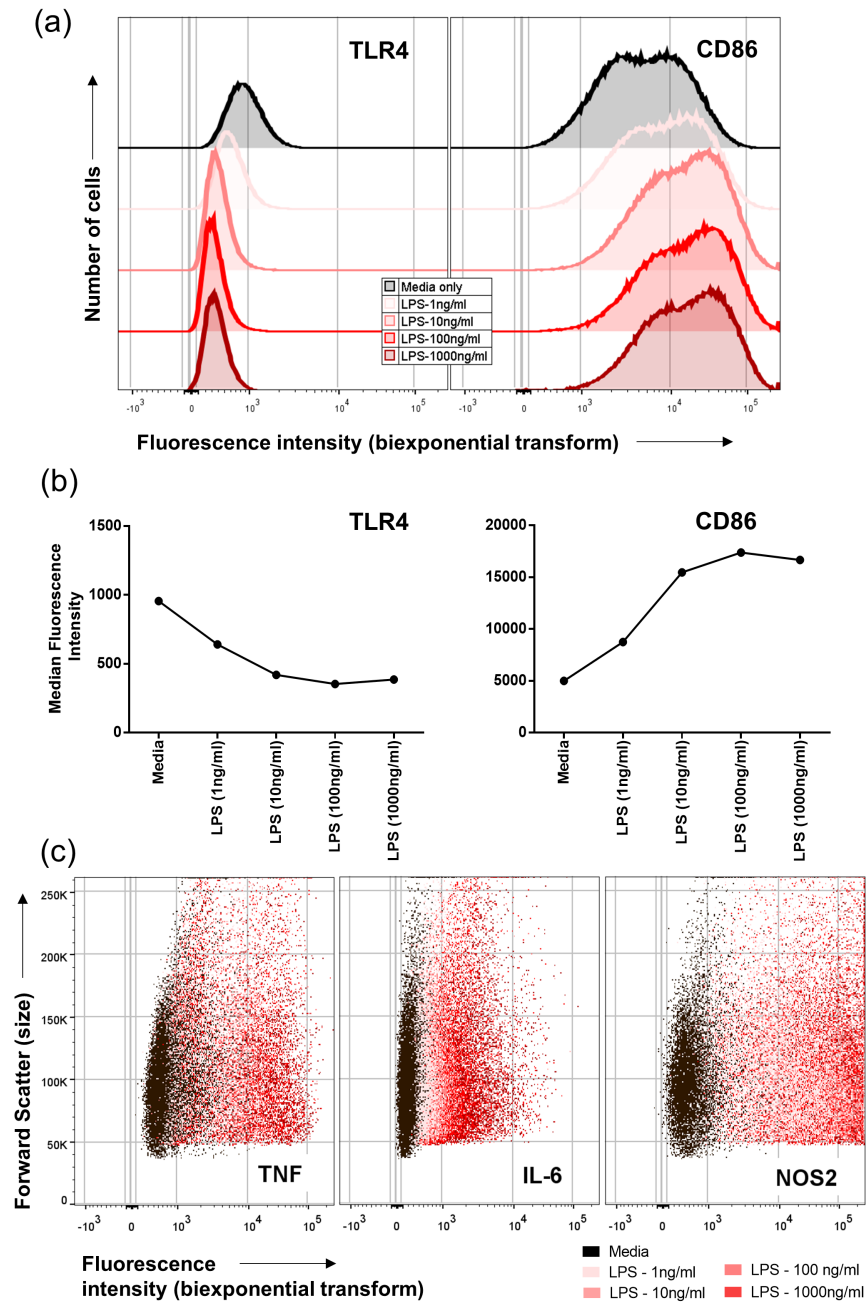


FIGURE 3.9: TLR4 expression distribution and cell-size effects are negligible in stimulated RAW264.7 cells.

Histograms showing a distribution of fluorescence intensity b Before-after plots showing median fluorescence intensity for TLR4 and CD86 in RAW264.7 cells cultured in media only or at 1, 10, 100 and 1000 ng/ml concentration of LPS for 12 hours c Bi-plot shows each cell as a dot with y-axis representing size of the cells and x-axis the fluorescence intensity of TNF, IL-6 and NOS2. Count of cells=50-100,000

3.5 First challenge of LPS shapes community composition

3.5.1 Inter-cellular communication drives macrophage community

Having shown community compositions change rapidly at approximately 8 hours into the first LPS stimulus (**Figure 4.3**), we wanted to know if the first LPS challenge does indeed change the community composition across LPS doses or whether this was just an effect seen at high doses of LPS. Towards this end, we treated RAW264.7 cells with 4, 8, 12 and 16 hours of BFA incubation in a total 16 hour LPS stimulation (**Figure 3.10**) to reveal that cytokines produced in single cells had distinct distributions for IL-6 and NOS2, especially, at longer incubations of BFA (**Figure 3.10a**) and community composition differences between 4 and 8 hr BFA and 12 and 16 hr BFA incubations were visually distinct (**Figure 3.10b**).

Histograms describing single-cell distributions of TNF, IL-6 and NOS2 revealed large proportions of populations to be positive for each protein at the 16hr and 12hr BFA incubation, and can be explained trivially by maximum accumulation effect appearing at longer incubation periods (**Figure 3.10a**). In 16 hour BFA community, a small proportion of TNF+ cells was found piled up at the highest fluorescence intensity bin. This may suggest that either a high TNF producing population is lost if the cells are allowed secretion for the first four hours (as this population is not seen in 12, 8 and 4 hr BFA incubations) or, alternatively, upon LPS stimulus a small proportion of TNF+ cells produce a lot more TNF than the rest of the population. These high producers appeared irrespective of LPS dose. Interestingly, effect on TNF expression upon secretion restriction for 12 (or 16) hours was not pronounced. The effect of LPS dose in terms of increasing median fluorescent intensity of TNF was more prominent in the shorter incubations of BFA suggesting the role of secretion in dampening the effect of TNF positivity and/or, simply, that higher doses of LPS correlate with higher proportion of TNF+ cells, that remain longer into the stimulus. TNF intensity distributions at high

doses of LPS (100 and 1000 ng/ml) at 4 hr BFA incubation seemed distinctly bi-modal compared to lower doses suggesting, that at higher doses, late phase TNF production characteristics of a population is more pronounced (**Figure 3.10b**, TNF).

IL-6 positive cells were distributed as a long right-tailed uni-modal population at 4hr and 8hr BFA incubations whereas the distribution appeared to be more bi-modal when secretion was restricted for more than or equal to 12 hours. The bi-modal population is interesting because the cells that belonged to the smaller mode were IL-6+ as well suggesting either a fraction of cells are high IL-6 producers in the first 4 hours into LPS stimulus or that restriction of secretion leads to high IL-6 producing cells that follow a distinct distribution to the majority population. Interestingly, despite restrictions in secretion IL-6 positivity titrated for all LPS doses and conditions (**Figure 3.10b**, IL-6).

NOS2 protein distribution showed positive cells titrated to LPS across the LPS doses but with 1 ng/ml stimulus leading to a more bi-modal response. Other higher doses seemed to increase NOS2 positivity comparably. However, NOS2, which is not secreted, is most affected at lower BFA incubations as is evident by its median fluorescence intensity increase with LPS dose (4 and 8 hr BFA incubation). In terms of NOS2, it must be noted that while NOS2 positivity of a cell is not affected much by restricting secretion, the amount of NOS2 made (median fluorescence intensity) is effected (**Figure 3.10a**, NOS2).

Combining the histogram data for each individual cell and visually inspecting community compositions across our treatment regime (LPS dose and BFA time), we find that communities that have secretion restricted for more than 8 hours are distinct from those that secrete for longer (**Figure 3.10b**). The time period between 0-8hr or 0-12hr into LPS stimulation may be crucial in shaping the heterogeneity of macrophage response to LPS. As shown previously, RAW264.7 cell communities responding to LPS have a higher

proportion of triple positive cells making TNF, IL-6 and NOS2. This is observed as dose of LPS increases and by increasing BFA time. Thus, implying the inflammatory response of these macrophage-like cells is not only stronger with LPS dose but also without community feedback. This suggests that inter-cellular communication is required for optimal resolution of macrophage responses to LPS.

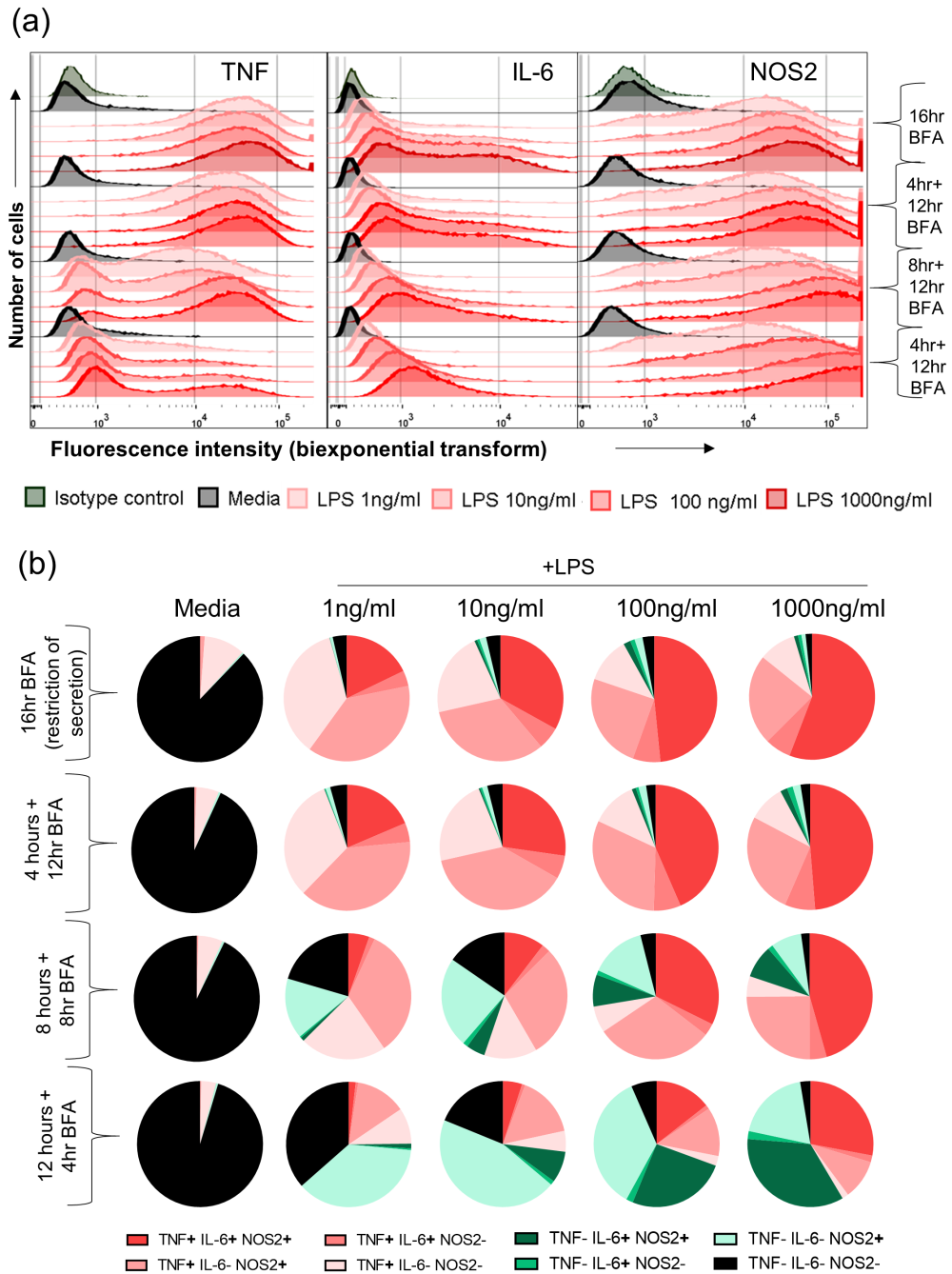


FIGURE 3.10: Restricting secretion of signalling proteins can give visual insights on community composition

a Histograms showing distribution of fluorescence intensity for TNF, IL-6 and NOS2 and **b** pie charts depicting sub-populations in RAW264.7 cells cultured in media only or at 1, 10, 100 and 1000 ng/ml concentration of LPS for **b** 16 hour LPS+BFA; 4 hour LPS and 12 hour LPS+BFA; 8 hour LPS and 8 hour LPS+BFA; 12 hour LPS and 4 hour LPS+BFA. Count of cells=50-100,000

3.6 Community-level effects are retained upon adding another cytokine

To test whether the effects we observed was restricted by our choice of TNF, IL-6 and NOS2, we expanded our panel to include two other inflammatory mediators IL-1b-pro and GM-CSF. We chose IL-1 β because it is an acute phase inflammatory cytokine (Zheng et al., 1995) and is widely implicated in inflammatory diseases (Ren and Torres, 2009). We chose the antibody for pro-IL-1 β or the inactive form as IL-1 β is released from cells with an alternative mechanism than ER/Golgi traffic as it lacks a signal sequence (Rubartelli et al., 1990). GM-CSF is a growth factor implicated in myeloid cell T-cell cross talk and GM-CSF producing macrophages can be instrumental in tissue damage (Becher, Tugues, and Greter, 2016). We included pro-IL-1 β and GM-CSF to see if community sub-populations could still be observed within the new panel (Appendix **figure 8.3**). Our results, indicated that an 8 hour divide exists when inflammatory communities change composition.

We next performed further experiments including pro-IL-1 β along with TNF, IL-6 and NOS2 to look at sub-populations based on the four proteins. A total of 16 theoretically possible sub-populations were plotted as communities whose secretion was restricted for 16, 12, 8 or 4 hour as shown in **Figure 3.11**. These results confirmed again that community level differences exist between LPS dose. Also, that restricting secretion, shows a change in community composition between the 8-12 hour time after LPS challenge (Figure 3.11).

Interestingly, community compositions were also indicative of what sub-populations are unlikely to appear (Figure 3.11) suggesting proteins that are unlikely to be expressed along side other.

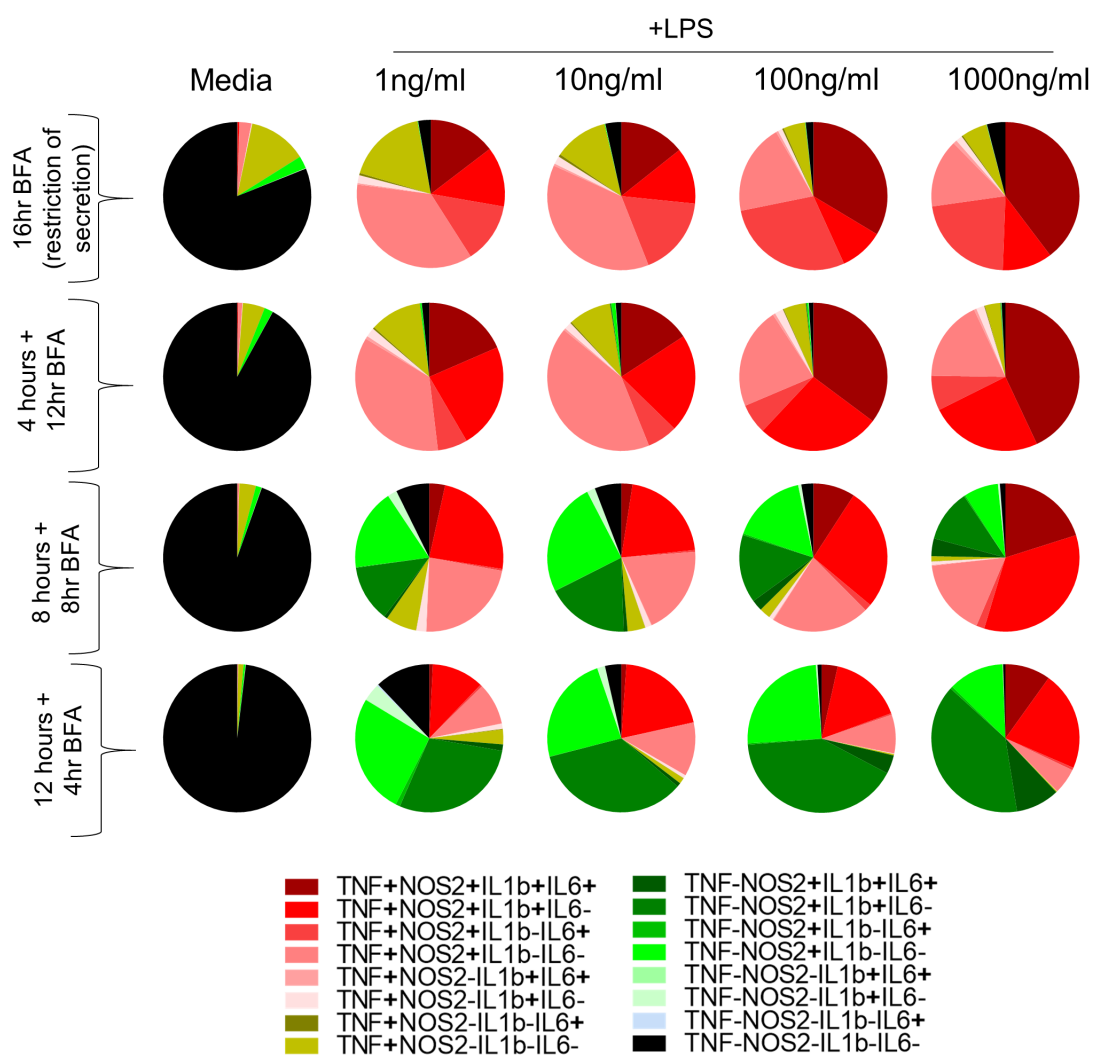


FIGURE 3.11: **Community composition complexity is increased on adding another cytokine**

Pie charts depicting sub-populations based on TNF, IL-6, NOS2 and pro-IL-1 β in RAW264.7 cells cultured in media only or at 1, 10, 100 and 1000 ng/ml concentration of LPS for a 16 hour LPS+BFA; 4 hour LPS and 12 hour LPS+BFA; 8 hour LPS and 8 hour LPS+BFA; 12 hour LPS and 4 hour LPS+BFA. Count of cells=50-100,000

3.6.0.1 Restriction of secretion alters responses to LPS

Next we analysed the four-dimensional data set from LPS and BFA treatments (**Figure 3.11**) using a Pearson's correlation matrix to show that communities with longer secretion do not correlate well with communities with secretion longer than 8 hours while communities of 4 hr and 8 hr BFA were strongly correlated as did 12 hr and 16 hr BFA communities. Communities with 4 hr and 8 hr BFA incubations when compared with 16 hr BFA communities had correlations value close to zero (**Figure 3.12**).

A pie-by-pie comparison reveals some correlation (<0.7) between communities that are treated with low doses LPS (1 and 10 ng/ml) and whose secretion has been restricted longer than 8 hr BFA with communities treated with high doses of LPS whose secretion is restricted for less than or equal to 8 hours. This suggests, although, community composition diversity is dependent on restriction of secretion but there exists a continuum of composition diversity which is also affected, if modestly, by the dose of LPS (**Figure 3.12**). Overall, our correlation analysis confirms what we have visually shown previously (**Figure 3.10**) that treatments where secretion is restricted for longer than 8 hours do not correlate with treatments where secretion restriction is less than 8 hours.

We further probed our data set with an ecological ordination metric Bray-Curtis dissimilarity to see how communities separate from each other representing qualitative and quantitative differences in community composition induced by LPS. The effect of LPS dose on communities is only apparent when secretion is restricted for less than 8 hours (**Figure 3.13**). The treatments where restriction of secretion is longer than 8 hours cluster close to each other suggesting antigen itself incapable of causing a differential effect when secretion is restricted. Control populations that are treated with BFA but not LPS all lie close to each other and away from the LPS stimulated samples and, thus, are distinct and distant in composition.

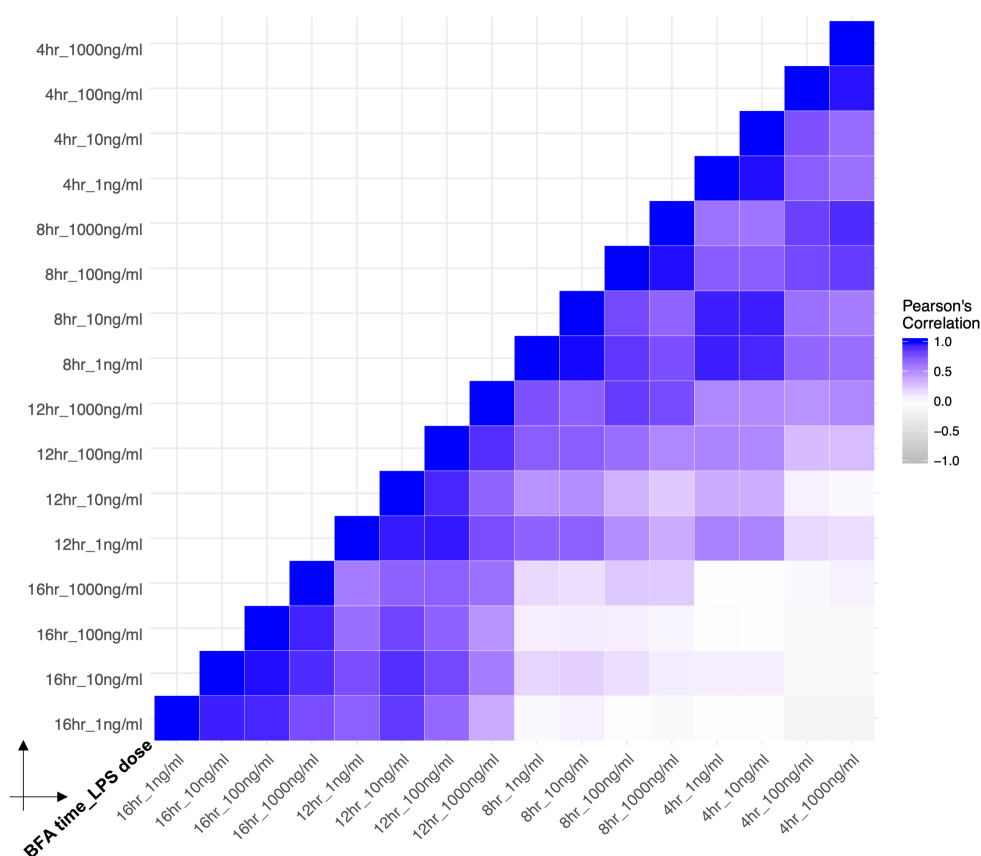


FIGURE 3.12: LPS stimulated RAW264.7 macrophages show weak to no correlation to those that have their secretion restricted for longer than 8 hours.

Pearson's co-efficient matrix displayed as heat map to compare linear correlations between RAW264.7 sub-populations as shown in **Figure 3.11**. Correlation value -1, 0 and 1 represent anti-correlation, no correlation and maximum correlation.

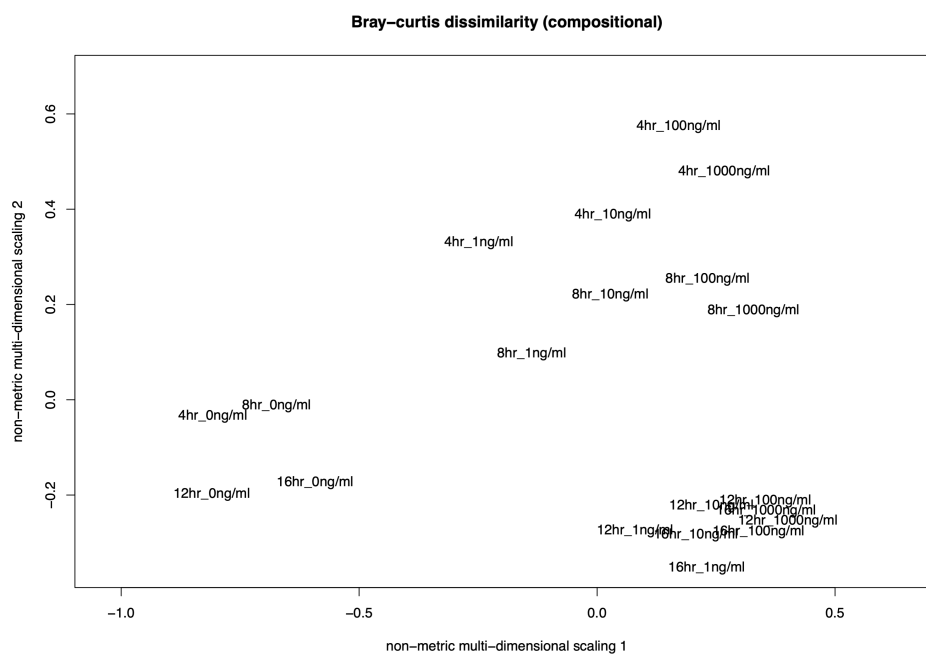


FIGURE 3.13: LPS stimulated RAW264.7 macrophages with secretion restricted for lesser than 8 hours are show separation with LPS dose

A Bray-Curtis dissimilarity matrix was calculated for population sub-populations based on RAW264.7 sub-populations as shown in **Figure 3.11** and the corresponding non-metric dimension plotted as an X,Y scatter plot. Shorter distances represent greater community similarity between treatments (LPS dose and BFA incubation time)

3.6.0.2 Isolated communities resemble communities whose secretion is restricted

Since restriction of secretion with BFA can stop autocrine/paracrine effects but also create an artificial environment for the cell. Therefore in order to recreate a condition where paracrine effects may have less effects, we plated an equal number of cells (250,000) alongside in a 24 well plate and in a T75 flask. A T75 flask is approximately 40 times the surface area of a well in a 24 well plate. Thus, by increasing the distance between cells and the volume of media, we checked the effect on the community composition of the cells. 4hr BFA time in a T75 visually appeared to be more akin to parallel treatments in a 24 well plate that had secretion restricted for 12 hours (**Figure 3.14**) with a correlation score of 0.89 and even correlated better (score=0.74) with 16hr BFA in 24 well as compared to the identical treatment in a 24 well (score=0.3). Since isolation does not stop autocrine signalling some of the sub-populations that appear in the cells cultured in T75 flask may be due to exclusive autocrine effects. However, the higher correlation to restriction secretion scenario must then suggest a greater role of paracrine effects in LPS induced communities.

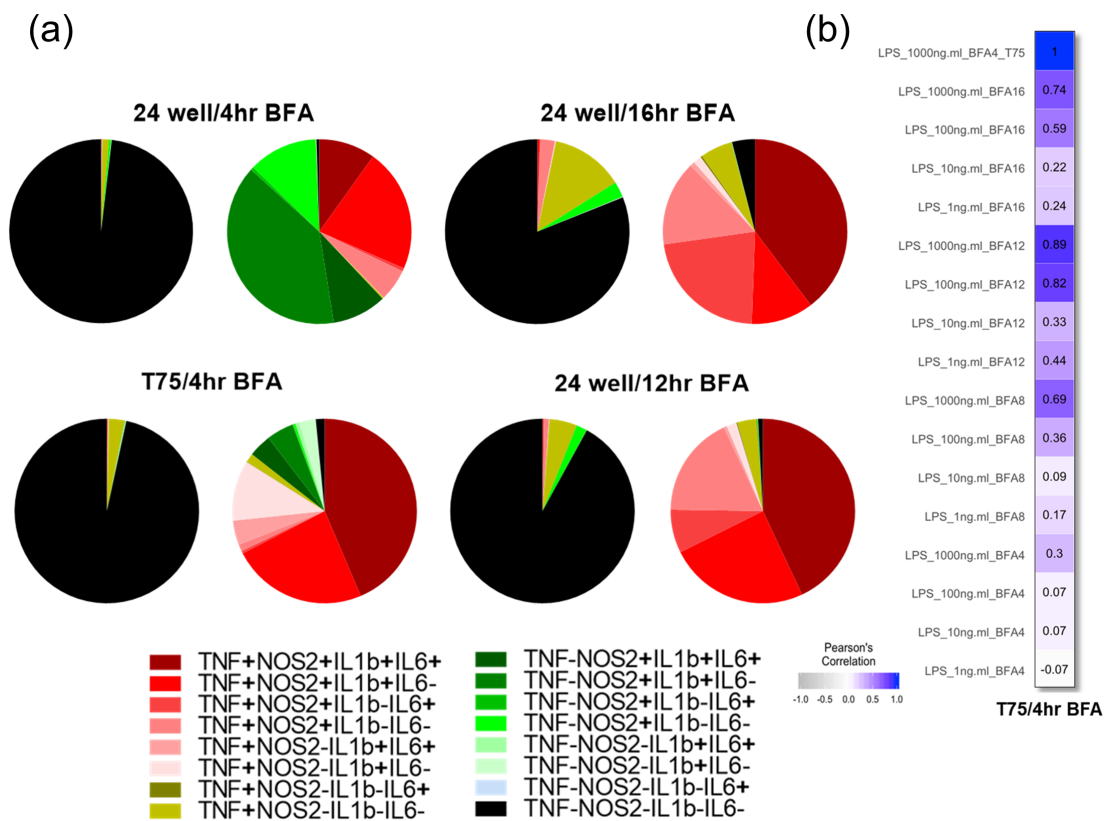


FIGURE 3.14: Cells stimulated in isolation and allowed to secrete make communities that are similar to secretion restricted (>8hr) communities

a Pie charts representing RAW264.7 communities based on TNF, IL-6, NOS2 and pro-IL1 β expression in cells grown 24 well plates or in T75 flasks. b Pearson's correlation between community grown in T75 flask versus other treatments (representing cells grown in 24 well plates).

3.6.1 Anti-TNF treatment does not disrupt macrophage response community

In previous sections, we have showed that TNF+ cells are an important part of the LPS-induced response community with TNF+IL6+NOS2+ to be a prominent identifier of LPS dose magnitude and increases as secretion of RAW264.7 cells are restricted. Further, we have also shown that upon LPS stimulation up to 97% cells are positive for TNF in the first 8 hours. This led us to question, if secreted TNF along with LPS has a strong effect in shaping the heterogeneous community-led response. A host of anti-TNF drugs are medically prescribed in conditions like rheumatoid arthritis (Seymour et al., 2001) to reduce the exacerbating effects of inflammation. Neutralising antibodies used in RAW264.7 cultures reduced the mRNA pro-inflammatory proteins like IL-6, NOS2, IL-12p40 by about 20% (**Figure 3.15**). TNF mRNA, however, did not show any decrease while TNF at the protein level showed 40% decrease in supernatant. IL-6 showed a similar decrease as well at the protein level when the highest concentration of anti-TNF was used (100ug/ml) (**Figure 3.15**). The results suggested that neutralising TNF may be reducing the overall levels of other TNF-inducible genes, however, it does not indicate whether this happens in all cells by decreasing the amount of TNF produced per cell or if it effect only a fraction of cells. We hypothesized if the decrease is due to TNF affecting a fraction of cells it could then further affect the community composition upon LPS stimulus.

No community level effects were observed when TNF was neutralised with a high dose (100 μ g/ml) of anti-TNF antibody and the composition of communities appeared qualitatively similar (data not shown). However, it was observed that anti-TNF antibodies increased the percentage of cells that were producing TNF when responding to 1000 ng/ml of LPS doubling it at 16 hours from stimulus. This may suggest a negative feedback loop that reduces the number of cells producing TNF. (**Figure 3.16**).

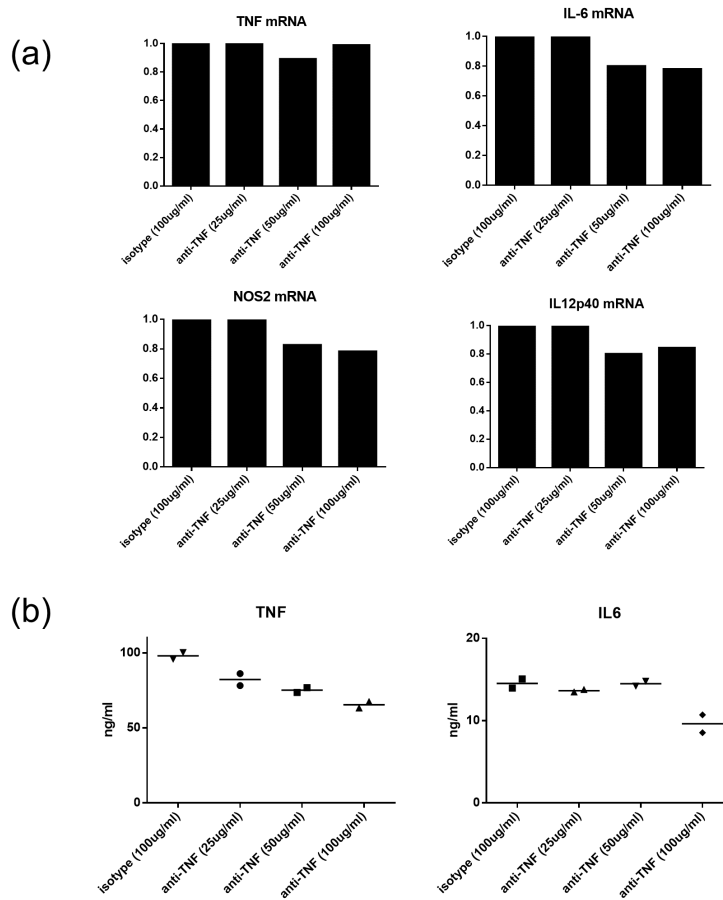


FIGURE 3.15: Anti-TNF neutralising antibody suppresses IL-6, NOS2 and IL12p40 mRNA up to 20%.

a Bar plots showing the fold repression of TNF, IL-6, NOS2 and IL12p40 mRNA Cells (n=1) and **b** scatter plots to show levels of TNF and IL-6 in the supernatant when treated with isotype control (100µg/ml) or anti-TNF neutralising antibody at 25, 50 and 100µg/ml concentration (n=2).

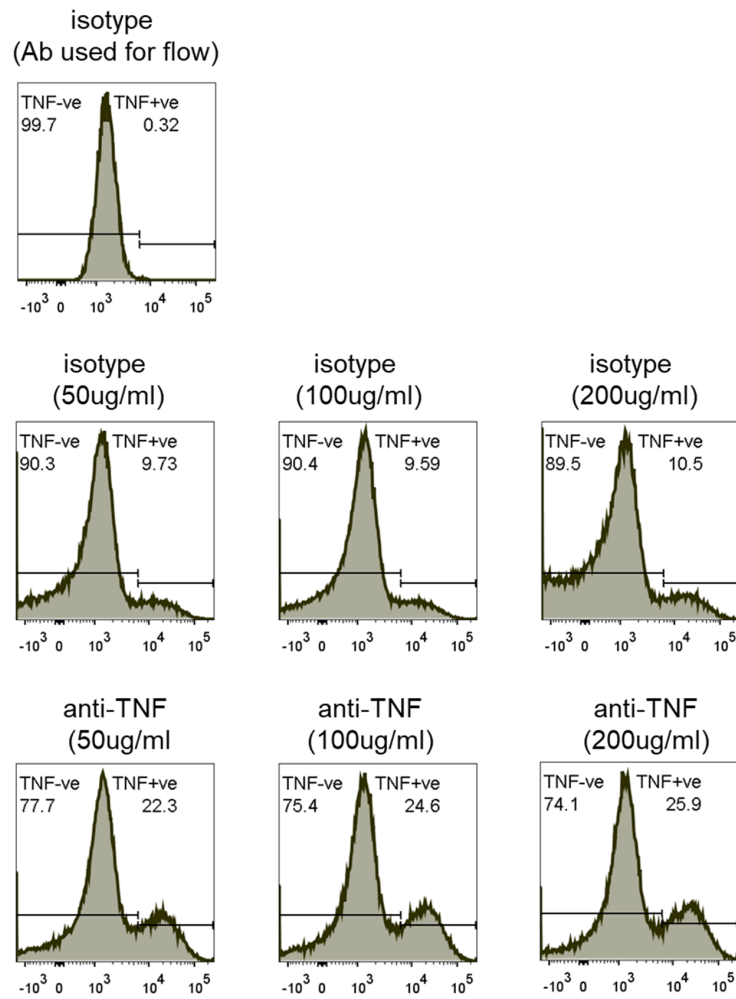


FIGURE 3.16: Neutralising TNF increases the number of late phase TNF producing cells

Histograms showing fluorescence intensity distribution of RAW264.7 cells cultured for 16 hour in LPS (12 hour LPS and 4 hour LPS+BFA). Histograms show percentage TNF+ population in three replicates (middle and bottom rows) treated with either isotype control or TNF neutralising antibody. Positive cell gating as per isotype control for antibody targeting TNF (top row)

3.6.2 Thioglycollate-elicited peritoneal macrophage response to LPS is heterogeneous

In order to verify if heterogeneous communities to LPS was not an effect limited to RAW264.7 cells, due to cell-line characteristics such as continuous growth and, cell-lines being adjusted to growing in cell culture media, we harvested thioglycollate-elicited peritoneal macrophages and cultured them *in vitro*.

We first characterised thioglycollate-elicited peritoneal macrophages (TEPMs) soon after harvest to look at surface protein expression to show that they are a highly heterogeneous population (**Figure 3.17**) as thioglycollate elicitation leads to monocyte recruitment without activation adding on to the tissue-resident peritoneal macrophage population. Among the four mice harvested, all had a similar size and granularity but could be differentiated using the F4/80 surface marker expression with typically 77-83% of the cells F4/80+, 9-15% F4/80 low and 5-6% F4/80 high (**Figure 3.17a&b**). CD86, as a co-stimulatory molecule, was bi-modally expressed (as seen in RAW264.7 cells, 3.9). These results suggested our harvest could consist of tissue resident (F4/80 high), a mix of monocyte-derived macrophages and small tissue residents (F4/80+) and infiltrating monocytes (F4/80 low). However, upon *in vitro* culture, this F4/80 expression pattern was lost (**Figure 3.18**) and, therefore, should not have large effects on the response to LPS.

Next, we looked at heterogeneous responses to LPS in peritoneal macrophages as a temporal snapshot at 16 hours of stimulation. As we have shown in previous sections, community transitions may occur at around 8 hour of LPS stimulus (**Figures 4.3, 3.10**) we either incubated the TEPM culture for 8 hour or 16 hour in BFA for a total of culture in LPS for 16 hour. Despite a longer BFA incubation of 8 hours (**Figure 3.19**, 8 hour + 8 hrs BFA) we could identify heterogeneous sub-populations in the *in vitro* peritoneal population across all doses of LPS and secretion restriction resulted in a visually distinct

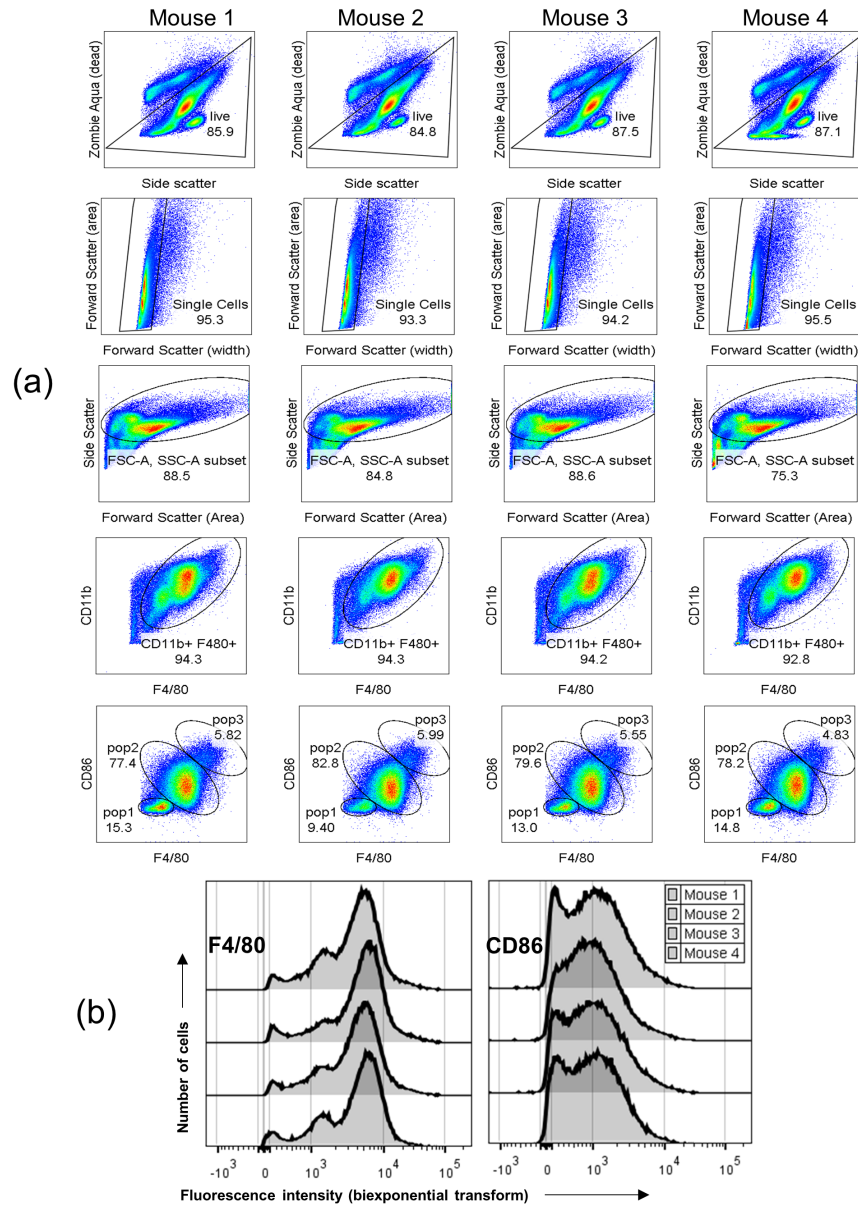


FIGURE 3.17: Surface expression of F4/80 shows distinct populations in thioglycollate-elicited peritoneal macrophages

Flow-cytometry gating shown for *ex-vivo* thioglycollate-elicited peritoneal macrophages (TPEM) to show a populations sub-types using bi-plots of F4/80 and CD11b/CD86. **b** Histograms to show distributions of F4/80 and CD86 fluorescence intensity. n=4 biological repeats

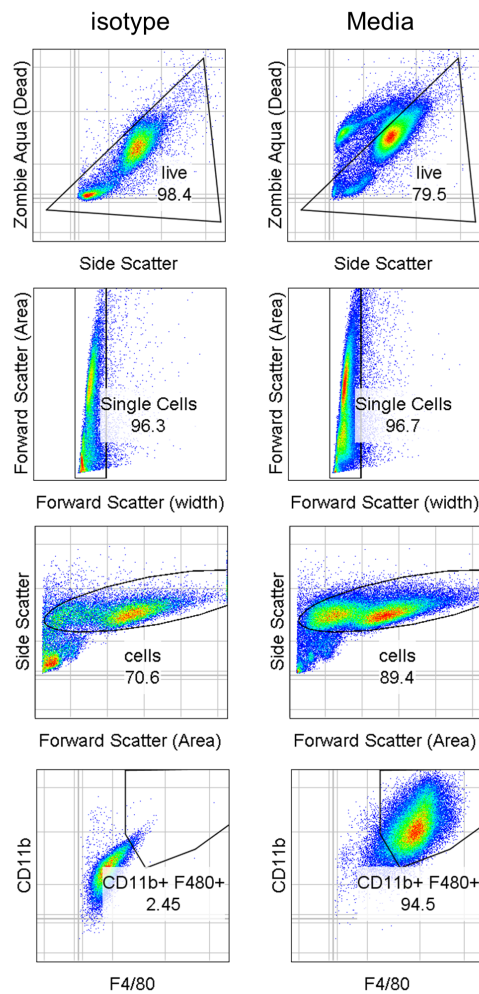


FIGURE 3.18: **F4/80** expression is more uniform upon *in vitro* culture of peritoneal macrophages

Flow-cytometry gating shown for cultured TPEMs for a period of 24 hours with CD11b and F4/80 expression (bottom row)

community composition.

LPS dose comparison in TEPMs (8 hours + 8 hr BFA, **Figure 3.19**) showed a heterogeneous population where negative cells, single positive TNF-IL6+NOS2-, double positive TNF-IL6+NOS2+ & TNF+IL6+NOS2- and the triple positive populations comprised the sub-populations in the community at 16 hours when cells were incubated in BFA for 8 hours. As the dose of LPS was increased number of negative cells reduced along with an increase in the triple positive and TNF-IL6+NOS2+ sub-populations as shown earlier in RAW264.7 cells (8 hours plus 8 hr BFA, **Figure 3.10**). However, a reduced proportion of cells that were overall positive for NOS2 were reported (13-42% among all conditions) as compared to 54-86% in RAW264.7 cells at 16 hours of LPS stimulation (**Figure 3.10**) suggesting fewer TEPMs make NOS2 or that NOS2 is switched on later into the LPS stimulus when compared to RAW264.7 cells. Similarly, overall IL-6 positive cells were higher in TEPMs (76-89%) than RAW264.7 (8-59%) with much reduced variability in TEPMs (4% variability compared to 50% in RAW264.7) co-efficient of variation).

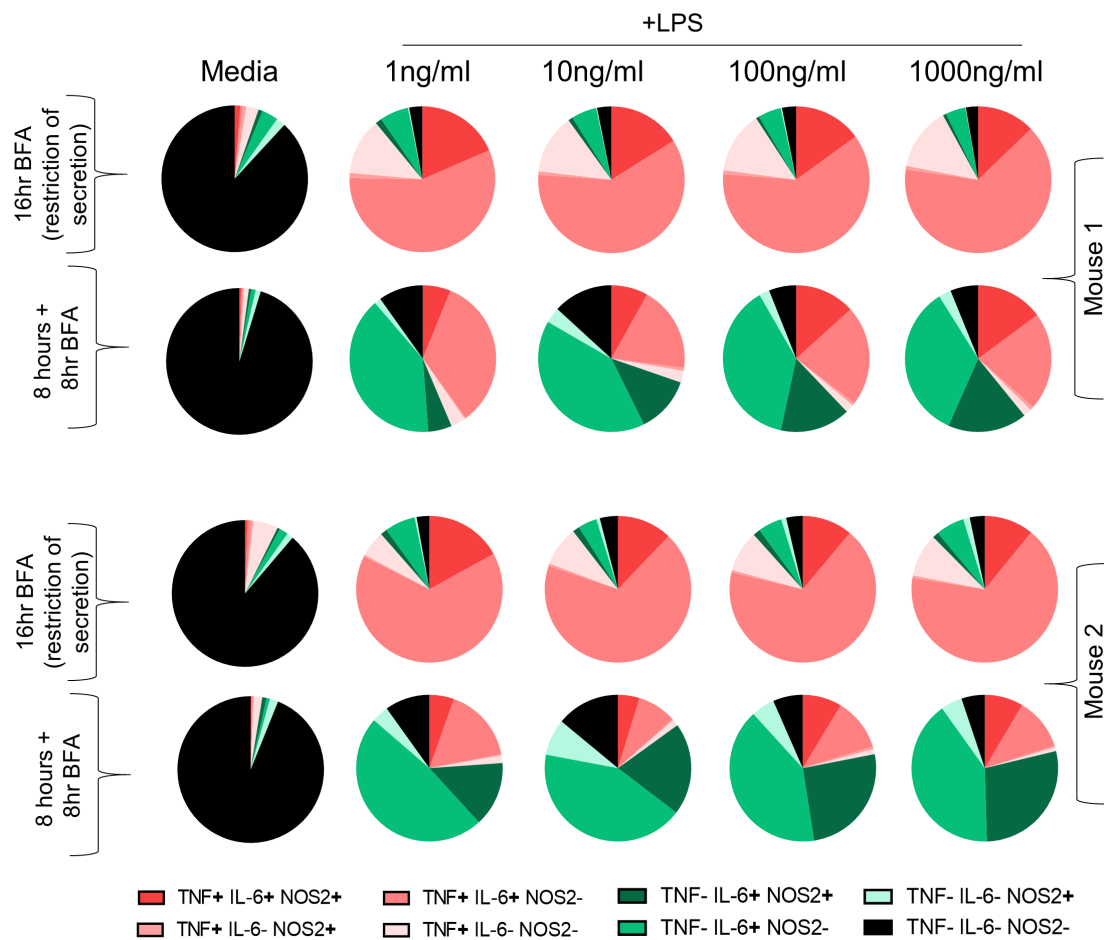


FIGURE 3.19: **Thioglycollate-elicited peritoneal macrophages for heterogeneous communities and are affected secretion restriction**

Pie charts depicting sub-populations in cultured TPMEs in media only or at 1, 10, 100 and 1000 ng/ml concentration of LPS for 16 hour LPS+BFA; 8 hour LPS and 8 hour LPS+BFA; 8 hour LPS and 8 hour LPS+BFA; 12 hour LPS and 4 hour LPS+BFA. Mouse 1 and 2 represent biological repeats. Count of cells = 50,000

3.7 Discussion

3.7.1 Conclusions

The results presented in this chapter regard macrophage heterogeneity as affected by temporal responses to LPS, LPS doses and intercellular communication. Heterogeneous responses presented as temporal snapshots of macrophage response to antigen, measuring three or more response proteins, can be visualised as a complex community of distinct sub-populations (**Figure 3.4**). Based on our results we make the following conclusions:

- Diverse community compositions indicate considerable population heterogeneity in RAW264.7 macrophages.
- Community compositions depend on LPS dose.
- TNF+IL6+NOS2+ and TNF-IL6+NOS2+ sub-populations are predominantly affected by LPS dose.
- Restricting inter-cellular communication leads to dissimilar community compositions.
- TNF blockade does not alter community composition but doubles the frequency of late-stage TNF positive cells.
- RAW264.7 cells at low density make more late-stage TNF positive cells. Community composition of this population resembles communities that have their secretion restricted.
- Thioglycollate elicited peritoneal macrophages (TPEMs) form distinct LPS-induced communities and are affected by secretion restriction. However, their response is distinct from RAW264.7 cells.

- Macrophage, both RAW264.7 and TPEM, communities responding to LPS rapidly change community composition between 8 and 12 hours of LPS stimulus

3.7.2 Visualisation method

In this chapter, firstly, we present a technique that can be used to compare temporal snapshots of protein expression for quantification of sub-populations within a LPS-activated macrophage population. This protein expression snapshot shows whether a cell is positive or negative for each of the measured fluorescently labelled antibodies on a flow cytometer. Pie charts, akin to those described in the SPICE software (Roederer, Nozzi, and Nason, 2011), represent a community of cells responding to an activator such as LPS at any particular time. Visualising heterogeneous sub-populations as a community can not only be used to probe the heterogeneity in LPS activated cells (Shalek et al., 2013) at a protein level but can also be used to enquire how heterogeneous communities may evolve in phenotypic changes such as in endotoxin tolerant or trained immune cells (Biswas and Lopez-Collazo, 2009; Netea, Quintin, and Van Der Meer, 2011). Further, this method allows exploring community composition of our selected proteins upon restriction of secretion that is known to alter response in bone-marrow derived dendritic cells in a paracrine dependent manner (Shalek et al., 2014) and other perturbations such as population density effects (Chen et al., 2015; Postat et al., 2018).

In general, visualising response as a community can be adapted to proteins of interest to probe consequences of heterogeneous protein expression on function. By temporally tracking communities with or without additional perturbations, it may be further possible to explore the ordering of community sub-populations in time. Interestingly, such ordering, analogously, has been shown using pseudo-temporal analysis of single-cell transcriptomic data of human myoblasts to map cell fate decisions (Trapnell et al., 2014).

Finally, our methods capture activation-induced heterogeneity as a community of diverse phenotypes and clearly describes the percentage of cells that are positive or negative for each/all measured proteins. However, this type of visualisation loses underlying fluorescence information at the per-cell level and does not describe the distribution within a positive population. In that sense, one cannot differentiate between high and low producers, or the absence of them from the pie-chart representation. For example, NOS2 expression in our dataset is seen to have high and low expressing cells even while most cells are positive (NOS2 histogram, Figure 3.10). As such, there may be additional differences in the amount that are overlooked by our method.

3.7.3 RAW264.7 macrophages respond as a community

It is shown that murine macrophage-like RAW264.7 cells, despite being a clonal population respond to LPS with considerable heterogeneity. In that sense, upon antibody staining for TNF, IL-6 and NOS2 at 16 hours, we find at least 5 and up to all 8 different possible sub-populations in the response. Two of the most under represented sub-populations were TNF+IL6+NOS2- and TNF-IL6+NOS2- cells across LPS doses and experiments. This suggested that these states are possibly short-lived and, thus, are never represented in our minimum 4 hour BFA accumulation.

Upon measuring four cytokines per cell (TNF, IL-6, NOS2 and pro-IL-1 β) we found up to 11 different sub-populations out of a possible 16 (2^4 , where 4 is the number of cytokines stained for). While, the addition of a cytokine, increased the number of possible sub-populations, not all possible sub-populations were found to exist in the community (ie those that represented at least 1% of the total population) suggesting, again that some sub-populations are not likely to exist within a community or undetectable with the current method.

This suggests while LPS does activate RAW264.7 cells, there is a secondary effect that shapes the course of inflammation and such diverse sub-populations require careful dissection of how this community is shaped.

While it is known that LPS dose has an effect on how much cytokine is produced at the population level (Amura et al., 1998; Yang et al., 2017; Matsuura et al., 2010), as per our knowledge, not much is known about how populations respond as a community to LPS dose. We show that LPS dose has considerable effect in community composition which may effect cell priming within a community that can shape hypo or hyper-responsiveness to second dose of LPS.

Further, we go onto show that communities are plastic in terms of relative frequencies of sub-population representation but the variability does not change the overall dose induced community composition. Plasticity in community composition can be attributed to a number of cell culture related factors such as cell density and plating, reagent concentration or temporal factors such as length of pre-stimulus or overnight incubation period, length of BFA incubation and, consequently, time-taken to harvest cells or errors in length of cell culture. Care was taken that these factors remained comparable between experiments and, thus, effects manifesting due to such errors must either be less or suggest that small perturbations of one or more of these factors can have large effects on community composition of macrophages responding to LPS (**Figure 3.7**).

Intuitively, triple and double positive populations are more pro-inflammatory than single positive or negative cells. When comparing LPS doses we find, by unbiased clustering, that TNF+IL6+NOS2+ and TNF-IL6+NOS2+ sub-populations were most different from the other sub-populations and were more prevalent in 100 and 1000 ng/ml LPS dose. This suggests that increasing LPS dose increases the inflammatory response even 16 hours into the LPS response. This is interesting because we also show

that almost 97% of all cells go through TNF in the first 8 hours of stimulus (4hr + 4hr BFA, **Figure 4.3**) when stimulated with 1000ng/ml of LPS. Since all RAW264.7 cells go through a TNF+ stage in the first eight hours, one explanation of the heterogeneous community composition could be due to this early TNF-release in an autocrine or paracrine manner, along with LPS, could shape the community compositions, as measured at a later time point (12 or 16 hours). Further, it may be speculated that TNF-IL6+NOS2+ cells which cluster along with TNF+IL6+NOS2+ cells, and are enriched in high doses of LPS may be a community of cells which have previously been triple positive and have, in time, lost TNF positivity (see correlation in **Appendix Figure 8.1**).

Interestingly, most TNF+ cells (sum of all TNF+ sub-populations) in the first 8 hours (97%, 4hr + 4hr BFA, **Figure 4.3**) switch off TNF (below 25%, 8hr + 4hr BFA, **Figure 4.3**) by 12 hours of LPS stimulus. This may be attributed to the anti-inflammatory IL-10 (Saraiva and O'Garra, 2010). IL-10 is known to be upregulated at mRNA levels in RAW264.7 cells at around 4 hours into stimulus (Zhu et al., 2018) and peak at 8 hours into LPS stimulus at the protein level in both mice (Van Laethem et al., 1998) and human macrophages (Chanteux et al., 2007; Giambartolomei et al., 2002). Further, studies in mice have also shown that knocking out IL-10 leads to increased TNF mRNA levels in the first 24 hours after LPS stimulus (Anderson et al., 2017).

Despite regulatory effects of IL-10, as discussed above, at 16 hours between 24-41% cells are TNF+ (sum of all TNF+ sub-populations, **Figure 3.7**). This could be because IL-10 is possibly not able to completely block TNF while it can also be because of the bi-phasic nature of NF- κ B activation. Upon TLR4/LPS endocytosis, a late phase NF- κ B activation has been shown to occur between 8-12 hours (Han et al., 2002) which can lead to a second wave of TNF production. Further a secondary NF- κ B activation can also occur because of TNF binding to its receptor TNFR (Hayden and Ghosh, 2014).

While TNF seemed to play a central role in our experiments with large LPS doses distinguishable by triple positive (TNF+IL6+NOS2+) populations and most cells going through a TNF+ phase in the early response to LPS, we were unable to disrupt community composition at a late stage (16 hours) into LPS stimulus by neutralising TNF in the cell culture. Interestingly, however, TNF+ cells (sum of all TNF+ subpopulations) doubled in percentage in comparison to control suggesting the lack of TNF in culture was promoting an inflammatory response. This late doubling of TNF+ cells could have an effect in the community composition after the 16 hour time point but this was not pursued further.

3.7.4 Community communication

Previously, using short and long BFA incubations to depict early and late phase response, we showed community consistency in 1000/1000 treatments. Since BFA, in addition to capturing accumulation, also restricts intercellular communication, we showed that community compositions switch to distinct community types at around 8 hours into LPS stimulus. Distinct bi-modal IL-6 production and lower NOS2 levels with almost all cells positive for TNF were the hallmark of the response when secretion was restricted (**Figure 3.10**). This 8 hour switch was yet again observed when community complexity was increased by adding pro-IL-1 β to our measurement (**Figure 3.11, 3.12, 3.13**). Our results indicate that loss of autocrine and paracrine signalling leads to an increased inflammatory response. While our disruption of autocrine and paracrine signalling is crude, it shows the importance of autocrine and paracrine signalling in RAW264.7 cells. We then plated the same number of RAW264.7 macrophages in a culture vessel that was approximately 40 times bigger than the usual culture plate to show that communities responding to LPS when cells are not clustered or near each other, correlate more to communities whose secretion is restricted (Fig 3.14). Since isolation is more likely to stop paracrine effects than autocrine, our results suggest that paracrine

signalling may be crucial for dampening the inflammatory response as previously suggested in bone-marrow derived dendritic cells at the mRNA level (Shalek et al., 2014) and in isolated human monocyte-derived macrophages (Xue et al., 2015).

Community structure of thioglycollate elicited peritoneal macrophages (TEPM) suggested that TPEMs respond to LPS in a heterogeneous manner and form communities that titrate to LPS dose and restriction of secretion makes the community appear distinct to when secretion is not restricted (Fig 3.19). However, the changes to community composition upon LPS titration is only modest and is likely to be due to the increased LPS sensitivity of primary cells to RAW264.7 cells. Interestingly, IL-6 production in TPEMs was bi-modal in comparison and NOS2 staining was moderate in comparison to unimodal analog responses observed for IL-6 and strong NOS2 staining in RAW264.7. Sub-populations such as single positive for IL-6 (TNF-IL6+NOS2-) which are prominent in TPEMs were not observed in RAW264.7 communities. This suggests that TPEMs and RAW264.7 have fundamental differences in how they respond to LPS and form different communities.

Chapter 4

Macrophage heterogeneity is a determinant of secondary LPS challenge

4.1 Introduction

Macrophages exposed to LPS twice can become hypo-responsive in their ability to produce cytokines (Biswas and Lopez-Collazo, 2009; Netea, Quintin, and Van Der Meer, 2011). In this chapter, we use visualisation and secretion restriction methods employed in Chapter 3 to investigate the effects of LPS-induced heterogeneous macrophage communities can affect the response-outcome to secondary doses of LPS in terms of community composition and population-level responses.

4.2 Aims

The aim of this chapter was to determine if RAW264.7 cells respond heterogeneously to secondary LPS challenges.

4.3 Second dose of LPS induces a hypo-response

4.3.1 Upon secondary exposure to LPS RAW264.7 cells make less of TNF, IL-6 and nitric oxide

We stimulated RAW264.7 cells for 24 hours with LPS and then re-stimulated with a second dose and collected cell supernatant. TNF, IL-6 and nitric oxide showed a significant decrease at the population level confirming that LPS can induce a hypo-response in RAW264.7 cells *in vitro* (Figure 4.1). When the first dose of LPS was small (10 ng/ml), the hypo-response induced at the population level was less pronounced than when cells were pre-treated with a higher dose of LPS.

While 1000/1000 treatment induced hypo-response in terms of TNF, IL-6 and nitric oxide, 10/1000 treatment induced hypo-response in terms of TNF and IL-6 but not nitric oxide. (Figure 4.1)

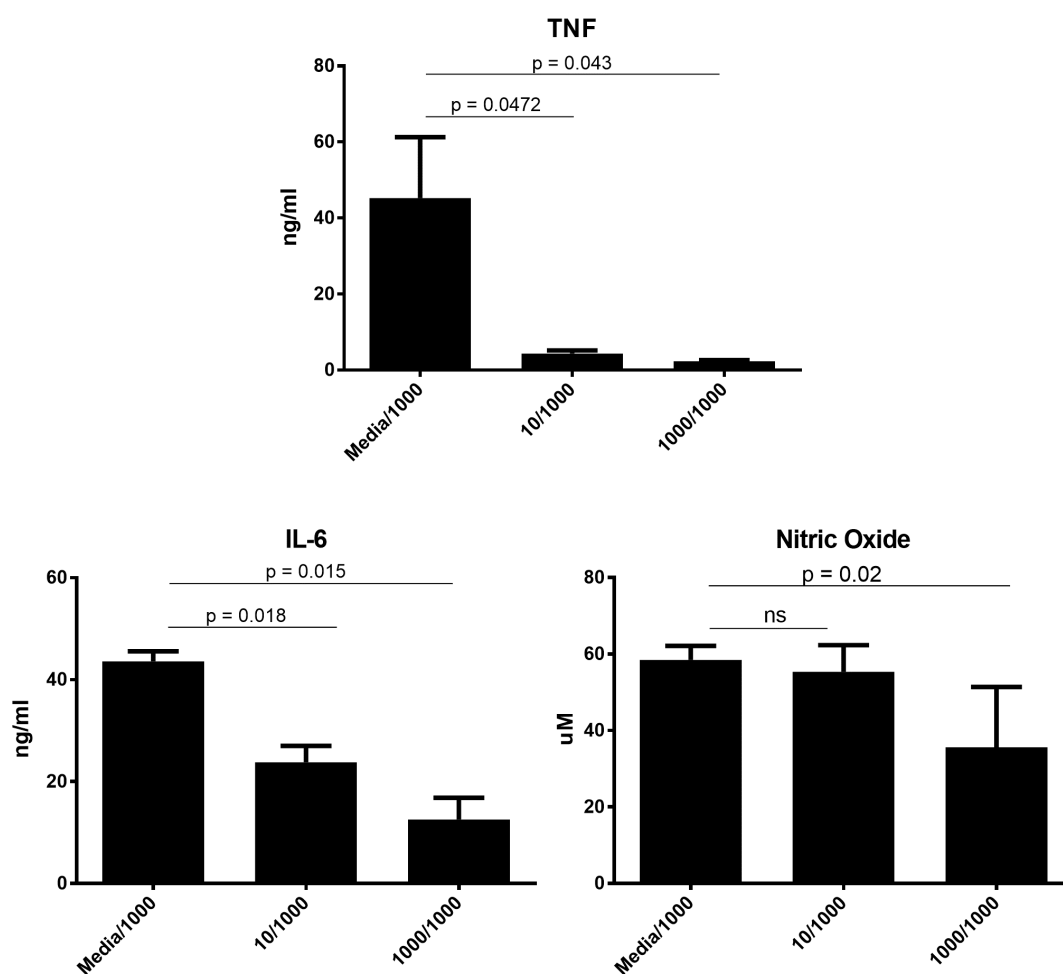


FIGURE 4.1: Re-stimulated RAW264.7 cells are hypo-responsive

Bar plots showing TNF, IL-6 and nitric oxide (NO) levels in RAW264.7 cells stimulated once (Media/1000), or twice (10/1000 or 1000/1000) where 10 and 1000 represent 10 and 1000 ng/ml of LPS post second stimulus at 24 hours into culture. p-values were calculated using paired t-tests (n=3-6, bars=standard deviation).

4.4 Community composition determines response to secondary stimulation with LPS

4.4.1 Heterogeneous community responses can be identified by protein accumulation

We next wanted to identify if a secondary dose of LPS, that induces a hypo- response at the population level (**Figure 4.1**) spur distinct communities compared to primary responses to LPS when probed at the single cell level. Twice-challenged cells showed similar consistency to cells that were challenged only once (**Figure 4.2a**) when community composition was compared at 16 hours post stimulus. This occurs both in the low (10ng/ml) and high dose (1000ng/ml) pre-stimulus (**Figure 4.2a**). Despite showing that a second dose of LPS induces hypo-responsiveness (with population level measurements **Figure 4.1** in RAW264.7 cells), at the single-cell level there were more cells that were overall positive for TNF (24% for 10/1000; and 12% for 1000/1000) and IL-6 (10% for 10/1000; and 16% for 1000/1000) as compared to approximately 6% and 10% TNF and IL-6 positive cells in single challenge (Media/1000) community (inferred from **Figure 4.2a**). Negative sub-populations were approximately twice as many in both 10/1000 and 1000/1000 communities when compared to the single challenge, Media/1000. However, these negative cells comprised of a small proportion of the total cells (approximately 10%). This indicated that upon a second challenge, cells switching on cytokine production may be delayed in time after stimulus, while there is also an increased population of negative cells that are part of the community.

In a separate experiment, to check if this delay in switching on cytokines, as suggested above, is evident, we compared communities of single challenge and two challenges of LPS after 24 hours (20 hours plus 4 hr BFA, **Figure 4.2b**). Indeed, cells that were overall positive for TNF in twice-challenged communities were 3.5 and 4 times (10/1000 and 1000/1000) higher than those exposed to LPS once. Cells that were overall

positive for IL-6 were twice more frequent in 1000/1000 communities when compared to Media/1000 suggesting late IL-6 production (like TNF) in twice-challenged cells. However, 10/1000 communities showed a decrease in IL-6+ cells at 24 hours (8%) from 10% at 16 hours when compared to approximately 10% and 12% IL-6+ cells in Media/1000 communities at 16 hr and 24 hr. This can be speculated as a differential effect that is seen due to the size of the pre-stimulus (10 vs 1000 ng/ml) but it must be noted that since 16 hr (**Figure 4.2a**) and 24 hr timepoint (**Figure 4.2b**) information is derived from two different experiments, this difference can also be attributed to empirical variability as shown previously (sub-section 3.4.4). Interestingly, negative cells between Media/1000 and 1000/1000 were 16% and 14% percent, respectively, showing both the treatments were unable to distinguish between non-responsive cells by this time point. 10/1000 community were, however, 31% negative being twice as high as Media/1000 (**Figure 4.2b**).

Figure 4.2a&b indicate that twice challenged communities have higher TNF (1000/1000 and 10/1000) and IL-6 (1000/1000) producing cells at 16hr and 24hr in twice challenged while NOS2 producing cells are lower or equal but community compositions are, by appearance, hard to distinguish, because sub-populations in the community that do show a change between Media/1000 and 10 or 1000/1000 are small populations. One subset, TNF+IL6-NOS2+, stands out at 16hr (**Figure 4.2a**) and 24hr (**Figure 4.2b**) of second stimulus and is 2-4 times (16 hour) and 3.6 times (24 hour) higher in twice-challenged cells compared to the Media/1000 community. As this sub-population represents 16% of 10/1000 (16 hour), 8% of 1000/1000 (16 hour), 17% of 10/1000 (24 hour) and 18% of 1000/1000 (24 hour) of the total community, it maybe an important part of the response when RAW264.7 cells are stimulated twice with LPS, and at least, between 16 and 24 hours of second stimulus.

As a visibly discernible hypo-response, in RAW264.7 (from the temporal snapshot of

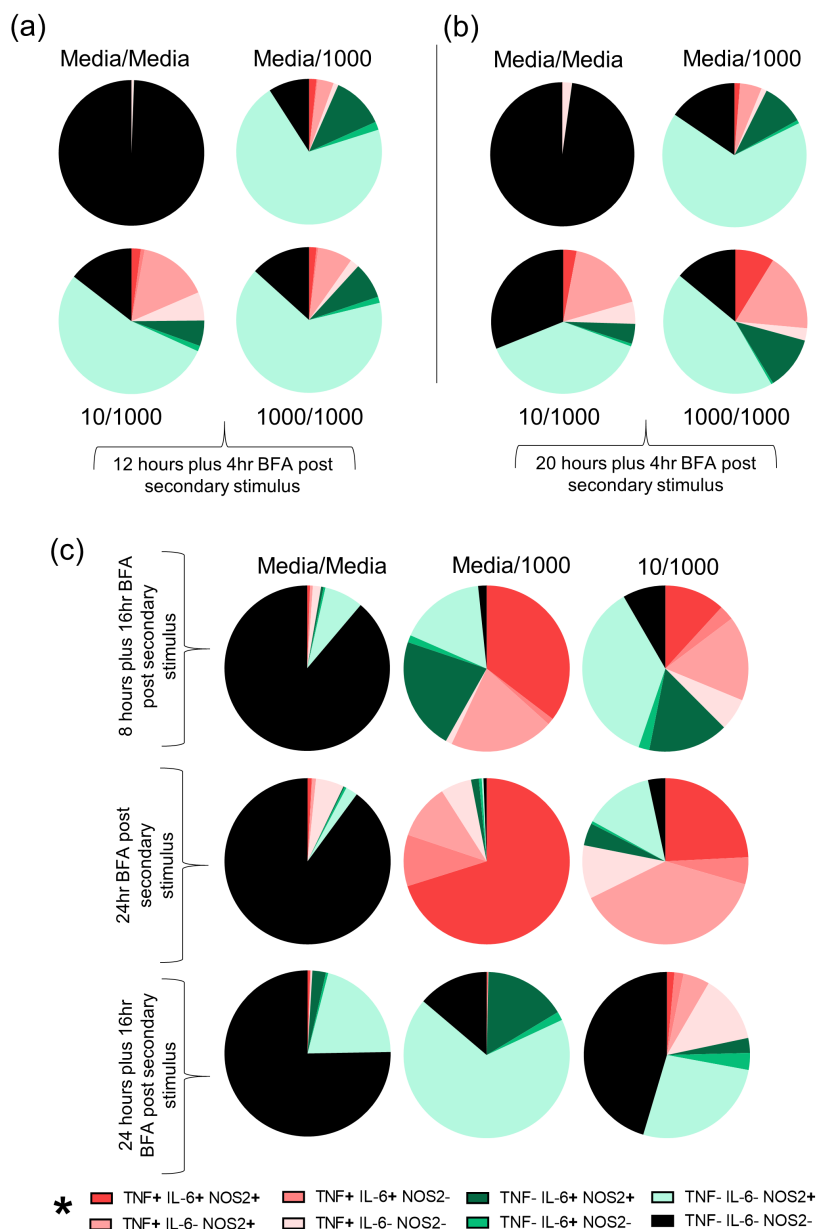


FIGURE 4.2: **Hypo-responsive communities appear more pro-inflammatory at 16 and 24 hours**

Pie charts representing sub-population frequencies of RAW264.7 cells stained for TNF, IL-6 and NOS2 when cells were either unstimulated (Media/Media), stimulated once (Media/1000), or twice (10/1000 or 1000/1000) at **a** 12 hour in LPS and 4 hour in LPS+BFA **b** 20 hour in LPS and 4 hour in LPS+BFA **c** 8 hour in LPS and 16 hour LPS+BFA; 24 hour LPS+BFA; 24 hour LPS and 16 hour LPS+BFA post second stimulus at 24 hours into culture. Count of cells=100,000.

the twice-challenged communities at 16 and 24 hour with 4 hour BFA incubation) was not observed, we then visualised communities by trapping proteins in the cells for longer to see if protein accumulation can be used to visualise hypo-response. Looking at accumulation of proteins over a 16 hour BFA incubation in a total of 24 hour stimulus (8 hour LPS and 16 hour LPS+BFA, **Figure 4.2c**) we show that approximately 38%, 32%, 80% of the 10/1000 community were TNF, IL-6 and NOS2 positive over the 24 hour period (8 hour LPS plus 16 hour LPS+BFA) compared to the Media/1000 community where TNF+, IL-6+ and NOS2+ cells were about 58%, 60% and 95% respectively. This showed that the response to a second dose of LPS is overall modest. In terms of community composition, notably, the triple negative (approximately 5-fold more) and the TNF-IL6-NOS2+ single positive sub-populations (2-fold greater) were prominent in the 10/1000 community while in the Media/1000 community the triple positive, TNF+IL6+NOS2+ and TNF-IL6+NOS2+ were 3 fold and 50% more respectively. This effect was exaggerated when we cultured cells for 24 hours in LPS with BFA (**Figure 4.2c**, 24 hr BFA) to show that approximately 70% of the Media/1000 community was triple positive in 24 hours, thus, suggesting that each of these 70% cells must have made all the three proteins in the 24 hour hour period. In contrast, triple positive sub-populations was limited to only 24% of all cells in a twice-challenged community. Similarly, there are 22% cells that do not make TNF in the entire 24 hour period in 10/1000 community whereas Media/1000 community suggests that all cells go through a TNF phase i.e. each cell makes TNF at some point during the 24 hour LPS stimulus.

Macrophages responding to a second challenge of LPS are hypo-responsive and this phenotypic change is known to persist for days (Biswas and Lopez-Collazo, 2009). In order to see if this could be captured in terms of heterogeneity of community between Media/1000 and 10/1000 we cultured cells for 40 hours post second stimulus (**Figure 4.2c**, 24 hr plus 16 hr BFA). 10/1000 community was found to be qualitatively different with certain TNF+ sub-populations such as TNF+IL6-NOS2+ and TNF+IL6-NOS2-

comprising 18% of the total population. In comparison, these sub-populations were negligible in the Media/1000 community (<0.5%) which had a higher percentage of TNF-IL6+NOS2+ cells (16%) in comparison to 3% in 10/1000. Also, 10/1000 community had 3 times more negative cells suggesting twice-challenged communities switch cytokines off faster.

Figure 4.2c suggests that IL-6 may be critical in determining the hypo-response in RAW264.7 cells with overall IL-6+ cells being consistently more in the Media/1000 community which is not apparent in the 4 hr BFA incubation experiments at 16hr and 24hr post secondary stimulus (**Figure 4.2a&b**). It is important to note here that long BFA incubations are restricting secretion and the ability of the communities to interact in an autocrine and paracrine manner indicating community compositions represented here may be affected by the lack of autocrine or paracrine effects.

4.4.2 Single-challenged communities undergo a compositional change at 8 hours of LPS stimulus

4 hour BFA incubation at 16 and 24 hour post second LPS stimulus showed few overall TNF+ cells while accumulation over 16/24 hour period showed up to 97% cells being TNF positive in the Media/1000 community (**Figure 4.2**). Such a high percentage of TNF+ cells (sum of all TNF+ sub-populations) suggested that most cells must then go through a TNF+ stage upon LPS stimulus. To test this we looked at the first 8, 12 and 16 hours of LPS stimulus with a short 4 hour BFA incubation. We found that indeed, and again, 97% cells were TNF+ in the first eight hours of the LPS response in the Media/1000 community (**Figure 4.3**, 4 hours plus 4 hr BFA). This finding is also in line with TNF being an early response protein (Bradley, 2008).

While 10/1000 community was 68% cells overall positive for TNF hyporesponsiveness was most pronounced in the 1000/1000 community with just 11% making TNF in the first eight hours of the response (**Figure 4.3**, 4 hours LPS plus 4 hr LPS+BFA). Interestingly,

the 10/1000 community shows a high percentage of TNF+ cells (6 times) higher than 1000/1000 community that switch off rapidly to 14% at 12 hours suggesting that a low dose pre-stimulus does not decrease the capability of a population of cells to switch on TNF compared to a higher dose pre-stimulus. Further, the communities of 10/1000 and 1000/1000 comprised of 7% and 10% negative sub-population confirming again that a small percentage of cells do not respond to the second dose of LPS (as opposed to 2% of cells in Media/1000).

The community structure in longer LPS stimulations (**Figure 4.3**, 8 plus 4 and 12 plus 4) of 12 and 16 hours exhibit similar subset composition as described earlier with less changes between 12 and 16 hours of LPS stimulus in terms of community composition. However, while overall TNF+ cells decrease over 8, 12 and 16 hours into LPS stimulus, the number of overall TNF+ cells first decrease (between 8 and 12 hours) then increase (between 12 and 16 hours) in both 10/1000 and 1000/1000 communities. This indicates a small percentage of cells become positive for TNF later when responding to the secondary stimulus, as shown earlier (**Figure 4.2a&b**).

We have shown that accumulation over long periods of LPS stimulation such as 16 hours and 24 hours show visual community differences in the single versus twice-challenged cells and that such a community-level switch occurs early on at around 8 hours into the LPS stimulus in Media/1000 community. We then restricted secretion for 16, 12, 8 or 4 hours during a 16 hour LPS stimulus (Media/1000) or re-stimulus (10/1000 or 1000/1000) (**Figure 4.4**) to show that, indeed, by trapping proteins longer in the cells we can again show that a visual change is observed in the community composition between 16 hour or 12 hour BFA incubations where effective secretion time is 0 hours and 4 hours in Media/1000 communities versus 8 hour. Further, community compositions change between 8 hour and 4 hour BFA incubation in Media/1000 community. Twice-challenged communities appear to be much less affected by BFA incubations, and as such, by environmental effects.

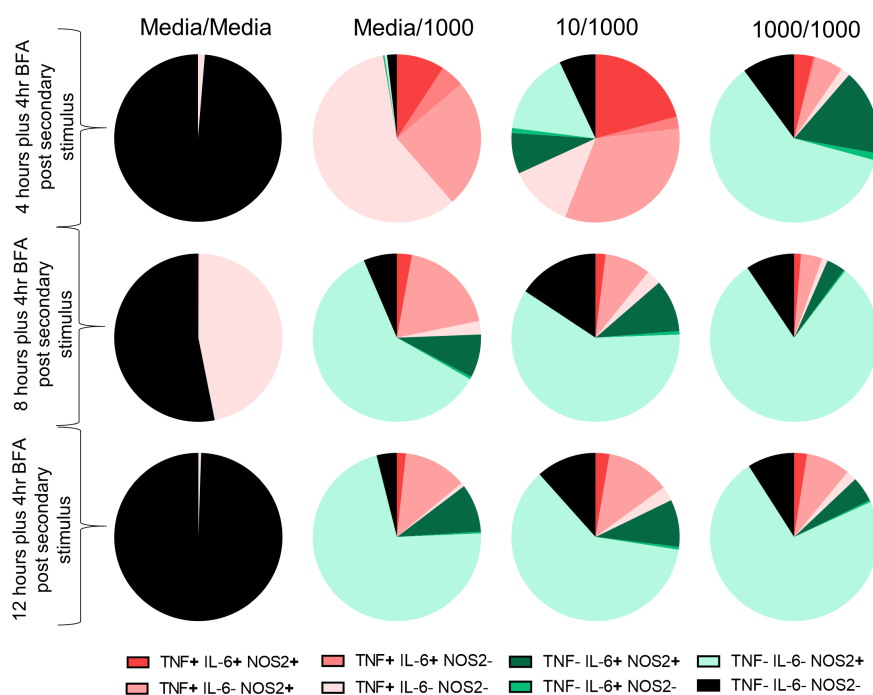


FIGURE 4.3: Hypo-responsive communities are more consistent in their response in the first 8 hours

Pie charts representing sub-population frequencies of RAW264.7 cells stained for TNF, IL-6 and NOS2 when cells were unstimulated (Media/Media), stimulated once (Media/1000), or twice (10/1000 or 1000/1000) for 4 hour in LPS and 4 hour LPS+BFA; 8 hour in LPS and 4 hour LPS+BFA; 12 hour in LPS and 4 hour LPS+BFA post second stimulus at 24 hours into culture. Count of cells=50,000-100,000.

Both temporal analysis (**Figure 4.2** and **4.3**) and longer BFA incubations (**Figure 4.4**) showed that cells that are challenged with LPS for the first time go through (approximately 97%) a TNF positive state within first 0-8 hours. In addition, the Media/1000 community changed after 8 hours into LPS stimulus. Twice-challenged communities, on the other hand, were hypo-responsive with fewer cells responding by producing TNF in the first 8 hours with 10/1000 communities showing compositional change to modest changes in the 1000/1000 community across BFA incubations (**Figure 4.4**)

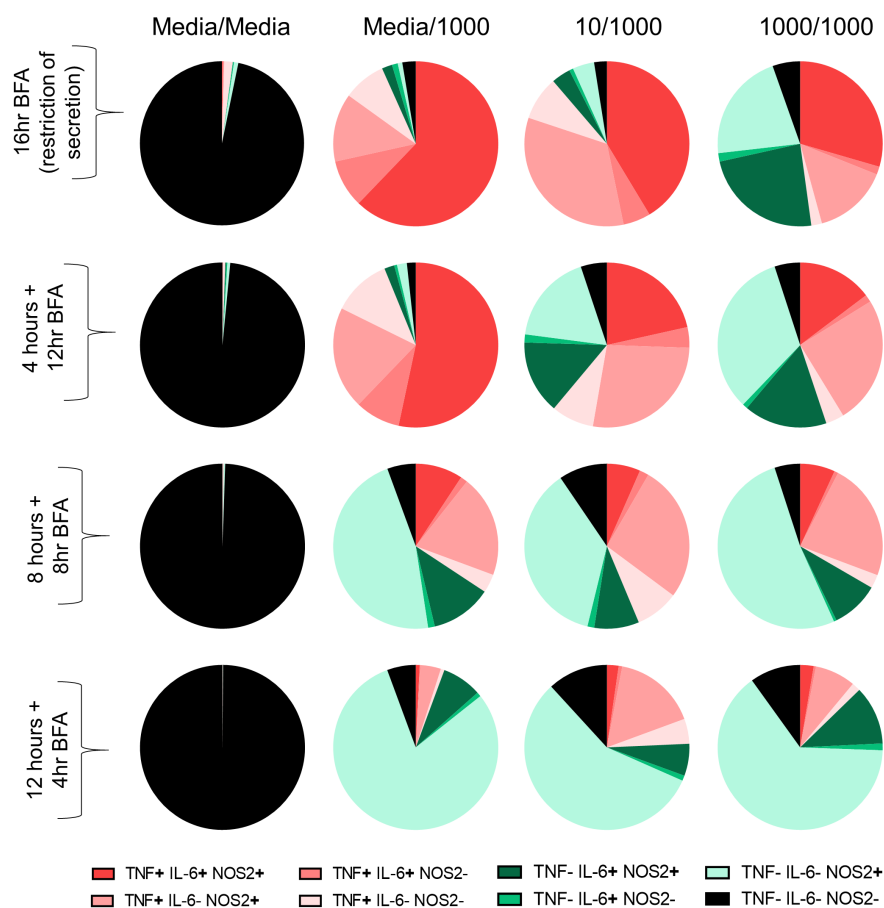


FIGURE 4.4: Prolonged restriction of secretion is associated with more modest changes in cells stimulated twice with LPS compared to cells stimulated once

Pie charts depicting sub-population frequencies of RAW264.7 cells stained for TNF, IL-6 and NOS2 when cells were unstimulated (Media/Media), stimulated once (Media/1000), or twice (10/1000 or 1000/1000) for 16 hour LPS+BFA; 4 hour in LPS and 12 hour LPS+BFA; 8 hour in LPS and 8 hour LPS+BFA; 12 hour in LPS and 4 hour LPS+ BFA post second stimulus at 24 hours into culture. Count of cells=50,000-100,000.

4.5 Discussion

4.5.1 Conclusions

The results presented in this chapter regard macrophage heterogeneity as affected by secondary response to LPS. Based on our results we make the following conclusions:

- Communities responding to a secondary LPS challenge are temporally more consistent.
- TNF+ cells in a hypo-responsive community are lower in the first 12 hours of the response.

4.5.2 Hypo-responsive communities

Populations challenged with LPS (1000 ng/ml) were hypo-responsive in the production of TNF, IL-6 and nitric oxide in the culture supernatant when pre-treated with 1000 ng/ml while populations pre-treated with 10 ng/ml failed to show hypo-response in levels of nitric oxide (**Figure 4.1**). Analysing community hyporesponsiveness, we found small difference in the communities of twice challenged and challenged populations at 16 and 24 hours. While 10/1000 and 1000/1000 communities had a higher proportion of negative cells when compared to communities that were treated with LPS only once (Media/1000) there were more TNF+ subpopulations in hyporesponsive communities. While TLR4 and TNF can induce a late phase NF- κ B activation, it is possible that IL-1 β that is only secreted upon the second challenge of LPS in RAW264.7 cells (**Appendix Figure 8.2**) can enhance higher activation of late-phase NF- κ B (Han et al., 2002).

Hyporesponsive cells appeared distinct as a community both when BFA was added for 16 hours post first 8 hours of LPS stimulus to capture the late phase inflammatory response in RAW264.7 which seemed to be dictated largely by the consistency and robustness in the community structure of 1000/1000 (**Figure 4.2**) and when shorter and

longer BFA incubations were used to probe the first 16 hours of inflammatory response by hypo-responsive communities (**Figure 4.3, 4.4**). The consistency in TNF+ subpopulations in 1000/1000 communities suggest that at the single cell level the hypo-responsive communities may be most resistant to making TNF. The most striking trait of hypo-responsiveness seemed to be that the population behaved as a distinct community of cells containing several phenotypes with respect to whether they were positive to TNF, IL-6 and NOS2. Our results suggest that while hypo-responses to LPS (endotoxin tolerance or trained immunity) do involve molecular signatures such as chromatin re-modelling and phenotypic changes as acknowledged in literature (Foster, Hargreaves, and Medzhitov, 2007; Biswas and Lopez-Collazo, 2009; Seeley and Ghosh, 2017), it is not a uniform effect in terms of response. As such, not all pre-stimulated populations respond to LPS as an all or none response but as a diverse community.

4.5.3 Summary and future work

Heterogeneity between a RAW264.7 population responding to LPS challenge versus those that were challenged twice was shown to be more modest in comparison to the first challenge. This is observed when communities are visually represented and compared in the first 8 hours or at later time points such as 12, 16 or 24 hours (**Figure 4.3**). Interestingly, changes in composition upon restricting secretion in twice-challenged communities was modest too (**Figure 4.3**). Numerous histone modifications, nucleosome modelling and DNA methylation have been suggested that suppress the production of inflammatory cytokines like TNF, IL-6 and NOS2 upon LPS tolerance (Seeley and Ghosh, 2017) despite this we observe heterogeneous sub-populations that remain in the community for longer than 16 hours. It will be interesting to check if these communities have any spatial preferences and we would like to explore this by looking at communities by immunofluorescence. It will be further useful to know whether sub-populations make IL-10 or TGF- β differentially. As RAW264.7 cells do not represent physiologically relevant macrophages we checked if our results could be extended to

primary cells we looked at thioglycollate-elicited peritoneal macrophages and found we can indeed find heterogeneous sub-populations. We think looking at heterogeneity in terms of community composition in macrophages responding to antigen can help us learn more about macrophage community composition, especially, in times of immunosuppression.

Chapter 5

Mathematical descriptions of population heterogeneity

5.1 Introduction

LPS-induced activation of macrophages marks the beginning of a complex immune response process. This can lead to resolution of infection when the inflammatory response is sufficient and controlled or, in cases, to the immune system switching from an overtly inflammatory response to an immuno-suppressive state that can lead to severe life threatening conditions like sepsis (Nathan and Ding, 2010; Rittirsch, Flierl, and Ward, 2008; Fleischmann et al., 2016). Mathematical understanding of this immune system failure can help develop strategies for interventions, and methods have been developed to describe the pro-inflammatory and immunosuppressive environment (Day, Metes, and Vodovotz, 2015; Maiti et al., 2015; Torres et al., 2019).

Models have gone further to predict the switch to immunosuppressive phenotypes of immune cells. Using concentrations of pro-inflammatory immune mediator proteins, such as cytokines, clinical outcomes of sepsis have been predicted using personalised models (Brady, R. et al., 2018). Inflammatory signalling by cytokines produced by immune cells can affect the cells themselves (autocrine), other like or unlike cells (paracrine), and sometimes have far reaching effects (endocrine), such as cytokines like

TNF and IL-1 β reaching the hypothalamus in the brain to modulate body temperature (Gourine et al., 1998). Modelling such a process in detail would require hundreds of parameters and can pose problems of over fitting (Lee et al., 2018).

Single cell-dynamics has been modelled to describe average behaviour of cells over time (Wilkinson, 2009). However, mean-field models discount the heterogeneity in macrophage responses, even in clonal populations, shown in cells of myeloid origins and described extensively in our current work in **Chapter 4**. Further, in the general introduction, (**Figure 1.4, Chapter 1**) we have discussed the reasons why these heterogeneous populations emerge. We hypothesise that heterogeneous responses of immune cells to LPS can hold the key to understanding how dissimilar effects can be produced from seemingly identical populations. Understanding the dynamics of this heterogeneity mathematically can provide critical information to drive testable hypothesis experimentally.

5.1.1 Aims

In this chapter, we aim to

1. Describe how an immunosuppressive phenotype can develop after repeated exposure to antigen using simple modelling paradigms with a specific aim to characterise immunosuppression (or hyporesponsiveness) in terms of population heterogeneity.
2. Modify our simple model to understand effects of signalling, given our empirical set up and description, to describe transition rates between sub-populations (or subsets described in **Chapter 4**).

5.1.2 Modelling - Methods employed

Ordinary Differential Equation (ODE) models were written as functions and numerically solved using the built-in ode45 solver in MATLAB. ode45 is implemented in MATLAB using Dormand-Prince pair, an explicit Runge-Kutta formula (Dormand and Prince, 1980).

Parameter estimation of ODE models was done using the function lsqcurvefit in MATLAB that uses non-linear curve fitting to find a vector of values that are a local minimiser to a sum of squares function using the Levenberg-Marquardt algorithm (Levenberg, 1944; Marquardt, 1963).

Bespoke code for implementing stochastic simulations algorithm (or the Gillespie algorithm) was written in MATLAB.

Parameter estimation of Gillespie-based models was performed by rejection-sampling of parameter values drawn from negative binomial, uniform and normal distributions. Parameter estimates were accepted if the model output fell in the 95 percentile confidence interval of the empirical dataset or within a error percentage mentioned in the relevant results section. Where possible, parameter space was bound based on numbers estimated from the ODE model.

MATLAB version 2017a was used for the purposed of coding and simulations.

5.2 Modelling paradigm

We describe temporal changes in population heterogeneity of a community of cells in terms of whether a sub-population of the community is expressing a particular protein or not. In other words, this community of cells is comprised of two phenotypes - one that

makes the inflammatory protein in question and the other that does not. (This partition into two phenotypes is generalised to allow more complex phenotypes, and to include the possibility of hypo-responsive cells, later in this chapter). Traditionally, models describing phenotypes have been modelled using chemical kinetics (Wilkinson, 2009). This assumes that the system has a high number of reactants and products and, thus, the behaviour is deterministic. Such models have been implemented widely using ordinary differential equations (ODEs). Although, these models can sometimes be solved analytically and describe average behaviour of a system, it fails to describe the stochasticity associated with single cell heterogeneity (Wilkinson, 2009).

ODE modelling assumes the reactants and products of the system to be continuous variables, while in contrast the phenotypes within a real population are always discrete. Stochastic modelling that is based on an underlying master equation describing the probability space of species (or phenotypes) assumes discrete numbers. The use of discrete numbers can then be used to describe biological experiments where a small number of species are involved (Wilkinson, 2009). Our experimental results showed large variation in proportion of cells positive for TNF (up to 52% co-efficient of variation) between experiments which raises the case for stochastic methods to describe the system, and suggests that average behaviour may not be sufficient to describe the system. Based on the above reasons, we use stochastic modelling, specifically, the Gillespie-Doob algorithm (Gillespie, 1976) to exactly simulate the time-evolution of communities of macrophage populations that are either positive or negative for one or more proteins.

5.2.1 Gillespie-Doob Algorithm

The Gillespie-Doob algorithm, as introduced in **Chapter 1**, describes the biological (or other) system based on reaction propensities and a state vector, X , that holds the number of each reactant (Gillespie, 1976). Reaction propensities are defined as probabilities that determine which reaction will occur in the next calculated time interval. These time

intervals (time to next reaction) are exponentially distributed random variables so that time is treated continuously rather than as fixed discrete steps. The algorithm first initialises time ($t = t_{initial}$) and state vector, X where $X = [X_1, X_2, \dots, X_n]$. A rate vector, R where $R = [R_1, R_2, \dots, R_M]$, holds the associated rate of each reaction of the defined M reaction channels. For example, in the system



R_1 and R_2 are the per-capita rates that govern X_1 to switching to X_2 , and vice versa, respectively.

The algorithm iterates over a user-defined number of iterations or until a fixed *in silico* time has elapsed. Upon each iteration, two random numbers are generated from a standard uniform distribution, n_1 and n_2 . Next a propensity vector, A_v , is calculated as the product of the rates governing state switch and the count of species in that state to obtain its probability or propensity of occurring when a reaction is fired. In a Gillespie-Doob simulation, containing two reaction channels as in **equation 5.1**, the propensity vector is calculated as the following

$$A_v = X_1 R_1, X_2 R_2 \quad (5.2)$$

and in vector pseudocode form as $A_v = [X_1 R_1 \ X_2 R_2]$. Next a combined propensity A_o is calculated by summing the individual propensities. Time to reaction is then calculated on the basis of A_o and random variable n_1 as

$$t_{next} = 1 / (\ln(n_1) A_o) \quad (5.3)$$

i.e. an exponential random variable with a mean of $1/A_o$. Once t_{next} is calculated, the algorithm calculates the reaction which will occur at this time based on the smallest

integer that is greater than n_2A_o . The selected integer (or index in pseudocode terms) then decides which reaction will occur (**equation 5.2**). In this way, the algorithm accounts for the two possible reactions in an unbiased way. The algorithm updates time to $t = t_{initial} + t_{next}$ and updates the count in the state vector e.g. increasing X_2 by 1 and decreasing X_1 by 1 if the forwards reaction is selected. The algorithm returns and starts a new iteration until a break in the simulation is encountered based on a user-defined number of iterations or maximum time, $t = t_{final}$.

5.2.2 Comparison with ODE and analytical solutions

We implemented the Gillespie-Doob algorithm in MATLAB using bespoke code, and tested it using a well characterised population growth model, the logistic equation. The logistic equation, in ODE form, can be written as

$$\frac{dx}{dt} = \beta x(1 - x_0/K) \quad (5.4)$$

where $\frac{dx}{dt}$ is the rate of change of a population, β is logistic growth rate, K the carrying capacity of a population while x_0 represents the initial population.

This ODE can also be explicitly solved analytically and its solution is given by

$$x_t = x_0K/(x_0 + (K - x_0)e^{-\beta t}) \quad (5.5)$$

In **Figure 5.1** 20 runs of model implementing the Gillespie-Doob algorithm were plotted. We show that the ODE solution for the same equation traces the average behaviour of our stochastic model over the entire solution trajectory. The correctness of the ODE solution implemented using `ode45` in MATLAB is further validated by plotting the analytical solution (given by **equation 5.5**) that explicitly calculates the population size at a given time, t . Thus, we conclude that our stochastic model is mathematically robust and can be further used to model problems set in our chapter aims.

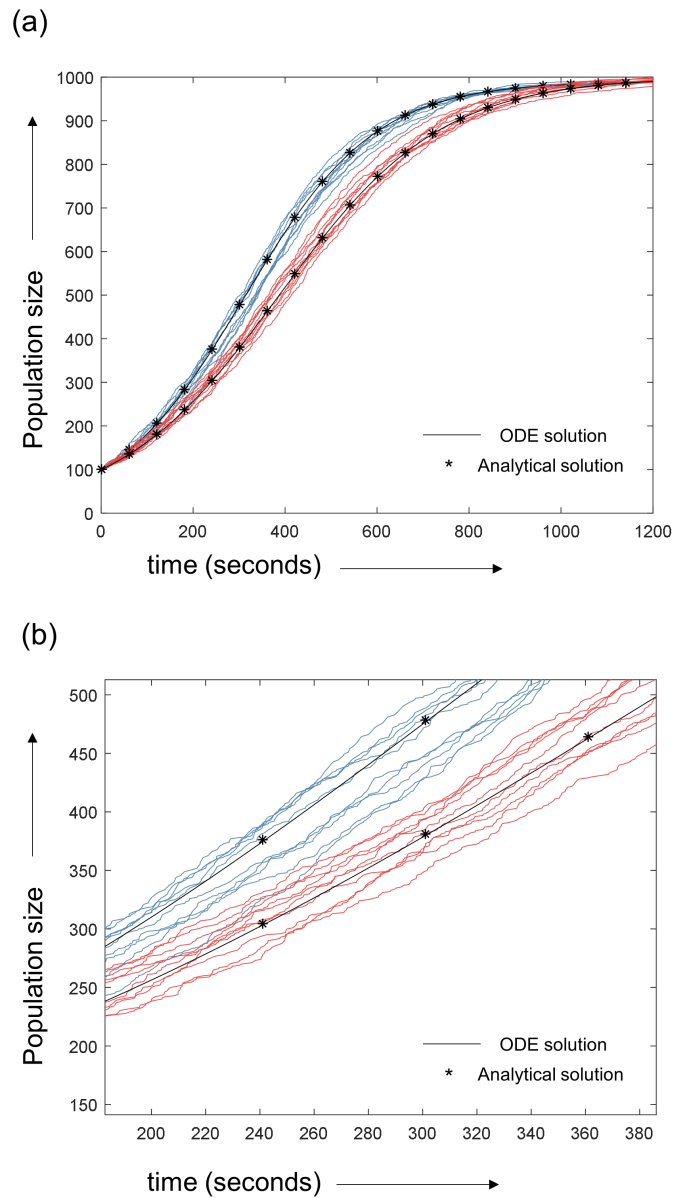


FIGURE 5.1: Gillespie model average represents the ODE solution and both are true to the analytical solution

20 stochastic runs of Gillespie based algorithm for solving a logistic equation with two different values of logistic rates (red and blue trajectories) and the same death rate and carrying capacity were plotted against the corresponding ODE solution and analytically predicted time-evolution of population count with (a) showing overall trajectories and (b) a closer look at the disposition of the three solutions

5.3 Modelling cell populations responding to LPS

5.3.1 Positive-state model definition

We first model the non protein-expressing negative state (N) or the protein-expressing positive state of a cell (P) as a 2-state model that has a fixed forward and backward rate describing the transition between positive and negative states (**Figure 5.2a**). We call this the positive-state model. The protein, modelled here, is physiologically only produced upon macrophage activation by antigens like LPS and is functionally inflammatory (Zhang and An, 2007). The response to LPS in the *in silico* cell environment is, therefore, modelled as a direct positive effect on the forward rate that describes the transition of a cell to the P state such that

$$\alpha_{LPS} = \alpha(1 + \mu L) \quad (5.6)$$

where α_{LPS} is the overall forward rate which takes into account the LPS in the environment, α is the forward rate in the absence of LPS, L is the concentration of LPS in the environment and μ is a constant that describes the magnitude of the response to LPS concentration. The linear assumption in **equation 5.6** is used for simplicity to induce plausible local LPS dynamics, bound between 0 and 1000, at the cost of introducing a single unknown, μ .

Upon describing the above model as an ODE, we have

$$\frac{dP}{dt} = N\alpha(1 + \mu L) - \beta P \quad (5.7)$$

where $\frac{dP}{dt}$ represents rate of change in the number of cells in the positive state with respect to time, P, N are the number of *in silico* cells in the positive and negative state respectively, β is the rate at which cells in the positive state change to negative state.

We model the decay of LPS concentration, L as a simple first order exponential decay in continuous time. This can then be expressed as

$$L(t) = L_0 e^{-\delta t} \quad (5.8)$$

where L_0 and $L(t)$ represent the concentration of LPS at time zero and t respectively, and δ is the constant LPS decay rate.

At a time dependent quasi-equilibrium, where the dynamics of L are assumed to occur on a slower time scale than those of P and N , **equation 5.7** can be used to write

$$P_{quasi}^* = \frac{N\alpha(1 + L_0 e^{-\delta t})}{\beta} \quad (5.9)$$

where rate of change of P , $\frac{dP}{dt} = 0$ and P_{quasi}^* represents the number of *in silico* cells in the positive-state at quasi-equilibrium. It can be inferred from **equation 5.9** that in the absence of LPS in the environment,

$$P^* = \frac{N\alpha}{\beta} \quad (5.10)$$

which is the equilibrium (P^*) dynamics for the simple case where 2 species switch between each other with rates α, β .

Further, **equation 5.7** can be re-written as

$$\frac{dP}{dt} = (T - P)\alpha(1 + \mu L) - \beta P \quad (5.11)$$

where T is total number of cells since $N + P = T$ at any given time.

Equation 5.11 can be exactly solved to the following closed form equation given the initial

condition $P(0) = 0$

$$P(t) = e^{\frac{L_0\alpha\mu e^{-\delta t}}{\delta} - t(\alpha+\beta)} \int_0^t T\alpha e^{\alpha t + \beta t - (L_0\alpha\mu e^{-\delta t})/\delta} (L_0\mu e^{-\delta t+1}) dt \quad (5.12)$$

5.3.1.1 Positive-state model simulation with arbitrary rates

We then simulate the positive-state model to show that over a period of 24 hour, 50% of the population is in positive state without LPS in the environment (**Figure 5.2b**). The simulation shows that in the absence of LPS the proportion of simulated cells that are in the positive-state are equal to those in the negative-state, thus, showing that the simulated results are true to the underlying analytically calculated equilibrium dynamics at $L=0$ (**equation 5.10**). Inflammatory proteins require activation (Zhang and An, 2007), and in the absence of a stimulus to activate an immune response the proportion of positive cells is likely to be small. This suggests that in a physiologically relevant context α must be small in comparison to β to constrain the positive-state proportion when there is no LPS in the environment (**equation 5.10**).

Next we simulate the effects of LPS dose by simulating the model, again with arbitrary rates ($\alpha = 0.005$ and $\beta = 1$) in **Figure 5.3** to illustrate that the magnitude of LPS concentration and its decay can affect how fast the positive-state proportion increases, how high the positive-state proportion rises and how fast the positive-state proportion becomes negative. Parameters for this model can be estimated to fit to the empirical results obtained at 16 hour or 24 hour upon the first challenge of LPS (**Figure 3.7, Chapter 4**) and, can be used to predict the time-evolution of positive proportions of inflammatory proteins (data not shown).

Next we simulated the model to mimic macrophage cell populations that induce a hypo-response from our empirical results in (**Figure 4.1, Chapter 4**) when stimulated with LPS twice in **Figure 5.4** to show that our current simplistic model definition cannot

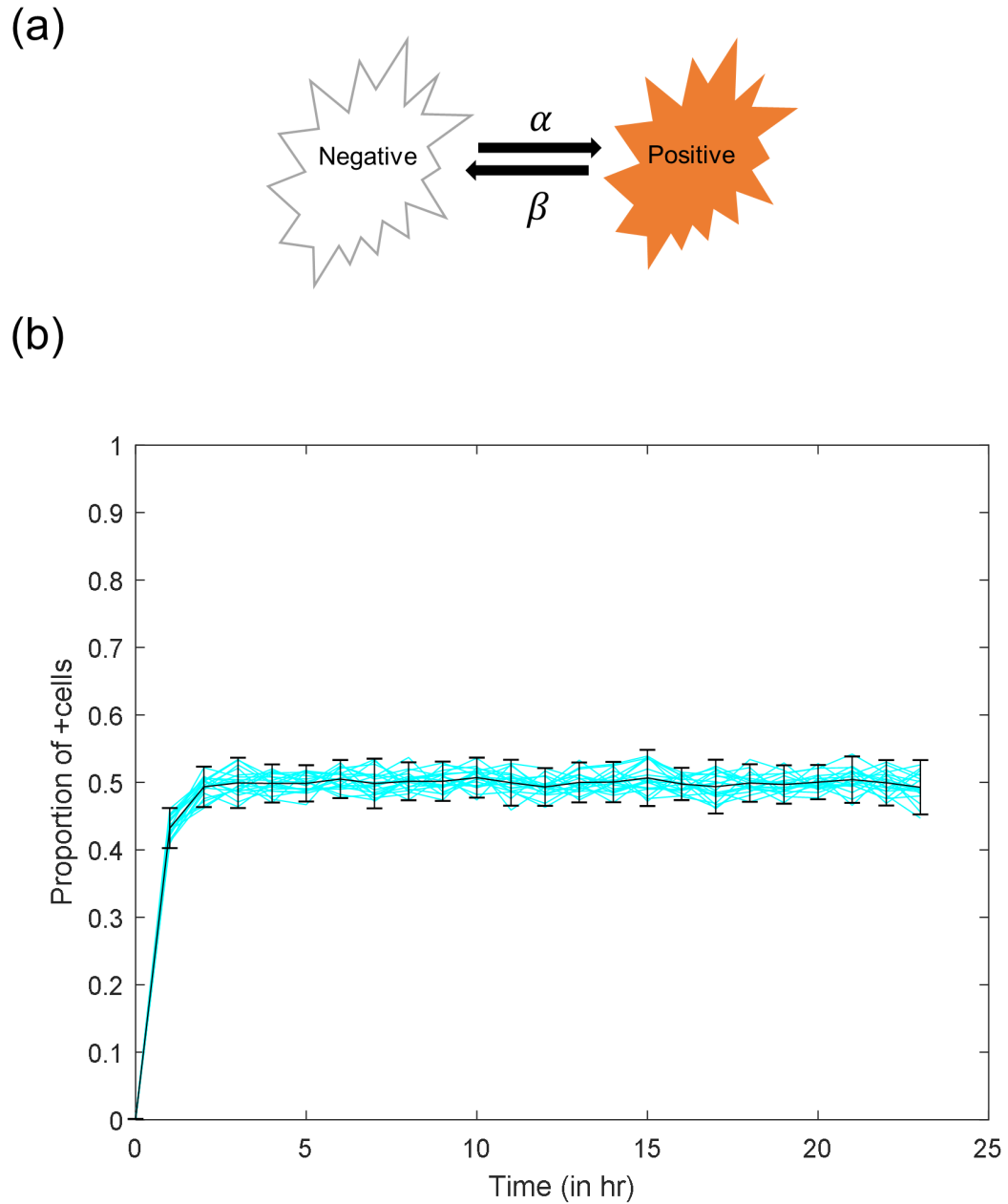


FIGURE 5.2: **Positive-state model description and output when there is no LPS in the environment**

(a) *In silico* cells in the positive-state model can assume two states. Negative and positive state transitions are defined by α and β rates (b) 20 stochastic realisations of the time-evolution of cells positive-state as a proportion of the total population when there is no LPS in the environment i.e. $L = 0, \alpha = 1, \beta = 1$. The bars denote 95% confidence intervals of the mean.

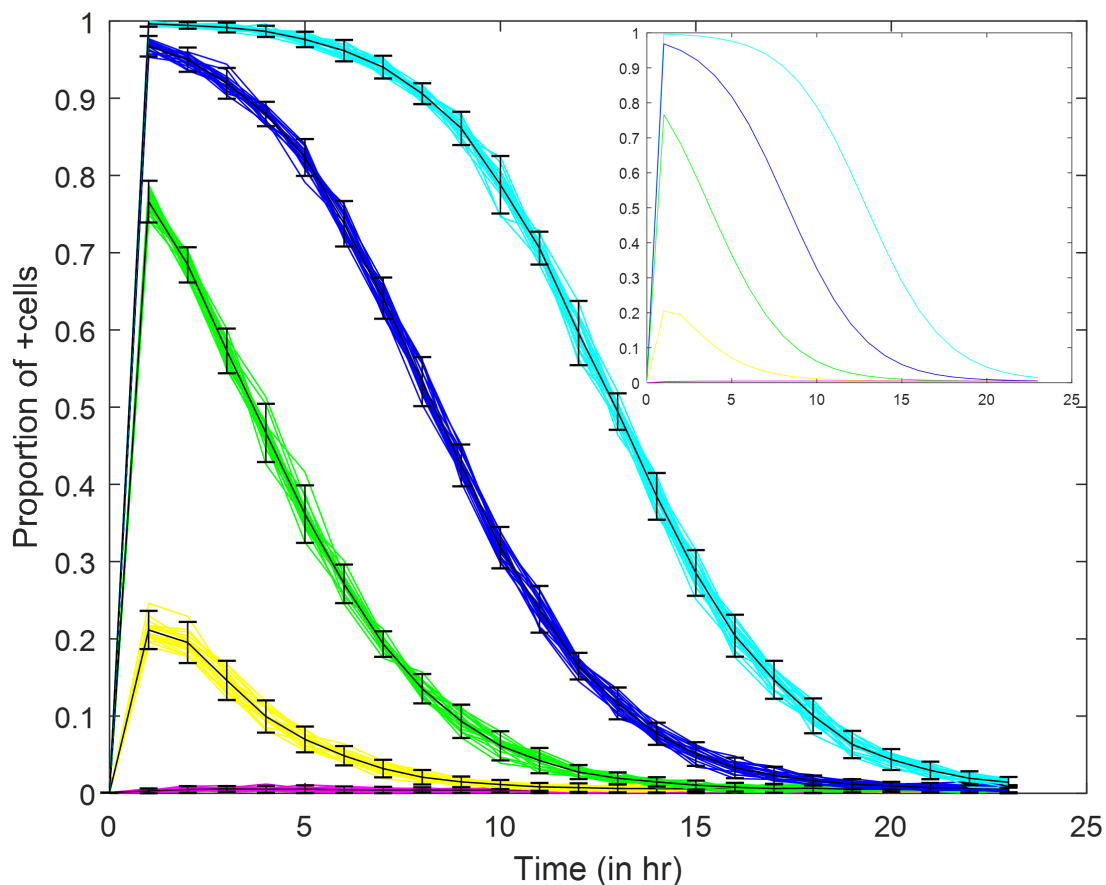


FIGURE 5.3: **LPS dose affects the rise and fall of positive cells differentially**

Positive-state model was simulated for LPS doses 0, 1, 10, 100 and 1000 with arbitrary forward rate ($\alpha = 0.005$, $\beta = 1$) with a fixed arbitrary LPS decay rate ($\delta = 0.5$). 20 stochastic runs for each dose (magenta=0, yellow=1, green=10, blue=100 and cyan=1000) were run for 24 simulated hour with bar graphs plotted in black representing 95% confidence interval of the mean (of all 20 trajectories for each dose). Inset represents the trajectories traced by the analytical solution of **equation 5.12** for LPS doses (magenta=0, yellow=1, green=10, blue=100 and cyan=1000)

induce a hypo-response in terms of predicting a smaller proportion of positive-state cells upon secondary stimulus. Artificially changing the values α and β at the beginning of the *in silico* secondary dose of LPS can induce hypo-response in terms of a smaller proportion of positive-state cells (data not shown). While this change of rates may provide a trivial explanation for hypo-responsiveness upon two doses of LPS, such a modification to the model would suggest that all macrophages upon secondary stimulus with LPS respond with a different rate. The idea that rates change per se for the population agrees with population-level studies on the hypo-responsive phenotype that posit that phenotypic changes reduce the amount of inflammatory proteins (Biswas and Lopez-Collazo, 2009). However, based on our experimental results (**Chapter 4**), we have shown that the response to a secondary LPS challenge is heterogeneous and is associated with overall lower proportions of macrophages positive for inflammatory proteins such as TNF, IL-6, NOS2 and pro-IL-1 β . This leads us to speculate that modelling hypo-responsive populations must include states that may capture a non-responsive state upon LPS challenge.

5.3.2 Non-responsive (nr) model definition

We next introduce two new cell states within the positive-state model to capture the hypo-responsive phenotype upon re-stimulus with LPS based on established knowledge (Biswas and Lopez-Collazo, 2009). This modified model (or nr-model) includes a non-responsive state which refers to an *in silico* cell that, temporarily, cannot respond to LPS along with a non-responsive (permanent) type that can no longer respond. Cells can transition into the non-responsive state by a rate γ from the positive state, thus constraining only cells that have responded to LPS to be able to make this transition. The non-responsive cell can then switch back to the negative state with a rate of β_2 . The *in silico* non-responsive cell can also switch to the non-responsive (permanent) state with a rate of γ_2 . Upon assuming this state, an *in silico* cell can no longer switch to any other

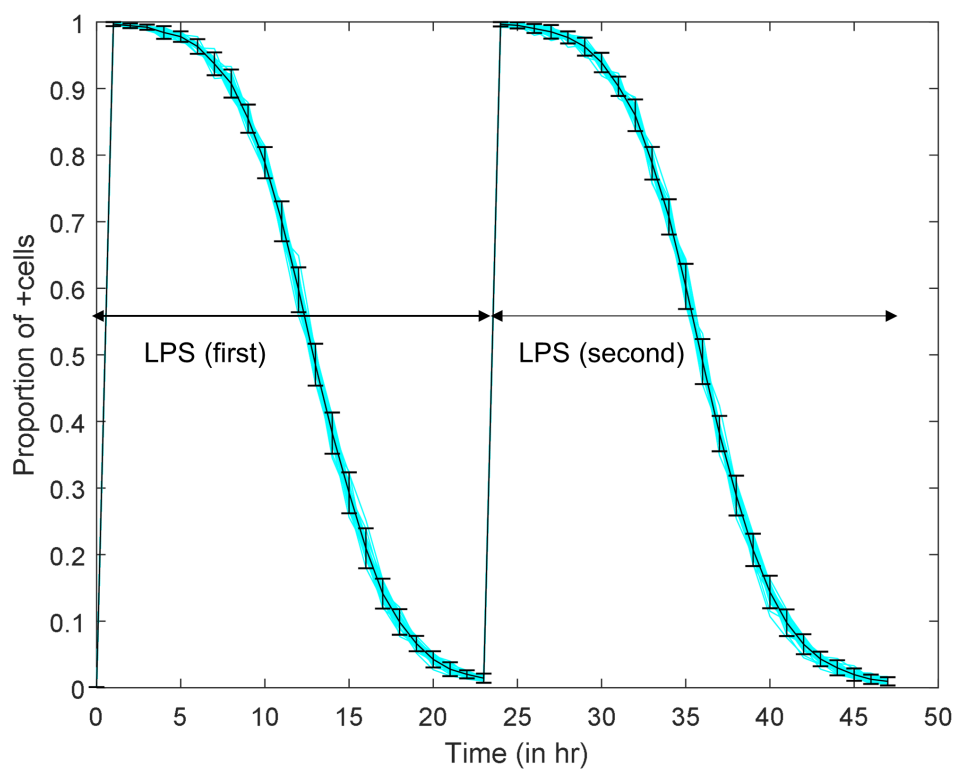


FIGURE 5.4: **Two temporally separated LPS doses induces similar response from *in silico* cells.**

Positive-state model was simulated for LPS dose of 1000 at 0 hour and a second dose of LPS at 24 hour and the time-evolution plotted between 0-48 hour with arbitrary forward rate ($\alpha = 0.005$, $\beta = 1$) and a fixed LPS decay rate ($\delta = 0.5$). 20 stochastic runs are plotted (magenta) with error bars (blue) representing 95% confidence interval of the mean (of all 20 trajectories for each dose).

state (**Figure 5.5**) and, therefore, becomes hypo-responsive for the duration of the simulation.

Simulating this model with arbitrary parameter values of $\alpha = 1$, $\beta = 1$, $\gamma = 1$, $\beta_2 = 1$, $\gamma_2 = 1$ to plot the trajectory for positive-state proportions, we show that the added complexity associated with the additional states (and the rates associated with them) can lead to a sharp decline in the peak of the positive-state and a longer right tail. The lower peak is because of the increased probability of leaving the positive state (with rates $\gamma = 1$ and $\beta_2 = 1$) while the right tail is due to contribution of more negative cells that can become positive later into the time-evolution as influenced by β_2 . Most interestingly, we can track the proportion of non-responsive (permanent) state over time (**Figure 5.6**, plotted in black). At quasi-equilibrium, the largest fraction comprises *in silico* of the permanently non-responsive state suggesting that the model tends to adopt a fully non-responsive (permanent) state.

5.3.2.1 nr model - Assumptions

As a basis for future, more complex, modelling studies, it is useful to be clear about the assumptions used in the nr model. These are enumerated below:

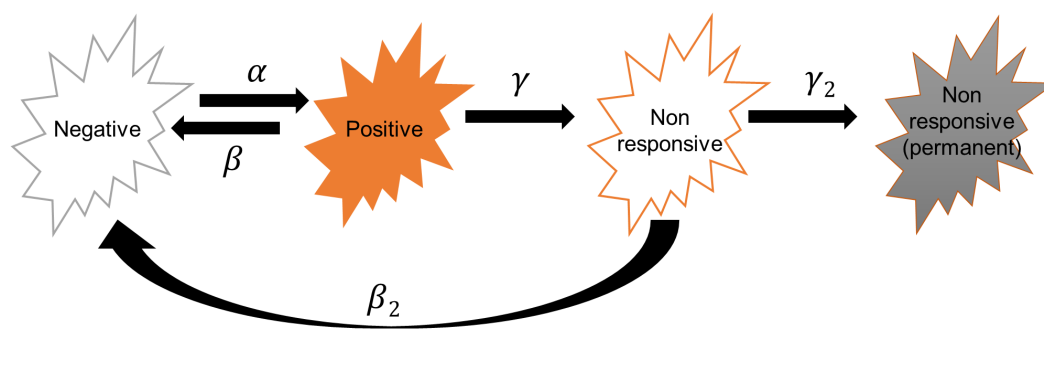
1. Individual proteins are treated independently by the model

Simulated cells respond to LPS and can be in a positive-state for an inflammatory protein. This activation of macrophages is treated without considering effects of cytokines being secreted in the environment and consequently, affecting the positive-state proportion for the inflammatory protein, under consideration.

2. In-silico cells in the negative proportion can only become positive.

The model does not allow for the non-responsive state to transition back to the positive state and, thus, forces the model to only allow for LPS-induced α dependent transition to the positive state.

3. A fixed arbitrary constant is used to model LPS utilisation/degradation

FIGURE 5.5: **nr model description**

a. *In-silico* cells can be in one of 4 different states that can transition via 5 routes upon stimulus. Negative, positive, non-responsive and non-responsive (permanent). Non-responsive cells can transition back to the negative-state or can transition to a non-responsive (permanent) state.

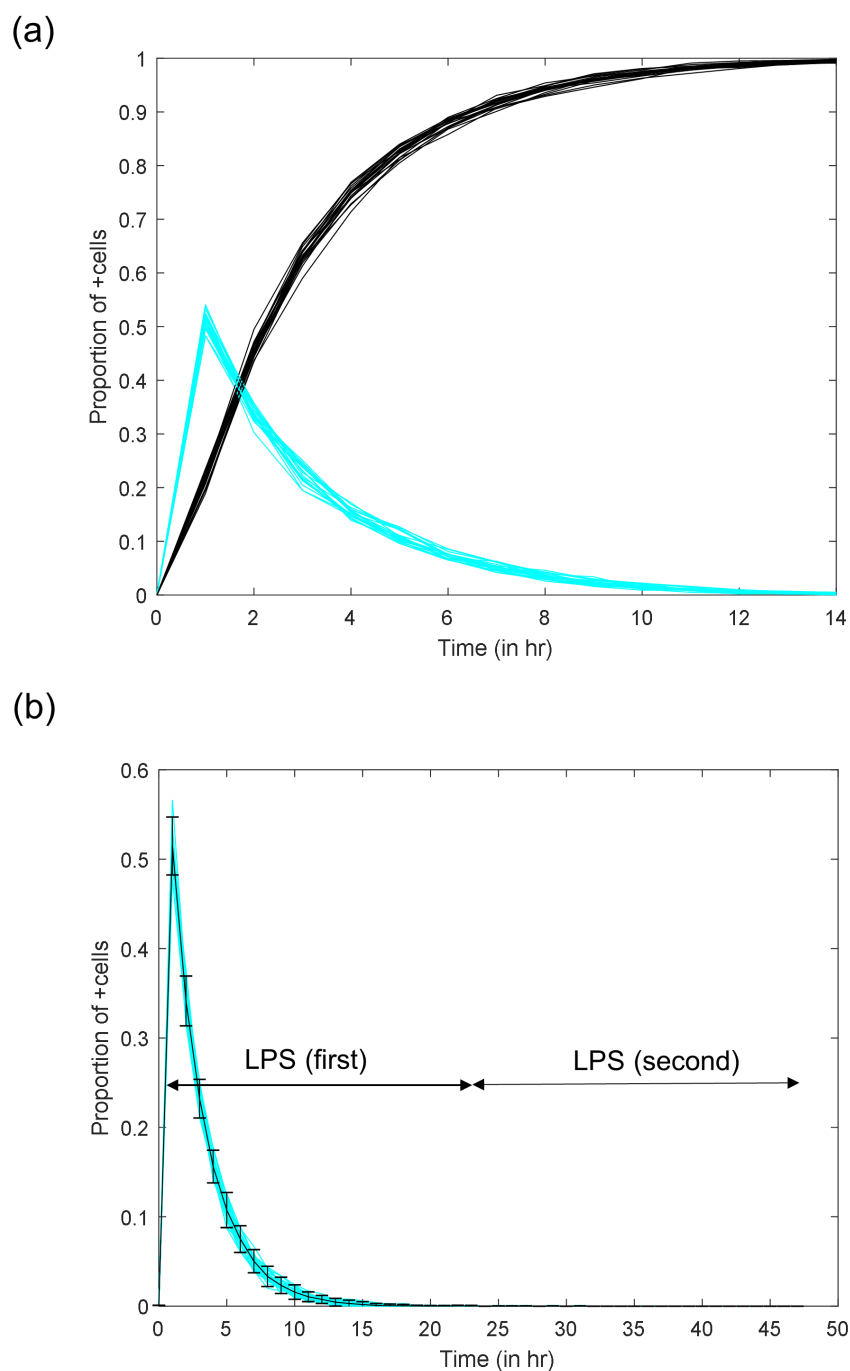
LPS bound to TLR4 is endocytosed and is related to late-phase activation of NF- κ B to initiate a second-wave of inflammatory proteins. This is not considered in the model. Thus, LPS degradation and endocytosis (or intake) is both modelled as simple exponential depletion from the environment.

4. Effects of cell density are ignored

There are no density-dependent or frequency-dependent processes within the modelling framework.

5.3.3 Parameter estimation - nr model

We then fitted our nr model to empirical data pertaining to TNF, IL-6, NOS2 and pro-IL-1 β positive cells at one temporal snapshot (16 hour of LPS stimulus), treating each cytokine independently. Since 16 hour was the end-point of our LPS stimulus experiments, we hoped to find a large number of parameter sets that would qualitatively match the end point proportions from our experiments, while revealing diverse trajectories of reaching that end point. We estimated parameters by drawing random

FIGURE 5.6: **nr model example output**

a. *In-silico* cells can be in 4 different states via 5 routes upon stimulation. Negative, positive, non-responsive and non-responsive (permanent). Non-responsive cells can transition back to the negative-state or can transition to a non-responsive (permanent) state. **b.** nr model was simulated with $L = 1000$ at 0 hour and a second dose ($L=1000$) at 24 hour. The time-evolution is plotted between 0-48 hour with $\alpha = 1$, $\beta = 1$, $\gamma = 1$, $\gamma_2 = 1$, $\beta_2 = 1$ and a fixed LPS decay rate ($\delta = 0.5$).

20 stochastic runs are plotted (magenta) with error bars (blue) representing 95% confidence interval of the mean (of all 20 trajectories for each dose) simulated

numbers from a negative binomial and normal distribution repeatedly, and then simulating the nr model using that parameter set, analysing upon each iteration if a set of parameter values approached the 95% confidence interval of the mean value of our empirical dataset at the simulated 16 hour time point (**Figure 3.7, Chapter 4**; n=4-5).

Next, we used the set of parameter sets as returned above (hereafter referred to as the 'rough fit') to fit to a more temporally resolved experimental data set (described in **Figure 4.3 in Chapter 4**) with data points at 8, 12, and 16 hour post primary and secondary challenge of LPS ('specific fit'). Primary or first challenge is represented as Media/1000 (LPS challenge with 100 ng/ml) while secondary challenge as 10/1000 and 1000/1000. Our empirical results were derived using flow cytometry to capture frequency of positive cells (TNF, IL-6, NOS2 and/or pro-IL-1 β) at a single-cell level and is based on at least n=85,000 cells per data point.

5.3.3.1 TNF

Analysing the parameter values from the 'rough fit' as described previously (**Figure 5.7a**), our results indicated that a wide range of parameter values can fit our empirical data set at 16 hour of LPS stimulus. On average, values of α (the rate at which *in-silico* cells become positive) was the highest, followed by β_2 (the rate at which a non-responsive cell transitioned to a negative state) and γ_2 (the rate at which non-responsive cells transition to the non-responsive (permanent) state). Mean values of β (the rate at which cells in the positive state can transition to the negative state) and γ_1 were comparable. The range of γ_1 values was the lowest among all parameter values. While, on average, all parameters were well represented (in magnitude) in the set of possible parameter values that fit to the experimental data, some individual parameter sets included parameter values which were very close to zero. This suggests that a diverse set of time-evolution trajectories can fit our experimental end point at 16 hour.

We next looked at the parameter values more closely by segregating them based on increasing values of α (**Figure 5.7b**). When values of α are less than the 25th percentile (of all predicted values of α) almost all parameters are, on average, greater than α . Higher values of γ_2 on average compared to β suggested a greater probability of simulated cells to transition to the TNF non-responsive state. A higher γ_2 than β_2 in these parameter sets suggest the greater probability of transitioning to the TNF non-responsive (permanent) state from the non-responsive state.

The parameter sets where α values were in the inter-quartile region of all predicted α values were very similar (to $\alpha < 25$ th percentile) in terms of differences between their means. However, β values were lower than α values, thus, increasing the chance of cells to transition from negative to TNF positive state even with decreasing LPS concentration.

Estimated parameter sets with α values (selected between 75th percentile and 1.2), mean β values were higher than γ_1 . This suggests TNF positive cells to have a higher probability to transition to TNF negative state than TNF non-responsive. In addition, since mean β_2 values were greater than γ_2 the probability of becoming non-responsive (permanent) was less.

Next, comparing parameter sets with the highest α values ($\alpha > 1.2$), mean β value was lower than mean γ while on the other hand β_2 was higher than γ_2 . In other words, while TNF positive cells had a higher chance of becoming TNF non-responsive based on this parameter set, the chances of becoming non-responsive (permanent) was lower (**Figure 5.7b**). In conclusion, we show that the 'rough fit' parameter estimation provided us with a diverse set of parameters that could fit the empirical data point at 16 hour, and that these parameter sets allow a diverse range of possible routes/trajectories of the nr model behaviour to fit that end point.

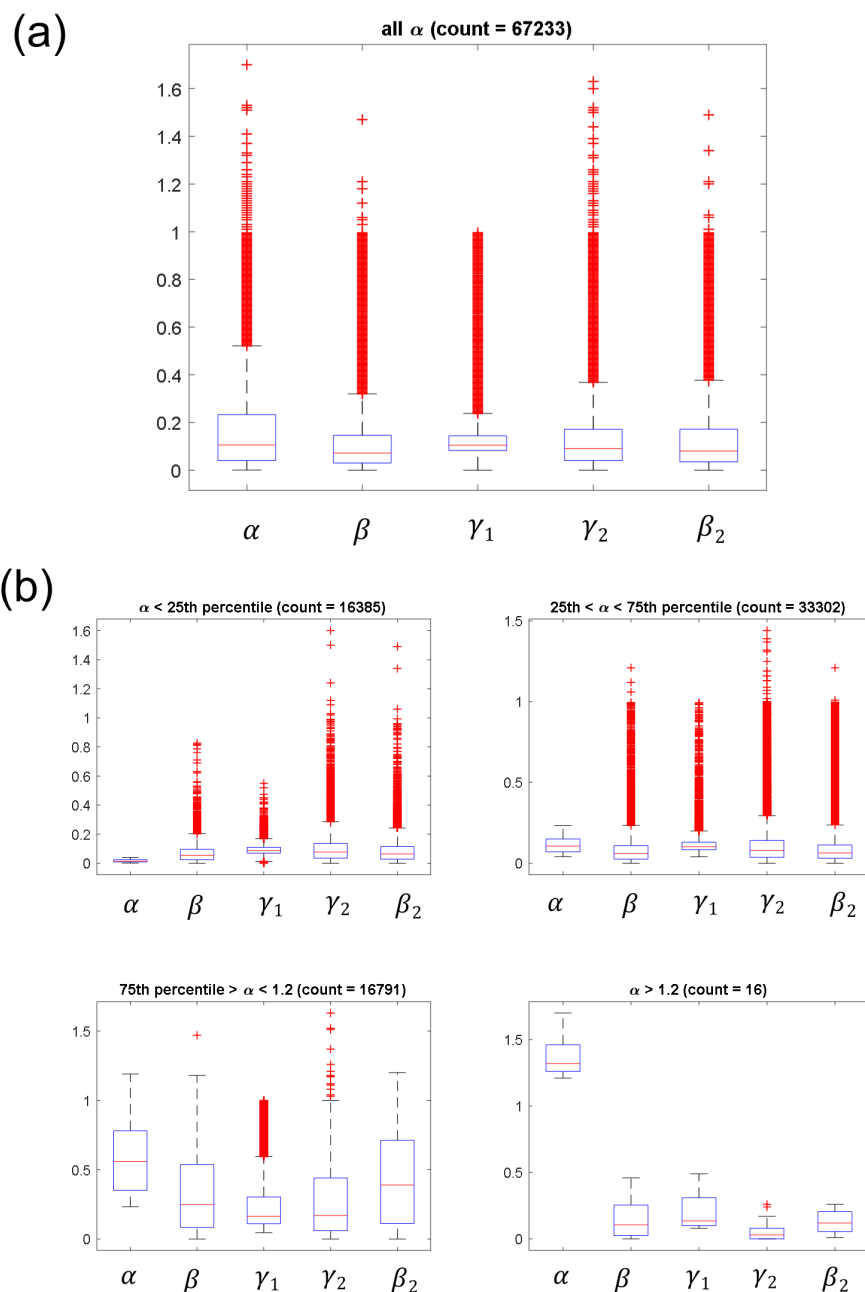


FIGURE 5.7: **Parameters estimation for TNF+ dataset reveal average α values greater than the other parameters**

Box and whiskers plot showing the calculated parameter values for nr model estimated based on empirical data point at 16 hour of LPS stimulus with 1, 10, 100 and 1000 ng/ml of RAW264.7 cells to obtain the frequency of TNF positive cells ($n=4-5$ for each LPS dose) a) Shows the overall parameter sets that were estimated b) Parameter sets were segregated based on the values of α

We next used parameter sets derived above (**Figure 5.8a**) to estimate parameters for the 'specific' fit (**Figure 5.8c**) as described in sub-section 5.3.3. Parameters that best approximated the empirical datasets were used to simulate the time-evolution of TNF positive cells over a 48 hour period. The first 24 hour period represented the first challenge while the 24-48 hour period represented second challenge.

Trajectories for the time-evolution of TNF positive cells (**Figure 5.8c**, 10/1000 and 1000/1000), do indeed, predict an overall hypo-response in both 10/1000 or 1000/1000 treatments such that the peak TNF positive population is higher in the first LPS dose compared to the second dose of LPS. TNF positive cells in the 10/1000 treatment during the first LPS dose appear to decrease faster as the LPS concentration in the first stimulus is lower (10 vs 1000) but also because of the added contribution of the increasing numbers in the non-responsive or non-responsive (permanent) states (**Figure 5.8c**). Model simulation also predicts the proportion of TNF positive cells at 16 hour (first dose) to be lower than at 40 hour (16 hour post second LPS) in 10/1000 and was observed in *in-vitro* experiments as well (**Figure 4.3, Chapter 4**). This is, however, not evident in the model simulation for the 1000/1000 treatment.

Overall, the parameter estimated nr model for TNF captures a hyporesponsiveness because of an increasing pool of non-responsive cells that cannot respond to LPS. In the nr model the non-responsive state (NRS) and non-responsive (permanent) state (NRPS), taken together, represent the number of non-responding cells at any given time during the simulation. The time-evolution of these TNF non-responding cells is shown in **Figure 5.9** for treatments 10/1000 and 1000/1000. When the first LPS dose is low (10/1000), the model predicts that about 50% of the population becomes either non-responsive or non-responsive (permanent) within the first 10 hour of the stimulus. This shows that upon the second LPS dose half the population is not immediately affected by LPS. Only cells in the non-responsive state transitioning to the negative state can go on to become

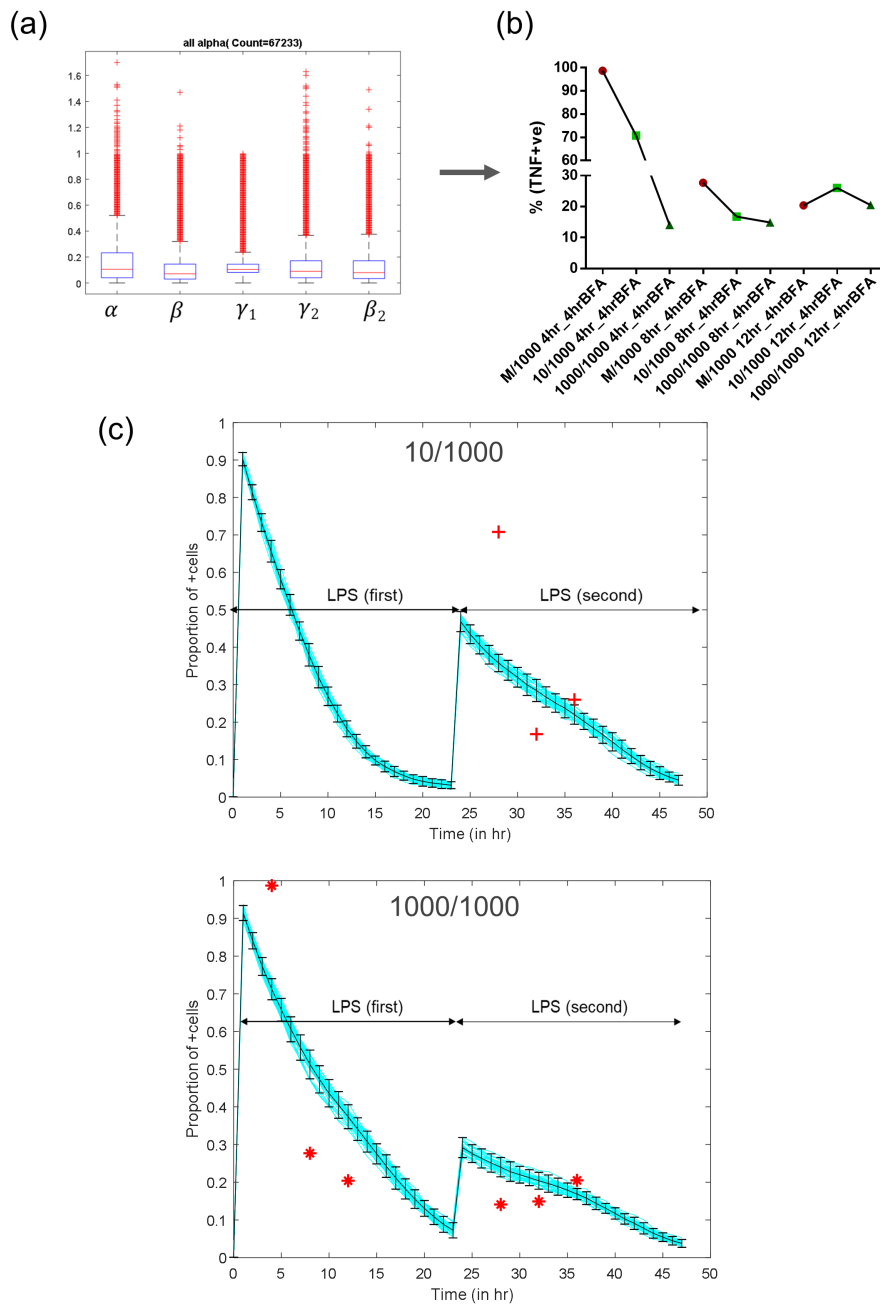


FIGURE 5.8: Peak TNF positive proportion decreases at second stimulus

a Box and whiskers plot showing the estimated parameters for TNF by nr model simulations based on empirical data as shown in before-after plot in **b**. **c** nr model was simulated for first LPS dose (10 or 1000) at 0 hour and a second dose of LPS (1000) at 24 hour and the time-evolution plotted between 0-48 hour with estimated forward rate $\alpha = 0.0128$, $\beta = 0.1828$, $\gamma = 0.0901$, $\gamma_2 = 0.0020$, $\beta_2 = 0.0161$ and a fixed LPS decay rate ($\delta = 0.5$). 20 stochastic runs representing TNF positive cells are plotted (cyan) with error bars (black) representing 95% confidence interval of the mean (of all 20 trajectories for each dose). Empirical data in red asterisks and crosses.

TNF positive. Thus, lower values of β_2 upon second LPS dose can affect the total pool of cells (negative state) available to respond to LPS and become TNF positive (**Figure 5.9**). This non-responding population (NRS + NRPS) increases yet again upon the second LPS dose and increases to up to 70% of the total population. When the first LPS dose is higher (1000/1000) within the first 24 hour of the simulation 70% of the population becomes non-responding (NRS + NRPS). Second LPS dose also increases the total number of non-responding cells up to about 80%. This increase is not as pronounced as in the case of the 10/1000 simulation as a high first dose reduces the number of negative (or cells available to respond to LPS) which in turn reduces the number of TNF positive cells that can further increase the non-responding cell population (**Figure 5.9**). Our model supports the idea that, that upon responding to LPS, macrophages become non-responsive very quickly and are unable to respond to a second LPS dose with equal numbers. TNF positive cells become non-responding with higher magnitudes of LPS and with repeated doses.

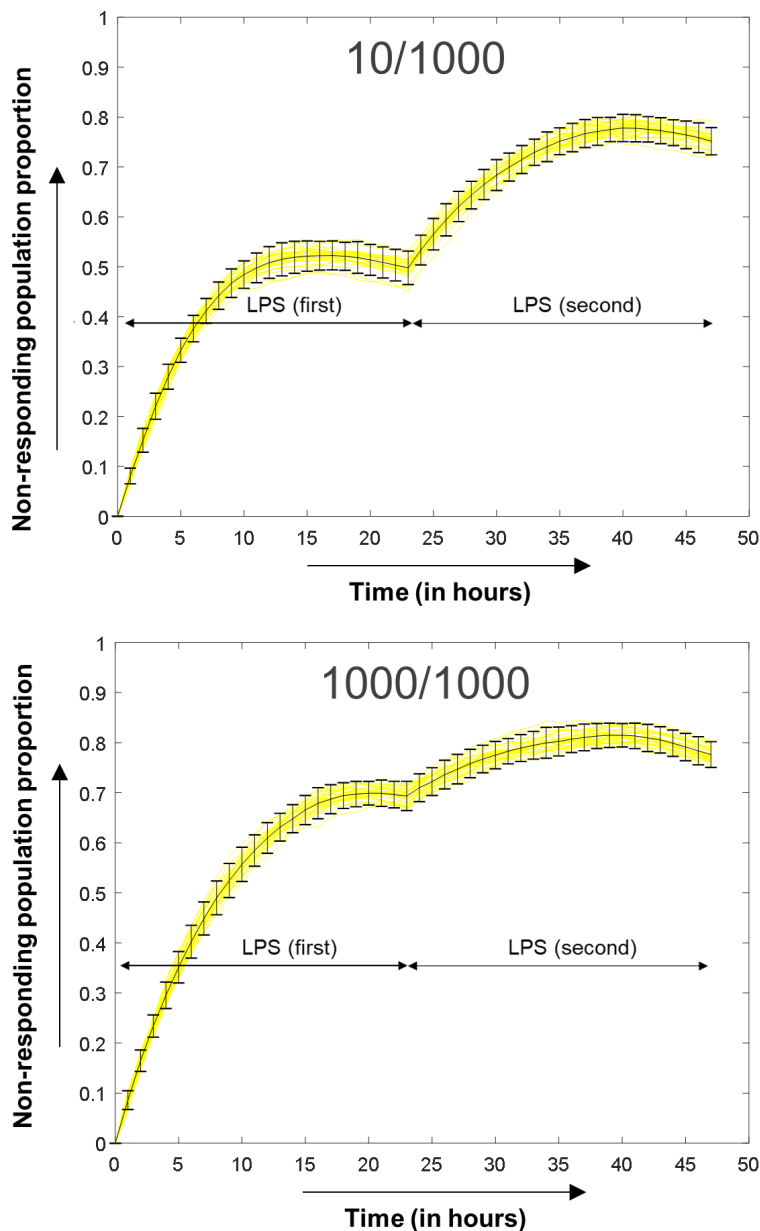


FIGURE 5.9: **Non-responding TNF population increases with first and second dose.**

Time-evolution of TNF non-responding states (non-responsive state, NRS + non-responsive permanent state, NRPS) over two LPS doses. First dose at 0 hour and second at 24 hour. 20 stochastic runs representing TNF (NRS+NRPS) are plotted (yellow) with error bars (black) representing 95% confidence interval of the mean (of all 20 trajectories for each dose)

5.3.3.2 IL-6

We then estimated parameters for IL-6 positive cells as described in sub-section 5.3.3 to first obtain a 'rough' fit of parameters and then a 'specific' fit to check if the model can explain empirical data pertaining to first (1000 only) and secondary challenges of LPS (10/1000 and 1000/1000; **Figure 5.10**).

IL-6 positive cells were greater during the first LPS dose in comparison to the second LPS challenge for both 10/1000 and 1000/1000 treatments, at least in terms of the initial peak in IL-6 positive population with approximately 50% of the cells responding to LPS for both challenges with the higher (1000) or lower (10) first dose (**Figure 5.10**; left panel). In 1000/1000 treatment, the proportion of cells that were IL-6 positive was higher throughout the duration of the stimulus (i.e. comparing 0-24 hours and 24-40 hours). This was not true for the 10/1000 population with a higher proportion of IL-6 positive cells 10 hour post secondary stimulus (34-48 hours) as compared to IL-6 positive cells between 10-24 hours post first LPS challenge. This suggests that in the hypo-responsive population (10/1000), while the initial peak of IL-6 positive population is lower, IL-6 positive populations do not switch off as fast as in the first challenge (**Figure 5.10**; left panel). This may suggest an explanation for an increased IL-6 amount in supernatant of twice challenged (10/1000) as compared to twice challenged (1000/1000) RAW264.7 cells in culture (**Figure 4.1, Chapter 4**).

We then looked at the proportion of cells in the non-responsive state (NRS) and non-responsive (permanent) state (NRPS) taken together to look at the time-evolution of non-responding IL-6 cell population (**Figure 5.10**; right panel). Our results indicate that the IL-6 non-responding population at low first dose increases up to approximately 80% within the first 5 hours corresponding to the decrease of IL-6 positive cells at first stimulus. This population steadily decreases over 24 hours and increases the proportion of cells in the negative state. This suggests that upon the second dose about 50% of the

population is available to respond to LPS. This explains the approximate halving of the total proportion of IL-6 positive cells at first and second stimulus (**Figure 5.10**; left panel). IL-6 non-responding population (NRS + NRPS) in 1000/1000 treatment at first dose reaches a total of 80% within the first five hours and decreasing slightly over 24 hours. The second dose of LPS increases this non-responding population to approximately 80% (**Figure 5.10**). Overall, the nr model parameters estimated for empirical IL-6 proportions predict that only half the *in-silico* population responds to LPS and a hypo-response to secondary dose is observed with a more pronounced effect in 1000/1000 treatment.

5.3.3.3 pro-IL-1 β

We then estimated parameters for the nr model to fit empirical results for pro-IL-1 β to observe model behaviour, using the methods outlined above in sub-section 5.3.3. As observed earlier for TNF and IL-6, pro-IL-1 β positive cells decreased upon the second dose of LPS for both 10/1000 and 1000/1000 treatments (**Figure 5.11**). Simulating the nr model with estimated parameters shows a sharp increase in pro-IL-1 β positive cells observed when LPS stimulus is low (10) or high (1000). Estimated parameter values were $\alpha = \beta = \gamma_1 = \gamma_2 = 0.05$ suggesting that upon LPS stimulus (first or second) cells in the negative state would switch on pro-IL-1 β and then transition to a non-responsive state or the negative state with equal probability. Further, based on a high β_2 value, cells transitioning to the non-responsive state can switch back to negative state ($\beta_2 = 6 * \gamma_2$). Overall, non-responding (NRS + NRPS) cells comprised 15-20% of the total population after first stimulus, while at the end of secondary stimulus for both (10/1000 and 1000/1000) reach 30% (**Figure 5.11**; right panel) of the total population. The results suggest that pro-IL-1 β non-responding populations may have a stronger effect, given above mentioned parameters, on overall pro-IL-1 β positive numbers when the population is challenged multiple times with LPS.

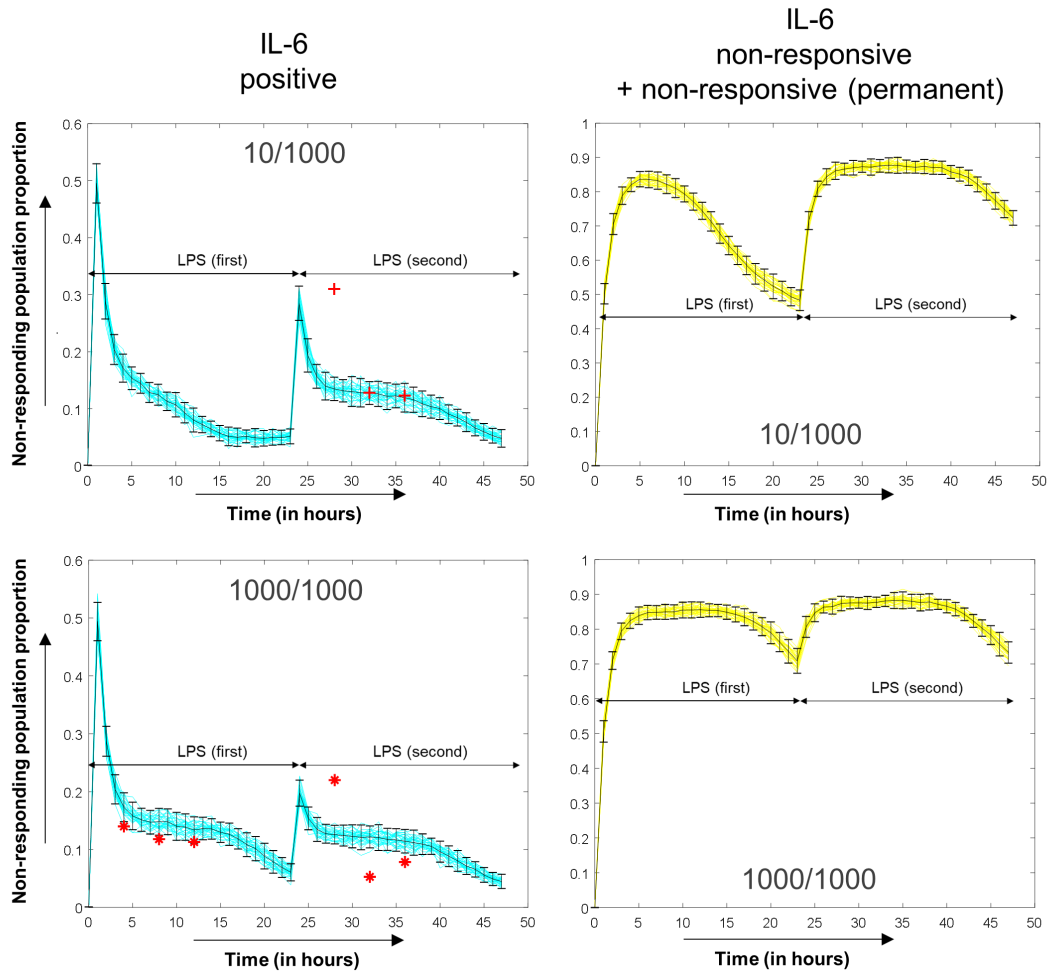


FIGURE 5.10: **IL-6 positive cells do not peak as high upon second dose of LPS**

a)nr model was simulated for first LPS dose (10 or 1000) at 0 hour and a second dose of LPS (1000) at 24 hours and the time-evolution plotted between 0-48 hours with estimated forward rate $\alpha = 0.1$, $\beta = 0.11$, $\gamma = 0.77$, $\gamma_2 = 0.01$, $\beta_2 = 0.14$ for IL-6 and a fixed LPS decay rate ($\delta = 0.5$). 20 stochastic runs representing IL-6 positive cells are plotted (cyan) with error bars (black) representing 95% confidence interval of the mean (of all 20 trajectories for each dose) representing 95% confidence interval of the mean (of all 20 trajectories for each dose)

b)Time-evolution of IL-6 non-responding states (non-responsive state, NRS + non-responsive permanent state, NRPS) over two LPS doses. 20 stochastic runs representing IL-6 (NRS+NRPS) are plotted (yellow) with error bars (black) representing 95% confidence interval of the mean (of all 20 trajectories for each dose). Empirical data in red asterisks and crosses.

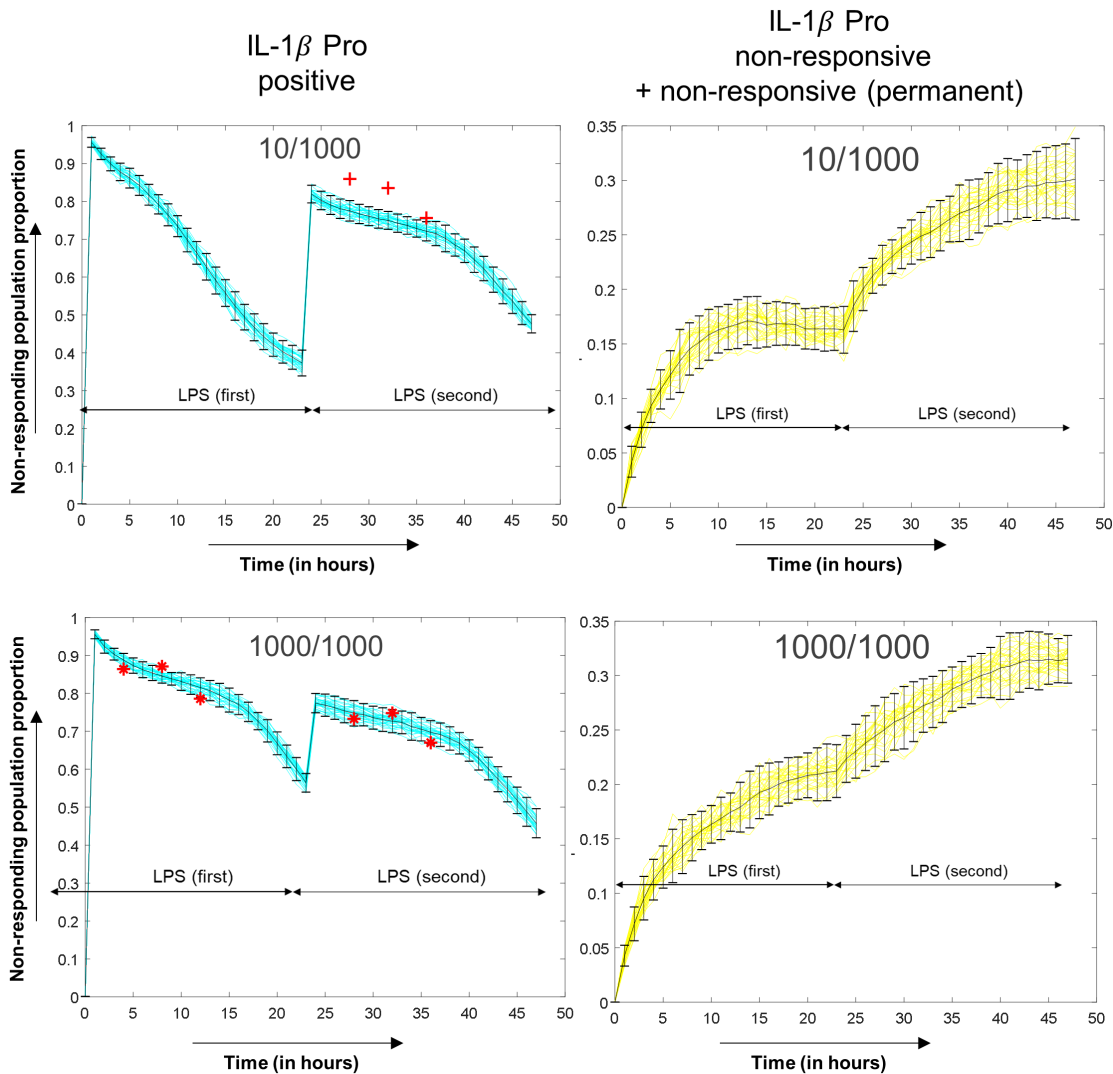


FIGURE 5.11: **pro-IL-1 β non-responsive cells increase steadily to 30% at 48 hours**

a nr model was simulated for first LPS dose (10 or 1000) at 0 hour and a second dose of LPS (1000) at 24 hours and the time-evolution plotted between 0-48 hours with estimated forward rate $\alpha = 0.05$, $\beta = 0.05$, $\gamma = 0.05$, $\gamma_2 = 0.05$, $\beta_2 = 0.3$ for pro-IL-1 β and a fixed LPS decay rate ($\delta = 0.5$). 20 stochastic runs representing positive cells are plotted (cyan) with error bars (black) representing 95% confidence interval of the mean (of all 20 trajectories for each dose). **b** Time-evolution of pro-IL-1 β non-responding states (non-responsive state, NRS + non-responsive permanent state, NRPS) over two LPS doses. 20 stochastic runs representing NRS+NRPS are plotted (yellow) with error bars (black) representing 95% confidence interval of the mean (of all 20 trajectories for each dose). Empirical data in red asterisks and crosses.

5.3.3.4 NOS2

NOS2 is upregulated upon LPS stimulus and catalyses nitric oxide, a potent mediator for inflammation (Bogdan, 2015). Using the empirical data point for NOS2 positive cells, we then estimated parameters that best fit the NOS2 dataset as outlined in sub-section 5.3.3. Parameter fitting for NOS2 revealed that it was difficult to fit the NOS2 positive empirical data points to the nr model, particularly, to the first challenge of LPS. Visualising the empirical data points it appears that NOS2 positive cells increase more slowly than suggested by the model fit upon LPS stimulus (**Figure 5.12**). The lower gradient in increasing NOS2 positive cells is also evidenced by published studies suggesting NOS2 requires additional signalling to LPS to be transcribed (Farlik et al., 2010).

The model, however seems to fit the second dose of LPS better and indicates a gradual decrease in overall NOS2 positive cells. 48 hours into the simulation, the model suggests that upto 60-65% remain positive for NOS2. While the number of non-responding cells (NRS + NRSP) increases, linearly, with LPS dose and time, only about 16% of the population is non-responding after 48 hours (post first and second stimulus). At 24 hours after first stimulus, this percentage is even lower (approximately 8%), suggesting hypo-response in terms of NOS2 positive cells, if any, may not be associated with the non-responding cell state.

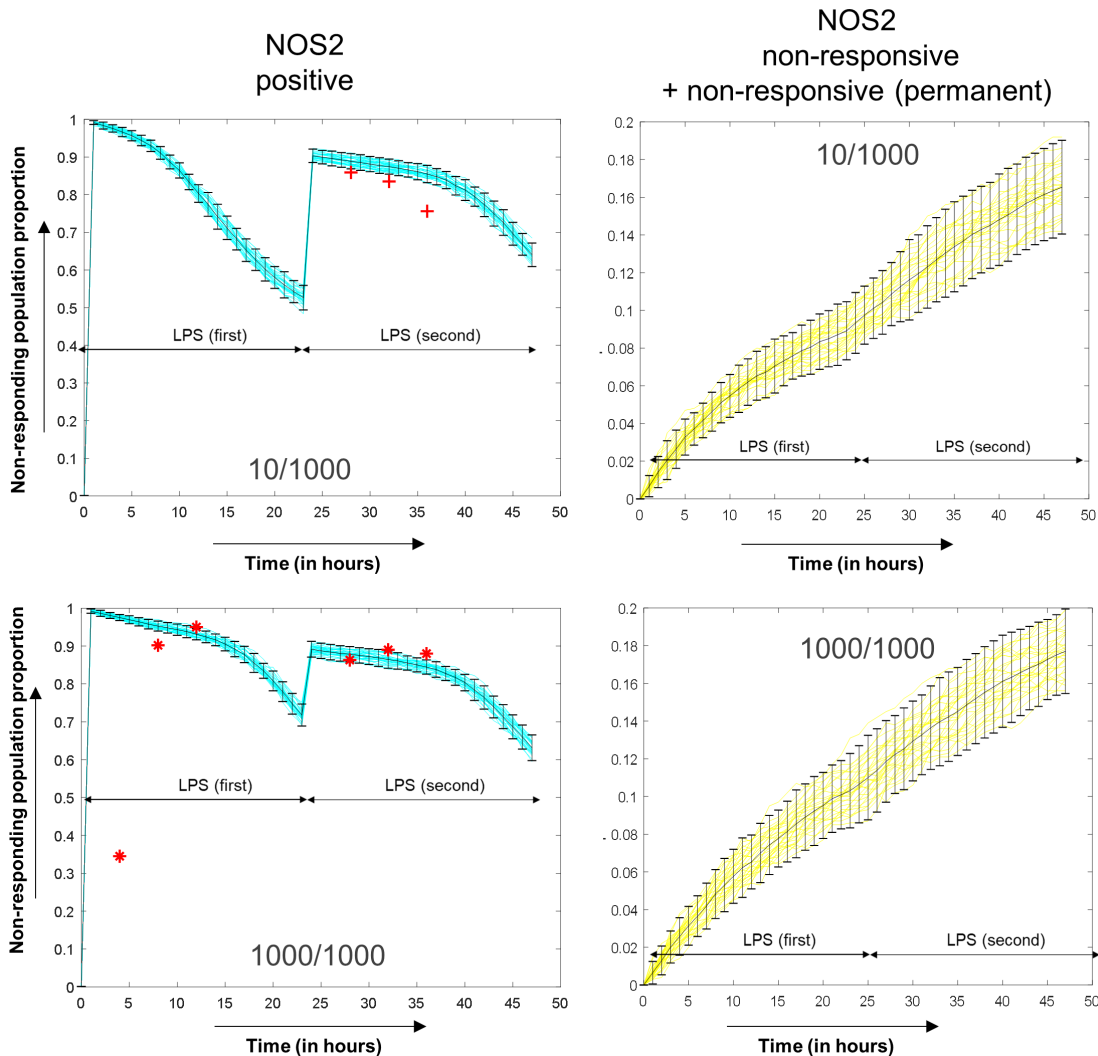


FIGURE 5.12: **NOS2 non-responding populations comprise just 8% after first LPS dose**

a nr model was simulated for first LPS dose (10 or 1000) at 0 hour and a second dose of LPS (1000) at 24 hours and the time-evolution plotted between 0-48 hours with estimated forward rate $\alpha = 0.0503$, $\beta = 0.0595$, $\gamma = 0.0068$, $\gamma_2 = 0.0405$, $\beta_2 = 0.0358$ for NOS2 and a fixed LPS decay rate ($\delta = 0.5$). 20 stochastic runs representing positive cells are plotted (cyan) with error bars (black) representing 95% confidence interval of the mean (of all 20 trajectories for each dose). **b** Time-evolution of non-responding states (non-responsive state, NRS + non-responsive permanent state, NRPS) over two LPS doses. 20 stochastic runs representing NRS+NRPS are plotted (yellow) with error bars (black) representing 95% confidence interval of the mean (of all 20 trajectories for each dose). Empirical data in red asterisks and crosses.

5.3.3.5 Non-responding states vary for each protein

Simulating the nr model for TNF, IL-6, pro-IL-1 β and NOS2 shows that non-responding states do form a part of the response to LPS. However, more interestingly, the number of cells in the non-responding states (NRS + NRPS) varied for each protein. In Figure 5.13, we show that TNF (67%) and IL-6 (54%) populations tend to show the highest proportion of non-responding cells in all of the four proteins considered. While NRS cells for TNF was high, the percentage of TNF NRPS cells is low at 2%, thus, suggesting TNF cells do not assume NRPS state and, as such, available to replenish the negative pool depending on the rate, β_2 . In the IL-6 population 16% of the cells at 24 hours become NRPS suggesting that a portion of the population after becoming IL-6 positive turns off its capability to turn on IL-6 (Figure 5.13).

pro-IL-1 β positive cells had comparable percentage of NRS (9.3%) and NRPS (11.6%) cells with approximately 21% non-responsive cells. NOS2 populations showed the lowest percentage of cells in the non-responding (10%) category with half each in the NRS and the NRPS state (Figure 5.13). Interestingly, for NOS2 17% cells remained in the negative state (data not shown) at 24 hours suggesting, cells may not assume a non-responding state for NOS2.

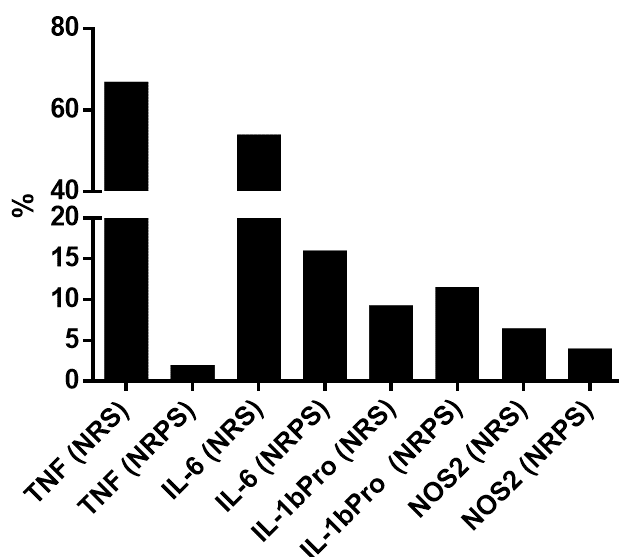


FIGURE 5.13: Non-responding states vary for each protein

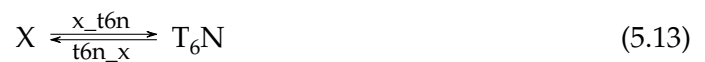
Bar plots showing percentage of non-responsive (NRS) and non-responsive (permanent) state (NRPS) for TNF, IL-6, pro-IL-1 β and NOS2 post first *in silico* LPS dose at 24 hours.

5.4 Modelling signalling in macrophage communities

In **Chapter 4**, we showed that macrophages responding to LPS, respond as communities of heterogeneous sub-populations. We further showed that these community compositions were affected by restriction of secretion (**Chapter 4, Figure 3.10**) by a chemical method, Brefeldin A (BFA) and isolation of macrophages by growing them in larger culture vessel and volume (**Chapter 4, Figure 3.14**). In order to describe communities within a macrophage population that evolve upon LPS stimulus, we expanded the nr model to a more general model that allowed transitions between each of the eight possible sub-populations made up of TNF, IL-6 and NOS2 positive cells. (For simplicity, LPS dynamics were not considered in this model.) The transitions were described for all forward and backward probabilities leading to a total of 56 (8 sub-populations capable of transitioning to 7 others) parameters are represented in a cube (**Figure 5.14a**) where each vertex can connect to seven other vertices. The underlying algorithm used was also a Gillespie-Doob based bespoke implementation of the model, referred to as the cube model in this chapter.

In the cube model, sub-populations TNF-IL6-NOS2-, TNF+IL6+NOS2+, TNF+IL6+NOS2-, TNF+IL6-NOS2+, TNF+IL6-NOS2-, TNF-IL6+NOS2+, TNF-IL6+NOS2-, TNF-IL6-NOS2+ are represented as X, T6N, T6, TN, T, 6N, 6 and N respectively for the sake of brevity.

Equation 5.13, 5.14 and **5.15** represent examples of reactions that are built into the model.





where x_{t6n} is the rate/probability with which negative cells (X) transition to triple positive (T6N) cells. The back rate $t6n_x$ then gives the rate at which the transition from triple positive to negative occurs. Similarly, **equation 5.14** and 5.15 describe the transition rates between $T, T6$ and N, T respectively.

The model can be simulated to obtain the time-evolution of each subset and define trajectories for the rise/fall of the sub-populations. The model can also be simulated to fit to an empirical end point to represent macrophage community *in silico*. Randomly sampled parameter values were used to simulate the cube model, with the outcomes plotted as a pie chart to represent a basic output (**Figure 5.14b**).

5.4.0.1 cube model - Assumptions

Assumptions made regarding the reactions in the cube model are as enumerated below:

1. All possible transitions within the cube model are allowed Cytokines expressed by macrophages can affect themselves or other macrophages. While NOS2 expression is dependent upon TNF and IFN- β cells can co-express both these proteins. Similarly, LPS induces TNF and IL-6 production while increased production of IL-6 may be associated with TNFR1 signalling via TNF binding in an autocrine or paracrine manner (see **Figure 1.3 in Chapter 1**).

2. No external perturbation of the model was allowed

The cube model only simulates transition probabilities which are, in turn, affected only by the number of cells of the relevant sub-population. LPS dynamics, and the possibility of density dependence and other non-linearities, are not considered.

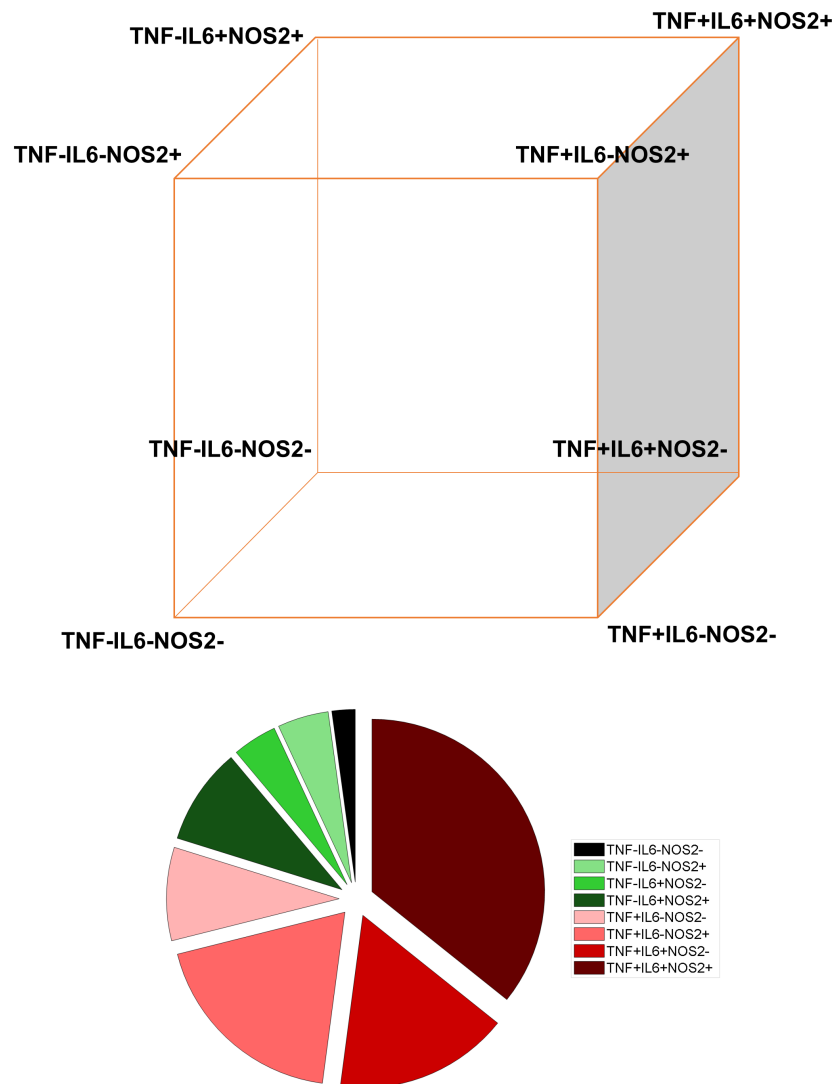


FIGURE 5.14: 8 sub-population of the community as represented on the vertices of the cube model

- a) Cube showing 8 different sub-populations used in the model that allows transitions via edges and diagonals. b) Representative example output of the cube model simulated with arbitrary parameter values to generate an *in silico* pie chart to represent community composition.

5.4.1 Parameter estimation

In order to explore possible parameter space for the transition probabilities or rates of the cube model, we estimated parameters based on our experimental data points where secretion was restricted by incubating cells stimulated with LPS in 4, 8 12 and 16 hours of BFA (**Figure 3.10, Chapter 4**). We estimated the parameters of the cube model by simulating the model with 56 random variables picked from a negative binomial distribution repeatedly for $5e10^6$ individual simulation runs to obtain sets of parameters that fitted 95% confidence interval of empirical data mean (n=3).

Parameter estimates for empirical data pertaining to 4 hour BFA (12 hour LPS + 4 hour LPS+BFA) and 8 hour BFA (8 hour LPS + 8 hour LPS+BFA) represent cases when restriction was restricted the least and we considered separately under the 'signalling' group.

As above, parameter estimates to 12 hour BFA (4 hour LPS + 12 hour LPS+BFA) and 16 hour BFA (16 hour LPS+BFA) were considered separately under the 'restricted secretion' group.

5.4.1.1 Estimated parameters - signalling

Parameter estimation, as described in the previous subsection, was used to fit experimental end points at 16 hours for the 'signalling group'. 2,464 possible parameter sets were obtained to fit the empirical data pertaining to 12 hour LPS and 4 hour LPS+BFA. For empirical data pertaining to 8 hour LPS and 8 hour LPS+BFA, 151 independent sets of parameters were estimated by the simulations. These parameter values were then plotted for each of the conditions to show mean and variance of the parameters in a box and whiskers plot (**Figure 5.15**)

Parameter estimations indicated that all transitions towards a triple positive sub-population i.e. t_{t6n} , n_{t6n} , 6_{t6n} , x_{t6n} , $t6_{t6n}$, tn_{t6n} and $6n_{t6n}$ were lowest among other parameter values. The parameter values predicted for x_{t6n} (transition rate describing the transition from triple negative to triple positive) to be the least variable and its mean the lowest overall among all estimated parameters. This suggests that triple positive sub-populations appear at a slow rate in LPS challenged community and are lost at a fast rate (as suggested by the corresponding back rates; **Figure 5.15a**) when secretion is not restricted. In fact, most of the large parameter values described the transition from the triple positive ($t6n$) state to a lesser inflammatory state (single or double positive) indicated that if some *in silico* cells are to transition to the triple positive state, a high probability will be associated with them to transition to a single or double positive state (**Figure 5.15a**).

Parameters such as 6_{tn} and $6n_{tn}$ were high and, also, interesting because they represented a diagonal on the cube which in *in vitro* terms can indicate cytokine/community based signalling as diagonally placed vertices in a cube are not directly connected to each other. This means that for a TNF-IL6+NOS2- cell to transition to a TNF+IL6-NOS2+ cell (6_{tn}) it has to switch off IL6 and switch on TNF and NOS2 (**Figure 5.15a**).

Parameter values for the 8 hour BFA empirical end point x_{t6n} was low, and one of the 5 lowest parameters by mean. The other parameters that had a lower mean were t_{t6n} , x_{6n} and tn_{6n} (**Figure 5.15b**). Similar to previous results for 4 hour BFA, 8 hour BFA results showed an overall decrease in the probability of transitioning to the triple positive state. The parameter $6n_{t6n}$, which dictates the transition from a double positive TNF-IL6+NOS2+ to triple positive cells, was on average higher than all other parameters that describe transitions to the triple positive sub-population. Interestingly, this suggests that cells that are positive for IL6 and NOS2 have a high tendency to

become triple positive upon secretion restriction. In other words, this can also mean that the triple positive sub-populations, upon switching off TNF, contribute to the TNF-IL6+NOS2+ sub-population.

The tn_6n parameter was one of the lowest while its corresponding reverse probability tn_6n was one of the highest in the estimates, suggesting a strong tendency of double positive TNF-IL6+NOS2+ to become TNF+IL6-NOS2+. Furthermore, the parameter x_tn had the highest mean value suggesting *in vitro* cells to transition upon LPS stimulus to TNF+IL6-NOS2+ sub-population with a high probability.

A correlation between parameters estimated for 4 and 8 hour BFA incubation empirical datasets were produced to see if some parameters are co-dependent and in any way redundant in the analysis (**Figure 5.16**). The average of top and bottom 5% correlation values were found to be 0.06 and -0.08. Maximum correlation and anti-correlation were 0.17 and -0.14. This suggests that the estimated parameters are independent and that when secretion is not restricted there is little or no co-dependence between the parameters.

5.4.1.2 Estimated parameters - secretion restriction

We next estimated parameters for the cube model, as described **subsection 5.4.1**, was used to fit experimental end points at 16 hours for the 'restricted secretion' group. 11 independent parameter sets were estimated for 12 hour BFA incubation while 118 parameter sets estimated for 16 hour BFA incubation.

Parameters estimated for the 12 hour BFA experimental end point, a high transition rate was predicted for negative cells to switch to TNF+IL6+NOS2+, triple positive sub-population (x_t6n) and, in addition, high transition rates for transitioning to the

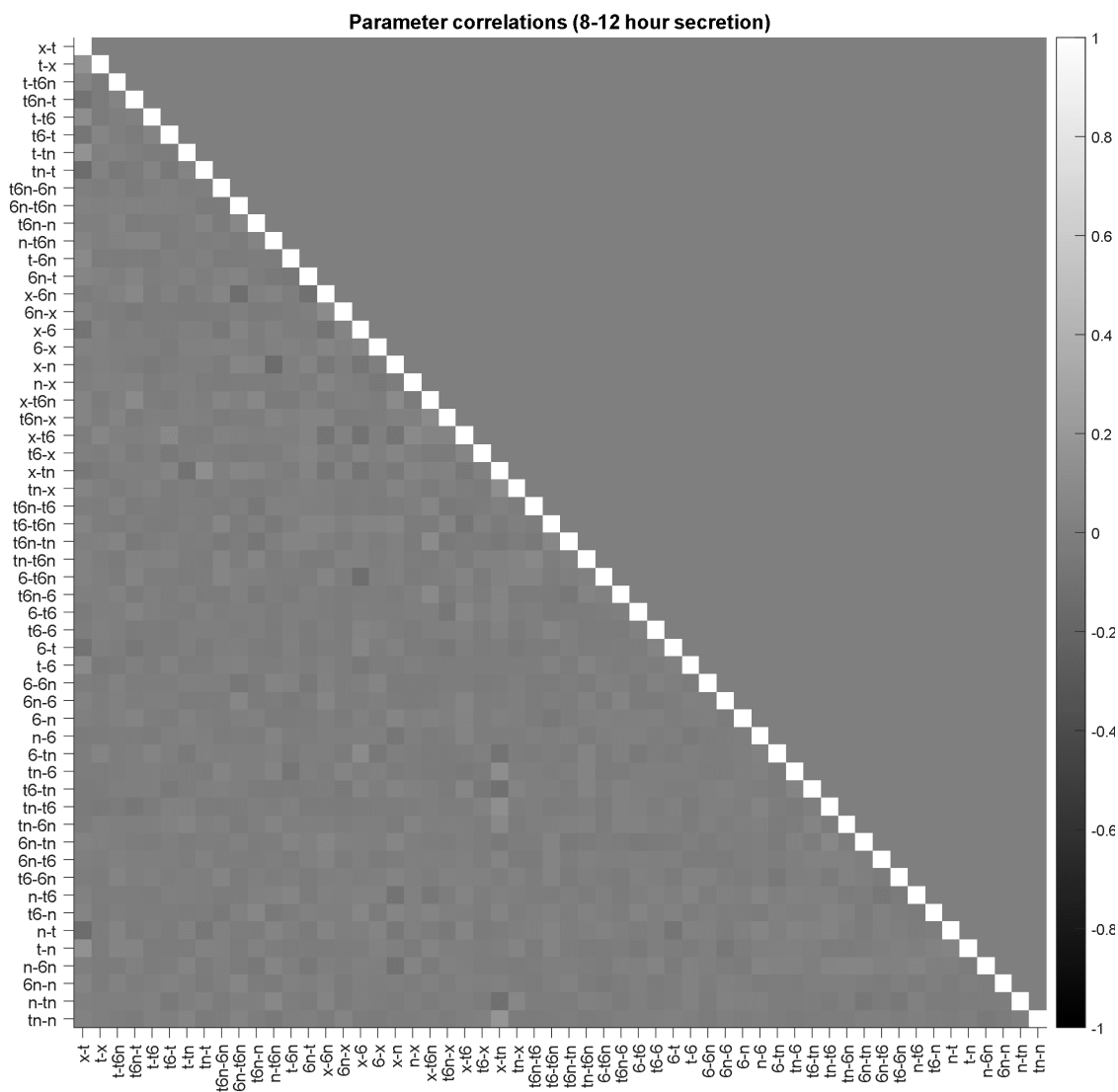


FIGURE 5.16: Parameter estimates for cube model (8/12hr secretion) show little to no correlation between them.

Spearman's correlation matrix was calculated and plotted as a heatmap with colour shading ranging between -1 (maximum anti-correlation) and 1 (maximum correlation). The diagonal values represent correlation of a parameter to itself and therefore is equal to 1 (white).

triple positive sub-population ($t6_t6n$, 6_t6n) were also observed. This suggested an overall high inflammatory potential when restriction is restricted for 12 hour (empirically)

Next we estimated parameters for 16 hour BFA experimental end point. Similar to the estimates for 12 hour BFA, parameter estimates for 16 hour BFA indicated that the diagonal transition rate (x_t6n) was the third largest among the estimated parameters. The parameters x_t and x_tn had the highest mean value among all parameters. Further, parameter estimates of x_6 and x_n also suggest that, when secretion is restricted, cells in the negative state have the highest probability to either transition to the TNF+IL6-NOS2+ or TNF+IL6-NOS2- state, or with lesser probability to the triple positive state (**Figure 5.17b**).

Correlation between parameters estimated for empirical datasets pertaining to 0 and 12 hour BFA incubation or restricted secretion showed slightly higher values of correlation between parameters (**Figure 5.18**). The average of top and bottom 5% correlation values were found to be 0.25 and -0.17. Maximum correlation and anti-correlation were 0.43 and -0.52. A higher on average correlation is expected as with decreased secretion and, therefore, increased accumulation the expectation of redundant transitions increase. Of note here, however, is the anti-correlation between x_tn and x_t (-0.52) suggesting a preference of *in-silico* cells to switch to triple positive (or double positive for TNF and IL-6) than become positive for TNF and NOS2.

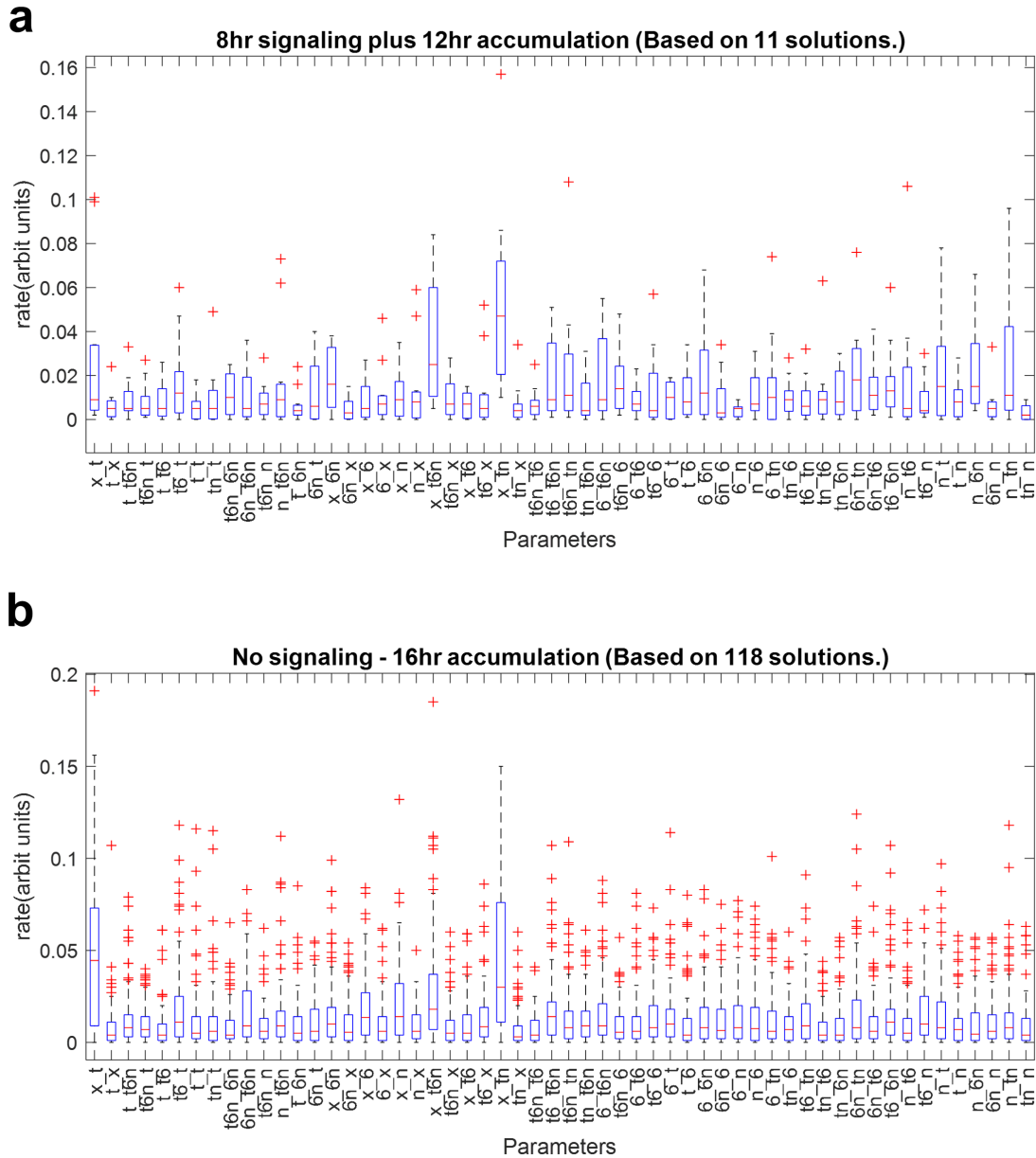


FIGURE 5.17: **Parameter estimation of cube model based on empirical dataset**

Box and whiskers plot to show the values of the parameters of the cube models as estimated based on empirical data pertaining to LPS stimulated macrophage community at 16 hour post stimulus with a) for 12 hour Brefeldin (BFA) incubation and b) 16 hour BFA incubation.

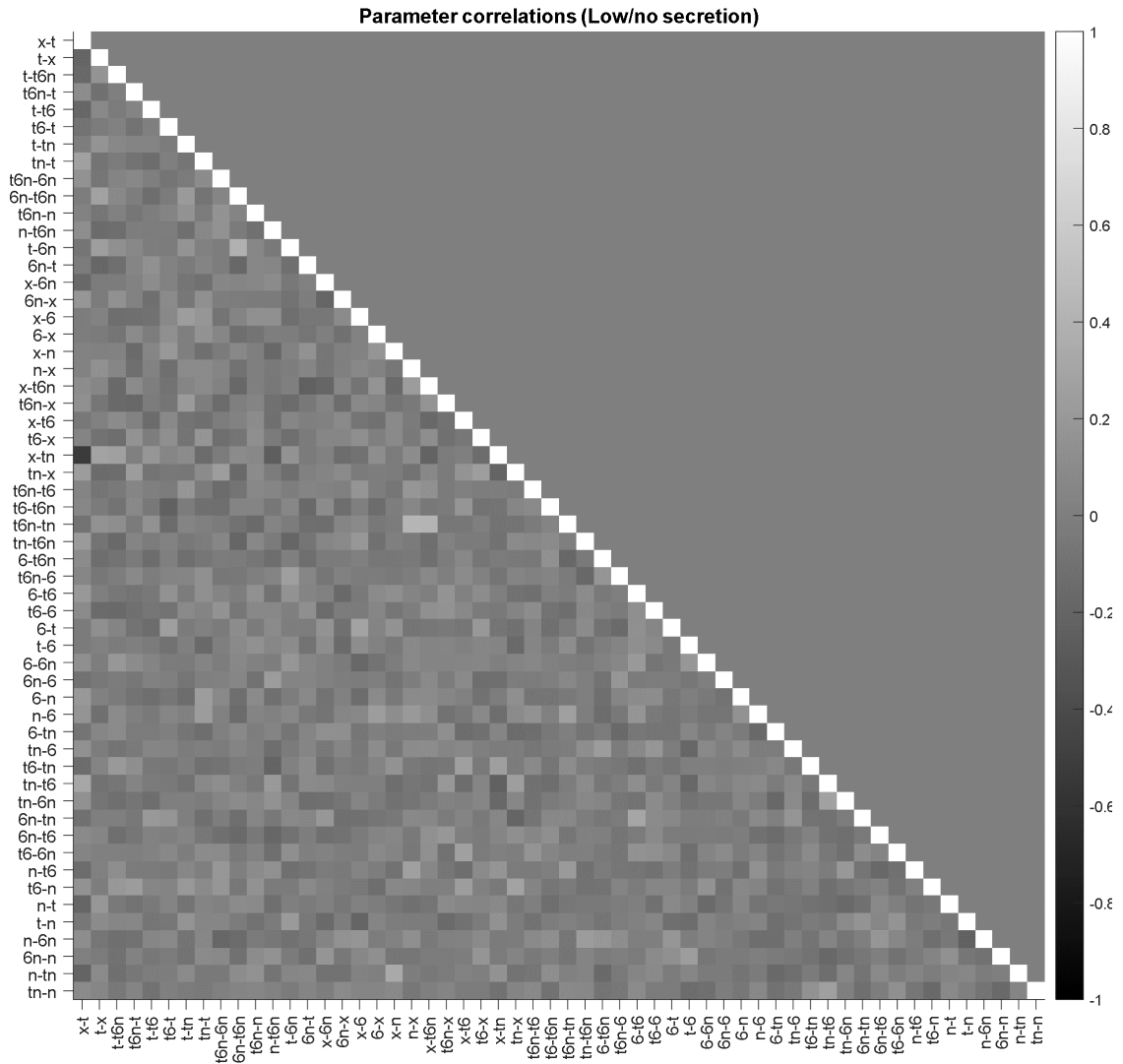


FIGURE 5.18: Parameter estimates for cube model (restricted secretion) show little correlation between them

Spearman’s correlation matrix was calculated and plotted as a heatmap with colour shading ranging between -1 (maximum anti-correlation) and 1 (maximum correlation). The diagonal values represent correlation of a parameter to itself and therefore is equal to 1 (white).

5.4.2 Simplified cube model did not fit experimental data

Since the number of parameters in the cube model is very high and our experimental data set is restricted to one time point, our model is prone to over fit the data. For this reason we checked if simpler cases of the cube model can fit the experimental data. We assumed that cells switching on to a protein positive state do so independently of other proteins. In terms of cube model transitions, this means that all parallel edges have equal rates, thus, a cell that is TNF+ can transition to a TNF+IL6+ state with an equal rate as compared to a negative cell that may transition to a IL6+ state. Also, all diagonal rates were fixed at 0 reducing the number of parameters of the model to not allow any such fast transitions.

We estimated parameters for cube model with equal rates for parallel edges to find that it was insufficient to fit the data with these parameters only. This suggests that parallel edges of the cube model requires unequal rates to fit the empirical data. It implicitly, also, suggests that community communication (differential rates and, speculatively diagonal transitions) may be important in shaping *in silico* communities that resemble the empirical macrophage communities.

The cube model is conceptually simple and parsimonious, but it includes a large number of parameters which need to be fitted to data, and therefore any conclusions drawn from this model ought to be treated with caution and considered in the context of other possible models. For example, the transition rates between cell-states may be dependent on the density of cell-states, introducing non-linearities which are not captured in the current model. To capture such non-linearities would require adding yet more parameters to the model. Nevertheless, if further data become available, and in particular data with a higher temporal resolution, then such considerations are worth pursuing.

5.5 Discussion

In conclusion, we use simple modelling approaches to help understand the possible mechanisms underpinning the complex dynamics observed in **Chapter 4**.

First, we model the proportion of cells positive for an inflammatory protein in response to LPS, treating each inflammatory protein independently, to show that:

- the addition of non-responding states within the model can be used to model hypo-response to a secondary dose of LPS; without such states, the model outputs cannot be readily matched to experimental observation.
- non-responding states (NRS + NRPS) vary in proportion, and evolve differentially, for various proteins when the parameters of the model are estimated from empirical results.
- While pro-IL-1 β , NOS2 and IL-6 positive cells can assume non-responsive and non-responsive (permanent) state, TNF positive cells do not become permanently non-responsive.

Second, we model sub-populations within a LPS responding macrophage community to show that:

- sub-population interdependence can be modelled in a heterogeneously responding community.
- restricting secretion globally can have specific effects on the transition probabilities of responding sub-populations, such as an increased transition rate for negative state to triple positive state or increased rates to respond to LPS stimulus.

5.5.1 Hypo-responsive populations modelled as distinct populations are different for different proteins

We create a simple model whose dynamics are dictated by LPS concentration in the environment to calculate the fraction of the population that is positive for a given cytokine or inflammation-associated protein. Upon adding non-responding states to the model, we mimic a hypo-responsiveness in terms of a decreased fraction of positive cells responding to a second *in-silico* LPS dose. We show that non-responding populations vary by size and also have a different composition for individual proteins. This is best displayed in **Figure 5.13** to show that while TNF non-responding population is comprised solely of a non-responsive (NRS) state each of the other protein populations comprise of NRS and non-responsive (permanent) state (NRPS) states. This specifically means that upon second dose of LPS some of the cells that are in the NRPS state for IL-6, IL- β Pro or NOS2 cannot respond to the stimulus.

LPS-induced tolerance has been shown to manifest through genes that become non-responsive or those that remain responsive (Foster, Hargreaves, and Medzhitov, 2007). Histone H3K4 trimethylation associated with transcription of IL-6 upon first challenge of LPS is lost when bone-marrow derived macrophages are challenged twice (Foster, Hargreaves, and Medzhitov, 2007). Histone modifications could be a mechanism by which NRPS cells, as defined in the nr model, manifest. NRS or non-responsive state in the model can represent cells that are temporarily attenuated such as by the reduction of TLR4 expression after LPS challenge (Nomura et al., 2000) or even fine-tuned by miRNA targeting of TLR4 (Chen et al., 2007; Teng et al., 2013; Jiang et al., 2018). Simulating the nr model for TNF (estimated parameters) revealed that TNF positive cells can become non-responsive but only about 2% of the population becomes non-responsive (permanent). This is interesting because histone modifications are known to occur for TNF (H3K9 dimethylated histones on promoter). However, while LPS-responsive genes are shown to be dependent on SWI/SNF dependent, *Tnf* is shown

to have little dependence (Ramirez-Carrozzi et al., 2006; Ramirez-Carrozzi et al., 2009). This may be a plausible reason why TNF cells do not become permanently non-responsive (NRPS) and requires further investigation.

It would then be interesting to experimentally test the presence or absence of NRS/NRPS states. Interestingly, the overall non-responding state (NRS + NRPS) had the highest representation in simulated models for TNF and IL-6. Intuitively, this may suggest that probing TNF or IL-6 negative cells within hypo-responsive community *in-vitro* may reveal more about the characteristics of LPS induced hyporesponsiveness or tolerance.

5.5.2 Modelling community inter-dependence

In order to understand signalling and its effects on sub-populations within a community of macrophages responding to LPS, we re-defined our model (cube model) to add 8 states representing 8 sub-populations of TNF, IL-6 and NOS2 (TNF+IL6+NOS2+, TNF+IL6+NOS2-, TNF+IL6-NOS2+, TNF+IL6-NOS2-, TNF-IL6+NOS2+, TNF-IL6+NOS2-, TNF-IL6-NOS2+). We also removed the LPS dynamics from the model to see how sub-populations evolve over time under implicitly constant LPS conditions. Fitting this model to experiments in **Figure 3.10, Chapter 4**, we show that LPS stimulation along with restriction of secretion has strong effects on transition rates of a cell in a negative state (TNF-IL6-NOS2-) to transition to the TNF+IL6-NOS2+ or TNF+IL6-NOS2- state. Interestingly, transition rates also suggested that cells in the negative state can also become single positive for TNF (TNF+IL6-NOS2-) or NOS2 (TNF-IL6-NOS2+) or IL6 (TNF-IL6+NOS2-) in decreasing order of probability. While it is apparent from our experimental results that secretion restriction does increase the proportion of triple positive sub-population, thereby suggesting an increase in overall inflammatory potential, our modelling results go a step further in suggesting the

overall rates at which this occurs. Parametrising the cube model can trace the time-evolution of sub-populations.

While simple cases of cube model that treat each protein independently were not able to fit the empirical data, our cube model sets up a modelling platform that can be used to model sub-population feedbacks that can modify community heterogeneity. This can be achieved by estimating the parameters of the cube model with additional more experimental data at different time points. The addition of density dependence and LPS dynamics within cube model framework may be able to explain the interdependence of states and their emergence. An addition of the dynamics of brefeldin and its effects on secretion may be built into the cube model to modify rates based on whether a cell at any given time is secreting or not. This not only effects the accumulation of the protein in the cell but also the autocrine/paracrine effects of the protein being secreted. While such possibilities were considered these were not attempted within the time stipulated for the thesis.

5.5.3 Summary and future work

We used simple mathematical models to understand hyporesponsiveness and by classifying responding populations into a negative, positive non-responsive (NRS) and non-responsive (permanent) state (NRPS). The model was able to capture apparent hyporesponsive behaviour for these proteins and provided output of the composition of NRS and NRPS state. Here, we propose the existence of, previously unknown cell states that explain macrophage hyporesponsiveness upon activation. Our model can be used for other cytokines and their expression at the single-cell level to find the relative proportion of NRS and NRPS states. However, it cannot be used to understand the mechanistic basis of single-cell protein expression behaviour. For this, individual-based

models will be required to be built.

However, the nr model does not capture how individual proteins are affected by the environment. We built a more complex model to capture this information and estimated the parameters of this model to fit empirical data pertaining to conditions at which secretion was restricted or not. Both our models answer different questions by suppressing complexity in underlying behaviour. nr model does not capture effects of community on individual proteins while cube does not capture LPS dynamics. This phenomenological approach proved useful in understanding heterogeneous population. The potential of the cube model, however, can be further explored with more experimental data.

In order to understand how macrophage communities evolve and interact it would be interesting to mathematically model communities based on future work suggested in **Chapter 4** such as the use of spatial information on how sub-populations of macrophages evolve. Using this information, more sophisticated individual based models maybe created to model emergent behaviour

Chapter 6

Dicer knock down affects composition, distribution and variability in LPS induced proteins

6.1 Introduction

miRNAs repress protein expression to act as a post transcriptional regulatory framework. Taken together, miRNAs regulate a myriad of cellular processes such as differentiation, development, homeostasis and regulate immune cells during an inflammatory response. The repression of messengerRNA (mRNA) by miRNAs is a many to many relationship where a miRNA can repress one or more proteins or many miRNAs can simultaneously target one mRNA. This allows miRNAs to have differential effects on protein targets, some being finely tuned by about 6% while others being repressed up to 50% (Guo et al., 2010; Baek et al., 2008).

miRNA primary transcripts are processed through a canonical pathway to become mature miRNAs that are cleaved by Dicer, an endonuclease, to their functional form which can then bind to their mRNA targets. While loss of individual miRNAs can have large effects on specific cellular and signalling processes, the loss of Dicer has been

shown to have global effects, such as loss of variability in expression of pluripotency factors by embryonic stem cells (ESCs) that is seen in otherwise uniform populations. This implies that in addition to affecting mean expression of their targets, miRNAs might also determine variance in gene expression. This variability in expression of pluripotency factors is attributed to the ability of ESCs to differentiate towards multiple cell fates (Kumar et al., 2014; Klein et al., 2015). The ability of miRNAs to increase noise (variability) in gene expression of highly expressed genes (Schmiedel et al., 2015) may contribute to differential expression of highly expressed genes (Shalek et al., 2013), such as pluripotency factors (Garg and Sharp, 2016). In this chapter, we question if disrupting the miRNA biomachinery by knocking down Dicer induce changes to LPS-stimulated macrophage communities as described in (**Chapter 4**).

6.2 Aims

1. To show if communities of LPS stimulated RAW264.7 macrophage change in composition upon knocking down Dicer.
2. Evaluate underlying expression patterns of our chosen proteins (TNF, IL-6, NOS2 and pro-IL-1 β) within the Dicer-deficient communities.
3. Theoretically investigate the effect of Dicer on kinetics of expression of pro-inflammatory proteins during LPS challenge.

6.3 Dicer expression in RAW264.7 cells can be knocked down for up to 72 hours

A global reduction in miRNAs can be induced in cells by knocking down Dicer (Kumar et al., 2007; Kumar et al., 2009). In order to characterise the effects of LPS in miRNA deficient macrophages, we transfected RAW264.7 cells with siRNA that specifically targeted the Dicer mRNA (**Figure 6.1**).

We checked protein levels of Dicer at 24 (first LPS stimulus) and 72 hours (harvest of cells) post transfection to show that Dicer levels were reduced at first LPS challenge and for the duration until cells were harvested for intra-cellular staining. Further the reduced levels across treatments show that LPS treatment did not affect the reduction in Dicer levels (**Figure 6.1**).

6.4 Dicer-knock down populations can make TNF and IL-6 and are hypo-responsive on secondary stimulus

We measured cytokine levels of TNF and IL-6 in Dicer knock down cells to confirm that secreted cytokines in Dicer knock down populations could be detected in the culture supernatant. Like untransfected RAW264.7 cells, Dicer knock down populations produced TNF and IL-6 on LPS challenge and were hypo-responsive on secondary challenges. Hypo-responsiveness was greater when the first challenge dose was higher (1000/1000 vs 10/1000, **Figure 6.2**) in both siDicer and NTC populations.

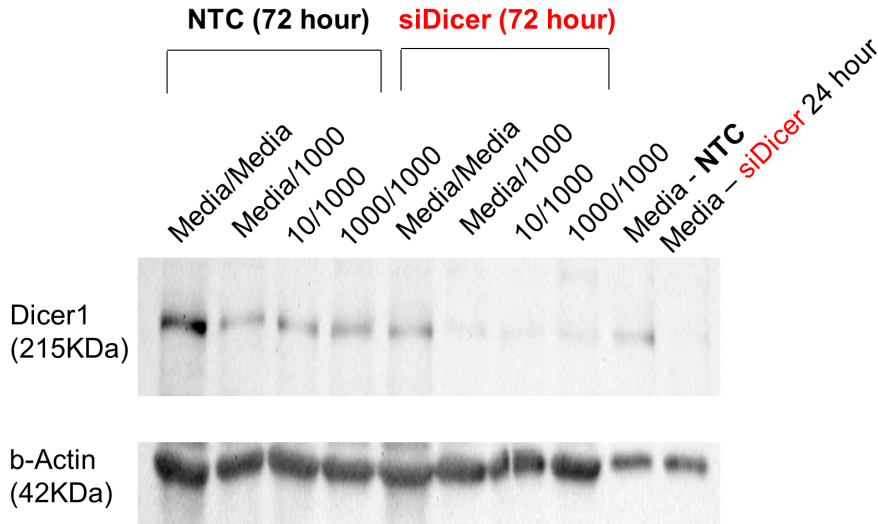


FIGURE 6.1: Dicer knock down in RAW264.7 cells

Western blots showing Dicer along with β -actin levels in untreated (Media/Media; Media), challenged (Media/100) and twice-challenged (10/10000; 1000/1000) RAW264.7 cells that were either transfected with not-template control (NTC) or an siRNA for Dicer.

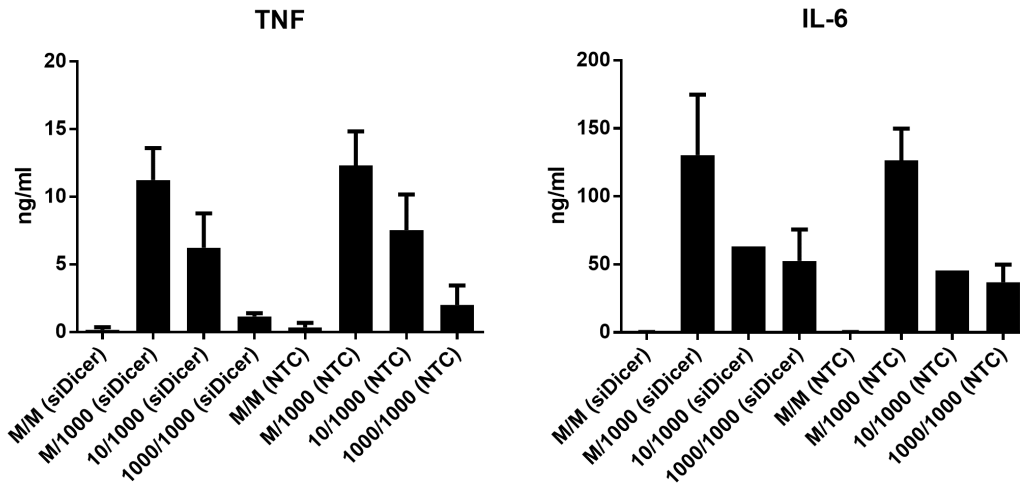


FIGURE 6.2: Dicer knock-down RAW264.7 cells are hypo-responsive

Bar-plots showing TNF and IL-6 levels in supernatant from untreated (M/M), challenged (Media/1000), twice-challenged (10/1000; 1000/1000) pertaining to siDicer and NTC treatments. n=2-3 for TNF; n=1-2 for IL-6.

6.5 Dicer knockdown induces changes in community composition

In order to visualise differences between communities responding to LPS for Dicer knock down, RAW264.7 cells we first looked at community structure at 24 hour (20 hour LPS and 4 hour LPS+BFA). RAW264.7 cells transfected with a non-targeting siRNA (NTC) or Dicer siRNA (siDicer) were challenged with 1, 10, 100 and 1000 ng/ml of LPS. We included a control for untransfected cells to account for any density-related effects due to cell isolation as seen before in **Chapter 4** as the transfections were carried out in culture plates with a surface area five times greater and a cell density (at plating) of approximately 50,000 (see **Chapter 2**). siDicer communities in comparison to untransfected and NTC communities showed compositional changes (**Figure 6.3**).

Communities between untransfected and non-targeting control (NTC) were very similar in the middle doses of LPS (10 and 100 ng/ml) while showing variation in the frequency of triple negative sub-population at 1 ng/ml (7% increase in NTC) LPS challenge and that of triple positive (TNF+IL6+NOS2+) and TNF+IL6-NOS2+ sub-populations at 1000 ng/ml. Compared to the untransfected community, NTC community (1000 ng/ml) comprised of approximately twice as many triple positive sub-populations with 16% TNF+IL6-NOS2+ sub-population compared to 9.5% in the untransfected control. Overall TNF+ cells, in that way, were twice as many in the NTC community (at 41% from 22.5%). These differences between untransfected and NTC communities (**Figure 6.3**) suggest that the transfection itself can affect community composition, possibly, due to the activation of TLR3 by double stranded RNA (Alexopoulou et al., 2001) or transfection reagent induced activation of interferon signaling (Guo et al., 2019). The above illustrates that untransfected communities should not be directly compared with siDicer communities. Due to this it must also be noted that transfected cells are activated and hence do not represent wild-type response for

which a knock-out cell line is preferable.

Comparing NTC and siDicer communities next, it was visually apparent that both the communities are sensitive to dose and triple positive and double positive TNF-IL6+NOS2+ sub-populations to be prominent at higher doses of LPS. At lower doses, both NTC and siDicer communities are dominated by the negative sub-population comprising 57% and 72.8% of the community. As miRNAs are known to repress protein expression, it is counter intuitive to expect more negative cells in population that has reduced Dicer expression (**Figure 6.3**). However, our results consistently showed a higher frequency of negative sub-population in siDicer communities (compared to NTC communities) across all doses of LPS at 24 hours post LPS challenge. This may suggest that miRNA as a regulatory network repress switching off of inflammatory mediators. Interestingly, the increased frequency of negative sub-population also accompanied a decrease in the frequency of the triple positive sub-population (5.3% to 3.3%, 100 ng/ml; 23% to 15.3%, 1000 ng/ml) in siDicer communities. This suggests that siDicer communities are less inflammatory overall with less cells producing all three proteins and more cells producing none. The double positive TNF-IL6+NOS2+, that we have earlier shown to be associated with higher doses of LPS and correlating with the triple positive population (**Chapter 4**), was marginally higher (26.5% compared to 24.8%, 1000 ng/ml; 10.6 % compared to 7%, 100 ng/ml) suggesting this sub-population to be affected differentially by Dicer knock down. At lower doses, fewer single positive TNF-IL6-NOS2+ sub-population were observed in siDicer communities and it may be speculated that single positive cells for NOS2 may switch to a negative sub-population faster in Dicer deficient environment (**Figure 6.3**). Overall the LPS dose effect observed between the communities was visualised by Bray-Curtis dissimilarity matrix that put untransfected and NTC close to each other while separating on the basis of LPS dose. siDCR communities on the other hand were distant from untransfected/NTC controls to suggest the differences in composition.

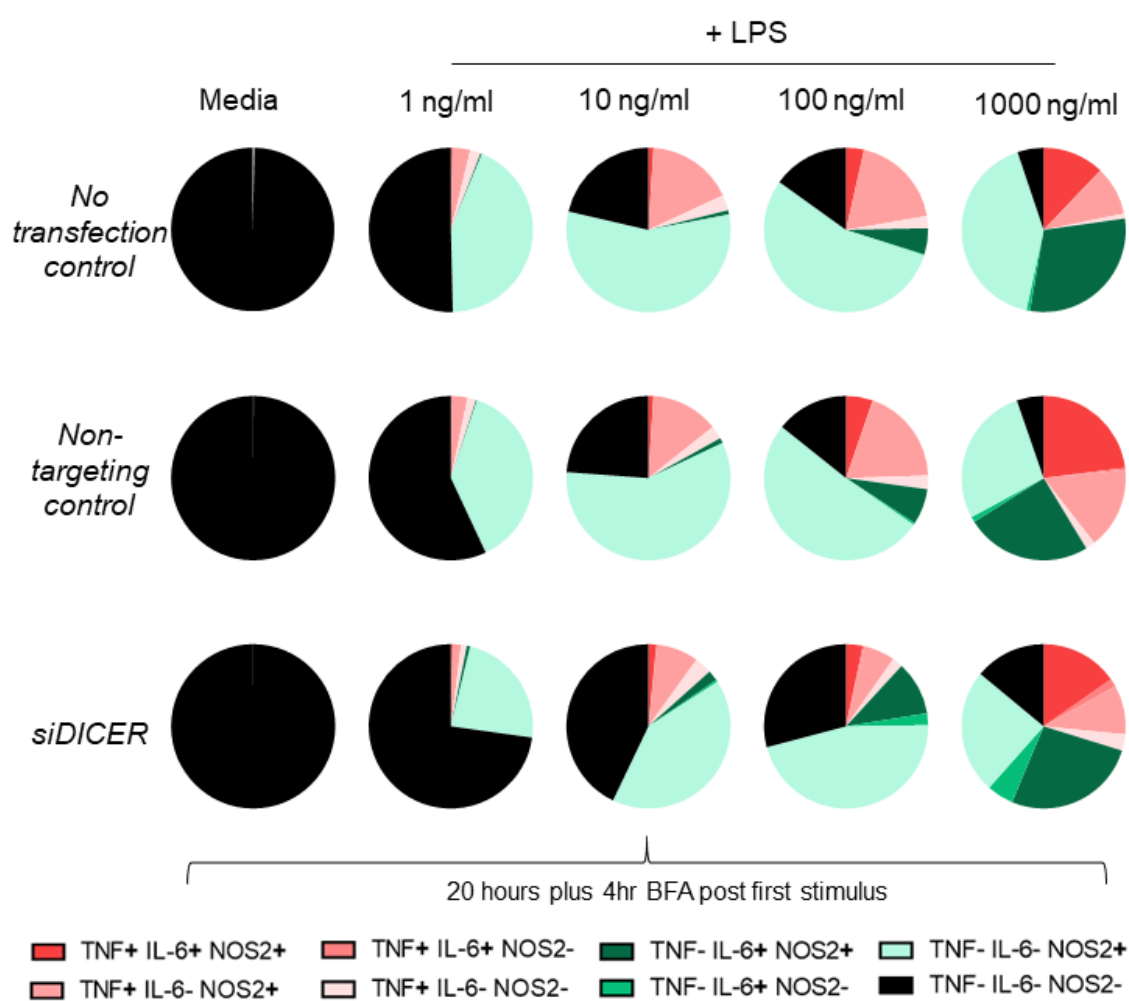


FIGURE 6.3: Dicer knock-down have an effect on triple positive and negative sub-populations

Pie charts derived from flow cytometry data representing community composition based on sub-populations of TNF, IL-6 and NOS2 positive cells for untransfected, NTC and siDicer groups treated with 0, 1, 10, 100 or 1000 ng/ml of LPS (20 hour LPS and 4 hour LPS+BFA). Count of cells=100,000.

(Figure 6.5a)

6.5.1 Twice challenged communities at 24 hours appear similar

Next, we looked at community compositions of cells that were challenged twice as compared to those that were challenged only once with LPS. Twice-challenged communities (10/1000 or 1000/1000, **Figure 6.4**), at 24 hours post secondary stimulus, were visually similar when compared to challenged communities between NTC and siDicer groups. Media/1000 or the single challenge community changed more in comparison (**Figure 6.4, 6.5b**).

While not directly comparable, untransfected twice challenged communities (Untransfected control, **Figure 6.4**) also appeared similar to NTC and siDicer groups, especially, the 10/1000 communities. Both 10/1000 and 1000/1000 communities showed a small increase in negative sub-populations in siDicer group compared to NTC. However, while 10/1000 siDicer community had more triple positive (TNF+IL6+NOS2+) sub-populations (8.7% compared to 4.2% in 10/1000 NTC). On the other hand, 1000/1000 community had a smaller triple positive population (13.6% in comparison to 23.50% in NTC). At the overall TNF+ cells, 10/1000 NTC and siDicer communities were both 31% positive while in 1000/1000, siDicer communities were only 30% overall positive for TNF (in comparison to 41% in NTC). The differences suggested a reduced inflammatory response from Dicer knock down 1000/1000 community at 24 hours post secondary stimulus stage (**Figure 6.4**).

The Media/1000 community between siDicer and NTC groups communities were the most distant (**Figure 6.5b**) and this was visually evident with the double positive, TNF-IL6+NOS2+ sub-population representing 30% of the entire community in siDicer group while the NTC group only comprised of 4% of this sub-population. In the Dicer knock down community, 10% cells were triple positive as compared to 2% in the NTC

group (**Figure 6.4**).

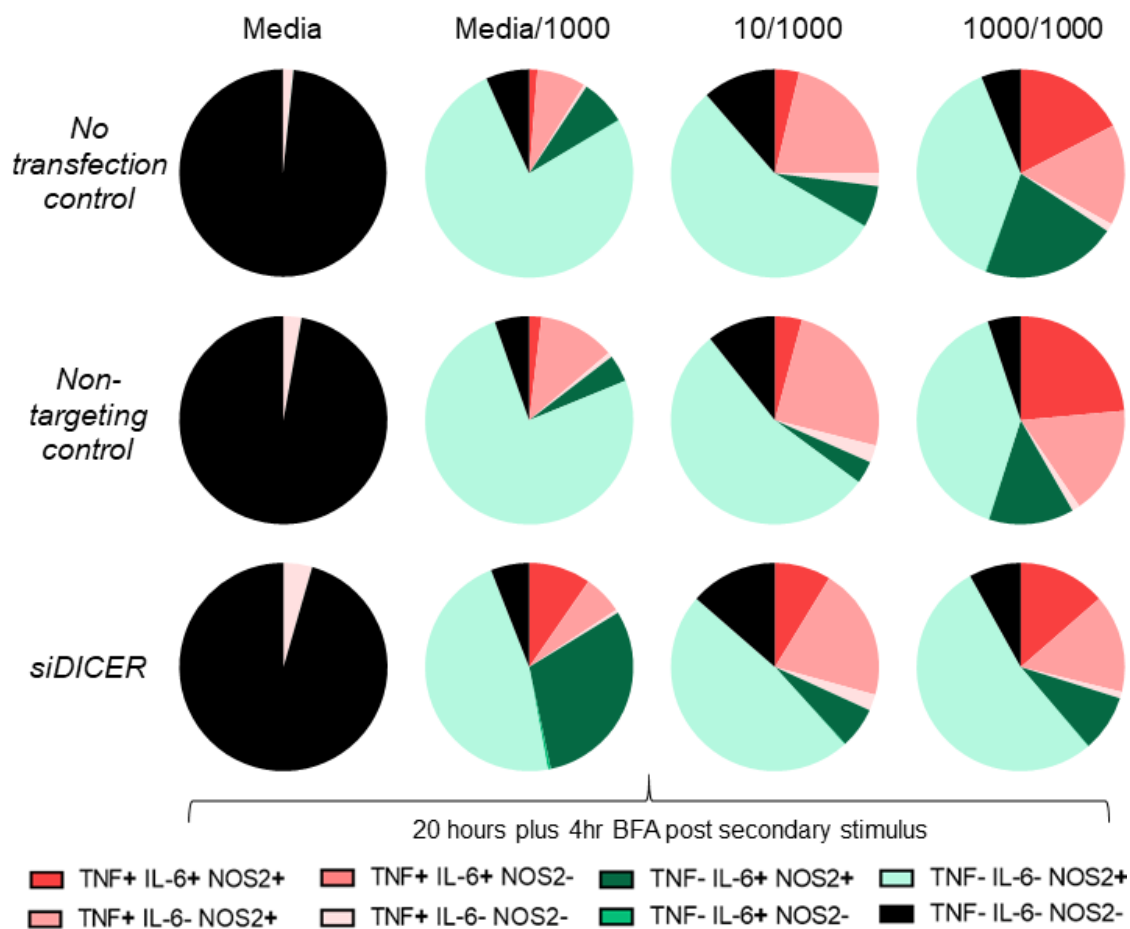


FIGURE 6.4: Hyporesponsive communities change little between NTC and siDicer groups

Pie charts derived from flow cytometry data representing community composition of TNF, IL-6 and NOS2 positive cells for untransfected, NTC and siDicer groups treated with 0, 1, 10, 100 or 1000 ng/ml of LPS (20 hour LPS and 4 hour LPS+BFA). Count of cell=100,000

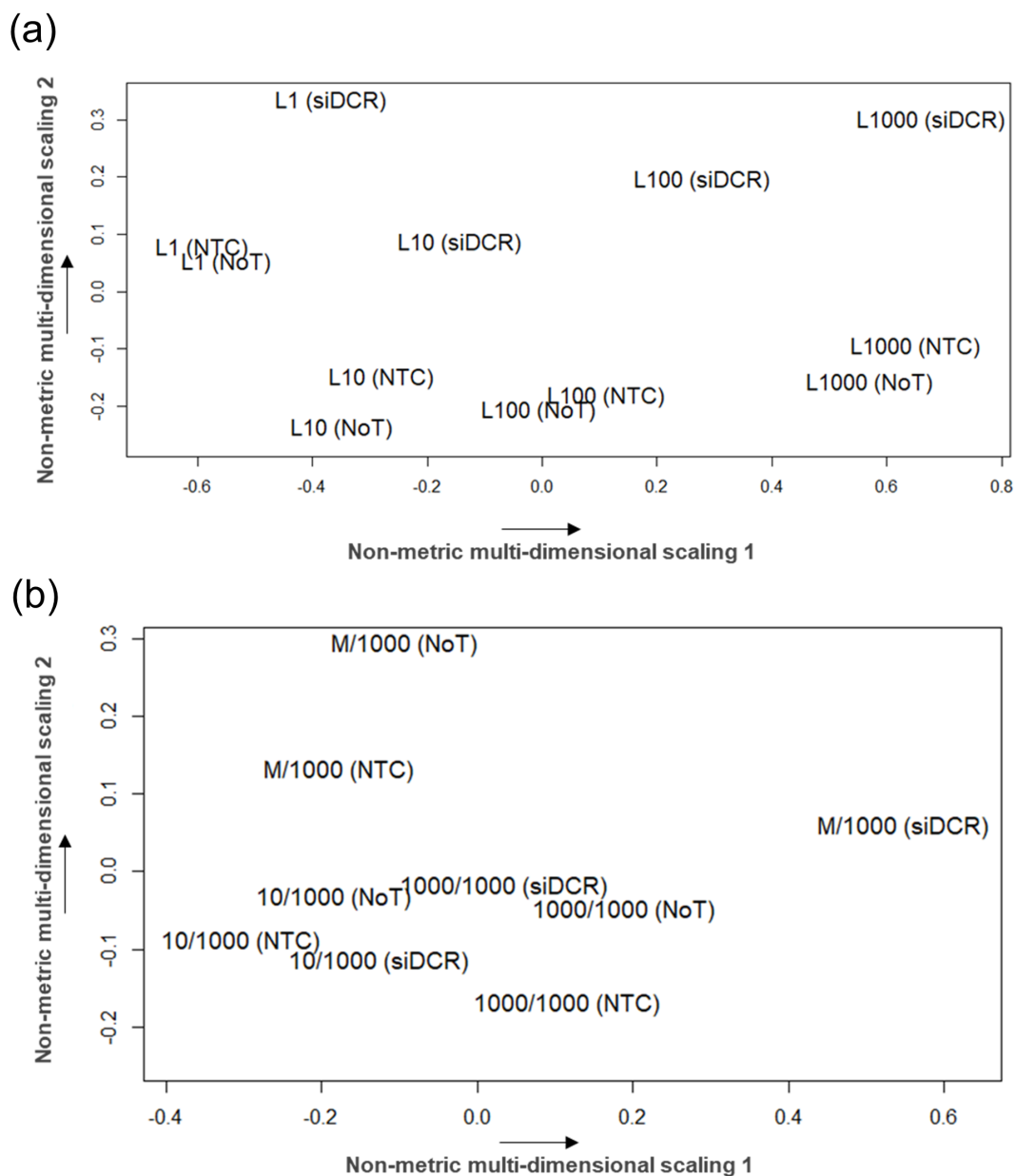


FIGURE 6.5: **Community compositions NTC and untransfected communities differ by LPS dose while hypo-responsive communities differ little.**

Bray-Curtis matrices representing community composition dissimilarities with respect to a) LPS dose titration and b) challenged and twice-challenged communities (M/1000; 10/1000; 1000/1000) across untransfected (NoT), NTC and siDicer groups.

6.6 Single positive pro-IL-1 β cells increase upon Dicer knock down in RAW264.7 cells

pro-IL-1 β is the immature form of IL-1 β , an acute-phase cytokine, and is implicated to have profound effects in inflammatory response and disease progression (Bent et al., 2018; Ren and Torres, 2009; Wojdasiewicz, Poniatoski, and Szukiewicz, 2014) upon caspase dependent cleavage. We included the pro-form of the cytokine in our panel to check if it introduces any new sub-populations upon Dicer knock down in RAW264.7 cells.

pro-IL-1 β was observed, plotted against TNF intensity in **Figure 6.6a**, and showed overall higher positive pro-IL-1 β populations upon Dicer knock down as compared to NTC. Higher number of pro-IL-1 β positive cells were, especially, more prominent at lower doses of LPS with respect to NTC or untransfected cells. The second quadrant of the bi-plots showed a high frequency of pro-IL-1 β +TNF $^-$ cells in Dicer knock down group (**Figure 6.6**). This led us to question if the increase in pro-IL-1 β positive cells were correlated to increased number of triple negative (TNF-IL6-NOS2 $^-$) sub-population observed to increase in Dicer knock down communities treated with LPS with greater frequencies at lower doses (**Figure 6.3**).

Indeed, upon gating sub-populations that were negative for TNF, IL-6 and NOS2, and then looking at pro-IL-1 β distribution, we found twice as many pro-IL-1 β positive cells in the siDicer treatment across all doses at 24 hours post stimulus (**Figure 6.6b**). NTC and untransfected groups both comprised of 2-4% of this single positive IL-1 β population at 100 and 1000 ng/ml LPS and between 4-9% at 1 and 10 ng/ml LPS. In siDicer treatment, single positive (pro-IL-1 β) cells represented between 14 and 29% of the population at 1 and 10 ng/ml respectively. At 100 and 1000 ng/ml LPS challenge, this sub-population represented 6 and 11% of the total population. Our results suggest that

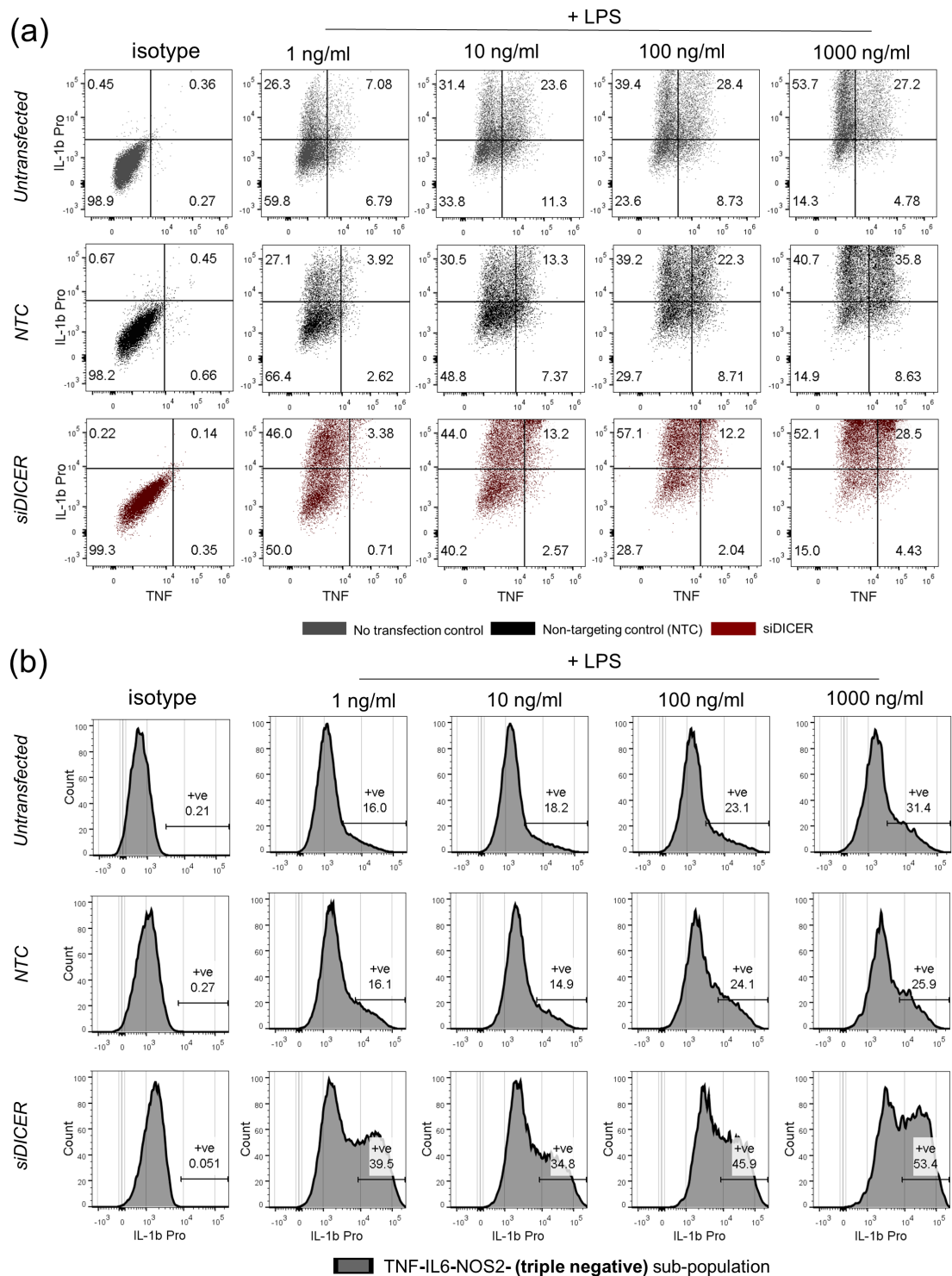


FIGURE 6.6: Dicer knock down increases pro-IL-1 β positive cells

Pre-gated a) flow cytometry (see methods) bi-plots between TNF and pro-IL- β fluorescence staining positive and negative populations and b) pro-IL-1 β intensity of TNF-IL6-NOS2- (negative) population for untransfected, NTC and siDicer groups across LPS treatments of 1, 100 and 1000 ng/ml. Isotype control (first bi-plot/histogram in each row for a) and b)) was used to gate positive and negative populations.

the miRNA regulatory framework plays an important role in regulating pro-IL-1 β populations that may persist, at higher frequencies even 24 hours post LPS stimulus.

6.7 pro-IL-1 β levels increase per cell upon Dicer knock down

We next looked at overall pro-IL-1 β distribution to see if Dicer knock down affects all cells producing pro-IL-1 β . Distribution of pro-IL-1 β was observed to be heavy right-tailed at low doses and distinctly bi-modal for untransfected and NTC controls. Dicer knock down, however, had profound effects on the distribution of pro-IL-1 β in the population. The population was distinctly bi-modal even at a low dose of LPS (1 ng/ml) suggesting more cells to become high-producers of pro-IL-1 β in the absence of miRNA regulation (**Figure 6.7a**). The bi-modality in pro-IL-1 β production increased with higher LPS dose and at the highest dose most of the population was high pro-IL-1 β producing (**Figure 6.7a**). This is further exemplified by the constant rise in the median pro-IL-1 β fluorescence intensity with respect to NTC peaking at 3 times the intensity 1000 ng/ml LPS treatment (**Figure 6.7b**). pro-IL-1 β intensity in Dicer knock down population showed between 2.8 to 4 times fold increase median intensity with respect to NTC consistently over different doses of LPS (**Figure 6.8a**). The highest dose (as represented by L1000 and M/1000) showed between 2.5-5 fold increase but high variability across experiments suggesting the absence of miRNAs might increase the noise in the production of IL-1 β within the population at the highest dose of LPS. The strong effect on pro-IL-1 β median intensity fold change was not as pronounced in the twice challenged population as compared to the challenged population, M/1000 (**Figure 6.8a**). This may suggest the hypo-responsive populations to be more resistant to the effect of miRNA loss-induced expression of pro-IL-1 β such that additional regulatory mechanisms may exist in a hypo-responsive population.

We then compared previously described single positive pro-IL-1 β positive population (**Figure 6.6b**) with the overall (all F4/80 positive cells) pro-IL-1 β distribution (**Figure 6.7a**) and found that single positive sub-population was distinct in their expression of pro-IL-1 β expression (**Appendix figure 8.4**).

An overall pro-IL-1 β increase in all cells upon Dicer knock down suggests there is a strong activation of pro-IL-1 β in the absence of Dicer and, consequently, miRNAs. We then looked at TargetScan (Agarwal et al., 2015) to look for conserved miRNA targets IL-1 β but found only poorly conserved targets (**Appendix Table 8.1**). Further, the 3' UTR (untranslated region) of the IL-1 β mRNA is short (495 nucleotides in mouse) which further decreases the likelihood (Matoulkova et al., 2012) of IL-1 β to be targeted by miRNAs.

6.8 TNF levels are affected at low dose of LPS upon knocking down Dicer

TNF expression was bi-modal at high doses (100 and 1000 ng/ml) while analog at low doses after 24 hours of LPS stimulus between untransfected, NTC and siDicer groups (**Figure 6.7a**). The median TNF produced (as indicated by the fluorescence intensity) by the population was similar at high doses with small increase in median TNF in low doses of LPS (**Figure 6.7b**). This suggested while the loss of miRNAs had no effect at high doses in overall amount, the same showed a positive knock on effect on how much TNF was being produced per cell. This is supported by the analog nature of the distribution of the staining. The fold change of median fluorescence intensity of TNF with respect to NTC showed that at low doses median TNF intensity is higher across two experiments while at high doses the fold change was not as high (**Figure 6.8b**). The media only (or stimulated) population showed an increase as more TNF staining was observed in siDicer than NTC in untreated cells (**Figure 6.8b**), however, the median intensity itself was not

comparable (**Figure 6.7b**). We also looked at the fold change in median intensity of TNF in hypo-responsive twice-challenged cells to find no difference in the intensity of TNF staining. This suggested that at 24 hours post secondary challenge miRNA effects in hypo-responsive cells do not have an effect suggesting limited miRNA-led regulation of TNF, at least at this time point (**Figure 6.8b**).

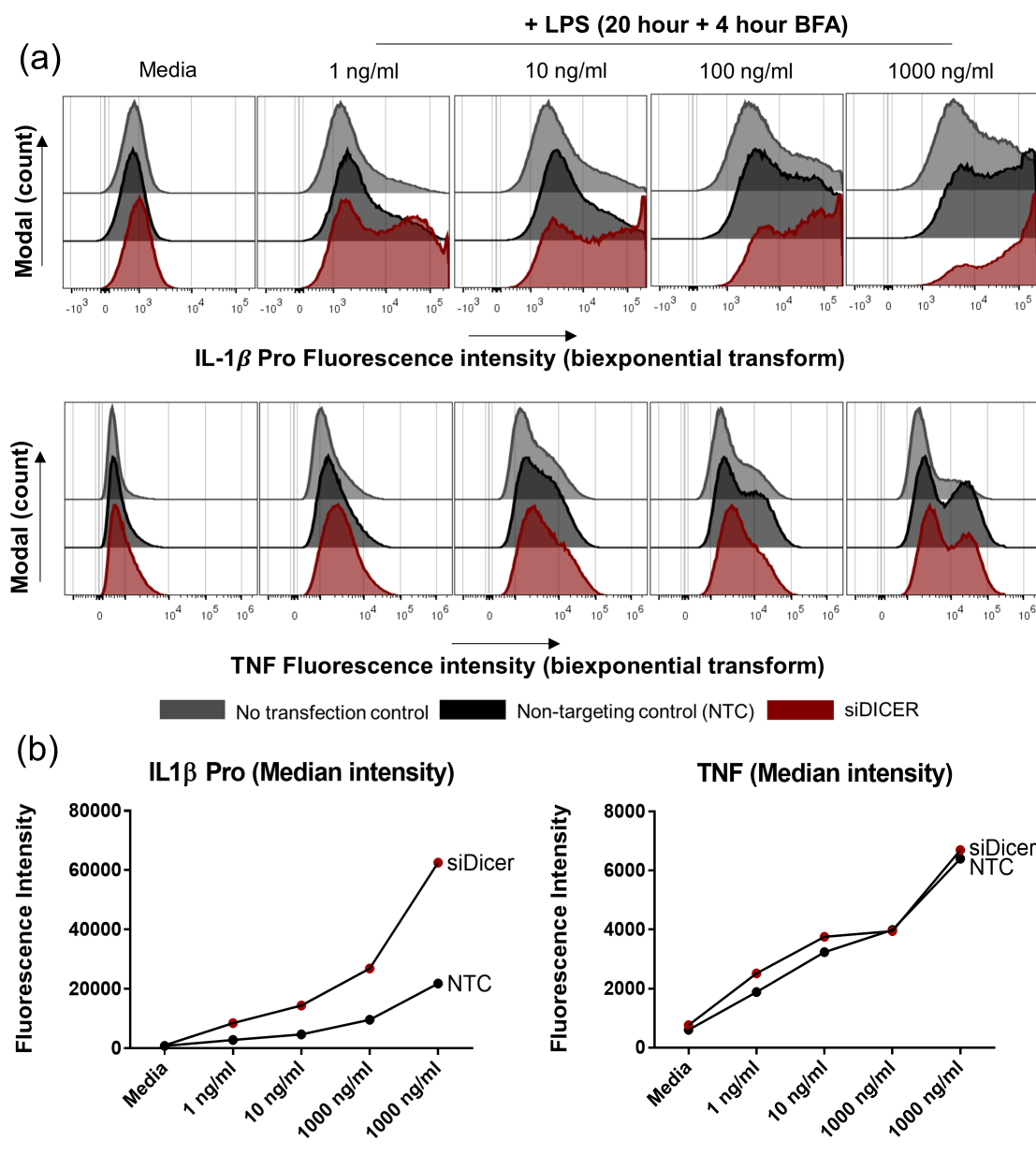


FIGURE 6.7: pro-IL-1 β shows positive fold change when compared to non-transfected controls.

Pre-gated (a) flow cytometry histograms for pro-IL-1 β and TNF fluorescence intensity for untransfected, NTC and siDicer groups are overlaid for comparison. (b) population median fluorescence intensity for NTC and siDicer groups each for IL-1 β Pro and TNF are represented in before-after plots. 1, 10, 100 and 1000 ng/ml of LPS treatment in per group.

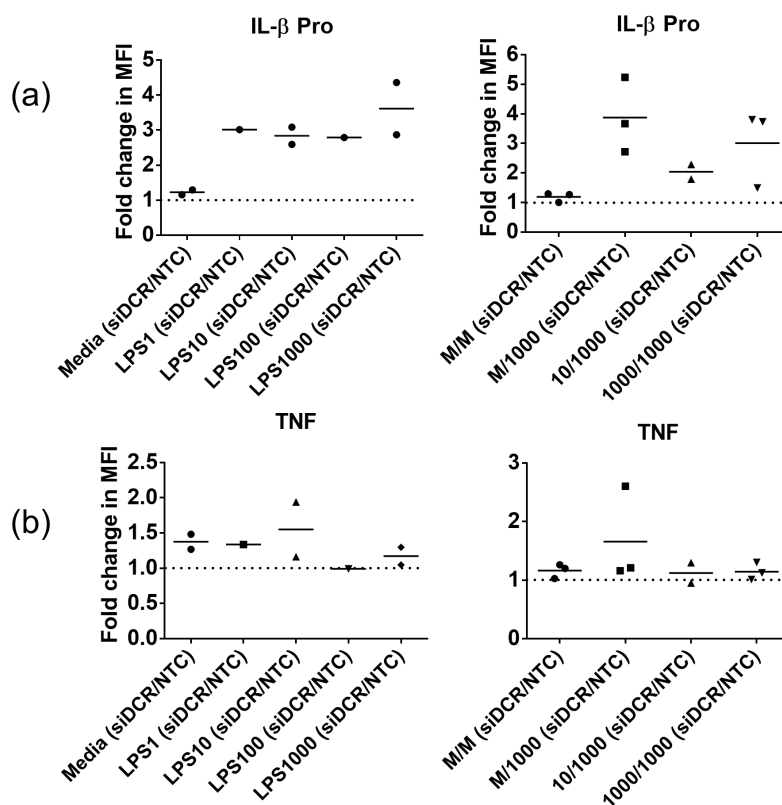


FIGURE 6.8: Dicer knock-down has subtle effects on TNF but profound effects on pro-IL-1 β expression

Scatter plots showing comparison of fold change in MFI (median fluorescent intensity) between siDCR and NTC groups for Media (0ng/ml), LPS1 (1 ng/ml), LPS1 (10 ng/ml), LPS1 (100 ng/ml) and LPS1000 (1000 ng/ml) and M/M, M/1000 (challenged), 10/1000 (twice-challenged) and 1000/1000 (twice-challenged) for a) pro-IL-1 β b) TNF

6.9 Dicer knock down populations have higher median IL-6 staining at high doses of LPS

Population distribution of IL-6 staining revealed distributions that were uni-modal across LPS doses in untransfected, NTC and siDicer groups (**Figure 6.9a**). The median intensity of siDicer group was comparable to that the NTC group except at the highest dose where the Dicer knock down population had a larger median intensity suggesting that Dicer knock down increased IL-6 production in the population but only at the highest dose (**Figure 6.9b**). However, when interpreting median intensity as a fold change between siDicer and NTC very small differences in the intensity fold change was variable at the highest dose and, therefore, were inconclusive (**Figure 6.10b**).

6.10 Dicer knock down decreases NOS2 levels in the population

NOS2 staining was observed to be bi-modal at 1, 10 and 100 ng/ml of LPS challenges in the untransfected control while at the highest dose of LPS (1000 ng/ml) the distribution of NOS2 staining was mostly uni-modal with most cells positive for NOS2 staining. NTC and Dicer populations were uni-modally distributed at 100 and 1000 ng/ml of LPS dose suggesting transfection to have a positive effect on the NOS2 staining of the cells (**Figure 6.9a**). However, the increase in median fluorescence intensity of NOS2 in the siDicer populations across LPS dose was linear in comparison to the NTC populations that had an higher median intensity at all doses which peaked at 1000 ng/ml LPS dose (**Figure 6.9b**). The lower NOS2 levels expressed as a fold change between siDicer and NTC groups at 100 ng/ml LPS dose showed a 20% drop in the median intensity of NOS2 staining. This drop increased to 40% at the highest dose of LPS. This was, however, not observed in Media/1000 (single-challenged) populations which had twice as many cells at LPS stimulus (**Figure 6.10a**). This leads to the speculation that when Dicer is available, the overall regulatory effect of miRNAs is to increase the production of NOS2 in

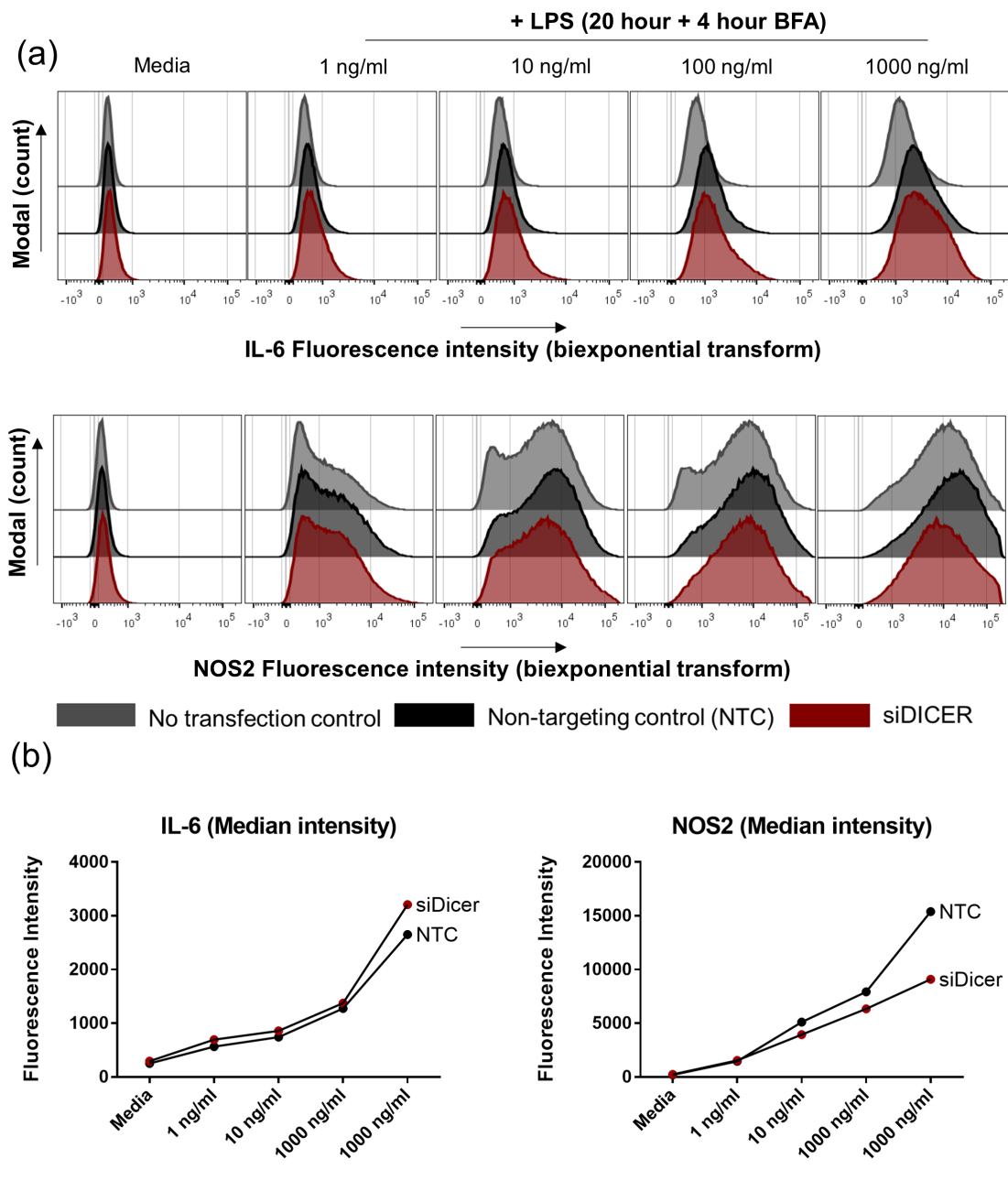


FIGURE 6.9: Dicer knock down decreases NOS2 levels in the population while IL-6 levels remain unaffected

Pre-gated (a) histograms for pro-IL-1 β and NOS2 fluorescence intensity for untransfected, NTC and siDicer groups are overlaid for comparison. (b) Population median fluorescence intensity for NTC and siDicer groups each for IL-6 and NOS2 are represented in before-after plots. 1, 10, 100 and 1000 ng/ml of LPS treatment in per group.

RAW264.7 but this effect is further dependent on the size and density of the population.

6.11 Dicer knock down affects the cell-to-cell variability of proteins

It has been shown using dual reporter systems (Schmiedel et al., 2015) and endogenous targets (Blevins et al., 2015) that miRNA affect the cell-to-cell variability interpreted using the co-efficient of variation (CV) statistic to represent variability. As CV is normalised to mean ($CV = \text{standard-deviation} / \text{mean}$), it can be indicative of the variability in the populations of different means. We calculated the CV of fluorescence intensities of each of our chosen proteins to check if Dicer knock down affected the cell-to-cell variability of protein expression.

Dicer knock down decreased the CV of pro-IL-1 β expression for all doses of LPS indicating that Dicer knock down has an overall effect of decreasing the variability of cells. This increased variability is stronger at low doses of LPS (or when the median intensity of the population is lower) in comparison to higher doses (**Figure 6.11**). The decrease in CV was observed when comparing challenged and twice-challenged populations in the expression of pro-IL-1 β as well. The above results suggest that pro-IL-1 β is expressed with greater variability in presence of Dicer, or consequently, mature miRNAs.

NOS2 CV was higher for the siDicer group when compared to its respective NTC control indicating that as Dicer is knocked down, the cell-to-cell variability of the NOS2 population increases (**Figure 6.11**). In populations challenged twice with LPS, the 1000/1000 treatment showed an increased CV upon Dicer knock down, the 10/1000 treatment had a smaller CV with respect to NTC suggesting, possibly, a small difference

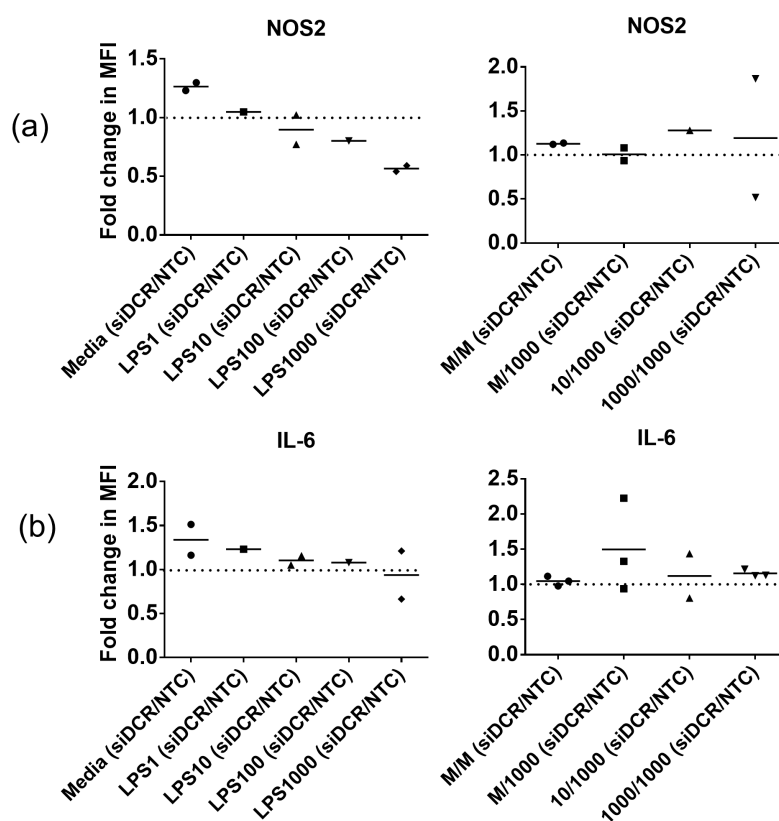


FIGURE 6.10: NOS2 fluorescence intensity shows negative fold change when compared to non-transfected controls.

Scatter plots showing comparison of fold change in MFI (median fluorescent intensity) between siDCR and NTC groups for Media (0 ng/ml), LPS1 (1 ng/ml), LPS1 (10 ng/ml), LPS1 (100 ng/ml) and LPS1000 (1000 ng/ml) and M/M, M/1000 (challenged), 10/1000 (twice-challenged) and 1000/1000 (twice-challenged) for a) NOS2 b) IL-6

in the two treatments as to how NOS2 variability is affected when populations are pre-stimulated with a low dose of LPS. Interestingly, the challenged (Media/1000) control population did not register a drop or increase in CV upon Dicer knock down suggesting the density of cells to have a role in maintaining the cell-to-cell variability (**Figure 6.11**).

TNF CV was found to be higher upon Dicer knockdown but this increase was less obvious or even absent at higher doses of LPS stimulus. The CV in twice-challenged population was unpredictable across the experimental repeats. IL-6 CV was mostly unchanged across the LPS doses and in twice challenged populations when compared siDicer was compared to NTC. Some of the repeats, however, showed an increase in the CV making overall predictions difficult (**Figure6.12**).

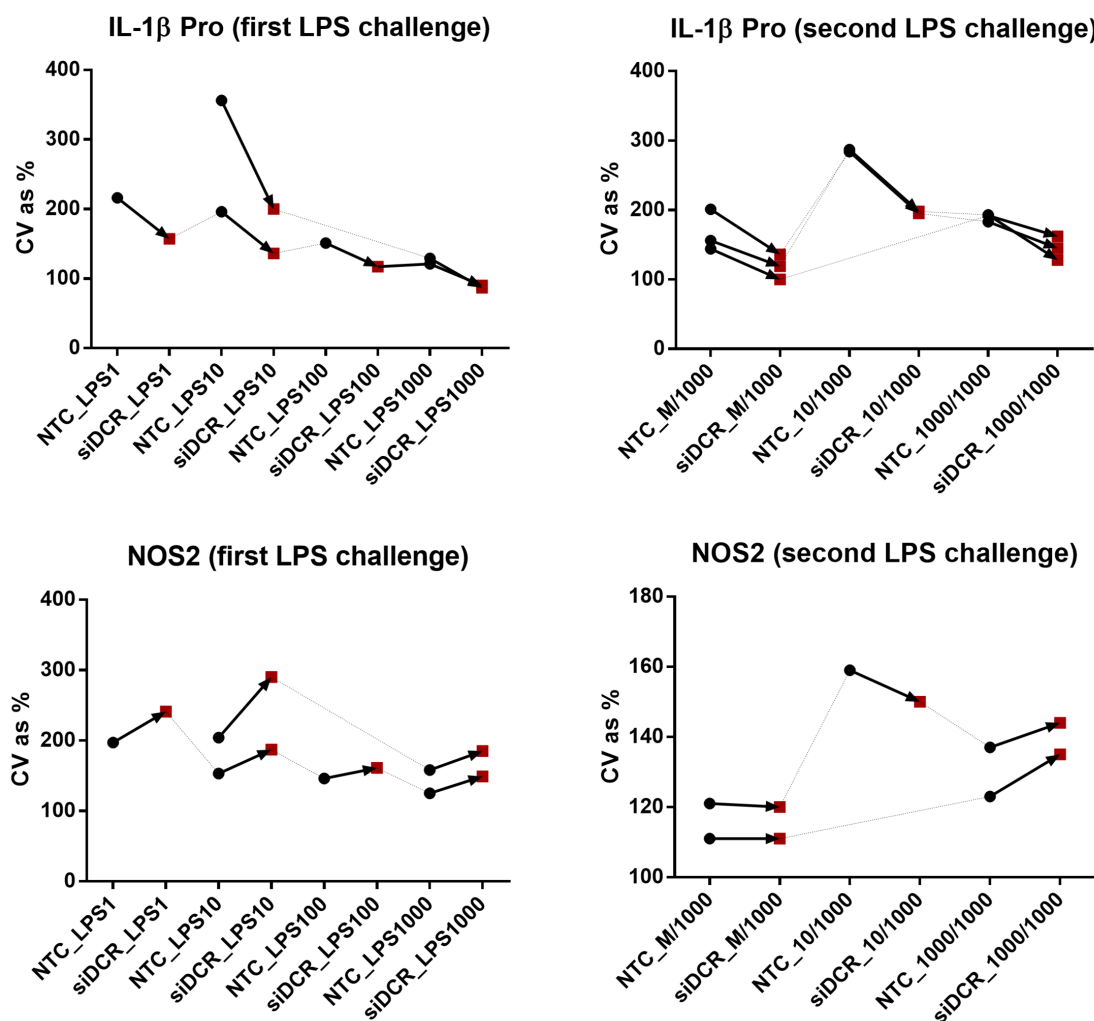


FIGURE 6.11: Dicer knock affects the cell-to-cell variability of pro-IL-1 β and NOS2

Before-after plots to show change in CV within NTC and siDicer groups for 1, 10, 100 and 1000 ng/ml of LPS treatment for first LPS challenge and M/1000, 10/1000 and 1000/1000 for second challenge for pro-IL-1 β and NOS2

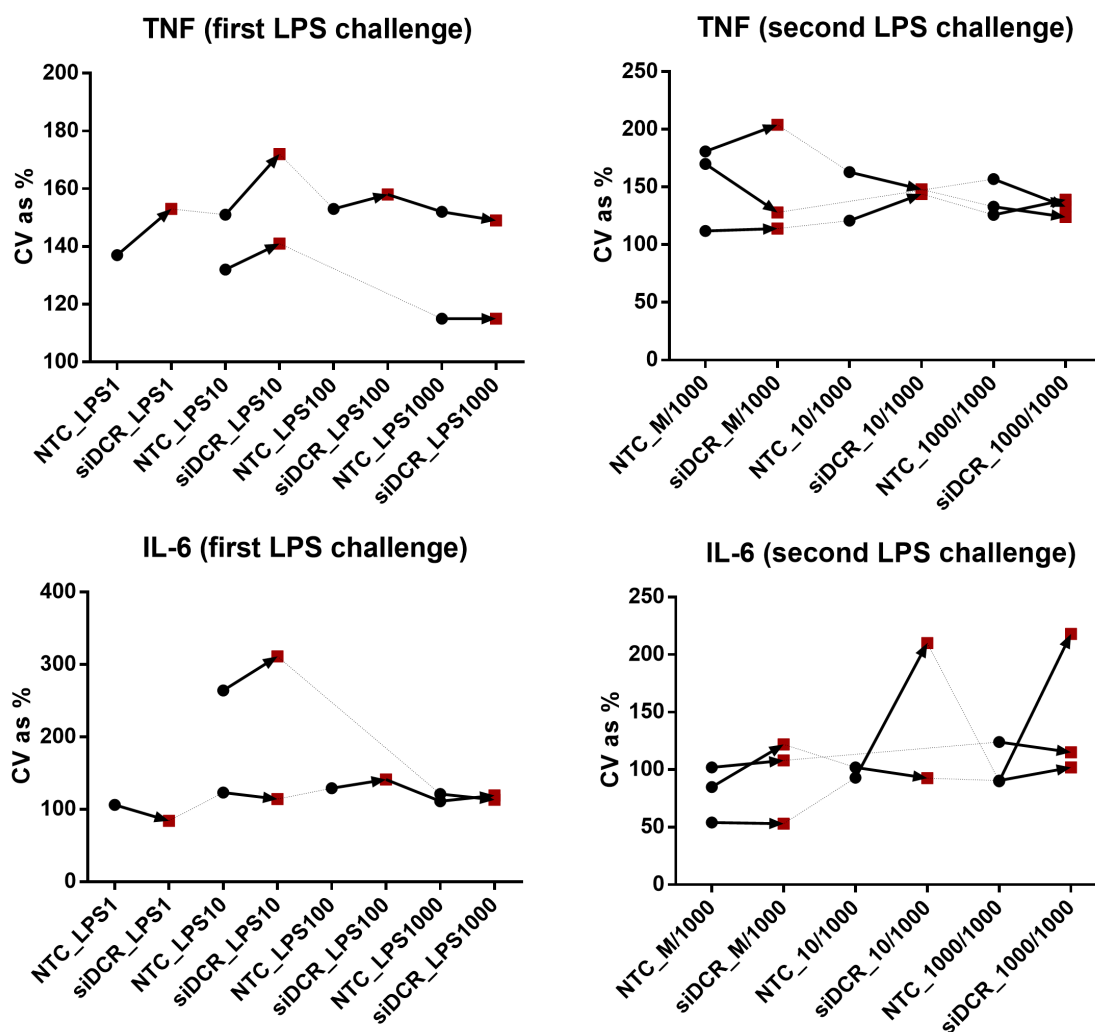


FIGURE 6.12: Dicer knock does not affects the cell-to-cell variability of TNF and IL-6

Before-after plots to show change in CV within NTC and siDicer groups for 1, 10, 100 and 1000 ng/ml of LPS treatment for first LPS challenge and M/1000, 10/1000 and 1000/1000 for second challenge for TNF and IL-6

6.12 *In-silico* cell states are sensitive to Dicer knockdown

We then questioned how the nr model (described in **Chapter 5**) fits the data obtained for overall pro-IL-1 β positive cells, especially, when Dicer is knocked down. Following the methods of **Chapter 5**, we estimated the parameters for nr model for NTC and siDicer separately and accepted parameters that fit (+/-5%) the number of pro-IL-1 β positive cells across all four LPS doses (**Figure 6.6a**) at 24 *in silico* hours.

Figure 6.13a shows that mean value of parameter β that describes the rate at which positive cells become negative was lower in siDicer and close in magnitude to the value of α . The value of α , the rate at which negative cells become positive, was similar between both NTC and siDicer. The parameter γ_1 , the rate at which positive cells turn non-responsive, was low for both treatments suggesting that fewer cells become non-responsive (NRS). The mean value of γ_2 , however, was higher in NTC than siDicer suggesting that a higher probability is associated with NRS cells to switch to the non-responsive (permanent) state (NRPS) in the NTC treatment. Further, mean β_2 value was lower in NTC (than in siDicer) suggesting, fewer cells to become negative from the NRS state (**Figure 6.13a**).

The results suggest that as γ_1 is low, majority of the transitions within the simulated models of NTC and siDicer will be effected by α and β values, especially, when LPS in the *in silico* environment decreases. This means that most of the variance in the trajectories of siDicer and NTC (**Figure 6.13b**) can be explained by a lower rate of switching off from positive to negative states. Further, the nr model simulation suggests that Dicer knock down may decrease the number of NRPS cells (because of the low γ_2 value) and increase the negative pool from a NRS state.

Figure 6.13 trajectories suggest that a variance in percentage positive pro-IL-1 β cells

is apparent from an early time point at low doses (1 and 10) whereas this variance is less pronounced in magnitude and at early time points at high doses of LPS (100 and 1000).

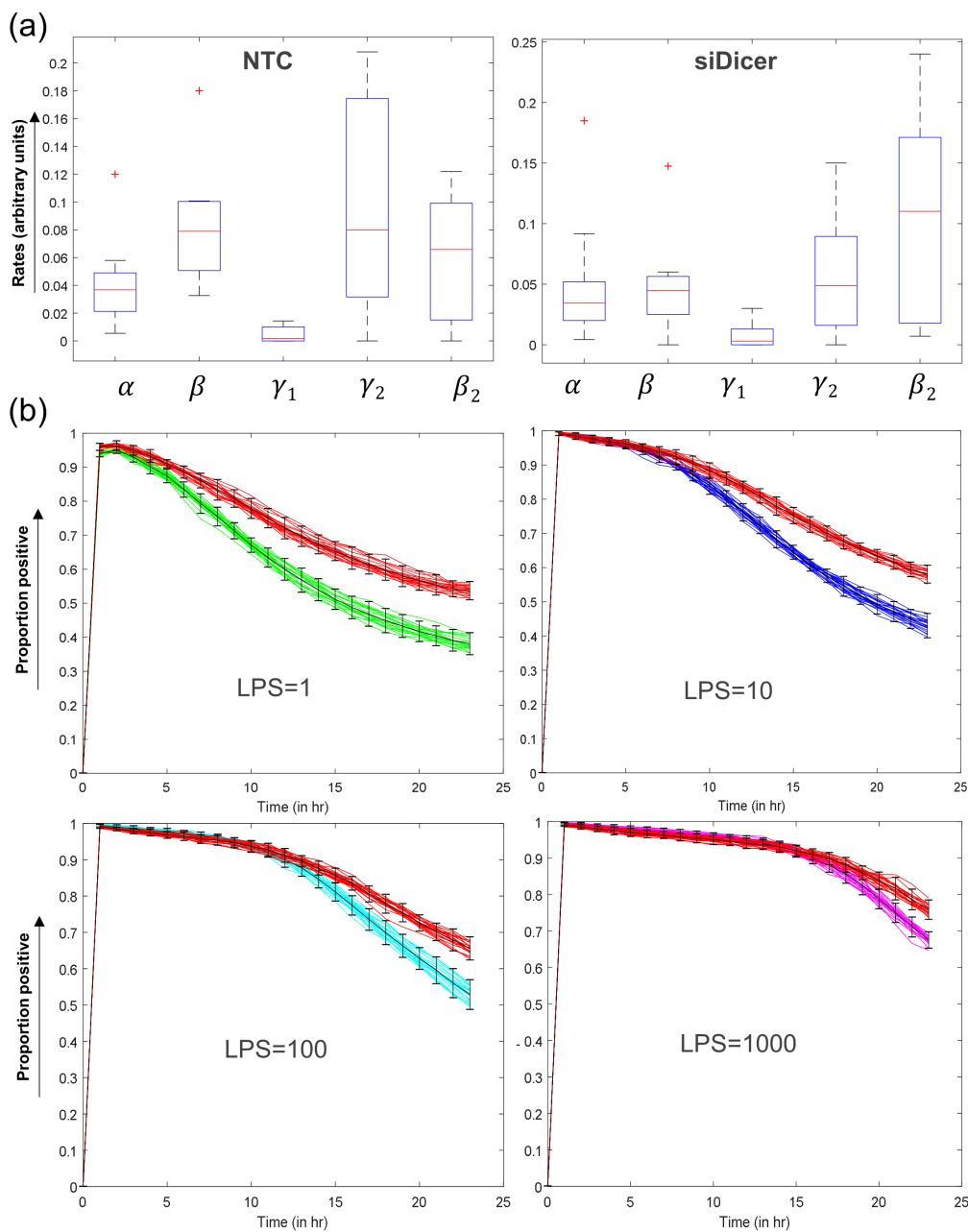


FIGURE 6.13: *In-silico* cell states are sensitive to Dicer knockdown

- a) Box and whisker plots showing estimated values of α , β , γ_1 , γ_2 , β_2 as estimated for NTC and siDicer treatments. Number of parameter sets estimated were 8 for NTC and 13 for siDicer b) Parameter values estimated in a for NTC and siDicer were averaged and used to simulate 20 stochastic runs of the nr model per treatment (NTC and siDicer) with error bars (black) representing 95% confidence interval of the mean (of all trajectories per dose). LPS 1, 10, 100 and 1000 for NTC in green, blue, cyan and magenta and all siDicer doses in red.

6.13 Discussion

6.13.1 Conclusions

In this chapter we looked at the effects of knocking down Dicer on RAW264.7 community composition when responding to a first or secondary dose of LPS. We show results pertaining to composition, distributions of inflammatory protein expression and cell-to-cell variability at 24 hours from first or secondary stimulus. We make the following observations in conclusion:

- We report compositional differences in Dicer knock down RAW264.7 macrophages to non-targeting control (NTC) communities.
- Dicer knock down has a strong positive effect on pro-IL-1 β expression
- TNF and IL-6 also have small positive effect on their expression level upon Dicer knock down while NOS2 is repressed.
- Cell-to-cell variability of NOS2 and pro-IL-1 β are affected differentially in Dicer knock down populations.
- Parameters estimated for nr state model to capture pro-IL-1 β positive cells for NTC and siDicer treatments, revealed that Dicer knock down can affect *in silico* cell states.

6.13.2 Dicer knock-down alters sub-population frequencies

We show that knocking down Dicer can either increase or decrease sub-population frequencies within a community of RAW264.7 cells responding to LPS. Describing community composition in terms of sub-populations of TNF, IL-6 and NOS2 producing cells, we show that the most pro-inflammatory sub-population TNF+IL6+NOS2+ decreases when Dicer is knocked down. Interestingly, TNF-IL6-NOS2- sub-populations increase upon Dicer knockdown. This suggests that Dicer or miRNAs, globally, increase the inflammatory potential of RAW264.7 cells while in the absence of this regulatory network, a larger proportion of negative cells are found with fewer triple positive populations. This suggests that these sub-populations may be maintained by a differential miRNA expression pattern as shown in cancer phenotypes such prostate cancer cells (Ambs et al., 2008). Interestingly, miRNAs are known to be determinants of inflammation in macrophages responding to bacteria (Zhou, Li, and Wu, 2018; Curtale, Rubino, and Locati, 2019) and have been shown to be differentially expressed upon secondary stimulus of LPS, in an endotoxin tolerised state (miR-146b, Renzi et al., 2015; miR-222, Seeley et al., 2018; miR-125a~99b~let-7e cluster, Curtale et al., 2018) to signify their relevance in phenotypic decisions. This may suggest that macrophage response to LPS is a consequence of communities that differentially express proteins and miRNAs.

This is further supported by the inflammatory sub-population TNF-IL6+NOS2+ which is present in communities responding to high LPS doses and is increased upon Dicer knock down. While this increase may be a variability in the experimental result it can also mean that miRNAs can also repress the inflammatory response by acting differentially on this sub-population.

Analysing triple negative sub-populations in Dicer knock down communities, we find that it is actually a heterogeneous population and is a mix of negative population (for TNF, IL-6, NOS2 and IL-1 β) and single positive IL-1 β population. We show that this

population is twice as frequent compared to NTC or untransfected RAW264.7 cells and are expressed bi-modally. Analysing the single positive pro-IL-1 β sub-population with respect to the overall distribution of pro-IL-1 β producing cells, this sub-population is uni-modal and a low producer of pro-IL-1 β (Appendix **figure 8.4**)

As, the pro-IL-1 β populations were twice as frequent we tested the percentage of positive cells per LPS dose for Dicer knock down populations and non-targeting controls (NTC) by fitting them to the nr model. Based on the parameter estimates we can speculate that while β (rate at which positive cells transition to negative) may be a prominent mechanism how Dicer may affect cell populations to attain the basal rate, alternative ways to reach the negative state can exist in Dicer knock down populations as exemplified by the higher β_2 rate (rate at which non-responsive cells transition to negative) in siDicer population (**Figure 6.13**). Our model suggests that underlying, mathematically modelled, states may be affected by knocking down Dicer.

6.13.3 Protein expression

As previously discussed, miRNAs play a role in changing overall frequencies of the inflammatory sub-populations in the LPS-induced community. Further it is observed that the absence of miRNAs can positively or negatively affect the overall expression, in terms of fluorescence intensity, of certain proteins. Whether the absence of miRNAs lead to repression or over-expression is dependent on what the overall additive effects of miRNAs (directly or indirectly targeting the protein of interest) is.

We show that pro-IL-1 β expression intensity increases up to 5-fold when comparing intensities of siDicer populations with respect to NTC upon LPS challenge. This increased expression intensity is also accompanied by a subsequent increase in the number of overall pro-IL-1 β positive cells in the Dicer knock down population. (Varol et al., 2017) showed increased pro-IL-1 β expression in Dicer-deficient mice microglia

suggesting Dicer-dependent activation to occur *in vivo* as well. This indicates that miRNA-mediated regulation may be uniformly relevant throughout the population and may or may not contribute to phenotypic fates in the responding community.

This being said, however, it is highly unlikely that these effects are caused directly by repression due to miRNA targeting of pro-IL-1 β based as the 3' UTR untranslated region (UTR) in mouse is 459 nucleotides in length with no conserved miRNA targeting sites (Appendix Table 8.1). It is also unlikely that a small 3' UTR may be targeted by poorly conserved miRNAs (Matoulkova et al., 2012). This suggests that the increase in pro-IL-1 β positive cells and its associated increase in intensity may be caused by additive effects of miRNAs targeting other regulatory proteins and signalling molecules and that miRNAs may be, collectively, dampening the ability of negative populations to turn positive and positive population to become hyper-responsive in terms of pro-IL-1 β expression. Alternatively, other Dicer-dependent non-coding RNA such as *Alu* (Kaneko et al., 2011) and activate the NLRP3 inflammasome (Gelfand et al., 2015) explaining the preferential activation of pro-IL1 β and not the other proteins measured in this study. This may be the reason why we observe increased single positive pro-IL-1 β cells upon Dicer knockdown.

We also observed an overall decrease in the intensity of NOS2 expression in the Dicer knock down population suggesting miRNAs, in a global sense, may encourage the production of NOS2 implying an opposite role in how miRNAs collectively, affect highly expressed proteins, perhaps suggesting their importance in LPS-induced response.

6.13.4 Cell-to-cell variability

While Blevins et al., 2015 suggest that cell-to-cell variability decreases in endogenous protein expression, Schmiedel et al., 2015 suggest that cell-to-cell variability may increase in highly expressed proteins that are also combinatorially targeted by miRNAs due to increase in the miRNA pool induced noise. In our results, we observe two highly

expressed proteins that showed disparate co-efficient of variance (CV) trends. Cell-to-cell variability decreases upon Dicer knock down for pro-IL-1 β suggesting miRNAs to have an overall tendency to increase the variance in pro-IL-1 β expression. This may explain how diverse IL-1 β populations were identified in our results (**Figure 6.7b**, Appendix **Figure 8.4**).

NOS2 expression showed increased CV upon the first challenge of LPS suggesting miRNAs to have a role of decreasing the noise in expression (**Figure 6.11**).

Both IL-1 β (459 nucleotides) and NOS2 (397 nucleotides) have short 3' UTRs and poorly conserved sites for miRNAs (appendix **Table 8.1**, **Table 8.2**) based on TargetScan predictions (Agarwal et al., 2015). Since, IL-1 β and NOS2 are unlikely to be miRNA targets because of a short 3'UTR (Matoulkova et al., 2012) and no conserved miRNA sites on them, it suggests that cell-to-cell variability affected by Dicer knock down may be a complex process and its effect to cell-to-cell variability may not be trivial.

6.13.5 Summary and Future work

Our observations, in this chapter, were limited to a single time-point (24 hours post primary or secondary stimulus) and was limited by the lack of complete Dicer. Also, we do not measure miRNA. Further, our hypo-response experiments showed compositional changes in challenged populations (Media/1000) that were different from the otherwise identified trends. While this could be an effect of a different starting population size in Media/1000 populations it remains to be tested. It must be noted that community composition is limited by the choice of proteins in our experimental set up and may not necessarily capture all possible sub-populations (inflammatory phenotypes) within the inflammatory response continuum that may be affected upon knocking down Dicer.

As future work, we would like to intra-cellularly stain for Dicer in populations responding to LPS to tease out heterogeneity that is either suppressed or expressed due

to miRNAs as a global regulatory system. Also, it would be further interesting to look at effects caused by knocking down Argonaute (miRNA-mRNA targeting) and Drosha (miRNA biomachinery).

Chapter 7

Discussion

7.1 Summary

In this thesis, we characterise population response of RAW264.7 to LPS and reveal communities underlying this response. We further find communities within a twice-challenged population that are otherwise known to be phenotypically distinct and hypo-responsive. Based on this, we build simple mathematical models to understand the heterogeneous basis for hypo-response and, more complex ones to determine how communities of RAW264.7 cells evolve in time. miRNAs have been known to fine-tune protein expression and cell-to-cell variability. To investigate if miRNAs have a role in maintaining or establishing LPS-induced heterogeneous communities in RAW264.7 cells, we knock down Dicer, a core protein in miRNA biogenesis pathway. Below we list our main findings:

RAW264.7 cells respond as communities to LPS

- Response to LPS is heterogeneous and can be visually represented as a complex community.
- Community composition is dependent on the magnitude of LPS dose.
- Restricting inter-cellular communication in RAW264.7 has large effects on community composition.

- Twice-challenged populations form communities that are more resistant temporally and perturbations to inter-cellular communication.

***In-silico* communities provide useful insights to underlying processes and sub-population transitions**

- Hypo-responsiveness can be modelled by including non-responding cellular states within a population responding to *in silico* secondary LPS challenge.
- Restriction of secretion promotes the transition of cells in the negative state to the triple positive (TNF+IL6+NOS2+) state.
- Inter-cellular communication can be mimicked by the cube model to gain useful insights such as rates that describe sub-population transition rates that can model time-evolution of community heterogeneity and point out towards possible interactions between the community.

miRNAs can have complex effects on fine-tuning of protein expression and community composition

- Community compositions are affected on knocking down Dicer.
- pro-IL-1 β expression is upregulated up to 5-fold but this is unlikely due to direct targeting of miRNAs.
- Variance in pro-IL-1 β expression decreases while it increases for NOS2.

7.1.1 Integration of mathematical modelling to experimental approaches in studying heterogeneity

Mathematical modelling of biological processes can precisely define dynamics of complex systems like multi-cellular organisms at the protein, cellular, or even organismal level. While complex agent-based models (ABM; Bonabeau, 2002) can be created to simulate emergent behaviour of a system, simple phenomenological models can be used to ask questions without having to understand the underlying system (Merks and Glazier, 2005). We approached the problem of representing heterogeneity and hypo-responsiveness in cell populations with simple phenomenological approaches.

Simplistic approaches, however, are often bound to failure and, thus, a large part of the mathematical modelling process involved the creation of models that did not explain our empirical data. However, upon adding and subtracting attributes or terms (Hammer and Pitchford, 2006) to various models we were able to describe hypo-responsiveness in terms of *in silico* cell states. This allowed us to explore the rates associated with the emergence of these states along with final outcomes in terms of composition of the population. Thus, approaching problems of biological complexity by iterating through simple models can be a useful modelling methodology.

Using pie charts to represent heterogeneity in macrophage communities helped us visualise the idea of macrophage sub-populations influencing each other in a continuum of heterogeneous communities responding to LPS and secondary effects. This inspired the idea to create the cube model (**Chapter 5**) to model sub-population transitions. The ideas explored with the cube model may be interesting to approach using individual-based or agent based methods. To model global miRNA behaviour with single-cell effects to model cell-to-cell variability in protein expression it may be useful to model macrophage populations at the single-cell level (as agents in an ABM, Bonabeau, 2002) to show how macrophage populations, fine-tuned by miRNAs emerge in time, micro-environment, and

antigen-induced response.

7.1.2 Innate immune responses are community-led

Variability in gene expression in eukaryotic cells (McAdams and Arkin, 1997; Elowitz, Levine, and Siggia, 2002; Paulsson, 2004) often has phenotypic consequences (Eldar and Elowitz, 2010; Blake et al., 2006). This suggests that genetically equal populations show considerable cell-to-cell variability that scales with abundance, particularly, of proteins that are stress induced (Bar-Even et al., 2006; Newman et al., 2006). Phenotypic heterogeneity conferred from heterogeneous gene expression in yeast has been shown to be a response mechanism to cope with environmental stress (Bódi et al., 2017). Similarly, variability in innate immune response to stimulus has been shown to be heterogeneous in mammalian immune cells (Shalek et al., 2013; Shalek et al., 2014). This is most notable in the high transcriptional variability of cytokines and their receptors upon stimulus in LPS stimulated phagocytes of human and mice origin (Hagai et al., 2018). Chapter 3 provides a visual representation of RAW264.7 cells that respond to LPS (as an external stimuli) as a community comprising of distinct sub-populations that may, in part, be a result of transcriptional variability of cytokines. The sub-population frequencies within the responding community are calculated from per-cell fluorescence staining levels against respective isotype controls to measure protein expression in binary yes or no terms. Using 3 or 4 highly expressed inflammatory proteins (TNF, IL-6, NOS2 and/or pro-IL-1 β) that result in a total of $8(2^3)$ or $16(2^4)$ sub-populations we show that response to LPS, indeed, triggers a heterogeneous response within the population.

While cytokine transcriptional variability may be one of the defining factors of the underlying heterogeneous response, immune cell response plasticity has been known to be affected by other factors such as autocrine and paracrine signalling (Xue et al., 2015; Caldwell et al., 2014; Shalek et al., 2014), and post-transcriptional regulation by miRNAs (Zhou, Li, and Wu, 2018). Temporal perturbations in transcription factors involved in

LPS induced genes may modulate response, as in the all or nothing response in NF- κ B activity during early phase activation (Mitchell and Hoffmann, 2018). While the early phase activation is via MyD88 signalling, the subsequent noisy and graded late phase activation is TRIF-mediated (Mitchell and Hoffmann, 2018).

We show at the protein level, that community composition is altered temporally, by increasing the magnitude of LPS and upon restricting secretion. The frequency of the triple positive (TNF+IL6+NOS2+) and double positive (TNF-IL6+NOS2+) sub-populations in the community increase upon stronger LPS stimulus suggesting that the dose of LPS affects sub-populations and not just the overall levels as indicated by the median fluorescence intensity of a single protein staining within a population. It is worth noting that certain sub-populations that are theoretically plausible (such as TNF+IL6+NOS2- or TNF-IL6+NOS2-) are absent or less frequent in RAW264.7 communities responding to LPS. This suggests certain sub-populations may either be rare or that community-mediated processes such as cytokine signalling can dampen their presence. We then show that a restriction of both autocrine and paracrine secretion can alter communities significantly making them more inflammatory. This alteration of communities was observed when secretion was restricted for longer than 8 hours but less than 12 hours suggesting this time to be crucial in shaping population heterogeneity. The possible contributors to this effect may be the activation of late phase NF- κ B which is TRIF-mediated and can lead to a graded, sensitive to noise response shaping the overall community into a heterogeneous population (Mitchell and Hoffmann, 2018). Other contributors to this effect may be the production of anti-inflammatory cytokine IL-10 (Saraiva and O'Garra, 2010) and TNFR1-TRADD mediated NF- κ B signalling with TNF binding to its own receptor (Hayden and Ghosh, 2014). It is possible that this graded response may then be disrupted with the restriction of secretion.

7.1.3 Twice-challenged communities do not change in composition in response to LPS

Innate immune cells pre-exposed to LPS show a dampened immune response when re-stimulated with LPS. This effect is physiologically relevant in the appearance of an immuno-suppressive phase in sepsis and is associated with increased mortality (López-Collazo and Del Fresno, 2013). The TLR4 response to LPS induces chromatin modifications priming anti-microbial effectors while silencing pro-inflammatory genes (Foster, Hargreaves, and Medzhitov, 2007).

In this thesis (**Chapter 4**) we show that RAW264.7 cells when challenged twice with LPS are hypo-responsive, as a population, in terms of secreted TNF and IL-6. However, at the single-cell level, challenged and single-challenged communities of TNF, IL-6 and NOS2 appear very similar. Interestingly, upon visually representing communities of challenged and twice-challenged populations at different time points, twice-challenged communities did not appear to change as much as the challenged community. This was observed to be true when secretion was restricted as well. This may mean that heterogeneity, in terms of, community composition is maintained in hypo-responsive communities despite the overall lower response. Whether a hypo-responsive population, that is phenotypically distinct from populations that are not pre-exposed to LPS are inherently heterogeneous or if certain 'rogue' triple positive or double positive cells remain within a hypo-responsive population remains an unanswered question. Such rogue populations may be important in chronic inflammatory settings such as atherosclerosis where macrophage response is continually shaped by the micro-environment (Chistiakov et al., 2015).

A bottom-up approach (Satija and Shalek, 2014) to characterise LPS challenged and twice-challenged populations by sequencing single-cells by RNA sequencing or by time-of-flight mass cytometry may be crucial to understand the continuum of

macrophage response communities. Building single-cell trajectories in pseudo-time to track how sub-populations, within a responding macrophage community, evolve (Trapnell et al., 2014) may further our understanding in the mediators of macrophage response heterogeneity. In Chapter 4, we conceived a mathematical model (cube model) that describes the time-evolution of macrophage sub-populations in terms of the probabilities associated with sub-populations switching between each other. Pseudo-time based parametrisation of this model to find probabilistic rates associated with appearance (or disappearance) of sub-populations over time can provide important clues to interdependences between sub-populations. Overall, single-cell based approaches, visual representations of heterogeneity and mathematically led-approaches to understanding how heterogeneity comes about in macrophage population can greatly benefit the understanding of macrophage communities and, even heterogeneous community responses in general.

7.1.4 MiRNAs can fine-tune expression but also community composition

MiRNAs fine tunes protein expression on a per cell basis acting as a post transcriptional regulatory framework. Interestingly, miRNA-mediated silencing can also result in lower cell-to-cell variability in endogenous proteins (Blevins et al., 2015) or an increase in the variance when multiple miRNAs target a single highly expressed protein (Schmiedel et al., 2015). In the results discussed in this thesis, protein expression variability (between cells) of pro-IL-1 β and NOS2 show opposite trends. The variability in the expression of pro-IL-1 β upon Dicer knockdown decreased suggesting Dicer (or miRNAs) when present, increases the variance in pro-IL-1 β expression.

Schmiedel et al., 2015 showed that highly expressed genes that are combinatorially targeted by miRNAs increase the extrinsic noise due to the variability in the miRNA pool itself. This extrinsic noise in the expression of the target protein expression then increases variability between cells. The idea of a variable pool of highly-expressed

miRNA has been recently suggested to be anti-correlated to predicted target gene expression using half-cell sequencing (Wang et al., 2019). These studies suggest that increased miRNA noise between cells adds to the extrinsic noise of target protein expression and has been shown, to computationally, favour the bi-modality in target protein distribution (Del Giudice et al., 2018). This effect was apparent at high doses of LPS in this study, in pro-IL-1 β expression where Dicer knock down population appeared to be more uni-modal than the (non-targeting) control population.

Dicer knock down pro-IL-1 β populations were not only less noisy but their expression increases up to 5-fold (**Chapter 6**). Interestingly, Il1b has a short 3' UTR (459 nucleotides) which decreases its susceptibility to combinatorial targeting (Matoulkova et al., 2012), especially, due to the lack of highly conserved miRNAs sites in the UTR (*source: Targetscan; Agarwal et al., 2015*). This begs the question if certain undiscovered miRNAs target Il1b or if knocking down Dicer can disrupt a series of regulatory proteins that keep pro-IL-1 β in check.

Garg and Sharp, 2016 proposed that noisy miRNA-mRNA circuits may be a source of generating phenotypic outcomes such that noisy genes under miRNA control may be susceptible to developing into physiologically different cells. Computational modelling of extrinsic noise was shown as a determinant of bi-modality (Del Giudice et al., 2018). We show that such a phenotypic variability can, indeed, be observed upon comparing LPS-challenged community compositions of Dicer knock down populations with Dicer unaffected communities. Further, of much interest, is why twice-challenged communities were more resistant to community composition change. This may mean that hypo-responsive communities as a population have reduced plasticity and yet form heterogeneous communities when analysed at the single cell-level.

7.1.5 Conclusion

Macrophages have been explored as communities but only recently been appreciated at the single-cell level. In this work we show that RAW264.7 macrophage-like cells respond to LPS as communities that consist of distinct sub-populations. This work demonstrates that a wealth of insight can be gained by single-cell studies with regards to the determinants of macrophage population heterogeneity and community responses. Finally, combining experimental results and mathematical approaches, our study can be used to probe heterogeneity in populations, not just limited to macrophages.

Chapter 8

Appendix

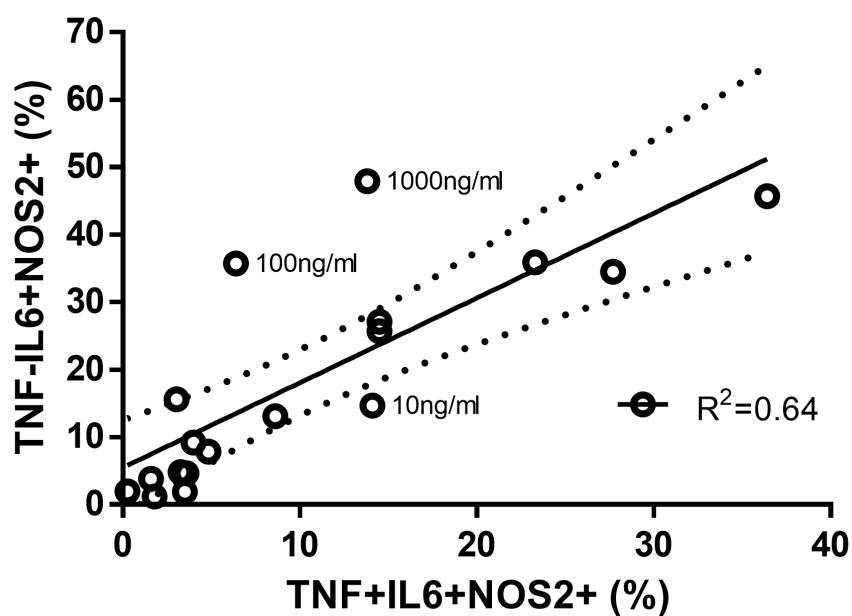


FIGURE 8.1: Triple positive cells and TNF- double positive cells correlate and may constitute similar populations

Scatter plot to show TNF+IL6+NOS2+ and TNF-IL6NOS2+ sub-populations from n=4-5 independent for treatments of 1, 10, 100 and 1000 ng/ml of LPS dose for 16 hours. R^2 value is used as the estimator for goodness of fit and dotted lines represent 95% confidence intervals.

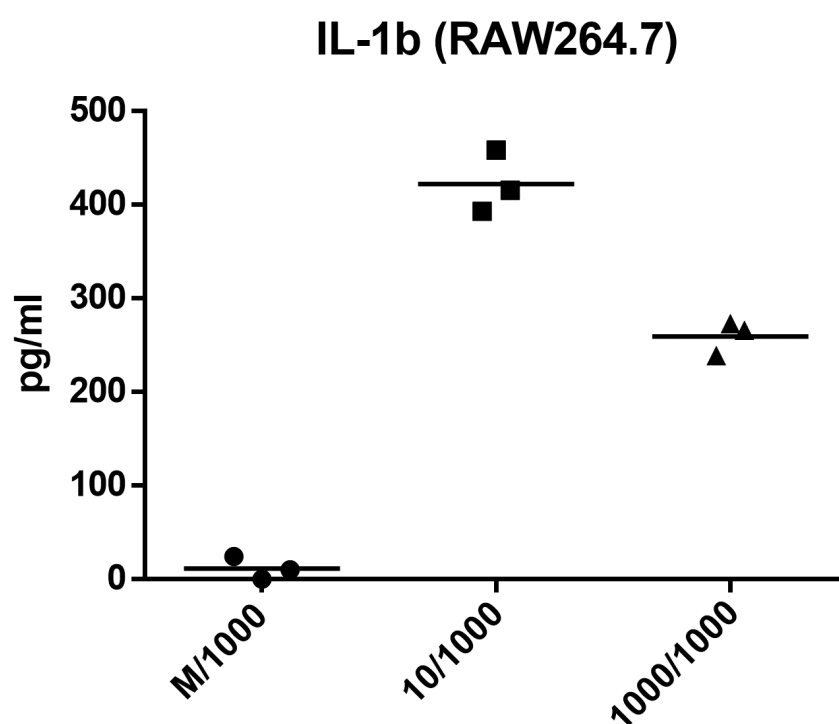


FIGURE 8.2: IL-1 β is secreted upon two doses of LPS in RAW264.7 cells

Scatter dot plot showing IL-1 β levels in RAW264.7 cells stimulated once (Media/1000), or twice (10/1000 or 1000/1000) where 10 and 1000 represent 10 and 1000 ng/ml of LPS post second stimulus at 24 hours into culture. n=3; mean levels indicated by horizontal line

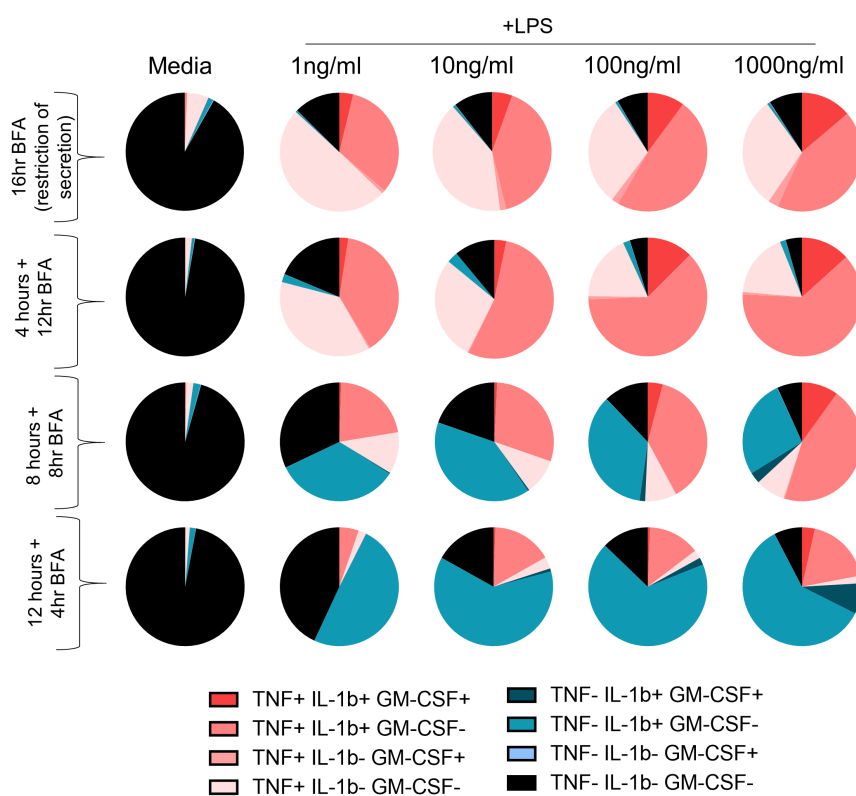


FIGURE 8.3: TNF, pro-IL-1 β and GM-CSF communities appear to change in composition on restricting secretion

Pie charts depicting sub-populations based on TNF, pro-IL-1 β , GM-CSF in RAW264.7 cells cultured in media only or at 1, 10, 100 and 1000 ng/ml concentration of LPS for a 16 hour LPS+BFA; 4 hour LPS and 12 hour LPS+BFA; 8 hour LPS and 8 hour LPS+BFA; 12 hour LPS and 4 hour LPS+BFA. Count of cells=50-100,000

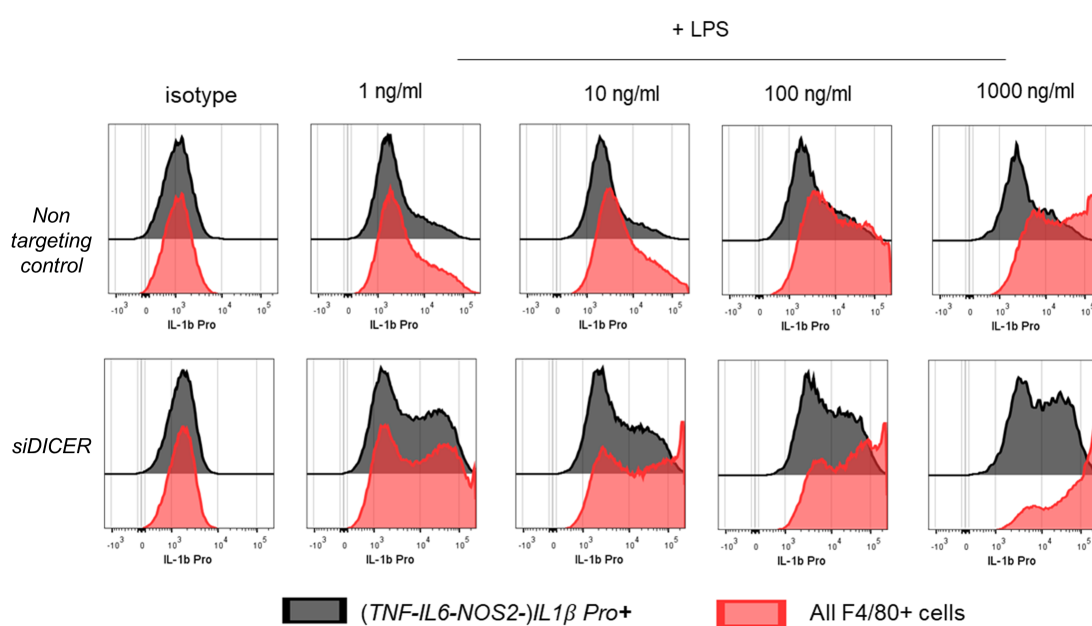


FIGURE 8.4: Single positive pro-IL-1 β have distinct expression profiles and are low producers

Histograms overlaid to compare expression intensity of single positive pro-IL-1 β staining compared to overall pro-IL-1 β staining for all gated F/480 positive macrophages for NTC and siDicer groups. Isotype controls (first plot, each row) are shown for comparison with positive populations for 1, 10, 100 and 1000 ng/ml of LPS treatment.

miRNA	Conserved sites	Poorly conserved sites
miR-138-5p	0	1
miR-455-5p	0	1
miR-125-5p/351-5p	0	1
miR-140-5p	0	1
miR-383-5p.2	0	1
miR-148-3p/152-3p	0	1
miR-129-5p	0	1

TABLE 8.1: TargetScan search for miRNAs targeting mouse IL-1 β mRNA

miRNA	Conserved sites	Poorly conserved sites
miR-130-3p/301-3p	0	1
miR-148-3p/152-3p	0	1
miR-302-3p	0	1
miR-291-3p/294-3p/295-3p/302-3p	0	1
miR-17-5p/20-5p/93-5p/106-5p	0	1
miR-33-5p	0	1

TABLE 8.2: TargetScan search for miRNAs targeting mouse NOS2 mRNA

List of Abbreviations

AGO	Argonaute
AP1	Activator protein 1
APC	Antigen Presenting Cell
BFA	Brefeldin A
CD	Cluster of Differentiation
CV	Co-efficient of Variation
DAMP	Damage-Associated Molecular Patterns
DGCR	DiGeorge syndrome chromosomal
GM-CSF	Granulocyte-Macrophage Colony-Stimulating Factor
Ig	Immunoglobulin
IL-1β Pro	Interleukin-1 β
IL-10	Interleukin-10
IL-6	Interleukin-6
INF	Interferon
IRF	Interferon Regulatory Transcription Factor
JAK	Janus Kinases
kDa	kilo Dalton
LPS	Lipopolysaccharides
NF-κB	Nuclear Factor - κ B
NLRP	Nucleotide-binding oligomerization domain, Leucine rich Repeat and Pyrin domain con
NOS2	Nitric Oxide Synthase 2
ODE	Ordinary Differential Equation

PAMP	Pathogen-Associated Molecular Pattern
PRR	Pattern Recognition Receptor
STAT	Signal Transducer and Activator of Transcription
SWI/SNF	SWItch/Sucrose NonFermentable
TGF-β	Transforming Growth Factor- β
TLR	Toll-Like Receptor
TNF	Tumour Necrosis Factor
TNFR	Tumour Necrosis Factor Receptor
UTR	Untranslated Region
XPO5	Exportin 5

References

- Agarwal, Vikram, George W Bell, Jin-Wu Nam, and David P Bartel (2015). Predicting effective microRNA target sites in mammalian mRNAs. *eLife* 4. Ed. by Elisa Izaurralde, e05005.
- Alexopoulou, L, AC Holt, R Medzhitov, and RA. Flavell (2001). Recognition of double-stranded RNA and activation of NF-kappaB by Toll. *Nature* 413 (6857), pp. 732–8.
- Allen, Nancy C., Naomi H. Philip, Lucy Hui, et al. (2019). Desynchronization of the molecular clock contributes to the heterogeneity of the inflammatory response. *Science Signaling* 12 (571).
- Almeida, Afonso R M, Inês F Amado, Joseph Reynolds, et al. (2012). Quorum-sensing in CD4+ T cell homeostasis : a hypothesis and a model. 3 (May), pp. 1–15.
- Amb, Stefan, Robyn L. Prueitt, Ming Yi, et al. (2008). Genomic profiling of microRNA and messenger RNA reveals deregulated microRNA expression in prostate cancer. *Cancer Research* 68 (15), pp. 6162–6170.
- Amura, C R, T Kamei, N Ito, M J Soares, and D C Morrison (1998). Differential regulation of lipopolysaccharide (LPS) activation pathways in mouse macrophages by LPS-binding proteins. *Journal of immunology (Baltimore, Md. : 1950)* 161 (5), pp. 2552–60.
- Anderson, Warren D., Andrew D. Greenhalgh, Aditya Takwale, Samuel David, and Rajanikanth Vadigepalli (2017). Novel influences of IL-10 on CNS inflammation revealed by integrated analyses of cytokine networks and microglial morphology. *Frontiers in Cellular Neuroscience* 11 (233), pp. 1–19.

- Antonioli, Luca, Corrado Blandizzi, Pál Pacher, Martin Williams, and György Haskó (2019). Rethinking Communication in the Immune System : The Quorum Sensing Concept. *Trends in Immunology* 40 (2), pp. 88–97.
- Arend, William P, Mark Malyak, Carla J Guthridge, and Cem Gabay (1998). INTERLEUKIN-1 RECEPTOR ANTAGONIST: Role in Biology. *Annual Review of Immunology* 16 (1), pp. 27–55.
- Ay, Ahmet and David N. Arnosti (2011). Mathematical modeling of gene expression: A guide for the perplexed biologist. *Critical Reviews in Biochemistry and Molecular Biology* 46 (2), pp. 137–151.
- Baek, Daehyun, Judit Villén, Chanseok Shin, et al. (2008). The impact of microRNAs on protein output. *Nature* 455 (7209), pp. 64–71.
- Bain, Calum C, Alberto Bravo-blas, Charlotte L Scott, et al. (2014). Constant replenishment from circulating monocytes maintains the macrophage pool in the intestine of adult mice. 15 (10).
- Bainbridge, J. W.B., C. Stephens, K. Parsley, et al. (2001). In vivo gene transfer to the mouse eye using an HIV-based lentiviral vector; efficient long-term transduction of cornealendothelium and retinal pigment epithelium. *Gene Therapy* 8 (21), pp. 1665–1668.
- Bar-Even, Arren, Johan Paulsson, Narendra Maheshri, et al. (2006). Noise in protein expression scales with natural protein abundance. *Nature Genetics* 38 (6), pp. 636–643.
- Bartel, David P. (2004). MicroRNAs: Genomics, Biogenesis, Mechanism, and Function. *Cell* 116 (2), pp. 281–297.
- Bartel, David P (2018). Metazoan MicroRNAs. *Cell* 173 (1), pp. 20–51.
- Bartel, David P and Chang-zheng Chen (2004). Micromanagers of gene expression : the potentially widespread influence of metazoan microRNAs. 5 (May), pp. 396–400.
- Becher, Burkhard, Sonia Tugues, and Melanie Greter (2016). GM-CSF: From Growth Factor to Central Mediator of Tissue Inflammation. *Immunity* 45 (5), pp. 963–973.

- Bell, Jessica H, Amy H Herrera, Ying Li, and Bruce Walcheck (2007). Role of ADAM17 in the ectodomain shedding of TNF- α and its receptors by neutrophils and macrophages. *Journal of Leukocyte Biology* 82 (1), pp. 173–176.
- Bent, Rebekka, Lorna Moll, Stephan Grabbe, and Matthias Bros (2018). Interleukin-1 Beta — A Friend or Foe in Malignancies? 19 (8).
- Berghaus, L J and J N Moore (2010). Innate immune responses of primary murine macrophage-lineage cells and RAW 264.7 cells to ligands of Toll-like receptors 2, 3, and 4. . . . *and Infectious Diseases* 33 (5), pp. 1–13.
- Berse, B, L F Brown, L Van de Water, H F Dvorak, and D R Senger (1992). Vascular permeability factor (vascular endothelial growth factor) gene is expressed differentially in normal tissues, macrophages, and tumors. *Molecular Biology of the Cell* 3 (2), pp. 211–220.
- Bezbradica, Jelena S and Ruslan Medzhitov (2009). Integration of cytokine and heterologous receptor signaling pathways. *Nature Immunology* 10 (4), pp. 333–339.
- Bianchi, Marco E. (2007). DAMPs, PAMPs and alarmins: all we need to know about danger. *Journal of Leukocyte Biology* 81 (1), pp. 1–5.
- Biswas, Subhra K. and Eduardo Lopez-Collazo (2009). Endotoxin tolerance: new mechanisms, molecules and clinical significance. *Trends in Immunology* 30 (10), pp. 475–487.
- Blake, William J., Gábor Balázsi, Michael A. Kohanski, et al. (2006). Phenotypic Consequences of Promoter-Mediated Transcriptional Noise. *Molecular Cell* 24 (6), pp. 853–865.
- Blevins, Rory, Ludovica Bruno, Thomas Carroll, et al. (2015). microRNAs Regulate Cell-to-Cell Variability of Endogenous Target Gene Expression in Developing Mouse Thymocytes. *PLoS Genetics* 11 (2), pp. 1–19.
- Bódi, Zoltán, Zoltán Farkas, Dmitry Nevozhay, et al. (2017). Phenotypic heterogeneity promotes adaptive evolution. *PLoS Biology* 15 (5), pp. 1–26.

- Bogdan, Christian (2015). Nitric oxide synthase in innate and adaptive immunity: An update. *Trends in Immunology* 36 (3), pp. 161–178.
- Bonabeau, Eric (2002). Agent-based modeling: Methods and techniques for simulating human systems. *Proceedings of the National Academy of Sciences of the United States of America* 99 (SUPPL. 3), pp. 7280–7287.
- Boone, David L., Emre E. Turer, Eric G. Lee, et al. (2004). The ubiquitin-modifying enzyme A20 is required for termination of Toll-like receptor responses. *Nature Immunology* 5 (10), pp. 1052–1060.
- Boucher, Dave, Mercedes Monteleone, Rebecca C Coll, et al. (2018). Caspase-1 self-cleavage is an intrinsic mechanism to terminate inflammasome activity. *The Journal of Experimental Medicine* 215 (3), 827 LP –840.
- Bradley, J R (2008). TNF-mediated inflammatory disease. *The Journal of Pathology* 214 (2), pp. 149–160.
- Brady, R., Frank-Ito, D.O., Tran, H.T., et al. (2018). Personalized mathematical model of endotoxin-induced inflammatory responses in young men and associated changes in heart rate variability. *Math. Model. Nat. Phenom.* 13 (5), p. 42.
- Burns, Kimberly, Fabio Martinon, Heike Pahl, et al. (1998). MyD88 , an Adapter Protein Involved in Interleukin-1 Signaling. *The Journal of Biological Chemistry* 273 (20), pp. 12203–12209.
- Caldwell, Andrew B, Zhang Cheng, Jesse D Vargas, Harry A Birnbaum, and Alexander Hoffmann (2014). Network dynamics determine the autocrine and paracrine signaling functions of TNF. *Genes & Development*, pp. 2120–2133.
- Campbell, I. L., M. Erta, S. L. Lim, et al. (2014). Trans-Signaling Is a Dominant Mechanism for the Pathogenic Actions of Interleukin-6 in the Brain. *Journal of Neuroscience* 34 (7), pp. 2503–2513.
- Carey FJ, Braude AI and M Zalesky (1957). Studies with radioactive endotoxin. III. The effect of tolerance on the distribution of radioactivity after intravenous injection of

- Escherichia coli endotoxin labeled with cr5. *Journal of Clinical Investigation* 37 (3), pp. 441–457.
- Cassado, Alexandra Anjos, Maria Regina D'Império Lima, and Karina Ramalho Bortoluci (2015). Revisiting mouse peritoneal macrophages: Heterogeneity, development, and function. *Frontiers in Immunology* 6 (MAY), pp. 1–9.
- Chalaris, Athena, Ulrike May, Georg H Waetzig, et al. (2019). Transgenic blockade of interleukin 6 transsignaling abrogates inflammation. 111 (3), pp. 1021–1029.
- Chan, Christopher, Liwu Li, Charles E McCall, and Barbara K Yoza (2005). Endotoxin Tolerance Disrupts Chromatin Remodeling and NF- κ B Transactivation at the IL-1 β Promoter. *The Journal of Immunology* 175 (1), 461 LP –468.
- Chanteux, Hugues, Amélie C Guisset, Charles Pilette, and Yves Sibille (2007). LPS induces IL-10 production by human alveolar macrophages via MAPKinases- and Sp1-dependent mechanisms. *Respiratory research* 8 (1), p. 71.
- Chaplin, David D. (2010). Overview of the immune response. *Journal of Allergy and Clinical Immunology* 125 (2 SUPPL. 2), S3–S23.
- Chen, Chih-chiang, Lei Wang, Arthur D Lander, et al. (2015). Organ-Level Quorum Sensing Directs Regeneration in Hair Stem Cell Populations Article Organ-Level Quorum Sensing Directs Regeneration in Hair Stem Cell Populations. *Cell* 161 (2), pp. 277–290.
- Chen, Wang, Deng Li, Hong Mei, et al. (2001). TAK1 is a ubiquitin-dependent kinase of MKK and IKK. *Nature* 412 (19), pp. 1–11.
- Chen, Xian-ming, Patrick L Splinter, Steven P O Hara, and Nicholas F Larusso (2007). A Cellular Micro-RNA , let-7i , Regulates Toll-like Receptor 4 Expression and Contributes to Cholangiocyte Immune Responses against *Cryptosporidium parvum* Infection *. 282 (39), pp. 28929–28938.
- Chen, Xiaoping, Mohamed El Gazzar, Barbara K. Yoza, and Charles E. McCall (2009). The NF- κ B factor RelB and histone H3 lysine methyltransferase G9a directly interact

- to generate epigenetic silencing in endotoxin tolerance. *Journal of Biological Chemistry* 284 (41), pp. 27857–27865.
- Chistiakov, Dmitry A., Yuri V. Bobryshev, Nikita G. Nikiforov, et al. (2015). Macrophage phenotypic plasticity in atherosclerosis: The associated features and the peculiarities of the expression of inflammatory genes. *International Journal of Cardiology* 184 (1), pp. 436–445.
- Chujo, Sonoko, Fumiaki Shirasaki, Miki Kondo-Miyazaki, Yuka Ikawa, and Kazuhiko Takehara (2009). Role of connective tissue growth factor and its interaction with basic fibroblast growth factor and macrophage chemoattractant protein-1 in skin fibrosis. *Journal of Cellular Physiology* 220 (1), pp. 189–195.
- Colotta, Francesco, Fabio Re, Marta Muzio, et al. (1993). Interleukin-1 Type 11 Receptor: A Decoy Target for IL-1 That Is Regulated by IL-4. *Science* 261 (July).
- Couper, Kevin N., Daniel G. Blount, and Eleanor M. Riley (2008). IL-10: The Master Regulator of Immunity to Infection. *The Journal of Immunology* 180 (9), pp. 5771–5777.
- Covert, Markus W, Thomas H Leung, Jahlionais E Gaston, and David Baltimore (2005). Achieving Stability of Lipopolysaccharide-Induced NF- κ B Activation. 309 (September), pp. 1854–1858.
- Croker, Ben A., Danielle L. Krebs, Jian Guo Zhang, et al. (2003). SOCS3 negatively regulates IL-6 signaling in vivo. *Nature Immunology* 4 (6), pp. 540–545.
- Csilla Holub, Marianna, Csaba Szalai, Anna Polgár, Sára Tóth, and András Falus (1999). Generation of 'truncated' interleukin-6 receptor (IL-6R) mRNA by alternative splicing; a possible source of soluble IL-6R. *Immunology Letters* 68 (1), pp. 121–124.
- Curtale, Graziella, Marcello Rubino, and Massimo Locati (2019). MicroRNAs as molecular switches in macrophage activation. *Frontiers in Immunology* 10 (MAR), pp. 1–13.
- Curtale, Graziella, Tiziana A. Renzi, Massimiliano Mirolo, et al. (2018). Multi-step regulation of the TLR4 pathway by the miR-125a~99b~let-7e cluster. *Frontiers in Immunology* 9 (SEP), pp. 1–16.

- Dai, Bo, Dan Wei, Ning Ning Zheng, et al. (2019). Coccomyxa gloeobotrydiformis polysaccharide inhibits lipopolysaccharide-induced inflammation in RAW 264.7 macrophages. *Cellular Physiology and Biochemistry* 51 (6), pp. 2523–2535.
- Day, Judy D., Diana M. Metes, and Yoram Vodovotz (2015). Mathematical modeling of early cellular innate and adaptive immune responses to ischemia/reperfusion injury and solid organ allotransplantation. *Frontiers in Immunology* 6 (SEP), pp. 1–19.
- Degterev, Alexei, Zhihong Huang, Michael Boyce, et al. (2005). Chemical inhibitor of nonapoptotic cell death with therapeutic potential for ischemic brain injury. *Nature Chemical Biology* 1 (2), pp. 112–119.
- Del Giudice, Marco, Stefano Bo, Silvia Grigolon, and Carla Bosia (2018). On the role of extrinsic noise in microRNA-mediated bimodal gene expression. *PLoS Computational Biology* 14 (4), pp. 1–26.
- Delgado, Mario, Wei Sun, Doina Ganea, and Javier Leceta (1999). VIP and PACAP differentially regulate the costimulatory activity of resting and activated macrophages through the modulation of B7.1 and B7.2 expression. *Journal of Immunology* 163 (8), pp. 4213–4223.
- Dinarello, Charles A. (2018). Overview of the IL-1 family in innate inflammation and acquired immunity. *Immunological Reviews* 281 (1), pp. 8–27.
- Divanovic, Senad, Aurelien Trompette, Sowsan F. Atabani, et al. (2005). Negative regulation of Toll-like receptor 4 signaling by the Toll-like receptor homolog RP105. *Nature Immunology* 6 (6), pp. 571–578.
- Doob, JL (1945). Markoff Chains—Denumerable Case. *Transactions of the American Mathematical Society* 58 (3), pp. 455–473.
- Dormand, J. R. and P. J. Prince (1980). A family of embedded Runge-Kutta formulae. *Journal of Computational and Applied Mathematics* 15 (2), pp. 203–211.
- Doyle, Sean E., Sagar A. Vaidya, Ryan O’Connell, et al. (2002). IRF3 Mediates a TLR3/TLR4-Specific Antiviral Gene Program. *Immunity* 17 (3), pp. 251–263.

- El Gazzar, Mohamed, Barbara K. Yoza, Jean Y.Q. Hu, Sue L. Cousart, and Charles E. McCall (2007). Epigenetic silencing of tumor necrosis factor α during endotoxin tolerance. *Journal of Biological Chemistry* 282 (37), pp. 26857–26864.
- Eldar, Avigdor and Michael B Elowitz (2010). Functional roles for noise in genetic circuits. *Nature* 467 (7312), pp. 167–173.
- Elowitz, Michael B, Arnold J Levine, and Eric D Siggia (2002). Stochastic Gene Expression in a Single Cell. *Science* 297 (August), pp. 1183–1187.
- Farlik, Matthias, Benjamin Reutterer, Christian Schindler, et al. (2010). Nonconventional initiation complex assembly by STAT and NF- κ B transcription factors regulates nitric oxide synthase expression. *Immunity* 33 (1), pp. 25–34.
- Ferreira, S. C., M. L. Martins, and M. J. Vilela (2003). Morphology transitions induced by chemotherapy in carcinomas in situ. *Physical Review E - Statistical Physics, Plasmas, Fluids, and Related Interdisciplinary Topics* 67 (5), p. 9.
- Fischer, Roman, Olaf Maier, Martin Siegemund, et al. (2011). A TNF receptor 2 selective agonist rescues human neurons from oxidative stress-induced cell death. *PLoS ONE* 6 (11).
- Fischer, Roman, Harald Wajant, Roland Kontermann, Klaus Pfizenmaier, and Olaf Maier (2014). Astrocyte-specific activation of TNFR2 promotes oligodendrocyte maturation by secretion of leukemia inhibitory factor. *Glia* 62 (2), pp. 272–283.
- Fitzgerald, Katherine A., Daniel C. Rowe, Betsy J. Barnes, et al. (2003). LPS-TLR4 Signaling to IRF-3/7 and NF- κ B Involves the Toll Adapters TRAM and TRIF. *The Journal of Experimental Medicine* 198 (7), pp. 1043–1055.
- Fleischmann, Carolin, Andre Scherag, Neill K.J. Adhikari, et al. (2016). Assessment of global incidence and mortality of hospital-treated sepsis current estimates and limitations. *American Journal of Respiratory and Critical Care Medicine* 193 (3), pp. 259–272.

- Flohé, S, E Dominguez Fernández, M Ackermann, et al. (1999). Endotoxin tolerance in rats: expression of TNF-alpha, IL-6, IL-10, VCAM-1 AND HSP 70 in lung and liver during endotoxin shock. *Cytokine* 11 (10), pp. 796–804.
- Foster, Simmie L, Diana C Hargreaves, and Ruslan Medzhitov (2007). Gene-specific control of inflammation by TLR-induced chromatin modifications. *Nature* 447 (7147), pp. 972–8.
- Friedman, Robin C, Kyle Kai-how Farh, Christopher B Burge, and David P Bartel (2009). Most mammalian mRNAs are conserved targets of microRNAs, pp. 92–105.
- Garbers, Christoph, Nathalie Jänner, Athena Chalaris, et al. (2011). Species specificity of ADAM10 and ADAM17 proteins in interleukin-6 (IL-6) trans-signaling and novel role of ADAM10 in inducible IL-6 receptor shedding. *Journal of Biological Chemistry* 286 (17), pp. 14804–14811.
- Garg, By Salil and Phillip A Sharp (2016). Single-cell variability guided by microRNAs, pp. 8–10.
- Gautier, Emmanuel L, Tal Shay, Jennifer Miller, et al. (2012). Gene-expression profiles and transcriptional regulatory pathways that underlie the identity and diversity of mouse tissue macrophages. *Nature immunology* 13 (11), pp. 1118–28.
- Gelfand, Bradley D., Charles B. Wright, Younghee Kim, et al. (2015). Iron Toxicity in the Retina Requires Alu RNA and the NLRP3 Inflammasome. *Cell Reports* 11 (11), pp. 1686–1693.
- Ghosn, Eliver Eid Bou, Alexandra A Cassado, Gregory R Govoni, et al. (2010). Two physically, functionally, and developmentally distinct peritoneal macrophage subsets. *Proceedings of the National Academy of Sciences of the United States of America* 107 (6), pp. 2568–73.
- Giambartolomei, Guillermo H., Vida A. Dennis, Barbara L. Lasater, P. K. Murthy, and Mario T. Philipp (2002). Autocrine and exocrine regulation of interleukin-10 production in THP-1 cells stimulated with *Borrelia burgdorferi* lipoproteins. *Infection and Immunity* 70 (4), pp. 1881–1888.

- Gillespie, Daniel T. (1976). A general method for numerically simulating the stochastic time evolution of coupled chemical reactions. *Journal of Computational Physics* 22 (4), pp. 403–434.
- Gillespie, Daniel T (1977). Exact Stochastic Simulation of Coupled Chemical Reactions. *The Journal of Physical Chemistry* 93555 (1), pp. 2340–2361.
- “Markov Processes: An Introduction for Physical Scientists” (1992). *Markov Processes*. Ed. by Daniel T. Gillespie. San Diego: Academic Press, pp. xix –xx.
- Gillespie, Daniel T. (2007). Stochastic Simulation of Chemical Kinetics. *Annual Review of Physical Chemistry* 58 (1), pp. 35–55.
- Gogos, Charalambos A., Eugenia Drosou, Harry P. Bassaris, and Athanassios Skoutelis (2002). Pro- versus Anti-inflammatory Cytokine Profile in Patients with Severe Sepsis: A Marker for Prognosis and Future Therapeutic Options. *The Journal of Infectious Diseases* 181 (1), pp. 176–180.
- Gordon, Siamon and Annette Plüddemann (2017). Tissue macrophages: heterogeneity and functions. *BMC Biology* 15 (1), p. 53.
- Gourine, Alexander V., Karin Rudolph, Johannes Tesfaigzi, and Matthew J. Kluger (1998). Role of hypothalamic interleukin-1 β in fever induced by cecal ligation and puncture in rats. *American Journal of Physiology - Regulatory Integrative and Comparative Physiology* 275 (3 44-3).
- Grell, Matthias, Matthias Lohden, Matthias Clauss, et al. (1995). The Transmembrane Form of Tumor Necrosis Factor Is the Prime Activating Ligand of the 80 kDa Tumor Necrosis Factor Receptor. *Cell* 83, pp. 793–802.
- Griffith, O W and D J Stuehr (1995). Nitric Oxide Synthases: Properties and Catalytic Mechanism. *Annual Review of Physiology* 57 (1), pp. 707–734.
- Grimes, Tyler, S. Steven Potter, and Somnath Datta (2019). Integrating gene regulatory pathways into differential network analysis of gene expression data. *Scientific Reports* 9 (1), pp. 1–12.

- Gundra, Uma Mahesh, Natasha M Girgis, Dominik Ruckerl, et al. (2014). Alternatively activated macrophages derived from monocytes and tissue macrophages are phenotypically and functionally distinct. *Blood* 123 (20), e110 LP –e122.
- Guo, Haitao, Justin B Callaway, and Jenny P-y Ting (2015). Inflammasomes : mechanism of action , role in disease , and therapeutics. 21 (7), pp. 677–687.
- Guo, Huili, Nicholas T. Ingolia, Jonathan S. Weissman, and David P. Bartel (2010). Mammalian microRNAs predominantly act to decrease target mRNA levels. *Nature* 466 (7308), pp. 835–840.
- Guo, Xiaomin, Huan Wang, Yang Li, et al. (2019). Transfection reagent Lipofectamine triggers type I interferon signaling activation in macrophages. *Immunology and Cell Biology* 97 (1), pp. 92–96.
- Guptasarma, Purnananda (1995). Does replication-induced transcription regulate synthesis of the myriad low copy number proteins of Escherichia coli? *BioEssays*.
- Hagai, Tzachi, Xi Chen, Ricardo J. Miragaia, et al. (2018). Gene expression variability across cells and species shapes innate immunity. *Nature* 563 (7730), pp. 197–202.
- Hammer, A. C. and J. W. Pitchford (2006). Mixotrophy, allelopathy and the population dynamics of phagotrophic algae (cryptophytes) in the Darss Zingst Bodden estuary, southern Baltic. *Marine Ecology Progress Series* 328, pp. 105–115.
- Han, Su Ji, Hyun Mi Ko, Jung Hwa Choi, et al. (2002). Molecular mechanisms for lipopolysaccharide-induced biphasic activation of nuclear factor- κ B (NF- κ B). *Journal of Biological Chemistry* 277 (47), pp. 44715–44721.
- Harfe, Brian D, Michael T McManus, Jennifer H Mansfield, Eran Hornstein, and Clifford J Tabin (2005). The RNaseIII enzyme Dicer is required for morphogenesis but not patterning of the vertebrate limb. *Proceedings of the National Academy of Sciences of the United States of America* 102 (31), pp. 10898–903.
- Hayden, Matthew S. and Sankar Ghosh (2014). Regulation of NF- κ B by TNF family cytokines. *Seminars in Immunology* 26 (3), pp. 253–266.

- Heinrich, Peter C, Iris Behrmann, Serge Haan, Heike M Hermanns, and Gerhard M Ullrich (2003). Principles of IL 6 type cytokine signaling and its regulating. *Biochemical Journal* 374, pp. 1–20.
- Hibi, Masahiko, Masaaki Murakami, Mikiyoshi Saito, et al. (1990). Molecular cloning and expression of an IL-6 signal transducer, gp130. *Cell* 63 (6), pp. 1149–1157.
- Hiscott, J, J Marois, J Garoufalos, et al. (1993). Characterization of a functional NF-kappa B site in the human interleukin 1 beta promoter: evidence for a positive autoregulatory loop. *Molecular and Cellular Biology* 13 (10), 6231 LP –6240.
- Hoadley, Margaret E. and Stephen J. Hopkins (2003). Simple, quantitative measurement of cytokine gene expression using an immunometric reverse transcriptase-polymerase chain reaction. *Journal of Immunological Methods* 282 (1-2), pp. 135–145.
- Horng, Tiffany, Gregory M Barton, and Ruslan Medzhitov (2001). TIRAP: an adapter molecule in the Toll signaling pathway. *Nature Immunology* 2 (9), pp. 835–841.
- Hoshino, Katsuaki, Osamu Takeuchi, Taro Kawai, et al. (1999). Cutting Edge: Toll-Like Receptor 4 (TLR4)-Deficient Mice Are Hyporesponsive to Lipopolysaccharide: Evidence for TLR4 as the Lps Gene Product. *The Journal of Immunology* 162 (7), pp. 3749–3752.
- Hotchkiss, Richard S, Craig M Coopersmith, Jonathan E McDunn, and Thomas A Ferguson (2009). The sepsis seesaw: tilting toward immunosuppression. *Nat Med* 15 (5), pp. 496–497.
- Hsu, Hailing, Jessie Xiong, and David V. Goeddel (1995). The TNF receptor 1-associated protein TRADD signals cell death and NF- κ B activation. *Cell* 81 (4), pp. 495–504.
- Hunter, Christopher A and Simon A Jones (2015). IL-6 as a keystone cytokine in health and disease. 16 (5).
- Jahnke, Tobias and Wilhelm Huisinga (2007). Solving the chemical master equation for monomolecular reaction systems analytically. *Journal of Mathematical Biology* 54 (1), pp. 1–26.

- Janeway Jr, Charles A, Paul Travers, Mark Walport, and Mark J Shlomchik (2001). *Immunobiology*. Garland Science.
- Janssens, Sophie, Kim Burns, Elisabeth Vercaemmen, Jurg Tschopp, and Rudi Beyaert (2003). MyD88S, a splice variant of MyD88, differentially modulates NF- κ B- and AP-1-dependent gene expression. *FEBS Letters* 548 (1-3), pp. 103–107.
- Jantsch, Jonathan, Valentin Schatz, Friedrich C Luft, et al. (2015). Cutaneous Na + Storage Strengthens the Antimicrobial Barrier Function of the Skin and Boosts Macrophage-Driven Host Defense, pp. 493–501.
- Ji, Zhiwei, Ke Yan, Wenyang Li, Haigen Hu, and Xiaoliang Zhu (2017). Mathematical and Computational Modeling in Complex Biological Systems. *BioMed Research International* 2017.
- Jiang, Kangfeng, Shuai Guo, Tao Zhang, et al. (2018). Downregulation of TLR4 by miR-181a Provides Negative Feedback Regulation to Inflammation. 9 (February), pp. 1–13.
- Jones, Simon a, Jürgen Scheller, Stefan Rose-john, et al. (2011). Therapeutic strategies for the clinical blockade of IL-6 / gp130 signaling. *The Journal of Clinical Investigation* 121 (9), pp. 3375–3383.
- Jun-Ming, Zhang and Jianxiong An (2007). Cytokines, Inflammation and Pain. *International Anesthesiology Clinics* 45 (2).
- June, Carl H., Jeffrey A. Bluestone, Lee M. Nadler, and Craig B. Thompson (1994). The B7 and CD28 receptor families. *Immunology Today* 15 (7), pp. 321–331.
- Kagan, Jonathan C., Tian Su, Tiffany Horng, et al. (2008). TRAM couples endocytosis of Toll-like receptor 4 to the induction of interferon- β . *Nature Immunology* 9 (4), pp. 361–368.
- Kalia, Vandana, Surojit Sarkar, Shruti Subramaniam, et al. (2010). Prolonged Interleukin-2R α Expression on Virus-Specific CD8+ T Cells Favors Terminal-Effector Differentiation In Vivo. *Immunity* 32 (1), pp. 91–103.
- Kalliolias, George D and Lionel B Ivashkiv (2016). TNF biology, pathogenic mechanisms and emerging therapeutic strategies. *Nature Reviews Rheumatology* 12 (1), pp. 49–62.

- Kampen, N.G. Van (2007). "Chapter X - The Expansion of the Master Equation". *Stochastic Processes in Physics and Chemistry (Third Edition)*. Ed. by N.G. Van Kampen. Third Edition. North-Holland Personal Library. Amsterdam: Elsevier, pp. 244–272.
- Kaneko, Hiroki, Sami Dridi, Valeria Tarallo, et al. (2011). DICER1 deficit induces Alu RNA toxicity in age-related macular degeneration. *Nature* 471 (7338), pp. 325–330.
- Kawamata, Tomoko and Yukihide Tomari (2010). Making RISC. *Trends in Biochemical Sciences* 35 (7), pp. 368–376.
- Khalil, N, O Berezney, M Sporn, and A H Greenberg (1989). Macrophage production of transforming growth factor beta and fibroblast collagen synthesis in chronic pulmonary inflammation. *The Journal of Experimental Medicine* 170 (3), 727 LP–737.
- Kitano, Hiroaki (2002). Computational Systems Biology. *Nature* 420 (November), pp. 206–210.
- Klein, Allon M, Linas Mazutis, David A Weitz, et al. (2015). Droplet Barcoding for Single-Cell Transcriptomics Applied to Embryonic Stem Cells Resource Droplet Barcoding for Single-Cell Transcriptomics Applied to Embryonic Stem Cells. *Cell* 161 (5), pp. 1187–1201.
- Kleinert, Hartmut, Andrea Pautz, Katrin Linker, and Petra M Schwarz (2004). Regulation of the expression of inducible nitric oxide synthase. 500, pp. 255–266.
- Kobayashi, Koichi, Lorraine D. Hernandez, Jorge E. Galán, et al. (2002). IRAK-M is a negative regulator of Toll-like receptor signaling. *Cell* 110 (2), pp. 191–202.
- Kong, Xiao Ni, He Xin Yan, Lei Chen, et al. (2007). LPS-induced down-regulation of signal regulatory protein α contributes to innate immune activation in macrophages. *Journal of Experimental Medicine* 204 (11), pp. 2719–2731.
- Kriegler, M., C. Perez, K. DeFay, I. Albert, and S. D. Lu (1988). A novel form of TNF/cachectin is a cell surface cytotoxic transmembrane protein: Ramifications for the complex physiology of TNF. *Cell* 53 (1), pp. 45–53.

- Kumar, Madhu S., Jun Lu, Kim L. Mercer, Todd R. Golub, and Tyler Jacks (2007). Impaired microRNA processing enhances cellular transformation and tumorigenesis. *Nature Genetics* 39 (5), pp. 673–677.
- Kumar, Madhu S., Ryan E. Pester, Cindy Y. Chen, et al. (2009). Dicer1 functions as a haploinsufficient tumor suppressor. *Genes and Development* 23 (23), pp. 2700–2704.
- Kumar, Manish, Sanjaya Kumar Sahu, Ranjeet Kumar, et al. (2015). MicroRNA let-7 Modulates the Immune Response to Mycobacterium tuberculosis Infection via Control of Article MicroRNA let-7 Modulates the Immune Response to Mycobacterium tuberculosis Infection via Control of A20 , an Inhibitor of the NF- k B Pathway. *Cell Host and Microbe* 17 (3), pp. 345–356.
- Kumar, Roshan M, Patrick Cahan, Alex K Shalek, et al. (2014). Deconstructing transcriptional heterogeneity in pluripotent stem cells.
- Lagos, Dimitrios, Gabriel Pollara, Stephen Henderson, et al. (2010). miR-132 regulates antiviral innate immunity through suppression of the p300 transcriptional co-activator. *Nature cell biology* 12 (5), pp. 513–9.
- Latz, Eicke, T Sam Xiao, and Andrea Stutz (2013). Activation and regulation of the inflammasomes. *Nature Reviews Immunology* 13, p. 397.
- Lavin, Yonit, Deborah Winter, Ronnie Blecher-gonen, et al. (2014). Tissue-Resident Macrophage Enhancer Landscapes Are Shaped by the Local Microenvironment. *Cell* 159 (6), pp. 1312–1326.
- Lee, Dongheon, Yufang Ding, Arul Jayaraman, and Joseph S Kwon (2018). Mathematical Modeling and Parameter Estimation of Intracellular Signaling Pathway : Application to LPS-induced NF κ B Activation and TNF α Production in Macrophages. *Processes* 6 (21), pp. 1–19.
- Lee, Timothy K, Elissa M Denny, Jayodita C Sanghvi, et al. (2009). A Noisy Paracrine Signal Determines the Cellular NF- k B Response to Lipopolysaccharide. 2 (93), pp. 1–10.

- Lema-Perez, Laura, Rafael Muñoz-Tamayo, Jose Garcia-Tirado, and Hernan Alvarez (2019). On parameter interpretability of phenomenological-based semiphysical models in biology. *Informatics in Medicine Unlocked* 15 (February), p. 100158.
- Levenberg, Kenneth (1944). A method for the solution of certain non-linear problems in least squares. *Quarterly of Applied Mathematics* 2 (14), pp. 164–168.
- Liew, F Y, S Millott, C Parkinson, R M Palmer, and S Moncada (1990). Macrophage killing of Leishmania parasite in vivo is mediated by nitric oxide from L-arginine. *The Journal of Immunology* 144 (12), 4794 LP –4797.
- Lin, Su Chang, Yu Chih Lo, and Hao Wu (2010). Helical assembly in the MyD88-IRAK4-IRAK2 complex in TLR/IL-1R signalling. *Nature* 465 (7300), pp. 885–890.
- Liu, Lin, Istvan Botos, Yan Wang, et al. (2008). Structural Basis of Toll-Like Receptor 3 Signaling with Double-Stranded RNA. *Science* 320 (5874), pp. 379–381.
- López-Collazo, Eduardo and Carlos Del Fresno (2013). Pathophysiology of endotoxin tolerance: mechanisms and clinical consequences. *Critical care (London, England)* 17 (6), p. 242.
- Ma, Chunyan, Yong Li, Min Li, et al. (2014). microRNA-124 negatively regulates TLR signaling in alveolar macrophages in response to mycobacterial infection. *Molecular Immunology* 62 (1), pp. 150–158.
- Mages, Jorg, Harald Dietrich, and Roland Lang (2008). A genome-wide analysis of LPS tolerance in macrophages. *Immunobiology* 212 (9-10), pp. 723–737.
- Maiti, Shreya, Wei Dai, Robert C. Alaniz, Juergen Hahn, and Arul Jayaraman (2015). Mathematical modeling of pro- and anti-inflammatory signaling in macrophages. *Processes* 3 (1), pp. 1–18.
- Marquardt, Donald W . (1963). An Algorithm for Least-Squares Estimation of Nonlinear Parameters. *Journal of the Society for Industrial and Applied Mathematics* 11 (2), pp. 431–441.
- Martinez, Fernando O and Siamon Gordon (2014). The M1 and M2 paradigm of macrophage activation: time for reassessment. *F1000prime reports* 6 (March), p. 13.

- Martins, M. L., S. C. Ferreira, and M. J. Vilela (2010). Multiscale models for biological systems. *Current Opinion in Colloid and Interface Science* 15 (1-2), pp. 18–23.
- Matoulkova, Eva, Eva Michalova, Borivoj Vojtesek, and Roman Hrstka (2012). The role of the 3' untranslated region in post-transcriptional regulation of protein expression in mammalian cells. *RNA Biology* 9 (5), pp. 563–576.
- Matsuura, Motohiro, Hideyuki Takahashi, Haruo Watanabe, Shinji Saito, and Kazuyoshi Kawahara (2010). Immunomodulatory effects of *Yersinia pestis* lipopolysaccharides on human macrophages. *Clinical and Vaccine Immunology* 17 (1), pp. 49–55.
- McAdams, H H and a Arkin (1997). Stochastic mechanisms in gene expression. *Proceedings of the National Academy of Sciences of the United States of America* 94 (3), pp. 814–819.
- Medvedev, AE, KM Kopydlowski, and SN Vogel (2000). Inhibition of lipopolysaccharide-induced signal transduction in endotoxin-tolerized mouse macrophages: dysregulation of cytokine, chemokine, and toll-like receptor 2 and 4 gene expression. *Journal of immunology (Baltimore, Md. : 1950)* 164, pp. 5564–5574.
- Medvedev, Andrei E, Arnd Lentschat, Larry M Wahl, Douglas T Golenbock, and Stefanie N Vogel (2002). Dysregulation of LPS-induced Toll-like receptor 4-MyD88 complex formation and IL-1 receptor-associated kinase 1 activation in endotoxin-tolerant cells. *Journal of immunology (Baltimore, Md. : 1950)* 169 (9), pp. 5209–5216.
- Medzhitov, Ruslan (2001). Toll-like receptors and innate immunity. *Nature Reviews Immunology* 1 (2), pp. 135–145.
- Medzhitov, Ruslan, Paula Preston-Hurlburt, Elizabeth Kopp, et al. (1998). MyD88 is an adaptor protein in the hToll/IL-1 receptor family signaling pathways. *Molecular Cell* 2 (2), pp. 253–258.
- Merks, Roeland M.H. and James A. Glazier (2005). A cell-centered approach to developmental biology. *Physica A: Statistical Mechanics and its Applications* 352 (1), pp. 113–130.
- Micheau, O., S. Lens, O. Gaide, K. Alevizopoulos, and J. Tschopp (2001). NF- B Signals Induce the Expression of c-FLIP. *Molecular and Cellular Biology* 21 (16), pp. 5299–5305.

- Micheau, Olivier and Jurg Tschopp (2003). Induction of TNF Receptor I-Mediated Apoptosis via Two Sequential Signaling Complexes. *Cell* 114, pp. 181–190.
- Miller, Melissa B and Bonnie L Bassler (2001). Quorum Sensing in Bacteria. *Annual Review of Microbiology* Vol. 55, pp. 165–199.
- Misumi, Y., Y. Misumi, K. Miki, et al. (1986). Novel blockade by brefeldin A of intracellular transport of secretory proteins in cultured rat hepatocytes. *Journal of Biological Chemistry* 261 (24), pp. 11398–11403.
- Mitchell, Simon and Alexander Hoffmann (2018). Identifying noise sources governing cell-to-cell variability. *Current Opinion in Systems Biology* 8, pp. 39–45.
- Mittal, Manish, Mohammad Rizwan Siddiqui, Khiem Tran, Sekhar P Reddy, and Asrar B Malik (2014). Reactive Oxygen Species in Inflammation and Tissue Injury. *ANTIOXIDANTS & REDOX SIGNALING* 20 (7).
- Mogensen, Trine H. (2009). Pathogen recognition and inflammatory signaling in innate immune defenses. *Clinical Microbiology Reviews* 22 (2), pp. 240–273.
- Mogensen, Trine H. and Søren R. Paludan (2005). Reading the viral signature by Toll-like receptors and other pattern recognition receptors. *Journal of Molecular Medicine* 83 (3), pp. 180–192.
- Molawi, Kaaweh, Yochai Wolf, Prashanth K Kandalla, et al. (2014). Progressive replacement of embryo-derived cardiac macrophages with age. 211 (11), pp. 2151–2158.
- Montaudouin, Caroline, Marie Anson, Yi Hao, et al. (2013). Quorum Sensing Contributes to Activated IgM-Secreting B Cell Homeostasis.
- Montminy, Sara W, Naseema Khan, Sara McGrath, et al. (2006). Virulence factors of *Yersinia pestis* are overcome by a strong lipopolysaccharide response. *Nature Immunology* 7 (10), pp. 1066–1073.
- Murakami, Masaaki, Masahiko Hibi, Naoko Nakagawa, et al. (1993). IL-6-induced Homodimerization of gp130 and Associated Activation of a Tyrosine Kinase. *Science* 260 (5115), pp. 1808–1810.

- Murray, James D. (2002). *Mathematical Biology I. An Introduction*. 3rd ed. Vol. 17. Interdisciplinary Applied Mathematics. New York: Springer.
- Murray, Peter J and Thomas A Wynn (2011). Protective and pathogenic functions of macrophage subsets. *Nature Reviews Immunology* 11 (11), pp. 723–737.
- Murray, Peter J., Judith E. Allen, Subhra K. Biswas, et al. (2014). Macrophage Activation and Polarization: Nomenclature and Experimental Guidelines. *Immunity* 41 (1), pp. 14–20.
- Muzio, Marta, Jian Ni, Ping Feng, and Vishva M Dixit (1997). IRAK (Pelle) family member IRAK-2 and MyD88 as proximal mediators of IL-1 signaling. *Science* 278 (5343), pp. 1612–1615.
- Nagelkerke, Sietse Q, Christine W Bruggeman, Joke M M den Haan, et al. (2018). Red pulp macrophages in the human spleen are a distinct cell population with a unique expression of Fc- γ receptors. *eng. Blood advances* 2 (8), pp. 941–953.
- Narazaki, Masashi, Kiyoshi Yasukawa, Takashi Saito, et al. (1993). Soluble forms of the interleukin-6 signal-transducing receptor component gp130 in human serum possessing a potential to inhibit signals through membrane-anchored gp130. *Blood* 82 (4), pp. 1120–1126.
- Nathan, Carl and Aihao Ding (2010). Nonresolving Inflammation. *Cell* 140 (6), pp. 871–882.
- Netea, Mihai G. and Jos W.M. van der Meer (2017). Trained Immunity: An Ancient Way of Remembering. *Cell Host & Microbe* 21 (3), pp. 297–300.
- Netea, Mihai G., Jessica Quintin, and Jos W M Van Der Meer (2011). Trained immunity: A memory for innate host defense. *Cell Host and Microbe* 9 (5), pp. 355–361.
- Netea, Mihai G., Claudia A. Nold-Petry, Marcel F. Nold, et al. (2009). Differential requirement for the activation of the inflammasome for processing and release of IL-1 β in monocytes and macrophages. *Blood* 113 (10), pp. 2324–2335.
- Netea, Mihai G., Leo A.B. Joosten, Eicke Latz, et al. (2016). Trained immunity: A program of innate immune memory in health and disease. *Science* 352 (6284), p. 427.

- Newman, John R.S., Sina Ghaemmaghami, Jan Ihmels, et al. (2006). Single-cell proteomic analysis of *S. cerevisiae* reveals the architecture of biological noise. *Nature* 441 (7095), pp. 840–846.
- Nomura, Fumiko, Sachiko Akashi, Yoshimitsu Sakao, et al. (2000). Cutting Edge: Endotoxin Tolerance in Mouse Peritoneal Macrophages Correlates with Down-Regulation of Surface Toll-Like Receptor 4 Expression.
- Novick, D., H. Englemann, D. Wallach, and M. Rubinstein (1989). Soluble cytokine receptors are present in normal human urine. *Journal of Experimental Medicine* 170 (4), pp. 1409–1414.
- Onizawa, Michio, Shigeru Oshima, Ulf Schulze-Topphoff, et al. (2015). The ubiquitin-modifying enzyme A20 restricts ubiquitination of the kinase RIPK3 and protects cells from necroptosis. *Nature Immunology* 16, p. 618.
- Owen, Markus R., Helen M. Byrne, and Claire E. Lewis (2004). Mathematical modelling of the use of macrophages as vehicles for drug delivery to hypoxic tumour sites. *Journal of Theoretical Biology* 226 (4), pp. 377–391.
- Park, Beom Seok and Jie Oh Lee (2013). Recognition of lipopolysaccharide pattern by TLR4 complexes. *Experimental and Molecular Medicine* 45 (12), e66–9.
- Paulsson, Johan (2004). Summing up the noise in gene networks. *Nature* 427 (6973), pp. 415–418.
- (2005). Models of stochastic gene expression. *Physics of Life Reviews* 2 (2), pp. 157–175.
- Paulsson, Johan, Otto G. Berg, and Måns Ehrenberg (2000). Stochastic focusing: Fluctuation-enhanced sensitivity of intracellular regulation. *Proceedings of the National Academy of Sciences of the United States of America* 97 (13), pp. 7148–7153.
- Pedraza, JM and Alexander Van Oudenaarden (2005). Noise Propagation in Gene Networks. 307 (March), pp. 1965–1970.
- Poltorak, Alexander, Xiaolong He, Irina Smirnova, et al. (1998). Defective LPS Signaling in C3H/HeJ and C57BL/10ScCr Mice: Mutations in Tlr4 Gene. *Science* 282 (5396), pp. 2085–2088.

- Postat, Jeremy, Romain Olekhnovitch, Fabrice Lemaitre, and Philippe Bousso (2018). A Metabolism-Based Quorum Sensing Mechanism Contributes to Termination of Inflammatory Responses, pp. 654–665.
- Raj, Arjun, Charles S Peskin, Daniel Tranchina, Diana Y Vargas, and Sanjay Tyagi (2006). Stochastic mRNA Synthesis in Mammalian Cells. 4 (10).
- Ramirez-Carrozzi, Vladimir R., Aaron A. Nazarian, Caiyi C. Li, et al. (2006). Selective and antagonistic functions of SWI/SNF and Mi-2 β nucleosome remodeling complexes during an inflammatory response. *Genes and Development* 20 (3), pp. 282–296.
- Ramirez-Carrozzi, Vladimir R., Daniel Braas, Dev M. Bhatt, et al. (2009). A Unifying Model for the Selective Regulation of Inducible Transcription by CpG Islands and Nucleosome Remodeling. *Cell* 138 (1), pp. 114–128.
- Rand, Ulfert, Melanie Rinas, Johannes Seh Werk, et al. (2012). Multi-layered stochasticity and paracrine signal propagation shape the type-I interferon response. *Molecular Systems Biology* 8 (584), pp. 1–13.
- Rappolee, DA, D Mark, MJ Banda, and Z Werb (1988). Wound macrophages express TGF-alpha and other growth factors in vivo: analysis by mRNA phenotyping. *Science* 241 (4866), pp. 708–712.
- Raschke, W C, San Diego, S Baird, and La Jolla (1978). Functional Macrophage Cell Lines Transformed by Abelson Leukemia Virus. (September).
- Redfield, Rosemary J (2002). Is quorum sensing a side effect of diffusion sensing ? 10 (8), pp. 365–370.
- Ren, Ke and Richard Torres (2009). Role of interleukin-1 β during pain and inflammation. *Brain Research Reviews* 60 (1), pp. 57–64.
- Renshaw, Eric (Aug. 1993). *Modelling biological populations space and time | Statistical physics, network science and complex systems*. Accessed: 2019-9-29.
- Renzi, Tiziana Ada, Marcello Rubino, Laura Gornati, et al. (2015). MiR-146b Mediates Endotoxin Tolerance in Human Phagocytes. *Mediators of Inflammation* 2015 (Mhc Ii).

- Reynolds, Joseph, Inês F Amado, Antonio A Freitas, Grant Lythe, and Carmen Molinaparis (2014). A mathematical perspective on CD4+ T cell quorum-sensing. *Journal of Theoretical Biology* 347, pp. 160–175.
- Rittirsch, Daniel, Michael A. Flierl, and Peter A. Ward (2008). Harmful molecular mechanisms in sepsis. *Nature Reviews Immunology* 8 (10), pp. 776–787.
- Roederer, Mario, Joshua L. Nozzi, and Martha C. Nason (2011). SPICE: Exploration and analysis of post-cytometric complex multivariate datasets. *Cytometry Part A* 79A (2), pp. 167–174.
- Rosadini, Charles V and Jonathan C Kagan (2017). Early innate immune responses to bacterial LPS. *Current Opinion in Immunology* 44, pp. 14–19.
- Rothe, M, V Sarma, V Dixit, and D Goeddel (1995). TRAF-2-mediated activation of NF-kappaB by TNF receptor 2 and CD40. *Science* 269 (September), p. 1424.
- Rubartelli, A, F Cozzolino, M Talio, and R Sitia (1990). A novel secretory pathway for interleukin-1 beta, a protein lacking a signal sequence. *eng. The EMBO journal* 9 (5), pp. 1503–1510.
- Said, Elias A, Franck P Dupuy, Lydie Trautmann, et al. (2010). Programmed death-1-induced interleukin-10 production by monocytes impairs CD4+ T cell activation during HIV infection. *Nature Medicine* 16 (4), pp. 452–459.
- Salamanca, Amalia Enríquez-de, Virginia Calder, Jianping Gao, et al. (2008). Cytokine responses by conjunctival epithelial cells: An in vitro model of ocular inflammation. *Cytokine* 44 (1), pp. 160–167.
- Saraiva, Margarida and Anne O’Garra (2010). The regulation of IL-10 production by immune cells. *Nature Reviews Immunology* 10 (3), pp. 170–181.
- Satija, Rahul and Alex K. Shalek (2014). Heterogeneity in immune responses: From populations to single cells. *Trends in Immunology* 35 (5), pp. 219–229.
- Schmiedel, Jörn M, Sandy L Klemm, Yinnan Zheng, et al. (2015). MicroRNA control of protein expression noise. *Science*.

- Schwandner, Ralf, Roman Dziarski, Holger Wesche, Mike Rothe, and Carsten J. Kirschning (1999). Peptidoglycan- and lipoteichoic acid-induced cell activation is mediated by Toll-like receptor 2. *Journal of Biological Chemistry* 274 (25), pp. 17406–17409.
- Scott, Charlotte L, Fang Zheng, Patrick De Baetselier, et al. (2016). Bone marrow-derived monocytes give rise to self-renewing and fully differentiated Kupffer cells, pp. 1–10.
- Seeley, John J and Sankar Ghosh (2017). Molecular mechanisms of innate memory and tolerance to LPS. 101 (January), pp. 107–119.
- Seeley, John J, Rebecca G Baker, Ghait Mohamed, et al. (2018). Induction of innate immune memory via microRNA targeting of chromatin remodelling factors. *Nature* 559 (7712), pp. 114–119.
- Seymour, H E, A Worsley, J M Smith, and S H L Thomas (2001). Anti-TNF agents for rheumatoid arthritis. *British Journal of Clinical Pharmacology* 51 (3), pp. 201–208.
- Shahrezaei, Vahid and Peter S. Swain (2008). Analytical distributions for stochastic gene expression. *Proceedings of the National Academy of Sciences of the United States of America* 105 (45), pp. 17256–17261. arXiv: 0812.3344.
- Shalek, Alex K, Rahul Satija, Xian Adiconis, et al. (2013). Single-cell transcriptomics reveals bimodality in expression and splicing in immune cells. *Nature* 498 (7453), pp. 236–240.
- Shalek, Alex K, Rahul Satija, Joe Shuga, et al. (2014). Single-cell RNA-seq reveals dynamic paracrine control of cellular variation. *Nature* 510 (7505), pp. 263–269.
- Sharma, J N, A Al-Omran, and S S Parvathy (2007). Role of nitric oxide in inflammatory diseases. *Inflammopharmacology* 15 (6), pp. 252–259.
- Shimazu, R, S Akashi, H Ogata, et al. (1999). MD-2, a molecule that confers lipopolysaccharide responsiveness on Toll-like receptor 4. *eng. The Journal of experimental medicine* 189 (11), pp. 1777–1782.
- Shimokado, Kentaro, Elaine W. Raines, David K. Madtes, et al. (1985). A significant part of macrophage-derived growth factor consists of at least two forms of PDGF. *Cell* 43 (1), pp. 277–286.

- Shin, Han Jae, Hayyoung Lee, Jong Dae Park, et al. (2007). Molecules and Kinetics of Binding of LPS to Recombinant CD14 , TLR4 , and MD-2 Proteins. *24* (1), pp. 119–124.
- Shooshtari, Parisa, Edgardo S. Fortuno, Darren Blimkie, et al. (2010). Correlation analysis of intracellular and secreted cytokines via the generalized integrated mean fluorescence intensity. *Cytometry Part A* *77* (9), pp. 873–880.
- Shouval, Dror S., Amlan Biswas, Jeremy A. Goettel, et al. (2014). Interleukin-10 Receptor Signaling in Innate Immune Cells Regulates Mucosal Immune Tolerance and Anti-Inflammatory Macrophage Function. *Immunity* *40* (5), pp. 706–719.
- Skiniotis, Georgios, Martin J Boulanger, K Christopher Garcia, and Thomas Walz (2005). Signaling conformations of the tall cytokine receptor gp130 when in complex with IL-6 and IL-6 receptor. *Nature Structural & Molecular Biology* *12* (6), pp. 545–551.
- Smolen, Paul, Douglas A. Baxter, and John H. Byrne (2000). Mathematical modeling of gene networks. *Neuron* *26* (3), pp. 567–580.
- Stamatakis, Michail and Nikos V. Mantzaris (2009). Comparison of deterministic and stochastic models of the lac operon genetic network. *Biophysical Journal* *96* (3), pp. 887–906.
- Su, Xiaoqin, Su Li, Min Meng, et al. (2006). TNF receptor-associated factor-1 (TRAF1) negatively regulates Toll/IL-1 receptor domain-containing adaptor inducing IFN- β (TRIF)-mediated signaling. *European Journal of Immunology* *36* (1), pp. 199–206.
- Swain, Peter S, Michael B Elowitz, and Eric D Siggia (2002). Intrinsic and extrinsic contributions to stochasticity in gene expression. *Proceedings of the National Academy of Sciences of the United States of America* *99* (20), pp. 12795–800.
- Taciak, Bartłomiej, Maciej Białasek, Agata Braniewska, et al. (2018). Evaluation of phenotypic and functional stability of RAW 264 . 7 cell line through serial passages, pp. 1–13.
- Taganov, Konstantin D, Mark P Boldin, Kuang-Jung Chang, and David Baltimore (2006). NF-kappaB-dependent induction of microRNA miR-146, an inhibitor targeted to

- signaling proteins of innate immune responses. *Proceedings of the National Academy of Sciences of the United States of America* 103 (33), pp. 12481–6.
- Takeda, Kiyoshi and Shizuo Akira (2004). TLR signaling pathways. *Seminars in Immunology* 16 (1), pp. 3–9.
- Tan, Yunhao, Ivan Zanoni, Thomas W. Cullen, Andrew L. Goodman, and Jonathan C. Kagan (2015). Mechanisms of Toll-like Receptor 4 Endocytosis Reveal a Common Immune-Evasion Strategy Used by Pathogenic and Commensal Bacteria. *Immunity* 43 (5), pp. 909–922.
- Tanaka, Toshio, Masashi Narazaki, and Tadamitsu Kishimoto (2014). IL-6 in Inflammation, Immunity, and Disease. 6 (Kishimoto 1989), pp. 1–16.
- Tannahill, G M, A M Curtis, J Adamik, et al. (2013). Succinate is an inflammatory signal that induces IL-1 β through HIF-1 α . *Nature* 496 (7444), pp. 238–242.
- Tay, Sava, Jacob J. Hughey, Timothy K. Lee, et al. (2010). Single-cell NF- κ B dynamics reveal digital activation and analogue information processing. *Nature* 466 (7303), pp. 267–271.
- Taylor, P.R., L. Martinez-Pomares, M. Stacey, et al. (2005). Macrophage Receptors and Immune Recognition. *Annual Review of Immunology* 23 (1), pp. 901–944.
- Teng, Gui-gen, Wei-hong Wang, Yun Dai, et al. (2013). Let-7b Is Involved in the Inflammation and Immune Responses Associated with Helicobacter pylori Infection by Targeting Toll-Like Receptor 4. 8 (2).
- Thattai, Mukund and Alexander Van Oudenaarden (2010). Intrinsic noise in gene regulatory networks. 2001 (Track II).
- Tomlin, Claire J and Jeffrey D Axelrod (2007). Biology by numbers: mathematical modelling in developmental biology. *Nature Reviews Genetics* 8 (5), pp. 331–340.
- Torres, Marcella, Jing Wang, Paul J. Yannie, et al. (2019). Identifying important parameters in the inflammatory process with a mathematical model of immune cell influx and macrophage polarization. *PLOS Computational Biology* 15 (7), e1007172.

- Trapnell, Cole, Davide Cacchiarelli, Jonna Grimsby, et al. (2014). The dynamics and regulators of cell fate decisions are revealed by pseudotemporal ordering of single cells. *Nature Biotechnology* 32 (4), pp. 381–386.
- Turner, Mark D., Belinda Nedjai, Tara Hurst, and Daniel J. Pennington (2014). Cytokines and chemokines: At the crossroads of cell signalling and inflammatory disease. *Biochimica et Biophysica Acta - Molecular Cell Research* 1843 (11), pp. 2563–2582.
- Van Laethem, J. L., R. Eskinazi, H. Louis, et al. (1998). Multisystemic production of interleukin 10 limits the severity of acute pancreatitis in mice. *Gut* 43 (3), pp. 408–413.
- Vannella, Kevin M., Luke Barron, Lee A. Borthwick, et al. (2014). Incomplete Deletion of IL-4R α by LysMCre Reveals Distinct Subsets of M2 Macrophages Controlling Inflammation and Fibrosis in Chronic Schistosomiasis. *PLoS Pathogens* 10 (9).
- Varol, Diana, Alexander Mildner, Thomas Blank, et al. (2017). Dicer Deficiency Differentially Impacts Microglia of the Developing and Adult Brain. *Immunity* 46 (6), 1030–1044.e8.
- Vught, Lonneke A van, Peter M C Klein Klouwenberg, Cristian Spitoni, et al. (2016). Incidence, Risk Factors, and Attributable Mortality of Secondary Infections in the Intensive Care Unit After Admission for Sepsis. *JAMA* 315 (14), pp. 1469–1479.
- Waetzig, Georg H, Philip Rosenstiel, Alexander Arlt, et al. (2004). Soluble tumor necrosis factor (TNF) receptor-1 induces apoptosis via reverse TNF signaling and autocrine transforming growth factor- β 1. *The FASEB Journal* 19 (1), pp. 91–93.
- Walpole, Joseph, Jason A. Papin, and Shayn M. Peirce (2013). Multiscale Computational Models of Complex Biological Systems. *Annual Review of Biomedical Engineering* 15 (1), pp. 137–154.
- Wang, Jing, Su Wu, Xin Jin, et al. (2008). Retinoic Acid-Inducible Gene-1 Mediates Late Phase Induction of TNF- α by Lipopolysaccharide. *The Journal of Immunology* 180 (12), pp. 8011–8019.

- Wang, Nayi, Ji Zheng, Zhuo Chen, et al. (2019). Single-cell microRNA-mRNA co-sequencing reveals non-genetic heterogeneity and mechanisms of microRNA regulation. *Nature Communications* 10 (1), pp. 1–12.
- Wilkinson, Darren J (2009). Stochastic modelling for quantitative description of heterogeneous biological systems. *Nature Reviews Genetics* 10 (February), pp. 122–133.
- Willenborg, Sebastian, Tina Lucas, Geert van Loo, et al. (2012). CCR2 recruits an inflammatory macrophage subpopulation critical for angiogenesis in tissue repair. *Blood* 120 (3), pp. 613–625.
- Wojdasiewicz, Piotr, A A Poniatowski, and Dariusz Szukiewicz (2014). The Role of Inflammatory and Anti-Inflammatory Cytokines in the Pathogenesis of Osteoarthritis. 2014.
- Wood, A. J. and J. B. Coe (2007). A fitness based analysis of Daisyworld. *Journal of Theoretical Biology* 249 (2), pp. 190–197.
- Wood, Andrew J, Graeme J Ackland, James G Dyke, Hywel T P Williams, and Timothy M Lenton (2008). Daisyworld : A Review. (2006), pp. 1–23.
- Wright, S D, P S Tobias, R J Ulevitch, and R A Ramos (1989). Lipopolysaccharide (LPS) binding protein opsonizes LPS-bearing particles for recognition by a novel receptor on macrophages. *The Journal of experimental medicine* 170 (4), pp. 1231–1241.
- Wright, S D, R A Ramos, P S Tobias, R J Ulevitch, and J C Mathison (1990). CD14, a receptor for complexes of lipopolysaccharide (LPS) and LPS binding protein. *Science* 249 (4975), 1431 LP –1433.
- Wynn, Thomas A., Ajay Chawla, and Jeffrey W. Pollard (2013). Macrophage biology in development, homeostasis and disease. *Nature* 496 (7446), pp. 445–455.
- Wynn, Thomas A. and Kevin M. Vannella (2016). Macrophages in Tissue Repair, Regeneration, and Fibrosis. *Immunity* 44 (3), pp. 450–462.
- Xiang, Qiang, L. Wen, M. H. Liu, et al. (2009). Endotoxin tolerance of RAW264.7 correlates with p38-dependent up-regulation of scavenger receptor-A. *Journal of International Medical Research* 37 (2), pp. 491–502.

- Xiao, Bin, Zhen Liu, Bo-sheng Li, et al. (2009). Induction of microRNA-155 during *Helicobacter pylori* Infection and Its Negative Regulatory Role in the Inflammatory Response. 200 (30).
- Xie, Qiang, Wen Wen Shen, Jian Zhong, et al. (2014). Lipopolysaccharide/adenosine triphosphate induces IL-1 β and IL-18 secretion through the NLRP3 inflammasome in RAW264.7 murine macrophage cells. *International Journal of Molecular Medicine* 34 (1), pp. 341–349.
- Xu, Guangxian, Zhaobo Zhang, Jun Wei, et al. (2013). microR-142-3p down-regulates IRAK-1 in response to *Mycobacterium bovis* BCG infection in macrophages. *Tuberculosis* 93 (6), pp. 606–611.
- Xue, Bin, Yifan Wu, Zhimin Yin, et al. (2005). Regulation of lipopolysaccharide-induced inflammatory response by glutathione S-transferase P1 in RAW264.7 cells. *FEBS Letters* 579 (19), pp. 4081–4087.
- Xue, Jia, Susanne V Schmidt, Jil Sander, et al. (2014). Resource Transcriptome-Based Network Analysis Reveals a Spectrum Model of Human Macrophage Activation. *Immunity* 40 (2), pp. 274–288.
- Xue, Qiong, Yao Lu, Markus R Eisele, et al. (2015). Analysis of single-cell cytokine secretion reveals a role for paracrine signaling in coordinating macrophage responses to TLR4 stimulation. 8 (381), pp. 1–13.
- Yamamoto, Masahiro, Shintaro Sato, and Hiroaki Hemmi (2003). Role of Adaptor TRIF in the MyD88-Independent Toll-Like Receptor Signaling Pathway. *Science* 301 (August), pp. 640–643.
- Yamasaki, K, T Taga, Y Hirata, et al. (1988). Cloning and expression of the human interleukin-6 (BSF-2/IFN beta 2) receptor. *Science* 241 (4867), 825 LP –828.
- Yang, Jing-Xing, Kou-Chou Hsieh, Yi-Ling Chen, et al. (2017). Phosphodiesterase 4B negatively regulates endotoxin-activated interleukin-1 receptor antagonist responses in macrophages. *Scientific Reports* 7, p. 46165.

- Yang, Sujuan, Julie Wang, David Douglass Brand, and Song Guo Zheng (2018). Role of TNF-TNF receptor 2 signal in regulatory T cells and its therapeutic implications. *Frontiers in Immunology* 9 (APR).
- Yasukawa, Hideo, Masahiko Hoshijima, Kenneth R. Chien, et al. (2003). IL-6 induces an anti-inflammatory response in the absence of SOCS3 in macrophages. *Nature Immunology* 4 (6), pp. 551–556.
- Yoda, Mayuko, Tomoko Kawamata, Zain Paroo, et al. (2009). Articles ATP-dependent human RISC assembly pathways. *Nature Structural & Molecular Biology* 17 (1), pp. 17–23.
- Yona, Simon, Ki Wook Kim, Yochai Wolf, et al. (2013). Fate Mapping Reveals Origins and Dynamics of Monocytes and Tissue Macrophages under Homeostasis. *Immunity* 38 (1), pp. 79–91.
- Yoshimura, A, E Lien, R R Ingalls, et al. (1999). Cutting edge: recognition of Gram-positive bacterial cell wall components by the innate immune system occurs via Toll-like receptor 2. *Journal of immunology (Baltimore, Md. : 1950)* 163 (1), pp. 1–5.
- Zhang, Guolong and Sankar Ghosh (2001). NF- κ B in defense and disease Toll-like receptor – mediated NF- κ B activation : a phylogenetically conserved paradigm in innate immunity. *Journal of Clinical Investigation* 107 (1), pp. 13–19.
- Zhang, Jun-Ming and Jianxiong An (2007). Cytokines, Inflammation, and Pain. *International Anesthesiology Clinics* 45 (2).
- Zhang, X and and DM Mosser (2008). Macrophage activation by endogenous danger signals. *Journal of Pathology* 214 (August), pp. 161–178.
- Zhang, Xia, Ricardo Goncalves, and David M Mosser (2008). The Isolation and Characterization of Murine Macrophages. *Current protocols in immunology / edited by John E.Coligan ...[et al.]* CHAPTER (November), Unit: 14.1.
- Zhao, Yang, Weilong Zou, Junfeng Du, and Yong Zhao (2018). The origins and homeostasis of monocytes and tissue-resident macrophages in physiological situation. (January).

- Zheng, Hui, Daniel Fletcher, Wieslaw Kozak, et al. (1995). Resistance to fever induction and impaired acute-phase response in interleukin-1 β -deficient mice. *Immunity* 3 (1), pp. 9–19.
- Zhou, Xikun, Xuefeng Li, and Min Wu (2018). miRNAs reshape immunity and inflammatory responses in bacterial infection. *Signal Transduction and Targeted Therapy* (September 2017), pp. 1–13.
- Zhu, Junyu, Li Luo, Lixing Tian, et al. (2018). Aryl hydrocarbon receptor promotes IL-10 expression in inflammatory macrophages through Src-STAT3 signaling pathway. *Frontiers in Immunology* 9 (SEP), pp. 1–14.
- Zhuang, John C. and Gerald N. Wogan (1997). Growth and viability of macrophages continuously stimulated to produce nitric oxide. *Proceedings of the National Academy of Sciences of the United States of America* 94 (22), pp. 11875–11880.
- Zigmond, Ehud, Biana Bernshtein, Gilgi Friedlander, et al. (2014). Macrophage-Restricted Interleukin-10 Receptor Deficiency, but Not IL-10 Deficiency, Causes Severe Spontaneous Colitis. *Immunity* 40 (5), pp. 720–733.
- Zou, Meijuan, Fang Wang, Aiqin Jiang, et al. (2017). MicroRNA-3178 ameliorates inflammation and gastric carcinogenesis promoted by *Helicobacter pylori* new toxin, Tip- α , by targeting TRAF3, pp. 1–14.